Exploring mechanisms of prostate tumourigenesis in mouse models

---

Adam Christopher Cox

1162217

MD Thesis, 2015

Cardiff University

Acknowledgements

I am eternally grateful to **Professors Alan Clarke** and **Howard Kynaston**, both of whom have provided limitless advice and guidance in helping to producing this thesis.

I am greatly indebted to **Mark Bishop** for carrying out genotyping, **Dr Kirsty Richardson** for assistance with FACS, and **Derek Scarborough** for histology services (all based at the School of Biosciences, Cardiff University). I also wish to thank **Dr David Griffiths** for making the time to analyse my histology slides, over and above his role as Consultant Histopathologist at University Hospital of Wales, Cardiff. My sincerest thanks are also extended to **Dr Karen Read**, **Dr Valerie Meniel**, and **Dr Aliaksei Holik** for their assistance in helping to overcome the daily struggles faced by a surgical trainee in the lab, and **Mr Matthew Jefferies**, my successor in this research, for being a great friend.

My heartfelt thanks are also extended to **Mr Owen Hughes**, Training Programme Director for Urology in Wales, and Consultant Urological Surgeon at the University Hospital of Wales, Cardiff for his constant encouragement and gentle reminders about thesis writing deadlines! I also acknowledge the **Wales Postgraduate Deanery**, and the **Specialist Training Committee** for allowing me to take the necessary time out of programme for research, and my **clinical supervisors** from the University Hospital of Wales, Cardiff and the Princess of Wales Hospital, Bridgend, for allowing me to take the occasional time out to complete my manuscript.

Finally and most of all, I want to thank my wife, **Sam**, and my son, **Dylan**, for their unwavering love and support in what have been the most challenging few years of my life. I don't know how I'll ever repay you…

Contents

Abstract **8**
Posters and Presentations **9**
Published Abstracts **10**
Abbreviations **11**

Chapter 1: General Introduction **13**
1.1 THE PROSTATE GLAND **13**
1.1.1. Prostate gland function 13
1.1.2. Embryology and prostate gland development 14
1.1.3. Anatomy of the human prostate 16
1.1.4. Histology of the normal human prostate 17
1.1.5. Histopathology of the human prostate and the zonal origin of PCa 18
1.1.6. Cellular organisation of human prostate epithelium 19
1.2. MOUSE PROSTATE ANATOMY **20**
1.2.1. Cellular organisation of mouse prostate epithelium 23
1.2.2. Why use a mouse model to study prostate tumourigenesis? 24
1.2.3. The limitations of using mouse models to study prostate cancer 24
1.3. PROSTATE CANCER **25**
1.3.1. Making a diagnosis of prostate cancer – Gleason score 28
1.3.2. TNM staging 31
1.3.3. Treatment of prostate cancer 32
1.3.3.1. Localised prostate cancer 32
1.3.3.2. Locally advanced prostate cancer 33
1.3.3.3. Metastatic prostate cancer 35
1.4. STEM CELLS AND STEM CELL THEORY **37**
1.4.1. Human prostate epithelial stem cells 37
1.4.1.1. Evidence for epithelial stem cells in normal prostate – rodent androgen cycling studies 38
1.4.1.2. Phenotypic relationship between epithelial cell types in the prostate 40
1.4.2. Do human prostate epithelial stem cells reside in the basal or luminal layer? 41
1.4.3. Epithelial stem cells in the murine prostate 42
1.4.3.1. Location of murine prostate epithelial stem cells 44
1.4.4. Prostate epithelial stem cell markers 45
1.4.5. Human prostate epithelial stem cell markers 45
1.4.6. Mouse prostate epithelial stem cell markers 51
1.4.7. Cancer stem cells 54
1.5. MODELLING PROSTATE CANCER IN VITRO **55**
1.5.1. Cell lines 55
1.6. MODELLING PROSTATE CANCER IN VIVO **56**
1.6.1. Xenograft models of prostate cancer 56
1.6.2. Constitutive/germline knockout models of prostate cancer 57
1.6.3. Transgenic T-antigen models of prostate cancer 60
1.6.4. Cre-LoxP Technology 62
1.6.5. Conditional knockout models of prostate cancer 64
1.7. β-CATENIN **68**

1.7.1. The structure and function of β-catenin 68
1.7.2. The role of β-catenin in cancer 72
1.8. PTEN **73**
1.8.1. PTEN structure and function 73
1.8.2. *The role of PTEN in PI3K/Akt/mTOR signalling* 74
1.8.3. PI3K/Akt/mTOR signalling in cancer 75
1.9. RAS: THE PROTO-ONCOGENE **77**
1.9.1. The structure and function of Ras 77
1.9.2. The role of Ras in MAPK signalling 79
1.9.3. The role of Ras in cancer 79

Chapter 2: Hypothesis and thesis aims **82**
2.1. HYPOTHESIS
2.2. THESIS AIMS

Chapter 3: Materials and Methods **84**
3.1. MOUSE COLONY **84**
3.1.1. Genotyping 85
3.1.2. Genotyping primers 85
3.2. TISSUE HARVESTING **86**
3.2.1. For immunohistochemistry (paraffin)
3.2.2. For primary tissue culture
3.3. IMMUNOHISTOCHEMISTRY (PARAFFIN) **86**
3.3.1. Primary antibodies 87
3.3.2. De-wax and rehydrate slides for immunohistochemistry 88
3.3.3. ***Method A:*** *Rabbit polyclonal primary antibodies (Envision)* 88
3.3.4. ***Method B:*** *Rabbit polyclonal primary antibodies (Biotin)* 88
3.3.5. ***Method C:*** *Mouse monoclonal primary antibodies (Envision)* 89
3.3.6. ***Method D:*** *Mouse/Rat polyclonal (Biotin)* 89
3.3.7. ***Method E:*** *Chicken polyclonal primary antibody (Biotin)* 90
3.4. HISTOPATHOLOGICAL CHARACTERISATION **91**
3.4.1. Haematoxylin and eosin staining 91
3.4.2. LacZ stain of prostate wholemounts 91
3.4.3. Characterisation of murine prostate tumours 91
3.4.4. Scoring proliferation 91
3.5. 3D PRIMARY PROSTATE EPITHELIAL STEM CELL CULTURE **92**
3.5.1. Creation of a prostate epithelial single cell suspension 92
3.5.2. Unsorted prostate epithelial cells 93
3.5.3. FACS enrichment: sorted prostate epithelial cells 94
3.5.4. Sorted cells 94
3.5.5. Passage of prostate epithelial stem cells in vitro 95
3.5.6. Quantifying self-renewal 96

Chapter 4: Investigating interactions between the Wnt, PI3K/Akt/mTOR, and MAPK pathways in prostate tumourigenesis **97**
4.1. INTRODUCTION **97**

4.1.1. PTEN is implicated in human prostate cancer 97
4.1.2. The PI3K/Akt/mTOR pathway and human prostate cancer 98
4.1.3. Beta-catenin is implicated in human prostate cancer 100
4.1.4. The Wnt pathway and human prostate cancer 102
4.1.5. KRAS and MAPK pathway signalling are implicated in human prostate cancer 102
4.2. CHAPTER AIMS **104**
4.3. RESULTS **104**
4.3.1. The probasin-Cre (PBCre4) transgene mediates DNA recombination of target alleles within the prostate epithelium 104
4.3.2. Beta-catenin and Pten single mutant mice display reduced survival, whereas Kras single mutant mice do not 106
4.3.3. Dominant, stablilised β-catenin results in progression from HGPIN to invasive adenocarcinoma associated with keratinised squamous metaplasia 108
4.3.4. Homozygous loss of Pten results in progression from HGPIN to invasive adenocarcinoma 109
4.3.5. Combinatorial mutations in β-catenin and/or Kras, with/without Pten loss, accelerates prostate tumourigenesis to lethal locally-advanced adenocarcinoma 109
4.3.6. Double and triple mutant mice model rapid disease progression from HGPIN to high-grade prostate cancer 112
4.3.7. The probasin-Cre transgene exhibits mosaic genetic deletion when transmitted maternally 114
4.3.8. Progression of prostate tumourigenesis in these mouse models correlates with Ki67 expression 117
4.3.9. Progression of prostate tumourigenesis in these mouse models correlates with AR expression 118
4.3.10. Progression of prostate tumourigenesis in these mouse models negatively correlates with p63 expression 119
4.3.11. Caspase-3 staining correlates with the number of pathways activated and disease progression, but not tumour grade 120
4.3.12. The pattern of expression of cytokeratins corroborates the expression of AR and p63 in each stage of prostate tumourigenesis 121
4.3.13. Beta-catenin single mutant mice display simultaneous activation of the Wnt, PI3K/Akt/mTOR, and MAPK pathways 123
4.3.14. PTEN single mutant mice display simultaneous activation of the Wnt, PI3K/Akt/mTOR, and MAPK pathways 125
4.3.15. Activated Wnt, PI3K/AKt/mTOR and Ras/MAPK pathways synergise to accelerate prostate cancer progression 129
4.4. CHAPTER CONCLUSION **134**
4.4.1. Dominant, stabilisation of β-catenin in murine prostate epithelium predisposes to adenocarcinoma and keratinising squamous metaplasia formation 134
4.4.2. Homozygous loss of PTEN predisposes mice to invasive adenocarcinoma of the prostate 138
4.4.3. Combinatorial activating mutations of β-catenin and/or Kras with/without Pten deletion cooperate to accelerate prostate tumourigenesis 141
4.4.4. AR correlates positively with prostate cancer aggressiveness 145
4.4.5. p63 correlates negatively with prostate cancer aggressiveness 146

4.4.6. Ki67 correlates positively with prostate cancer aggressiveness 146
4.4.7. Probasin-Cre demonstrates unwanted mosaic genetic deletion when inherited maternally 147
4.5. CHAPTER SUMMARY **147**

Chapter 5: Establishing a 3D primary tissue culture assay to explore self-renewal in murine adult prostate epithelial stem cells (PrSCs) **148**
5.1. INTRODUCTION **148**
5.1.1. Cancer stem cell theory 148
5.1.2. The origin of human cancer stem cells 149
5.1.3. In vitro and in vivo experiments have provided evidence for PrSC/CSCs 150
5.1.4. Why use mouse models to study the function of PrSC/CSCs? 152
5.1.5. FACS enables prospective identification of purported PrSCs/CSCs 152
5.1.6. Trop2 is a candidate PrSC marker 153
5.2. CHAPTER AIMS **154**
5.3. RESULTS **154**
5.3.1. Validation of proposed stem cell markers in autochthonous mouse models of human prostate cancer 154
5.3.1.1. CD44 155
5.3.1.2. FRMD4a 156
5.3.1.3. Notch1 157
5.3.1.4. Notch4 158
5.3.1.5. Trop2 158
5.3.2. Optimisation of PrSC 3D tissue culture assay 159
5.3.3. Prostate epithelial stem cells possess the antigenic profile $Lin^-CD49f^+Sca1^+Trop2^{Hi}$ 162
5.3.4. PrSC organoids demonstrate self-renewal in vitro 166
5.3.5. Assay optimisation 170
5.4. CHAPTER CONCLUSION **176**
5.4.1. Primitive prostate epithelial cells that possess the antigenic profile $Lin^-CD49f^+Sca1^+Trop2^{Hi}$ display stem cell characteristics in vitro 176
5.4.2. PrSC organoids are shown to be spherical and largely undifferentiated by IHC 176
5.4.3. Trop2 is co-expressed in both human and mouse prostate 177
5.4.4. Trop2 poses a therapeutic target for the treatment of prostate cancer 178
5.4.5. Novel primary tissue culture techniques are valuable but subject to criticism 178
5.4.6. Optimisation of this 3D primary tissue culture assay provides a baseline standard with which to compare the function of SC/CSCs in mouse models of tumourigenesis 180
5.4.7. The technical demands of this 3D primary cell culture assay may prevent its widespread adoption 180
5.5. CHAPTER SUMMARY **181**

Chapter 6: General Discussion **182**
Thesis Summary **188**
References **190**

Abstract

Many cell signalling pathways contribute to prostate cancer (PCa) initiation and survival, but the interplay between them remains poorly understood. In this thesis, conditional transgenic models were employed to investigate the impact of mutating the proto-oncogenes β-catenin, and Kras, and the tumour suppressor gene PTEN, alone and in combination within the murine prostate.

β-catenin and Pten single mutants display progression from PIN to invasive adenocarcinoma that appears similar to human Gleason pattern 3. Tumours demonstrate co-activation of the Wnt, PI3K/Akt/mTOR, and Ras/MAPK pathways. Kras single mutants develop PIN but do not progress to adenocarcinoma. Double and triple mutants develop more aggressive tumours comparable to Gleason pattern 4. Furthermore, double and triple mutants display upregulated Wnt, PI3K/Akt/mTOR and Ras/MAPK signalling. Expression of p63 negatively correlates with tumour grade, and moreover, progression from PIN to invasive adenocarcinoma is characterised by the synergistic elevation of AR and Ki67, which parallels human PCa.

Malignant transformation of a normal prostate epithelial stem cell (PrSC) gives rise to the cancer stem cell (CSC), which may contribute to castrate-resistant PCa. In this study a 3D primary tissue culture assay was optimised to allow maintenance and expansion of prostate cells that display stem-like characteristics *in vitro*.

PrSCs can be isolated by fluorescence activated cell sorting for the antigenic profile $Lin^{-}Sca1^{+}CD49f^{+}Trop^{Hi}$, and consistently form spherical structures in Matrigel. PrSCs can withstand multiple round of passage *in vitro*, and demonstrate the ability to maintain an undifferentiated state. PrSC spheres possess a basal phenotype, supporting a basal location of PrSCs in prostate epithelium.

In summary, these mouse models of PCa demonstrate cooperation between important cell signalling pathways in prostate tumourigenesis, and provide a platform for testing novel therapeutics. In addition, the successful isolation and cultivation of cells with stem-like attributes will allow their unique biological properties to be explored further, providing a baseline standard with which to compare the function of CSCs.

Posters and Presentations

1. **Welsh Urological Society** (19th April 2013)
   Development of an *in vitro* assay to enrich for prostate epithelial stem cells
   - ***awarded Huw Wiliiams memorial prize for best paper presentation***

2. **British Association of Urological Surgeons (BAUS) AGM** (18th June 2013)
   Investigating synergy between Wnt, PI3K and MAPK pathways in models of prostate tumourigenesis *in vivo* and *ex vivo*
   - ***nominated for podium presentation in "Leading Lights" session***

3. **European Cancer Stem Cell Research Institute Conference** (24th-26th July 2013)
   Development of a 3D primary tissue culture assay to explore self-renewal in prostate epithelial stem cells

4. **Welsh Urological Society** (8th November 2013)
   Exploring synergy between β-catenin, Pten and K-ras mutations in prostate cancer *in vivo* and *ex vivo*

5. **Society of Academic and Research Surgery (SARS)** (9th January 2014)
   Evaluating the roles of Wnt, PI3K, and MAPK pathways in prostate cancer
   - ***nominated for Patey prize to represent the BAUS Section of Academic Urology***

6. **BAUS Section of Academic Urology** (9th January 2014)
   Establishing a 3D primary tissue culture assay to explore self-renewal in murine adult prostate epithelial stem cells

7. **Royal Society of Medicine Urology section: Malcolm Coptcoat Spring short papers prize session** (6th March 2014)
   a) Optimisation of a primary tissue culture assay to purify adult murine prostate epithelial stem cells
   b) The Wnt, PI3K/Akt/mTOR, and MAPK pathways synergise to accelerate prostate tumourigenesis
   - ***awarded 1st prize for best poster presentation***

8. **American Urological Association AGM** (19th May 2014)
   Wnt, PI3K/Akt/mTOR, and MAPK signaling cooperate to accelerate prostate tumorigenesis in the mouse

Published Abstracts

COX, A.C., JEFFERIES, M.T., KYNASTON, H.G., CLARKE, A.R. **2014**. Evaluating the roles of Wnt, PI3k and MAPK pathways in prostate cancer. British Journal of Surgery, 101 (S4): 2 – 49

COX, A.C., JEFFERIES, M.T., KYNASTON, H.G., CLARKE, A.R. **2014**. Establishing a 3D primary tissue culture assay to explore self-renewal in murine adult prostate epithelial stem cells (PrSCs). British Journal of Surgery, 101 (S4): 56 – 68

COX, A.C., JEFFERIES, M.T., KYNASTON, H.G., CLARKE, A.R. **2014**. Wnt, PI3K/Akt/mTOR, and MAPK signaling cooperate to accelerate prostate tumorigenesis in the mouse. J Urol, Vol. 191, No. 4S, Supplement, e509

Abbreviations

ADT	Androgen deprivation therapy
AMH	Anti-Müllerian hormone
AP	Anterior lobe of mouse prostate
APC	Adenomatous polyposis coli
AR	Androgen receptor
ARR	Androgen responsive region
AZ	Anterior zone (of prostate)
BPH	Benign prostatic hyperplasia
BrDU	Bromodeoxyuridine
CK	Cytokeratin
Cre	Cre recombinase
CRPC	Castration-resistant prostate cancer
CSAP	Cryosurgical ablation of the prostate
CSC	Cancer stem cell
CT	Computerised topography
CZ	Central zone (of prostate)
DLP	Dorsolateral lobes of mouse prostate
EBRT	External beam radiotherapy
EPE	Extra-prostatic extension
FACS	Fluorescence-activated cell sorting
HGPIN	High-grade prostate intraepithelial neoplasia
HIFU	High-intensity focused ultrasound
IHC	Immunohistochemistry
LADY	LPB promoter driving the large-T antigen
LAPC	Locally-advanced prostate cancer
LGPIN	Low grade PIN
LN	Lymph node

LoxP	Locus of phage crossing over
LPB	Large probasin promoter
MA	Meta-analysis
MAPK	Mitogen-activated protein kinase
MIS	Müllerian Inhibitory Substance
mPCa	Metastatic prostate cancer
MRI	Magnetic resonance imaging
NE	Neuroendocrine
NOD/SCID	Non-obese/severe combined immunodeficiency
PAP	Prostate acid phosphatase
PB	Probasin
PCa	Prostate cancer
PCR	Polymerase chain reaction
PIN	Prostate intraepithelial neoplasia
PrSC	Prostate epithelial stem cell
PSA	Prostate specific antigen
PZ	Peripheral zone (of prostate)
RCT	Randomised controlled trial
RP/RRP	Radical (retropubic) prostatectomy
SC	Stem cell
SR	Systematic review
TAC	Transit-amplifying cell
TNM	Tumour node metastasis staging
TRAMP	Transgenic adenocarcinoma of the mouse prostate
TURP	Transurethral resection of prostate
TZ	Transitional zone (of prostate)
UGS	Urogenital sinus
VP	Ventral lobe of mouse prostate

Chapter 1: General Introduction

1.1 THE PROSTATE GLAND

The prostate gland is largely an androgen-sensitive exocrine gland of the male mammalian reproductive system. The following section focusses on the function, anatomy, embryology, and histopathology of the prostate in both the human and mouse. In addition, the similarities and disparities between human and mouse prostate will be described with the aims of emphasising the pros and cons of mouse models in studying prostate tumourigenesis, and the evidence for stem cells and cancer stem cells in both species.

1.1.1 Prostate gland function

The prostate gland, one of the male accessory glands, is exclusive to mammals. Other male mammalian accessory glands can include the vesicular glands, seminal vesicles, ampullary glands, bulbourethral glands, and preputial glands. The products of these glands serve to nourish and activate spermatozoa, to clear the urethral tract prior to ejaculation, to serve as the vehicle of transport of the spermatozoa in the female tract, and to plug the female tract after placement of spermatozoa to aid fertilisation. While accessory glands are usually described as tubulo-alveolar, they vary in their number, organisation and in their distribution in different species.

The main function of the prostate is secretory; it contributes around 30% of the ejaculate (Fair and Cordonnier, 1978). Due to its surrounding muscular stroma, the prostate forces emission of prostatic fluid to mix with seminal fluid during ejaculation. Prostatic secretions contain various important molecules which all play important roles in reproductive homeostasis. Many of these important substances are listed in table 1.

	Constituent name	Function	Reference
Proteins	Prostate acid phosphatase (PAP) and Prostate specific antigen (PSA)	Semen liquefaction	Fair and Cordonnier (1978)
	Leucine aminopeptidase	Antigen presentation, processing of spent bioactive peptides (oxytocin, vasopressin, enkephalins), and vesicle trafficking to the plasma membrane	Matsui et al. (2006)
	Diamine oxidase	Degrades polyamines spermine, spermidine, putrescine and affects motility	Le Calve et al. (1995)
	B-Glucuronidase	Catalyses carbohydrates for sperm nutrition, roles in sperm acrosome reaction and maturation of spermatozoa	Hall and Killian (1987), Kareskoski and Katila (2008)
	Plasminogen activator	Promotes fibrinolysis and sperm motility	Maier et al. (1991)
	Complement (C3 and C4)	Sperm agglutination	Azim et al. (1978)
	Transferrin and transferritin	Immunological role; binds iron thus impeding bacterial survival	Barthelemy et al. (1988)
	Growth factors	Sperm motility	Iyibozkurt et al. (2009)
Non-proteins	Citrate	Essential for sperm mitochondrial function, a buffer	Cappello et al. (2012)
	Polyamines (spermine, spermidine, putrescine)	Regulate cell growth and gene expression and promote sperm motility	Rubinstein and Breitbart (1990), Lefevre et al. (2011)
	Zinc	Stabilises chromatin in sperm	Canale et al. (1986)
	Myoinositol	Regulates seminal plasma osmolarity and volume, sperm motility, capacitation, and acrosome reaction	Condorelli et al. (2012)
	Cholesterol	Sperm capacitation	Osheroff et al. (1999)

Table 1: Some of the important constituents of mammalian prostatic secretions and their effects

1.1.2 Embryology and prostate gland development

In man, the development of the male and female genitourinary tract is identical until 7 weeks gestation. A male foetus develops in the presence of a Y-chromosome which encodes the SRY (sex-determining region Y) protein. The SRY protein enables testicular differentiation and the production of androgens including testosterone. The indifferent gonad comprises two zones: the medulla in males differentiates into the testis, whereas the cortex involutes, giving rise to vestigial remnants. In addition to the SRY protein and androgens a third factor is required for male development, anti-Müllerian hormone (AMH), also known as Müllerian Inhibitory Substance (MIS) (Munsterberg and Lovell-Badge, 1991). AMH/MIS prevents female genital ductal differentiation causing the Müllerian (paramesonephric) duct to degenerate which forms

the prostatic utricle. At approximately week 8 the fetal testis produces testosterone and as a consequence, the human prostate begins to develop at about the 10th week of gestation. As a result, the initial outgrowths of the prostatic buds from the urogenital sinus (UGS) occur in response to the binding of 5α-dihydrotesterone to androgen receptors localised in the surrounding mesenchymal tissue (Shannon and Cunha, 1983, Lasnitzki et al., 1989, Takeda et al., 1985, Takeda and Chang, 1991). These prostatic buds begin as solid cords of epithelial cells that elongate and undergo extensive branching morphogenesis during the latter stages of fetal growth to develop primitive lumens (Timms, 2008). During weeks 13 to 15, serum testosterone elevates and remains high until week 25, which in turn induces epithelial differentiation. At this point, the 3 important epithelial populations are distinct – luminal, basal and neuroendocrine cells (Timms, 2008). At week 25 testosterone level diminishes and the gland remains in a quiescent state until puberty. During the postnatal period and under the influence of androgens, the ducts form true patent lumens, and the epithelial cells lining the acini fully differentiate to synthesise a variety of secretory products (as listed in table 1 earlier). During puberty, serum testosterone increases to induce epithelial proliferation and the formation of a mature, adult prostate. Hypogonadism of ageing can occur with increasing age beyond 45-50 years, which in turn leads to prostate gland involution and atrophy.

Development of the murine prostate begins at around embryonal day 10 (E10) when the UGS is evident at dissection (Staack et al., 2003). The UGS is an endodermal tube derived from hindgut, which is clearly demarcated by E13–14 (Staack et al., 2003). At this time the Leydig cells within the fetal testes differentiate, synthesise and secrete testosterone (Pointis et al., 1980). Testosterone and its metabolites stimulate the Wolffian ducts and mesonephric tubules to form the epididymi, vasa deferentia, seminal vesicles, and efferent ducts. At approximately E14–15, and similar to events in the human at 7-8 weeks gestation, the Sertoli cells of the murine fetal testes initiate production of AMH/MIS, which elicits destruction of the Müllerian (paramesonephric) ducts in males (Kuroda et al., 1990). The prostatic buds emerge from the urogenital sinus epithelium at approximately E17 and grow and branch within the surrounding urogenital sinus mesenchyme, forming their characteristic pattern which reflects the eventual lobar structure of the gland (Cunha et al., 1987, Timms et al., 1994). Branching morphogenesis continues postnatally and is almost complete by 2-3 weeks of age (Sugimura et al., 1986a).

1.1.3 Anatomy of the human prostate

The human prostate lies inferior to the urinary bladder within the pelvis and both are separated from the rectum posteriorly by Denonvilliers' fascia, a variable sheet of fused fibromuscular layers that extends upward to cover the seminal vesicles at the superior, posterior aspect of the prostate. The prostate is conical in shape and its base is intimately related to the bladder neck superiorly while the apex is directed downward and is in contact with the superior part of the urogenital diaphragm. The human prostate is surrounded by a prominent fibromuscular stroma, which is vastly more abundant than in the rodent, extending beyond the outer perimeter of the gland to form a distinct capsule separating the prostate from periprostatic fat. The capsule is best defined histologically in the posterior and lateral portions of the human prostate. The adult prostate is separated into fused zones that are anatomically distinct, have characteristic histological features, and importantly, have specific predisposition to benign or malignant neoplastic change. Although lobes are recognisable in the developing human prostate, the lobar classification is more frequently used for anatomical or surgical description (see table 2).

Prostate lobe	Corresponding prostate zone
Anterior (isthmus)	Mainly transitional zone
Posterior	Part of the peripheral zone
Median (or middle)	The central and transition zones
Lateral	Spans all zones

Table 2: Each anatomical prostate lobe corresponds to part(s) of a pathological zone. The terminology relating to prostate lobar anatomy is commonly used in gross anatomy or for surgical description. Prostate lobes do not precisely correspond to individual prostate zones; indeed the lateral lobes (readily visible during transurethral surgery) span all zones.

The human prostate is composed of the anterior fibromuscular stroma, which is devoid of glandular components, the periurethral transitional zone (TZ), the peripheral zone (PZ), and the central zone (CZ) (McNeal, 1981a, McNeal, 1981b). The CZ surrounds the ejaculatory ducts and comprises the portion of the prostate from where the ejaculatory ducts enter the urethra, near the prostatic utricle at the verumontanum, to the base. The TZ is located interiorly between the urethra and the surrounding PZ and CZ while the PZ is found on the posterolateral aspects of the prostate. The distinction between these anatomical zones is shown in figure 1.

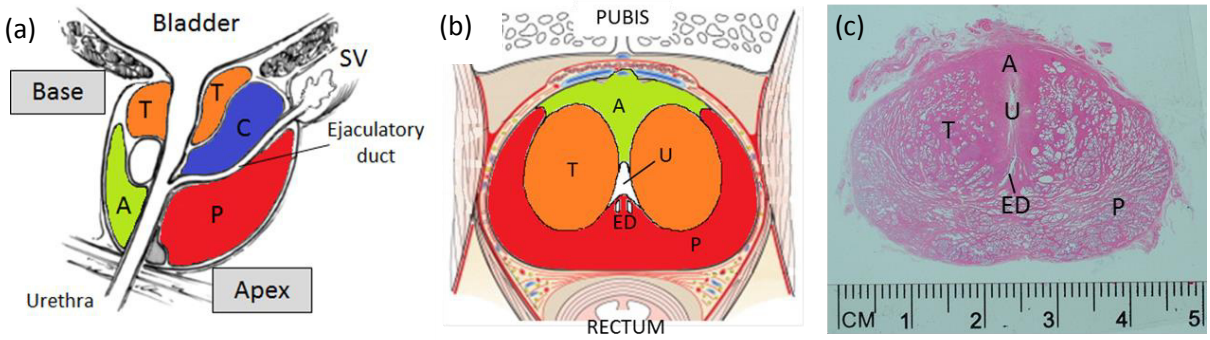

Figure 1: Anatomy of the normal human prostate. (a) Illustration of a sagittal section through the prostate demonstrating the orientation of the base (most cranial aspect) and the apex (most caudal aspect). Adapted from McNeal (1969) in Valkenburg and Williams (2011) (b) Schematic representation of the prostate in axial section through the base of the prostate highlighting its intimate relation to the pubis (anteriorly) and rectum (posteriorly). Adapted from Walz et al. (2009) (c) An H&E section through the base of a prostate removed following an open radical retropubic prostatectomy for localised prostate cancer. The striking demarcation delineating the transition (T) and peripheral (P) zones are due the patient's young age; in older men these planes would be more indistinct. *U*, urethra; *ED*, ejaculatory duct; *A*, anterior fibromuscular stroma. H&E slide (c) courtesy of Dr David Griffiths, Consultant Histopathologist, University Hospital of Wales, Cardiff.

1.1.4 Histology of the normal human prostate

The CZ within human prostate consists of large complex glands demonstrating greatly irregular luminal contours, epithelial tufting, papillary formations, and with frequent Roman arches or cribriform patterning that lacks cytological atypia (Shappell et al., 2004). Secretory cells in the CZ are irregularly arranged with large nuclei at multiple levels to adjacent cells and visible basal cells. Acini in the CZ are separated by fewer bands of compact smooth muscle fibres than the PZ and TZ.

Benign glands of the PZ are larger and have a tufted or undulating luminal border intermediate between that of the frequently-folded CZ and rounded TZ glands. Secretory cells of the PZ are columnar with a regular luminal border and smaller, more uniform, flattened basal nuclei. The PZ fibromuscular stroma is abundant with loosely woven, randomly arranged muscle fibres separated by irregular spaces and numerous collagen fibres.

The TZ acini are distributed uniformly and are more rounded in shape with compactly arranged smooth muscle and collagen fibres in the stroma surrounding them. Secretory cells of the TZ are columnar with regular small basal nuclei, whereas flattened basal cells with slender dark nuclei lie parallel to the basement membrane.

Representative examples of normal human prostate, highlighting the zonal differences, are demonstrated in figure 2.

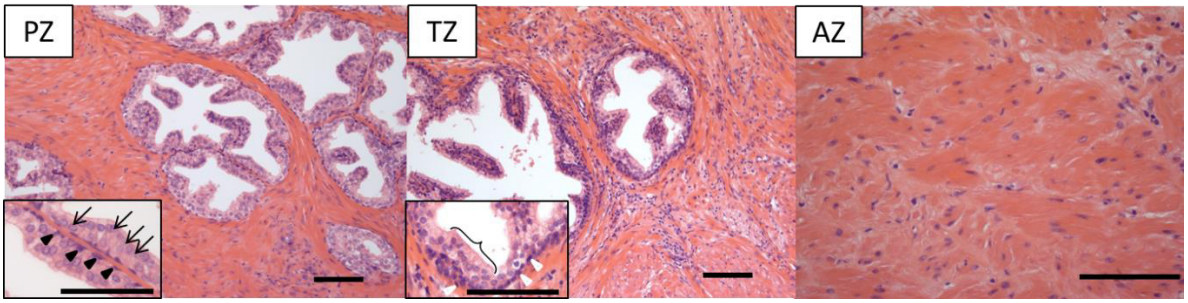

Figure 2: Histology of normal human prostate. The above photographs were taken from the RRP specimen in figure 1(c) above, thus the central zone (CZ) is not shown. Peripheral zone (PZ): acini have irregular tufted luminal epithelium with irregularly arranged multilevel large round nuclei (black arrows), whereas the regular location of basal cells can be clearly seen here (black arrowheads). The PZ is intermediate in its appearance between the CZ (not shown) and TZ. Transitional zone (TZ): acini are more rounded; the luminal secretory border consists of orderly columnar cells (braced bracket) with regular small basal nuclei, and white arrowheads highlight the flatter dark nuclei of basal cells. The anterior zone (AZ) is devoid of epithelium; instead it is comprised of fibromuscular stroma. H&E slides courtesy of Dr David Griffiths, Consultant Histopathologist, University Hospital of Wales, Cardiff.

1.1.5 Histopathology of the human prostate and the zonal origin of prostate cancer

The TZ is the exclusive site of benign prostatic hyperplasia (BPH) in the human and is associated with ageing. BPH is seen in 80-90% of radical prostatectomy (RP) specimens but less than 20% of clinically significant PCas originate here (McNeal, 1992). TZ tumours often have a characteristic histological appearance, usually composed of well differentiated tumours. They are felt to arise as the result of precursor lesions called atypical adenomatous hyperplasia (or adenosis), that are distinct from prostatic intraepithelial neoplasia (PIN), including high-grade PIN (HGPIN), seen in the PZ. In contrast to its common occurrence in the PZ, PIN/HGPIN is rarely seen in the TZ.

The PZ contains the majority of glandular tissue in the normal human prostate and is the most frequent site of PCa origin (McNeal et al., 1988). Conversely, the CZ is rarely the site of origin for PCa, although it can be involved through direct invasion from a PZ tumour. The fact that the PZ is located at the posterolateral aspects of the prostate, explains anatomically why digital rectal examination is mandatory in the assessment of men with suspected PCa. DRE allows assessment of both prostate and tumour volumes, and can help differentiate localised from locally-advanced tumours to determine suitability for surgery based on the likelihood of a curative tumour excision. The PZ is the exclusive site of PIN/HGPIN in the human prostate (De Marzo et al., 2003). Epithelial hyperplasia analogous to that seen in TZ BPH does not occur in the PZ, instead epithelial proliferation occurs within the confines of pre-existing normal gland profiles, and is deemed low- or high-grade PIN based on nuclear morphology (Bostwick et al., 1996).

1.1.6 Cellular organisation of human prostate epithelium

Three phenotypically distinct cell types are readily identifiable within a two-layered epithelium: luminal secretory cells, basal cells, and rare, scattered neuroendocrine cells (see figure 3). The presence of a fourth population, prostate epithelial stem cells, is discussed in detail later (see section 1.4.1).

The normal, adult human prostate demonstrates sophisticated cellular organisation. Terminally differentiated luminal cells constitute the majority of normal and malignant prostate and they are reliant on androgens for their survival and thus express high levels of androgen receptor (AR) (Bonkhoff and Remberger, 1993), CD57 (Liu et al., 1997), PSA and PAP. Paradoxically the basal layer, which is independent of androgens and thus expresses low levels of AR, is largely undifferentiated and comprises approximately 10% of prostate epithelial cells. The basal cells are closely adherent to the basement membrane and lack secretory activity. They express CD44 (Liu et al., 1997), Bcl-2 (Bonkhoff et al., 1998), telomerase (Paradis et al., 1999) and p63 (a p53 homolog) (Signoretti et al., 2000). Basal and luminal cells can be further discriminated by their expression of specific cytokeratins; basal cells express cytokeratins 5 (CK 5) and 14, whereas luminal cells express CK 8 and 18 (Sherwood et al., 1991). Neuroendocrine cells (NE) are relatively few (1% in humans, <0.3% in mice) terminally differentiated, androgen-insensitive cells scattered throughout the basal epithelial compartment and they readily express synaptophysin and chromogranin A (Shappell et al., 2004). Despite the fact that cells with NE-

like expression are routinely found in prostate cancer (PCa), their precise function is unknown. However, evidence suggests that NE cells are a post-mitotic cell type derived from luminal cells (Bonkhoff et al., 1991, Bonkhoff et al., 1995).

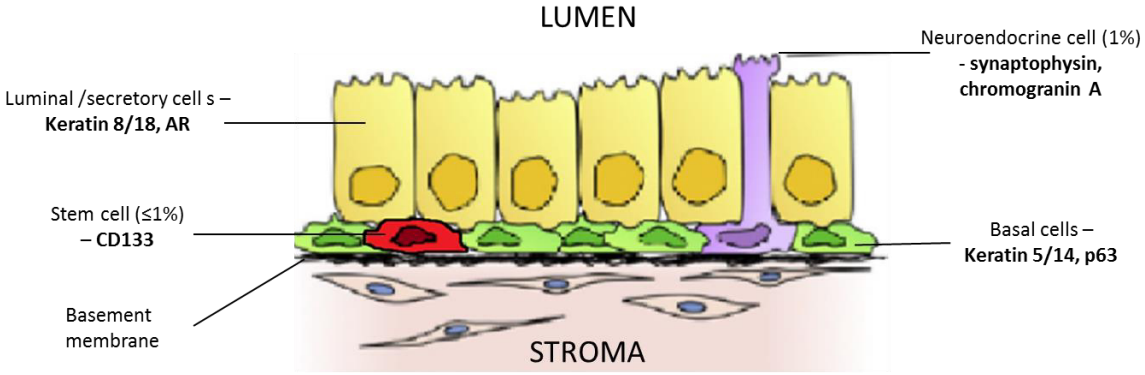

Figure 3: Schematic representation of human prostate epithelial morphology. The terminally differentiated columnar luminal cells secrete protein-rich fluid into the lumen of prostate acini and are intimately related to relatively undifferentiated basal cells, seen here uniformly adjacent to the basement membrane. Neuroendocrine cells are distinguishable from basal cells and represent approximately 1% of the cellular population. Stem cells represent ≤1% of the total cell population (approximately 1% of basal cells). Biomarkers to identify each population are shown here **in bold**. Adapted from Oldridge et al. (2012).

Without the supporting stromal microenvironment, the prostate epithelial compartment is reportedly ill-equipped to function independently. Thus so-called "mesenchymal-epithelial crosstalk" (Cunha et al., 2004), is vital for epithelial cell development *in utero (Hayward and Cunha, 2000)*, for sustaining growth and cell maintenance, and epithelial cell differentiation (Hall et al., 2002, Berry et al., 2008).

1.2 MOUSE PROSTATE ANATOMY

In stark contrast to the human, mouse prostate is divided into separate lobes; namely the anterior prostate (AP), which is intimately related to the concave aspect of the seminal vesicles along its entire length, the ventral lobes, and the dorsal and lateral lobes, often collectively called the dorsolateral lobes (see figure 4).

(a)

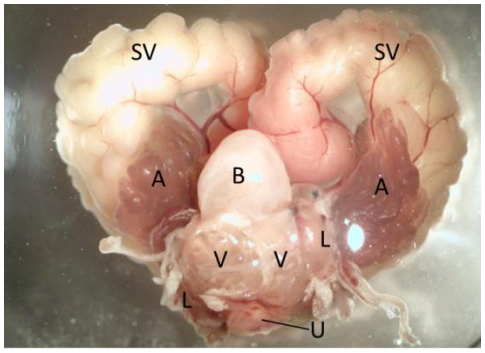

(b)

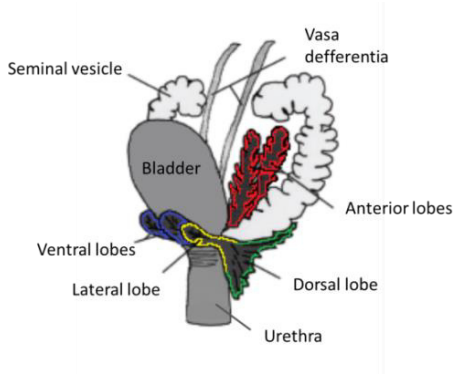

Figure 4: Anatomy of the mouse genitourinary tract. (a) Photograph of the genitourinary tract from a wild-type mouse, aged 100 days, dissected en bloc. *A*, anterior lobe; *B*, bladder; *L*, lateral lobe; *SV*, seminal vesicles; *U*, urethra (cut); *V*, ventral lobe; dorsal lobe hidden from view posteriorly. (b) Cartoon of mouse genitourinary tract with each lobe highlighted in colour, adapted from Valkenburg and Williams (2011).

Individual lobes are invested by a thin mesothelial-lined capsule, appreciable microscopically, that separates one lobe from another. Mouse prostate lobes are composed of a series of blind-ending branching ducts or tubules, which in turn are surrounded by a thin fibromuscular tunica of smooth muscle cells interspersed with eosinophilic collagen. Glandular cells are separated from the capsule by loose fibroadipose connective tissue where blood vessels and nerves are found. The abundant dense fibromuscular stroma present in human prostate is not comparable to the mouse; here it is less complex and sparse (Tsujimura et al., 2002, Shappell et al., 2004). Due to these fundamental differences in the anatomical organisation of the prostate between the human and mouse, mouse models may not be adequate or suited to address the staging issues related to extra-prostatic extension, and thus progression to T3 disease, in human PCa (see section 1.3.2).

Each lobe of the mouse prostate has a distinctive histological appearance, and these differences can be appreciated in figure 5.

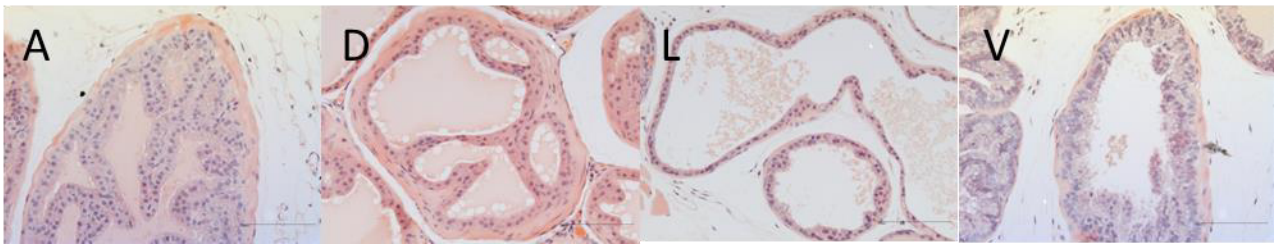

(a)

(b)

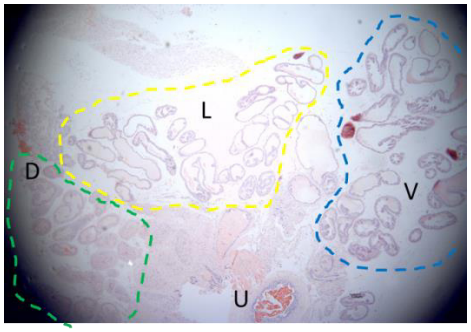

Figure 5: Normal mouse prostate. (a) Histological appearance of 10% formalin-fixed, paraffin-embedded sections stained with haematoxylin and eosin from all four lobes of wild-type murine prostate aged 100 days taken at 40x magnification, scale bars represent 100µm. (b) Spatial relationship of the lobar anatomy (at 4x magnification) in the axial/transverse plane through the urethra, at or near the level of the SV junction (anterior lobe not shown). *A*, anterior lobe; *D*, dorsal lobe; *L*, lateral lobe; *U*, urethra; *V*, ventral lobe.

The mouse DP is lined by simple columnar and occasionally stratified, tufted epithelium. The degree of infolding is intermediate between the AP and the flatter luminal borders of the LP and VP. The secretory cells of the DP have central to basally located small uniform nuclei containing inconspicuous or small nucleoli. Gland lumens contain homogenous eosinophilic secretions. The LP has flatter luminal edges, with only sparse infoldings, with the abundant luminal space containing more particulate eosinophilic secretions. The epithelium is cuboidal to low columnar, with small uniform basally located nuclei.

Histologically the mouse AP normally demonstrates a more papillary and cribriform growth pattern than the other lobes, with cuboidal to columnar epithelial cells containing typically central nuclei with inconspicuous to small nucleoli, and eosinophilic granular cytoplasm. The gland lumens contain abundant slightly eosinophilic secretions.

The mouse VP has flatter luminal edges and only focal epithelial tufting or in-folding. The abundant luminal spaces contain homogenous pale serous secretions. The nuclei are small, uniform, typically basally located, and have inconspicuous to small nucleoli.

The mouse dorso-lateral prostate (DLP) has, for around 50 years, been reported as being most homologous to the human PZ, perhaps because the majority of adenocarcinomas in genetically-engineered mice originated here (Price, 1963, Roy-Burman et al., 2004). More recently this has been disputed (Shappell et al., 2004). Each developing lobe in the embryo remains recognisable in the postnatal and adult mouse prostate, as the lobes described previously. Even though the developing lobes are recognisable in the human embryo, they are not readily identifiable in the adult (Price, 1963). There is therefore no existing supporting evidence for a direct relationship between the mouse prostate lobes and the specific zones in the human prostate (Shappell et al., 2004).

1.2.1 Cellular organisation of mouse prostate epithelium

The glands of each mouse prostate lobe appear to have normal cell populations homologous to the human prostate. However, in contrast to human prostate, the murine prostate structure is much simpler and consists of a luminal-like epithelium in direct contact with the basement membrane, a discontinuous layer of fewer basal cells, and a minor population of NE (see figure 6). The location of murine prostate stem cells is felt to be within the basal subpopulation.

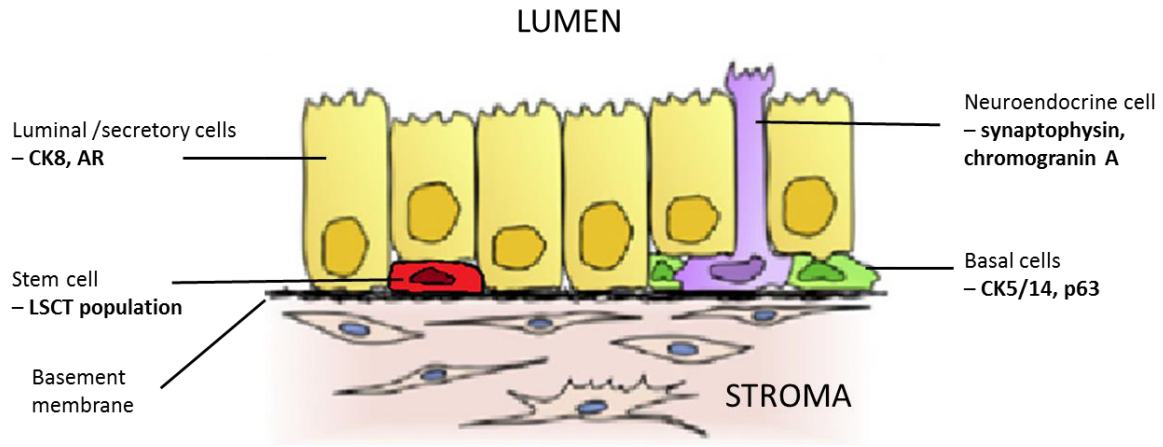

Figure 6: Schematic representation of murine prostate epithelial morphology. In contrast to the human, mouse prostate epithelium contains a discontinuous layer of basal cells. Neuroendocrine cells represent approximately 0.3% of the cellular population. Stem cells are estimated to represent ≤1% of the total cell population. Biomarkers expressed by each population are shown here **in bold**. *LSCT*; when murine prostate epithelia are FACS-sorted, the $Lin^{-}Sca\text{-}1^{+}CD49f^{hi}Trop\text{-}2^{hi}$ fraction enriches for a population with stem-like properties (see later). Adapted from Oldridge et al. (2012).

Limited markers exist for secretory cell differentiation in the mouse prostate but as in humans, CK8 has been shown to stain luminal cells in normal mouse prostate (Lukacs et al., 2010). The basal population in histologically normal murine prostates is readily identified by staining with CK5 (DiGiovanni et al., 2000, Lukacs et al., 2010) and also CK14 (Kim et al., 2002). Immunostaining for chromogranin (Garabedian et al., 1998) and/or synaptophysin (Lukacs et al., 2010) demonstrates a minor population of neuroendocrine cells in the normal mouse prostate totalling approximately 0.3% (Bostwick et al., 1996).

1.2.2 Why use a mouse model to study prostate tumourigenesis?

The mouse and human genomes are approximately 95% identical, and share many structurally similar genes and genomic alterations implicated in prostate cancer (Maser et al., 2007). In addition, technology exists to allow prostate-specific genetic modification of the mouse genome, such as the Cre-loxP system (see section 1.6.4). The small size and short gestation time of mice, along with their relative affordability, means that large populations to study lesions of interest can be generated quickly. The prostate of both species are androgen sensitive and both have glands with three distinct epithelial cell populations and similar functions. Both species also have male accessory organs that develop from the Wolffian ducts and the urogenital sinuses. Even though some aspects of prostate anatomy and histology are homologous between the two species, there are also, as already described, marked dissimilarities.

1.2.3 The limitations of using mouse models to study prostate cancer

No single mouse model has fully recapitulated the molecular and pathological events that constitute human prostate cancer through its stages of development and progression. In particular no model describes spontaneous development of bony metastases, which is a consistent feature of advanced PCa in men (Mundy, 2002) and the most significant cause of morbidity (Singh and Figg, 2005). Cancers, and therefore metastases, in mice tend to be of mesenchymal origin whereas metastases in humans generally originate from epithelial cells (DePinho, 2000). One further consideration is that in mice, as in the human disease, tumourigenesis and the time to development of the prostate lesion of interest exhibits variability despite established transgenic technologies. Genetic background in addition to environmental factors could conceivably have important effects on lesion development and/or

progression in genetically modified models of prostate cancer. In one study using inbred mice (Gingrich et al., 1996), despite each mouse beginning with a similar genetic background, stochastic variability in the timing of tumour development and progression was observed. Primary pathologies ranged from hyperplasia to adenocarcinoma that arose within a 10 – 24 week period with metastases occurring by 28 weeks in either the lymph nodes or lungs.

1.3 PROSTATE CANCER

Prostate cancer (PCa) is acknowledged as one of the most important medical problems facing the male population worldwide. Indeed, it is the commonest cancer diagnosed in men, outnumbering both lung and colorectal cancer. This equates to approximately 25% of newly diagnosed UK male cancers (CRUK, 2012) and 23% in Wales (Welsh Cancer Intelligence and Surveillance Unit, 2009). In 2009 over 40,000 British men were diagnosed with PCa, with around 2,000 of these in Wales (WCISU, 2009). It is the 2nd leading cause of cancer death worldwide after lung cancer, accounting for approximately 200,000 deaths per year (CRUK, 2012) with 546 deaths per year on average in Wales (WCISU, 2009).

The PCa incidence rate has increased in recent years, whereby it crudely affects approximately 135 per 100,000 UK-wide (CRUK, 2012). This can be further appreciated in Wales where it affects around 162 per 100,000 men, up from 90 per 100,000 in 1995 (WCISU, 2009). PCa shares a strong association with age therefore it is of greater concern in developed countries where, like the UK and mainland Europe, there is an ageing population with improving health. In the UK, between 2007 and 2009, roughly 75% of PCa cases were diagnosed in men aged 65 years and over (see figure 7).

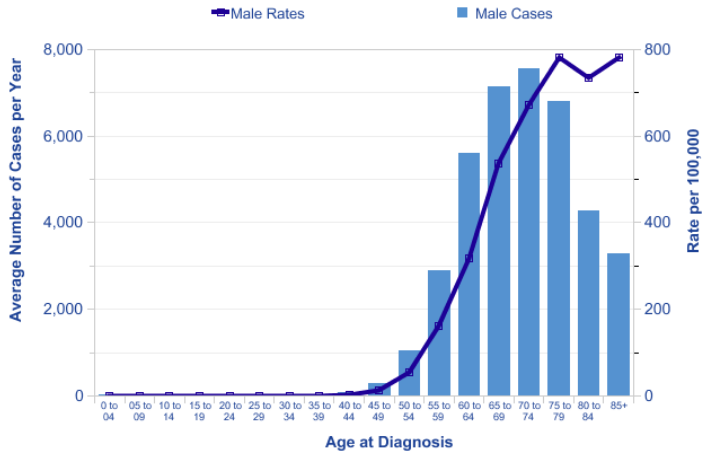

Figure 7: Prostate cancer incidence as a function of age. Age-specific incidence rates increase sharply from around age 50, peaking in men aged 75 and over (CRUK, 2012).

Similarly substantial increases in incidence have been reported in recent times for many countries around the world. The prostate cancer incidence trend for the UK is shown in Figure 8.

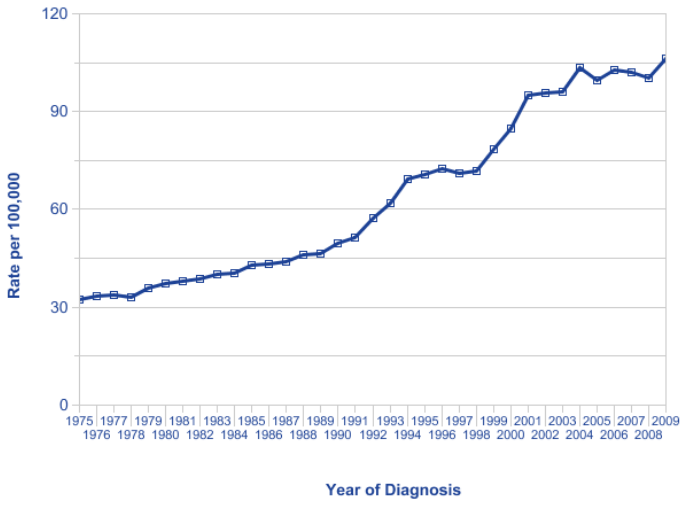

Figure 8: Prostate cancer age-standardised incidence trend for the UK. This data illustrates how the overall the incidence rate increased by three times between 1975 and 2009; almost 50% between 1993 and 2005 but remained relatively stable since then.

Incidence trends for younger men have continued to rise year on year since the mid-1970s (see Figure 9). The largest increase has been in men aged 45-54, with the European age-

standardised rate having increased by eight times between 1975-1977 and 2007-2009. For men aged 85 and over, there has been a decrease in the incidence rate since the mid-1990s, and the rate for men aged 75-84 has also decreased slightly since the early 2000s. Hence increased incidence is not applicable to the elderly group, yet the death rate is rising in this population. This trend is noted in other countries and is probably an indication of improving health in elderly men. As general health improves, ones chance of dying ***of*** PCa, rather than ***with*** PCa, increases considerably.

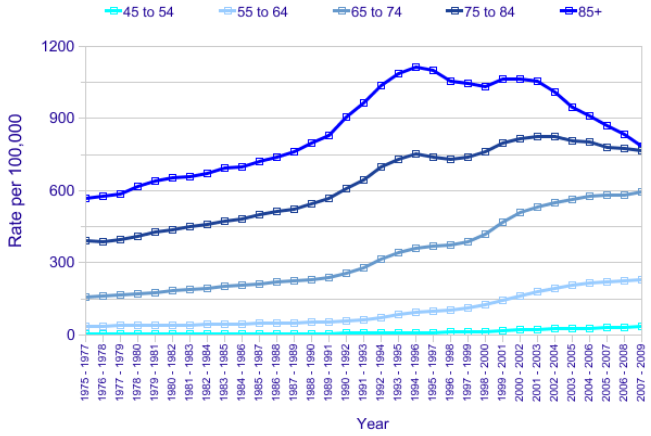

Figure 9: Prostate cancer incidence trends for the UK by age group. For men <75 years, incidence trends continue upwards to 2009. For men aged 75-84 and >85 the incidence has decreased and plateaued respectively, after 1996 (CRUK, 2012).

Analysis of incidence trends have concluded that much of the apparent increase in PCa incidence is a result of improvements in detection; before 1989 as a consequence of increasing rates of transurethral resection of the prostate (TURP), and afterwards through the rising use of PSA testing. This is due to greater awareness of prostate cancer through media publicity and focused screening of at-risk individuals despite the lack of a national screening programme such as UK screening for breast or cervical cancer. Similarly the USA has reported that increased detection rates through PSA testing has been a major factor (Potosky et al., 1995), to such an extent that approximately 75% of US men over 50 years have had a PSA test (Sirovich et al., 2003). Published estimates for the level of PSA screening in Europe vary but are much lower, estimated at 10-20% (Bray et al., 2010). The future burden on healthcare services that prostate

cancer poses can be appreciated given the current lifetime risk of developing prostate cancer is estimated to be 1 in 9 UK-wide, having increased from 1 in 14 in 2004 (CRUK, 2012).

1.3.1 Making a diagnosis of prostate cancer – Gleason score

In 1966, American pathologist Donald Gleason created a unique grading system for PCa based on tumour morphology. Specifically it classified the degree of loss of the normal glandular tissue architecture (i.e. shape, size and differentiation of the glands) at low power. (Mellinger et al., 1967, Gleason and Mellinger, 1974). Rather than assign the worst grade as the overall tumour grade, each tumour was defined as the sum of the two most common patterns and reported as the Gleason score. It has since been revised (Epstein et al., 2005) because its interpretation and application had evolved significantly following its inception. However it remains, over 40 years on, one of the most powerful prognostic factors in PCa (Epstein, 2010). The Gleason score is allocated to a prostate needle biopsy or a radical prostatectomy specimen by a consultant histopathologist. It is estimated that upgrading is seen in approximately 1/3 of prostatectomy specimens and downgrading is evident in 5%, when compared to the pre-operative needle biopsy Gleason score, demonstrating some of the limitations of applying a Gleason score to needle biopsy samples where tumour heterogeneity may exist.

The classic Gleason scoring diagram (see figure 10) shows five basic tissue patterns that are referred to as tumor "grades", each being represented by a number from 1 to 5. Grade 1 represented well differentiated adenocarcinoma with the best prognosis, whereas grade 5 denoted poorly differentiated or anaplastic adenocarcinomas and thereby the worst grade. Originally a score of between 2 and 10 was obtained from adding the first and second most predominant patterns i.e. the primary pattern comprised >50% and the secondary pattern <50% but >5%.

Currently Gleason grades 1 and 2 are largely obsolete highlighting a paradigm shift in prostate cancer reporting that led to the revised Gleason scoring system in use today (Epstein et al., 2005). Low grade cancers (scores 2-4) are rarely seen on needle biopsy because they are predominantly located anteriorly in the transition zone and tend to be clinically insignificant. At TURP for clinical BPH, which samples the transition zone, Gleason score 2–4 cancer may still be diagnosed but it is uncommon. Due to the success of α-adrenergic receptor antagonists for

lower urinary tract symptoms TURP in itself is uncommon, further contributing to the rarity of a Gleason score 2–4 diagnosis. For practical purposes this change has translated into the virtual disappearance of Gleason score 2–4 on needle biopsy in contemporary practice. In 1991, 24% of pathologists made a diagnosis of Gleason score 2–4 on biopsy, which decreased to 2.4% in 2001 (Ghani et al., 2005).

In current practice Gleason 3+3=6 is the score with best prognosis. The original Gleason system also predated the use of immunohistochemistry; it is likely that with immunostaining for basal cells, many of the original 1+1=2 adenocarcinomas of the prostate would today be regarded as adenosis, a benign mimic of prostate cancer (Epstein et al., 2005). Similarly many of the cases historically diagnosed as cribriform Gleason pattern 3 adenocarcinoma would now be called cribriform high-grade prostatic intraepithelial neoplasia (PIN) if labelled with basal cell markers (Amin et al., 1994).

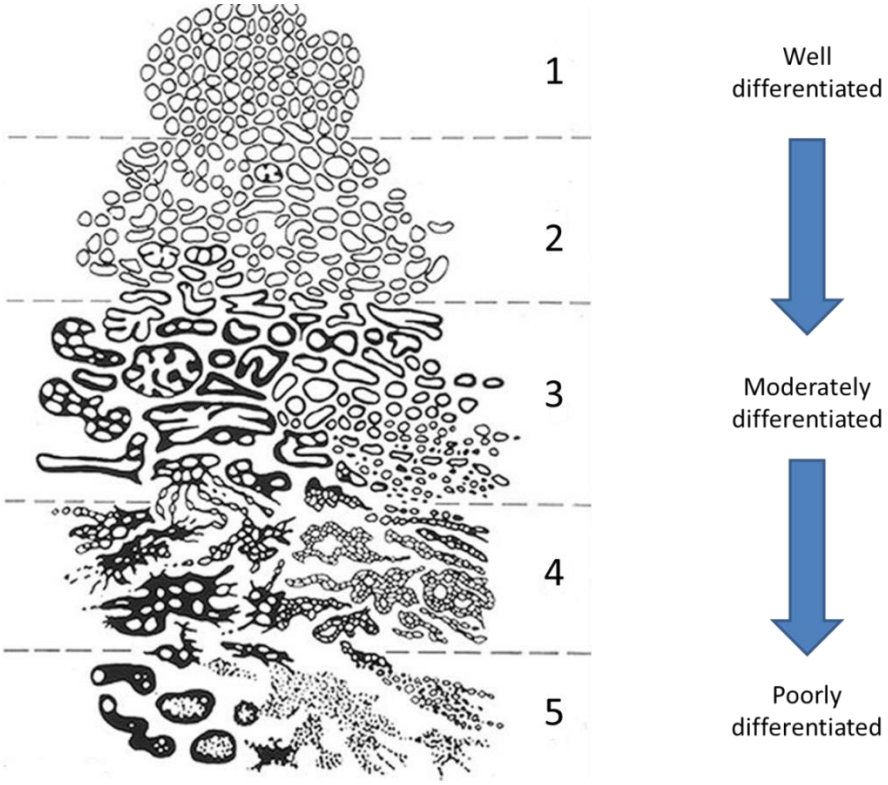

Figure 10: The original Gleason scoring system is outdated. In Gleason's era there was no screening for prostate cancer other than digital rectal examination; serum prostate specific antigen had yet to be discovered. Typically limited numbers of needle biopsies were taken from an area of palpable disease only. Consequently the grading of prostate cancer in multiple cores from different sites of the prostate and/or grading multifocal tumour in a prostatectomy specimen was unimportant. Adapted from Epstein (2010).

A number of other important amendments have been made since the Gleason grading system was revised (see figure 11). Secondary patterns of *low* grade (i.e. pattern 3) are not reported if representing less than 5% of tumour volume and a higher grade pattern is present. Conversely, secondary patterns of *higher* grade disease should always be reported, even if less than 5% in total. There has also specific guidance for needle biopsies, whereby the primary pattern and the highest grade should be recorded; secondary pattern should be ignored (Epstein et al., 2005). More recently, guidance for prostatectomy specimens states that Gleason score should be based on the primary and secondary patterns with a comment on the tertiary pattern if present (Epstein, 2010).

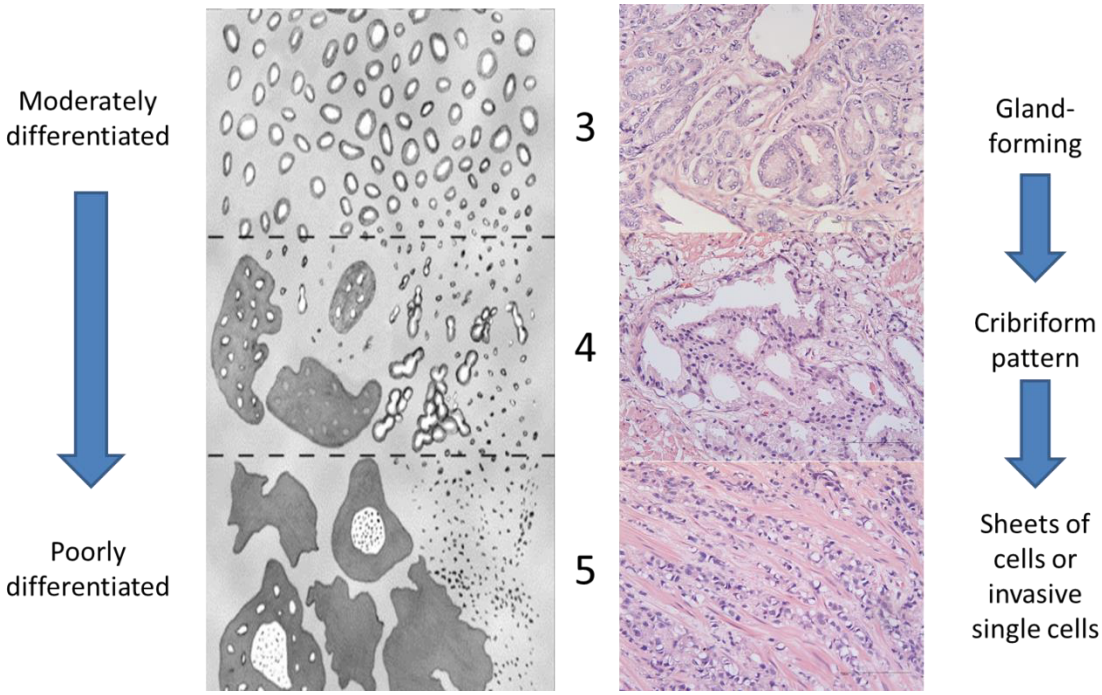

Figure 11: The modified, updated Gleason scoring system. Patterns 1 and 2 are largely obsolete in contemporary practice but may rarely still be diagnosed following TURP. Pattern 3 above displays moderately-differentiated carcinoma with large nuclei and prominent nucleoli, variable infiltrative glands that are closely packed but irregularly separated, of relatively circumscribed structure. Pattern 4 demonstrates the pathognomonic cribriform (or bridging) pattern with smaller hyperchromatic nuclei, but could have poorly-formed irregular glands. Pattern 5 carcinomas possess minimal glandular differentiation, and range from infiltrating single cells to solid sheets of tumor cells (as seen here). Diagram adapted from Epstein (2010). Photographs taken from anonymous TURP H&Es courtesy of Dr David Griffiths, Consultant Histopathologist, University Hospital of Wales, Cardiff, and were taken at 40x magnification, bars represent 100µm.

1.3.2 TNM staging

Prostate cancer is staged using the TNM classification, which is clearly outlined in table 3. This allows assessment of the tumour (T), lymph nodes (N) and metastases (M), which in turns affords accurate prognostic information and enables further treatment and/or follow-up to be planned.

T stage			
T1: impalpable or undetectable radiologically	**T2**: confined to prostate	**T3**: through prostate capsule	**T4**: fixed or invades adjacent structures e.g. rectum/bladder
T1a: ≤5% of TURP chips	**T2a**: ≤ half of one lobe	**T3a**: extra prostatic extension	
T1b: >5% of TURP chips	**T2b**: > half of one lobe	**T3b**: invades seminal vesicles	
T1c: Detected on needle biopsy	**T2c**: both lobes		

N Stage	**M stage**
Nx: nodes cannot be assessed	**Mx**: metastases cannot be assessed
N0: lymph nodes clear	**M0**: no evidence of metastases
N1: lymph nodes infiltrated with tumour	**M1:** distant metastases present

Table 3: TNM classification for prostate cancer. Clinical evaluation of any prostate cancer is made using digital rectal examination, however pathological analysis following radical retropubic prostatectomy (RRP) with pelvic lymph node dissection allows most accurate T and N staging. For men undergoing prostate-sparing treatments, such as radiotherapy or androgen deprivation, final T and N stage is made using a combination of the needle biopsy report and radiological assessment, usually with magnetic resonance imaging (MRI). To rule out or confirm the presence of bone metastases, isotope bone scintigraphy is the gold-standard investigation, as is computerised topography (CT) for visceral or lymph node metastases beyond the pelvis. Adapted from *TNM Classification of Malignant Tumours – 7th Edition* (UICC, 2009).

Important anatomical implications should be borne in mind for PCa prognosis, namely extra-prostatic extension (EPE), formerly extracapsular extension. Standard pathological staging of RRP specimens states the absence or presence of EPE, stage pT2 or pT3 tumours respectively, a prognostic cut-off for increased risk of disease progression after RRP (Epstein et al., 1996, De Marzo et al., 2003). Nerve bundles, which can enable transmission of EPE, are located in the

posterolateral aspect of the gland, with the largest nerve plexus at the base and a smaller one at the apex (McNeal, 1992). Hence the typical site of EPE is the posterolateral aspect of the prostate, particularly at the base, which is also the common route for direct invasion into the seminal vesicles i.e. stage pT3b (McNeal, 1992).

1.3.3 Treatment of prostate cancer

1.3.3.1 Localised prostate cancer

Improvements in detecting early disease and its treatment may have been refined but controversy regarding the most appropriate therapy for men with clinically localised PCa still remains (Albertsen et al., 2005). Established curative treatment options for men with localised prostate cancer include radical retropubic prostatectomy (RRP), radical radiotherapy and brachytherapy, along with active surveillance (deferred treatment). Cryosurgical ablation of the prostate (CSAP) and high-intensity focused ultrasound (HIFU) have more recently emerged as alternative therapeutic options for men with localised PCa (Fahmy and Bissada, 2003, Rees et al., 2004, Han and Belldegrun, 2004, Beerlage et al., 2000). Both HIFU and CSAP have been developed as minimally invasive procedures, which have potentially the same therapeutic efficacy as established surgical and non-surgical options, with reduced therapy-associated morbidity (Heidenreich et al., 2012). While HIFU is still considered an experimental treatment, the American Urological Association considers CSAP a true alternative therapeutic option.

The discovery of reliable biomarkers will ensure more accurate differentiation between indolent and lethal phenotypes to better guide management of men with newly diagnosed prostate cancer (Garber, 2011, Cuzick et al., 2011, Ding et al., 2011). More sophisticated imaging modalities will also ensure better imaging for those who choose to defer or forego treatment of localised PCa (Zaheer et al., 2009). Undoubtedly before these technological advances to come into fruition, we will be privy to the outcomes of well awaited trials comparing management options for localised PCa.

The Prostate cancer Intervention Versus Observation Trial (PIVOT) randomised 731 men (mean age 67 years) with localised prostate cancer to surgery or watchful waiting, and the two main endpoints from this trial were overall survival, and PCa-specific survival. Forty three percent of

men had low-risk, 36% had intermediate-risk, and 20% had high-risk prostate cancer (Wilt et al., 2012). The most salient results from PIVOT included no apparent difference between RRP and observation for men with low-risk PCa, whereas those with high-risk disease demonstrated significantly better PCa-specific survival after surgery. However, PIVOT failed to recruit the desired number of study participants, and as such, the trial was underpowered to detect the intended differences between RRP and observation (Catalona, 2012). The on-going ProtecT trial (Prostate testing for cancer and Treatment) aims to evaluate the effectiveness, cost-effectiveness and acceptability of treatments for men with localised prostate cancer; over 100,000 men with localised PCa have been randomised to active surveillance, radical prostatectomy or radical radiotherapy (ProtecT, ISRCTN20141297, Lane et al., 2010). In the hope of determining the most appropriate treatment for localised PCa, primary outcome measures will include: disease progression (biochemical and clinical), treatment complications, quality of life and sexual function, and ultimately PCa-specific survival and overall survival.

1.3.3.2 Locally advanced prostate cancer

There is no universally agreed definition of locally advanced prostate cancer (LAPC) (NICE, 2014). It includes a spectrum of disease ranging from tumour invading through the capsule of the prostate (pT3a) to those with T4 cancer that may be invading the bladder or rectum and/or has spread to pelvic lymph nodes (any T, and N1 – see section 1.3.2). The management of men with 'localised' prostate cancer but with a high-risk of extracapsular disease (i.e. Gleason score ≥ 8, or PSA > 20) may also be considered under this heading. Few effective treatment options for LAPC exist but they include systemic (androgen deprivation) or local therapy. Mounting evidence supports the use of a multimodality approach (Lowrance et al., 2012), including a combination of external beam radiation therapy (EBRT) with androgen deprivation therapy (ADT) or radical retropubic prostatectomy (RRP) with adjuvant EBRT.

Multiple randomised controlled trials (RCTs) have demonstrated a survival advantage to combined EBRT and ADT compared with either modality alone (Bolla et al., 2002, Bolla et al., 1997, D ' Amico et al., 2008, Pilepich et al., 2005, Roach et al., 2008, Widmark et al., 2009). To further add weight to the growing body of evidence, a systematic review (SR) and meta-analysis (MA) concluded that men given neoadjuvant hormone therapy prior to EBRT showed significant

improvements in clinical and biochemical disease-free survival as well as overall survival (Shelley et al., 2009b). Most recently, data from the PRO7 Trial co-ordinated by the UK Medical Research Council (MRC) have shown that combining EBRT with neoadjuvant ADT in patients with LAPC improved the overall survival rate at 7 years (p=0.03) compared with ADT alone (Warde et al., 2011). This multicentre phase III RCT recruited 1,205 patients with LAPC from the UK, the USA and Canada and randomised their treatment to either ADT alone or a combination of ADT and radiotherapy. In the latter group there was substantial overall survival and disease specific survival benefit, hence in view of these data, the benefits of ADT and EBRT in combination should be discussed with all patients considering a curative treatment approach (NICE, 2014).

As yet there has been no neo-adjuvant ADT in combination with adjuvant ADT surgical trial, which is the most efficacious strategy of androgen deprivation in men treated by EBRT for high-risk disease (i.e. Gleason score ≥ 8, or PSA > 20) (NICE, 2014). Neo-adjuvant ADT has so far failed to improve outcomes after surgery; ten studies were analysed as part of a SR and MA to compare the effect of neo-adjuvant ADT prior to RRP versus RRP alone (Shelley et al., 2009b). Neo-adjuvant ADT prior to RRP resulted in clinical and pathological down-staging along with a reduction in positive surgical margin rates (Schulman et al., 2000), however no improvement in overall and disease-free survival was seen (Aus et al., 2002, Baert et al., 1998, Klotz et al., 2003). Likewise, for men undergoing RRP as primary therapy for LAPC, the addition of adjuvant ADT did not improve overall survival in a separate SR and MA (Shelley et al., 2009a), however one of only two trails eligible for this review reported a survival advantage in a small cohort of lymph node–positive (N1) surgical patients treated with adjuvant ADT (Messing et al., 2006). More recently the control arm of the South West Oncology Group (SWOG) S9921 study identified the largest prospective group of men receiving immediate adjuvant ADT after RRP for high-risk localised PCa (Dorff et al., 2011). Originally designed to compare outcomes of adjuvant therapy with ADT alone, or in combination with mitoxantrone chemotherapy after RRP, these results from the control arm of SWOG S9921 were published early in view of their favourable 5-year biochemical failure-free survival and overall survival (92.5%, and 95.9% respectively, median 4.4 years). With the main trial outcomes still yet to report, these preliminary data make a compelling argument for counselling all men with high-risk PCa after radical RRP about the merits of adjuvant ADT.

An important aspect of RP in LAPC is to unearth the risk of adverse pathological features, such as upgrading/upstaging of disease or margin positivity. The role and benefit of adjuvant EBRT in this context has been demonstrated by three seminal RCTs that randomised men with positive margins, seminal vesicle invasion or EPE to receive adjuvant EBRT or conservative management (Thompson et al., 2009, Bolla et al., 2012, Wiegel et al., 2014). Men randomised to adjuvant EBRT in all three trials benefitted from improved biochemical progression-free survival and local control. Only one trial demonstrated significant improvements in metastasis and overall survival, with a median follow-up of 12.7 years (Thompson et al., 2009). The initial improvement in clinical progression-free survival seen at 5 years by Bolla et al. (2005), was not maintained at 10 years (Bolla et al., 2012). The currently-recruiting Medical Research Council RADICALS (Radiotherapy and Androgen Deprivation in Combination after Local Surgery) trial will evaluate the advantages of EBRT (adjuvant versus early salvage) and ADT in combination following RRP (Parker et al., 2007).

1.3.3.3 Metastatic prostate cancer

Huggins and Hodges (1941) were first to report the effect of surgical castration and oestrogen on the progression of metastatic prostate cancer (mPCa). Their pioneering work demonstrated the responsiveness of PCa/mPCa to ADT (Huggins and Hodges, Feb 2002, Huggins et al., 1941). Since then, androgen deprivation strategies have become the mainstay of mPCa management. After initially responding to ADT, most men with advanced PCa will eventually progress within 12-48 months depending on the disease burden, host factors and inherent tumour biology (Antonarakis and Eisenberger, 2011). As such the current gold-standard treatment could be seen as being palliation, especially given that there is no conclusive evidence to show that ADT extends life (Heidenreich et al., 2012).

After failing ADT, PCa evolves into a new clinically and molecularly heterogeneous androgen-independent state known as castration-resistant prostate cancer (CRPC), which invariably metastasises before becoming fatal (Antonarakis and Eisenberger, 2011). Androgen receptor signalling remains active even at castrate levels of serum testosterone, contrary to original understanding that disease progression after gonadal ablation implied androgen-independent

escape mechanisms (Chen et al., 2004a). One way in which CRPC maintains AR signalling is by overexpressing CYP17 (17α-hydroxylase/C17,20-lyase), a key enzyme in extragonadal (adrenal, prostatic, and intratumoral) androgen biosynthesis. As a result abiraterone acetate, an oral CYP17 inhibitor has been approved for use in the post-docetaxel chemotherapy setting, where it has shown an overall survival benefit of 3.9months compared to placebo and prednisolone (14.8 vs 10.9m respectively) (de Bono et al., 2011). Other treatment options for CRPC are shown in figure 12.

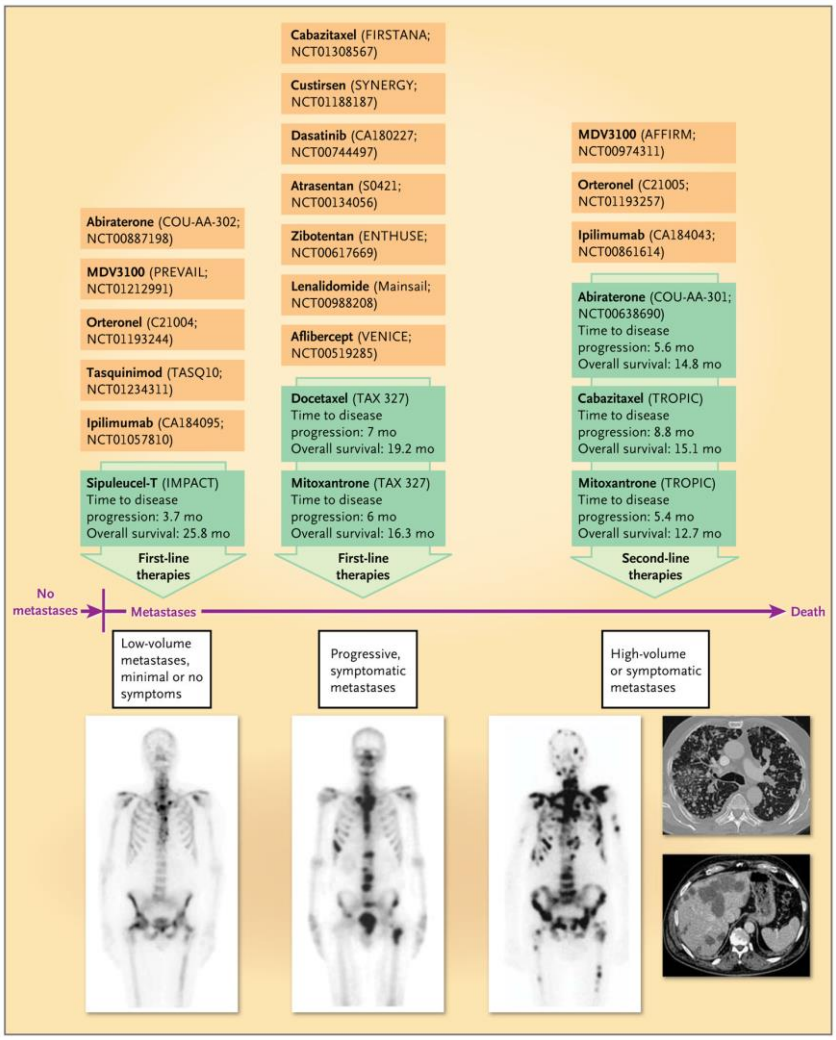

Figure 12: Evidence-based therapies for metastatic CRPC, and selected emerging treatments. Isotope bone scans show the typical course of metastatic CRPC from limited bone involvement (left) to progressive bone metastases (centre) to widespread metastases (right). The CT scans on the far right show visceral (lung and liver) metastases. Green boxes indicate agents that are currently approved in the USA by the Food and Drug Administration for the treatment of metastatic CRPC. The effects of these agents on disease progression and overall survival are shown. Orange boxes indicate selected agents currently in phase 3 drug development. Figure taken from Antonarakis and Eisenberger (2011).

The identification of validated clinical, radiological, biological, and/or genomic biomarkers could in future aid PCa management by enabling risk stratification and better patient selection for specific therapies, in addition to helping quantify response to treatment by acting as surrogates of clinical benefit (Antonarakis and Eisenberger, 2011).

Stem cell (SC) and cancer stem cell (CSC) theory are widely accepted concepts in the pathophysiology of many cancers and similarly prostate epithelial stem cells have been assigned a role in prostate cancer. Residual CSCs following conventional therapies such as ADT, EBRT and chemotherapy, may be responsible for treatment failure and the development of CRPC. Hence, understanding the aetiology and pathophysiology of PCa will help to underpin the development of better treatment options for advanced PCa. More specifically an understanding of prostatic epithelial biology is important because the evolution of CRPC may reflect a stem–like state of the tumour (Reya et al., 2001).

1.4 STEM CELLS AND STEM CELL THEORY

Many adult tissues, including blood, skin and intestine, are maintained by a subpopulation of cells known as SCs; one that possesses the ability to self-renew (maintenance of an undifferentiated state) and produce progeny that undergo further differentiation. Adult SCs generate only the differentiated lineages appropriate for the tissue in which they reside, and are thus referred to as either multipotent or unipotent. Multipotent stem cells have the ability to form all the differentiated cell types of a given tissue, such as in the prostate. In some cases, a tissue contains only one differentiated lineage and the SCs that maintain the lineage are described as unipotent, such as those in skin. Tissue homeostasis depends on a balance between SC self-renewal and differentiation (Watt and Driskell, 2010).

1.4.1 Human prostate epithelial stem cells

Evidence in support of the prostate epithelial stem cell (PrSC) niche has been increasing for over three decades. Early androgen depletion/repletion experiments in rats identified populations of androgen-independent cells (English et al., 1985, English et al., 1987) with the ability to re-

form duct-like structures, similar to human prostate acini, *in vitro* (Montpetit et al., 1988). Aspects of their data went on to develop later understanding that the prostatic epithelium is maintained by a single cell lineage system in which PrSCs comprise a subpopulation of the basal cells. This notion has more recently been supported by indirect evidence that basal and luminal cells are derived from a common precursor (Verhagen et al., 1992, Xue et al., 1998, van Leenders et al., 2000, Hudson et al., 2001). However in contrast, data from other researchers has led to the opposing hypothesis that both basal and luminal cells are independently capable of self-renewal (Evans and Chandler, 1987). Nonetheless identification and characterisation of PrSCs is important because they may represent a major target of carcinogenesis as well as a potential source of benign prostatic hyperplasia (BPH) (De Marzo et al., 1998, Reya et al., 2001). BPH and prostate cancer, both disorders of cell differentiation and cell proliferation, are major causes of morbidity and mortality in elderly men. There is evidence that the expansion and/or neoplastic transformation of PrSCs is the cause of BPH and/or PCa (Isaacs and Coffey, 1989, Schalken and van Leenders, 2003). Therefore, the immunophenotypical characterisation of PrSC candidates could provide novel therapeutic targets to use as adjuncts to standard therapies for treatment of BPH and PCa.

1.4.1.1 Evidence for epithelial stem cells in normal prostate – rodent androgen cycling studies

The ground-breaking experiments by English et al. (1985, 1987) defined the temporal effects of androgen replacement on prostatic cell population dynamics. They revealed that ADT in rats led to prostate gland atrophy due to apoptosis of almost all terminally-differentiated epithelial cells; namely androgen-dependent epithelial, endothelial and periacinar stromal cells. Upon readministration of testosterone, the gland regenerated and resumed normal secretory function. The rodent prostate is able to undergo several cycles of regression/regeneration, which postulates for the presence of a robust, androgen-independent population of PrSCs with the profound, innate ability for self-renewal and differentiation to an androgen-dependent luminal population. Further advances were made by Montpetit et al. (1988) when clones of androgen-independent cells were isolated from primary culture of rat prostate. When seeded into soft agar, these androgen-independent cell lines formed distinct foci suggesting their potential for tumourigenesis (Montpetit et al., 1988).

Following on from these seminal discoveries, Isaacs and Coffey (1989) proposed a hierarchical SC theory of prostate organisation in a precursor-progeny relationship. Slowly proliferating androgen-independent SCs within the basal compartment give rise to a second population of more rapidly-cycling androgen-independent, but androgen-responsive, transit-amplifying cells (TACs). Their capacity for self-renewal is greatly diminished however when following a limited number of population doublings, they were postulated to terminally differentiate into luminal secretory cells.

Experiments in opposition to this "classical" stem cell theory have hypothesised that basal and luminal cells are derived from independent lineages – the "two lineage" model (see figure below). A Cardiff group studied the proliferative activity of basal and luminal epithelial cells in the rat prostate after castration (Evans and Chandler, 1987). Although castration induced widespread apoptosis of up to 90% of the luminal cells, no compensatory hyperplasia of the basal cells was noted in response (Evans and Chandler, 1987). Instead cell proliferation and histological appearances suggested that both the basal and secretory cells entered a quiescent state upon castration. The proliferative potential of luminal cells persisted up to three months after castration and during androgen-induced regeneration of the prostate proliferation was evident in both basal and luminal cell compartments. Similarly, it was shown in the rat that after castration-induced atrophy, androgen-induced regeneration led to an enhanced proliferative response particularly of luminal cells (Evans and Chandler, 1987, English et al., 1987). There is also evidence to support the "two lineage" theory in human prostate whereby human prostatic luminal cells are capable of self-renewal following repletion of androgen after castration (van der Kwast et al., 1998). These opposing stem cell theories are illustrated in figure 13.

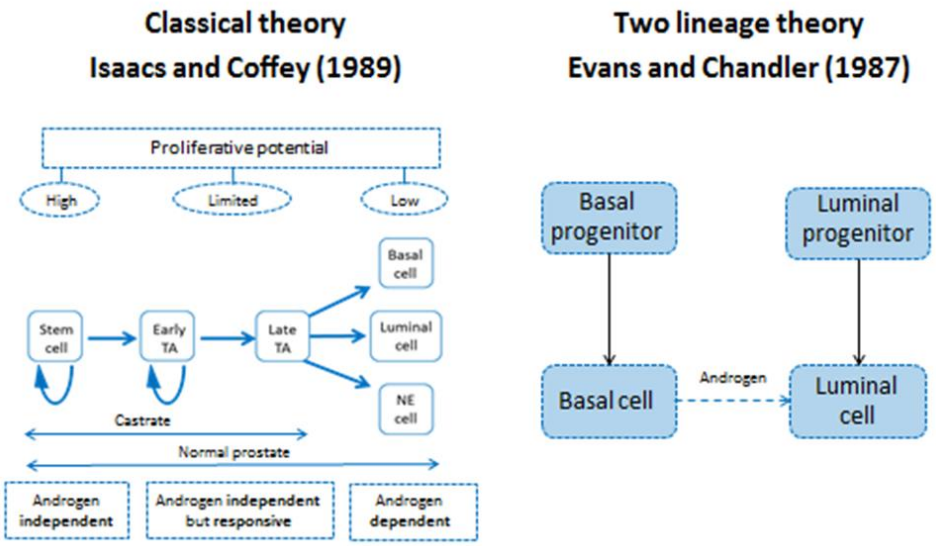

Figure 13: Schematic representation of the two proposed stem cell theories. In spite of these conflicting stem cell theories, the persistence of luminal secretory cells after androgen cycling in the "two lineage" theory does not wholly expunge the "classical" theory. The two stem cell models may be reconciled by assuming that in the presence of androgens, a certain number of AR-positive basal cells (Bonkhoff and Remberger, 1993) possess the ability to differentiate into luminal cells, to compensate for luminal cell loss following androgen deprivation (van der Kwast et al., 1998).

1.4.1.2 Phenotypic relationship between epithelial cell types in the prostate

Basal and luminal cells were first reported to be distinguishable in the human prostate due to their varying affinity to toluidine blue (Dermer, 1978), whereby it exhibits a strong affinity for basal cells while secretory cells are poorly stained. Dermer (1978) went on to describe how cells located nearer gland lumina were occupied by cells with a basal like morphology and which exhibited a strong affinity for toluidine blue. These early data suggest that basal cells are capable of proliferation and may be a source of luminal cells. Indeed co-localisation of basal cell-specific cytokeratins (denoted by prefix *CK*) with the proliferation-associated antigen Ki67 highlighted that the proliferative compartment in the prostate resides within the basal layer as evident in normal and hyperplastic tissues (Bonkhoff et al., 1994). Following on from these studies, methods of multiple immunocytological staining were developed that enabled the identification of a cell population intermediate from basal and luminal cells by the expression of differentiation stage-specific CKs (Verhagen et al., 1992, Xue et al., 1998, van Leenders et al., 2000, Hudson et al., 2001). Each group described how basal cells develop a luminal phenotype by way of an intermediate population. Similar experiments later detected a gradual shift from

expression of basal to luminal CKs via a transit-amplifying population (Robinson et al., 1998). The aforementioned experiments (Verhagen et al., 1992, Xue et al., 1998, van Leenders et al., 2000, Hudson et al., 2001) describe simultaneous immunocytological staining for up to three CKs. The least-differentiated basal stem cell population, containing stem cells, expresses only CK5/14, whereas CK15, 17, and 19 are expressed as the cells differentiate, initially with CK14 but then without. CK15 and 17 are restricted to intermediate basal cells but CK19 continues to be expressed as the cells become CK8/18-positive. The process ends with the loss of CK19, leaving only CK8/18 in the fully differentiated secretory population (Hudson et al., 2001). CK19 has been implicated in the differentiation of many different epithelial tissues in which there is a transition between differentiated phenotypes (Stasiak et al., 1989). This differentiation process is depicted below in figure 14.

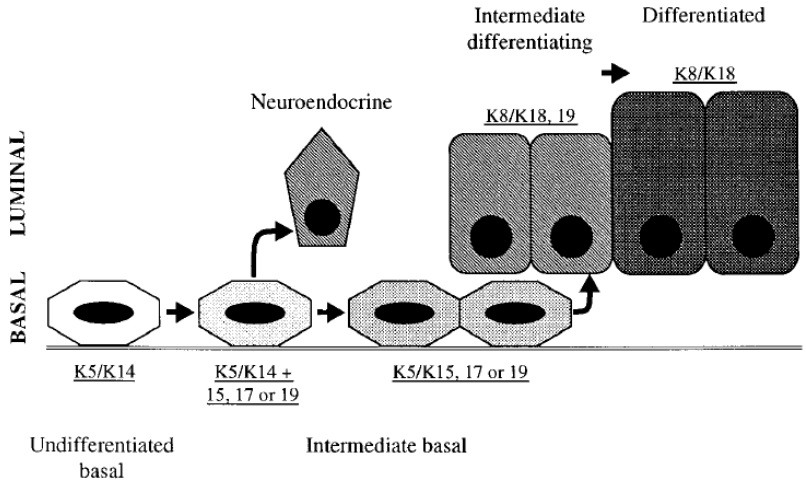

Figure 14: Hypothetical differentiation pathway for human prostate epithelial cells based on patterns of keratin staining. The prefix *CK* is interchangeable with *K* as used in this figure. Basally located undifferentiated cells (K5 and 14 only) give rise to an intermediate transit amplifying population expressing K19. These cells differentiate into luminal cells with transient co-expression of K19, 8, and 18 before complete differentiation into cells expressing K8/18 only. Adapted from Hudson et al. (2001).

1.4.2 Do human prostate epithelial stem cells reside in the basal or luminal layer?

There is a consistent body of evidence that PrSCs reside in the basal layer. Here, a small subpopulation of cells with the antigenic profile $\alpha_2\beta_1$integrin^{Hi}CD133^{+} display SC characteristics: they are quiescent and have a high proliferative potential *in vitro* and they are capable of constructing functional prostate acini-like structures *in vivo* (Richardson et al., 2004). More

recent molecular characterisation of these cells by the same group reveals that they do not express AR at mRNA level (Maitland et al., 2011), suggesting that they are not dependent on androgen for their survival, nor are they androgen-responsive. In support of a basal location for PrSCs, CD49f and Trop2 were identified as candidate surface antigens after interrogation of prostate-specific microarray databases (Goldstein et al., 2008). Trop2 discriminated basal cells into 2 populations, both of which were verified as basal cells by quantitative PCR, and only $Trop2^{Hi}$ cells were able to efficiently form prostate spheres *in vitro* (Goldstein et al., 2008) and regenerate prostate structures in a xenograft model *in vivo* (Goldstein et al., 2010).

1.4.3 Epithelial stem cells in the murine prostate

The preferential survival of prostate basal cells following androgen depletion/repletion experiments (English et al., 1987) led to the hypothesis that PrSCs reside within the basal layer of the gland (Isaacs and Coffey, 1989). Furthermore, this notion is supported by the fact that mice bearing a germline inactivation of, and therefore are null for, the basal cell marker *p63* fail to develop a prostate (Signoretti et al., 2000). This suggests that the PrSC resides within the p63-expressing subpopulation. Later Signoretti et al. (2005) showed that *p63* is required for commitment to the prostate cell lineage and, importantly, luminal cells of the prostate originate from p63-positive basal progenitor cells. In contrast, another group (Kurita et al., 2004) observed that fetal urogenital sinus tissue from *p63*-null mice transplanted as an allograft regenerated prostate ductal tissue in immunodeficient mice that lacked identifiable basal cells but did contain cells that expressed typical luminal markers. Although this finding suggests basal and luminal cells are derived from separate lineages, an alternative explanation might be that in the absence of *p63* the prostate does not develop normal stratified epithelia. The transcription factor *p63* is a homologue of the tumour suppressor *p53* but unlike *p53*, which is dispensable for normal development, *p63* is critical for the development of stratified epithelial tissues such as epidermis and breast (Barbieri and Pietenpol, 2006).

The location of epithelial SCs in the murine prostate has been, and continues to be, a contentious issue. Unlike human prostate, the mouse gland can be subdivided into ventral and dorsolateral lobes which are made up of individual ducts that drain into the urethra independently. These ducts can be separated into proximal, intermediate, and distal regions in

both mice, which is depicted in figure 15 (Sugimura et al., 1986a, Tsujimura et al., 2002), and rats (Jesik et al., 1982, Lee et al., 1990).

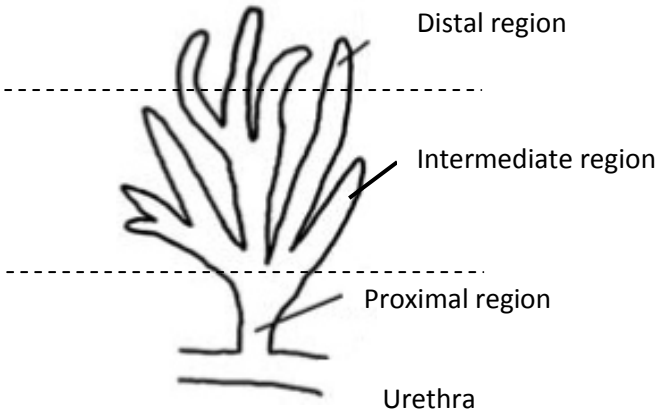

Figure 15: Schematic representation of a mouse prostate duct. The urethra, proximal and distal regions of the prostate are highlighted. Adapted from Korsten et al. (2009).

Label-retention studies on murine prostate have demonstrated that the majority of cells with stem-like features are located proximally, whereas greater numbers of luminal cells are found more distally at the tips of individual ducts. Label retention is well reported to be one method of mapping the location of stem cells on the assumption that cells displaying stem-like properties are quiescent, hence they are able to retain a DNA label for a lengthened period of time due to their infrequent entry into the cell cycle. In contrast, density of the label in question is rapidly diminished in actively dividing cells.

Tsujimura et al. (2002) described that in the proximal portions of the dorsal and ventral prostate, a high proportion of both basal and luminal cells were found to retain the BrdU label, even after multiple rounds of androgen involution–regeneration. In addition, Tsujimura et al. (2002) claim that the proximal cells of mouse prostatic ducts are quiescent, have a high proliferative potential, and give rise to large, glandular structures that produce prostatic secretory products in culture. These data strongly suggest that prostatic epithelial stem cells are concentrated in the proximal region of the ducts; however they admit that the distal region of the gland contains a population of actively proliferating cells as supported by others (Sugimura et al., 1986b, Cunha et al., 1987). The distal tips of the dorsal and lateral rat prostates undergo significant growth when combined with embryonic UGS mesenchyme and

implanted under the renal capsule (Kinbara et al., 1996). These findings were interpreted to mean that SCs reside in the distal region of prostatic ducts; however this experiment failed to include tissue from the proximal region for comparison which is a weakness in their study design (Kinbara et al., 1996). The observed growth of the distal region could be explained by the presence of young rapidly-proliferating TACs (Tsujimura et al., 2002). Other tissues exhibit the inherent ability of self-renewal, highlighting that a post-stem cell population of young TACs are capable of undergoing significant growth. These include skin (Taylor et al., 2000, Oshima et al., 2001), bone marrow (Williams, 1993, Berardi et al., 1995), and liver (Fausto, 2000, Strain and Crosby, 2000).

Enrichment for PrSCs from the proximal region of the mouse prostate has also been performed based on Sca-1 (stem cell antigen-1) expression (Burger et al., 2005). Cells expressing Sca-1 from the proximal region displayed a 17-fold higher in vivo proliferative potential than Sca-1^- ($p<0.001$) and Sca-1^+ cells obtained from the remaining ductal regions had far less growth potential than Sca-1^+ proximal cells ($p<0.001$) (Burger et al., 2005).

1.4.3.1 Location of murine prostate epithelial stem cells

In contrast to human prostate, there is still uncertainty as to whether the PrSC population in mice has a luminal or basal phenotype, as there is evidence in support of both hypotheses. As discussed earlier (see section 1.4.1.1), and in opposition to a solely basal phenotype, is the notion that BrDU- label-retaining cells are present both in the luminal and basal compartments (Tsujimura et al., 2002). Furthermore, using genetic lineage-marking, one study demonstrated that castration-resistant Nkx3.1-expressing cells are rare luminal cells that express Nkx3.1 after castration, can self-renew *in vivo* and can reconstitute prostate ducts in a single-cell allograft experiment (Wang et al., 2009).

In contrast, there is a greater body of evidence to suggest that mouse prostate SCs possess a basal phenotype akin to human prostate. In both species, a subset of basal cells are androgen-independent and can exhibit higher proliferative potential than luminal cells (Bonkhoff and Remberger, 1996). In addition, murine basal prostate epithelial cells can differentiate into luminal cells both *in vitro* and *in vivo* (Xin et al., 2007). Studies in mice have led to the

identification of Sca-1^+ cells as a subpopulation of prostate epithelial cells with SC characteristics (Xin et al., 2005, Burger et al., 2005).

1.4.4 Prostate epithelial stem cell markers

The majority of markers used to isolate prostate cells that are capable of displaying stem-like qualities, are not shared by both human and mouse. The prospective identification of enriched SC and/or progenitor/transit-amplifying subpopulations in mouse prostate is important for investigating the self-renewal properties of SCs. This will in turn enable their role in cancer initiation and propagation to be explored, so as to exploit their potential as novel drug targets in the pre-clinical setting. Notwithstanding, identification of these populations from human prostate would be the most sought-after goal and result in greatest therapeutic benefit; that of improved PCa survival and ultimately cure. Therefore, it would be useful to identify antigens found on stem/progenitor cells from both the mouse and human prostate.

1.4.5 Human prostate epithelial stem cell markers

In the normal human prostate, basal cells express CD44, whereas luminal cells express CD57. Liu et al (1997) were able to isolate the two major epithelial cell populations by utilising their differential expression of surface markers CD44 and CD57 by fluorescence activated cell sorting (FACS). Their work demonstrated that CD44-expressing basal cells were capable of differentiation into luminal cells when cultured in combination with dihydrotestosterone, and a synthetic mimic of the stromal microenvironment, Matrigel. This was proven by the detection of secreted PSA in the culture medium, which is an innate function of luminal cells but not basal cells. Unsurprisingly $CD57^+$ cells continued to secrete PSA, but interestingly PSA production was also noted in the $CD57^-$ population. This was hypothesised to be due to contamination with residual luminal cells or differentiation of $CD44^+$ cells. Given that basal cells exhibit one property of SCs, differentiation, (Bonkhoff and Remberger, 1996), they were felt to constitute the reservoir of progenitors that mature into luminal cells.

Following this experiment, cells that express $\alpha_2\beta_1$-integrins were selected from $CD44^+$ basal cells by FACS, and shown to possess features in-keeping with SCs (Collins et al., 2001). Integrins, which mediate attachment of cells to extracellular matrix proteins of the basement membrane,

have proven effective in identifying SCs in such tissues as skin and testis. Epidermal SCs had earlier been shown to express higher levels of integrins $\alpha_2\beta_1$, which was used to discover the location of SCs within the epidermis, and to isolate them on their ability to adhere to type IV collagen *in vitro* (Jones et al., 1995). Collins et al (2001) hypothesised that PrSCs could share similar molecular properties to other SCs , and thus they questioned whether integrin $\alpha_2\beta_1$ could facilitate adhesion to type I collagen and laminin-1, in addition to type IV collagen; a feature restricted to the basal cells of the prostate (Knox et al., 1994). They found that basal cells expressing this molecular signature comprised up to 15% of the subpopulation. Furthermore, high surface expression of the α_2-integrin subunit on human prostate epithelium correlates with increased colony forming ability in 2D-culture, and the potential to regenerate a fully differentiated prostate epithelium in an allograft model. Immunohistochemical analysis revealed colonies predominantly contained cells that stained intensely with the basal cell-specific marker 34βE12. Luminal cells correctly stained with antibodies against PAP and PSA, in addition to AR.

To further facilitate the isolation and characterisation of prostate epithelial stem cells, the same group later showed that by sorting for $\alpha_2\beta_1$-integrin^{hi}CD133^{+}, they were able to refine a subpopulation that expanded both *in vitro,* and *in vivo* following transplantation in the flank of athymic male mice. In adherent culture, this population of interest totalled 0.75%. In a colony-forming assay, clonal CD133^{+} cells were enriched at an approximately 10-fold greater efficiency than the non-selected basal population, and CD133^{-} cells had a 4 to 5-fold greater efficiency than non-selected basal cells. They later became the first group to successfully isolate and characterise the CSC population from human prostate tumours using the antigenic profile CD44$^{+}\alpha_2\beta_1$-integrin^{hi}CD133^{+} (Collins et al., 2005). These CSCs, representing a small fraction of the total cells comprising the tumour, were capable of self-renewal and proliferation *in vitro*, and differentiated to recapitulate the phenotype of the tumour from which they were derived. However, this study lacked the so-called, “ultimate test” of tumourigenicity, transplantation *in vivo*, but went on to state that they had provided compelling evidence that the CD133-derived cultures were tumorigenic, as they were shown to be invasive in Matrigel. The quantity of CD133-expressing cells was not influenced by tumour grade, or the source of tumour cells, which included primary prostate cancers and metastatic deposits, whereby their proportion (approximately 1%) remained small in all experiments.

Schmelz et al (2005) aimed to identify subpopulations of prostate epithelial cells with the potential for proliferation and differentiation from core biopsies of normal human prostate taken from RRP specimens. The members of the CK6 family are structural proteins associated with hyperproliferation and aberrant differentiation, and as such, CK6 expression was tested *in vivo* as a structural marker to identify PrSC candidates. Evidence in support of $CK6a^+$ cells being candidate prostatic stem cells includes: the presence of $CK6a^+$ cells in foetal, juvenile and adult prostatic glands; the niche-like distribution pattern; the abundance in the foetal urogenital sinus enriched in stem cells; the differentiation potential; the proliferation potential; and finally the amplification potential of these $CK6a^+$ cells (Schmelz et al., 2005).

Work with murine PrSCs has revealed commonalities between them and stem-like cells originating from other tissues, including the mammary gland (Lawson et al., 2007). In breast cancer, earlier discovery had identified $CD44^+CD24^-$ cells as being both clonogenic and tumorigenic (Al-Hajj et al., 2003). These cells were xenografted into the mammary fat pad of NOD/SCID mice (see section 1.6.1) and shown to possess the ability to proliferate extensively, to give rise to diverse cell types with reduced developmental or proliferative potential, and to serially passage *in vivo* up to four generations (Al-Hajj et al., 2003). This led another group to later question whether $CD44^+CD24^-$ cells from human prostate cancer defined a population of cancer stem cells (Hurt et al., 2008). They showed that human prostate cancer cells with the $CD44^+CD24^-$ phenotype display stem cell characteristics such as clonogenicity, tumorigenicity, and the ability to grow into spherical organoids in non-adherent culture. These organoids displayed stem-like gene signatures; over-expression of genes associated with 'stemness', including *Oct-3/4*, *BMI-1*, *smoothened*, and *β-catenin*. Furthermore, tumours from mice injected with $CD44^+CD24^-$ cells were phenotypically similar to tumours resulting from mice injected with total cells from the immortalised LNCaP cell line. This indicates that $CD44^+CD24^-$ cells satisfy the CSC brief. Additionally, $CD44^+CD24^-$ cells contain a molecular signature originally identified in breast tumorigenic cells (Liu et al., 2007), further drawing similarities between breast cancer and PCa.

Despite the growing body of evidence for PrSCs, a fundamental question remains as yet unanswered: whether all basal cells possessed stem cell characteristics and could give rise to terminally differentiated cells of the organ, or whether only a subpopulation of basal cells have tissue regenerative capacity? Goldstein et al. (2008) attempted to address this by sorting for

the marker Trop2^{Hi}, from the population enriched for the antigenic profile CD49f^{+}. They elegantly demonstrated how tumour-associated calcium signal transducer 2 (TACSTD2/Trop2/M1S1/GA733-1) (Fornaro et al., 1995), allows discrimination between two basal cell subpopulations. Furthermore they provided evidence that not all basal cells have SC characteristics; the Trop2^{Hi} cells displayed 'stemness' in *in vitro* and *in vivo* assays. The value of the Trop2 marker is further enhanced because it can isolate sphere-forming stem/progenitor cells from both the human prostate and the murine prostate, the latter of which will be discussed later.

Up to this point no group had managed to identify the antigenic profile of a functionally pure human PrSC population in order distinguish multipotent SCs from progenitors with more limited self-renewal potential. Guo et al. (2012) served to interrogate combinations of cell surface antigens EpCAM, CD44 and CD49f to differentiate SCs from progenitors and luminal cells by way of a tissue regeneration assay, in which total benign prostate cells induce tubule formation (differentiation) supported by human fetal prostate stroma in a tissue regeneration model. They were the first group to report 3 distinct epithelial populations with unique properties:

1. **EpCAM^{+}CD44^{+}CD49f^{hi}** - basal cells capable of forming abundant spheres
2. **EpCAM^{+}CD44^{-}CD49f^{hi}** - basal non sphere-forming cells (true SCs) with significantly increased tubule induction activity
3. **EpCAM^{+}CD44^{-}CD49f^{lo}** – true luminal cells that lack both sphere-forming and tissue regenerating potential

These data go some way to support those outlined by others (Richardson et al., 2004, Lang et al., 2010), whereby CD133 was reported to be a marker of human PrSCs. Their experiments demonstrated how these cells were incapable of forming spheres, but readily formed proliferative monolayers in 2D culture. In addition, $\alpha_2\beta_1$integrin^{hi}CD133^{+} cells induced acinar-like outgrowths *in vivo*, suggesting that CD133^{+} cells possess similar properties to the EpCAM^{+}CD44^{-}CD49f^{hi} subpopulation. Moreover, other human studies have reported that CD133 does not enrich for sphere-forming cells (Garraway et al., 2010).

Few surface molecules are currently available for enriching both murine and human prostate tissue stem/progenitor cells, but CD166 is one such antigen (Jiao et al., 2012). CD166 has been shown to enrich the sphere-forming ability of benign primary human prostate cells *in vitro* and induce the formation of tubule-like structures *in vivo*. Similarly, its expression is upregulated in human PCa, especially in CRPC samples. Its role as a murine stem/progenitor cell marker will be expanded upon later.

Human PrSC markers are summarised in table 4.

Human SC marker	Description	Source of tissue	Evidence
CD44	CD44+ cells occupy a basal location. Differentiation, as reflected by PSA production, can be detected when CD44+ cells are co-cultured with stromal cells. Thus, CD44+ basal cells possess characteristics of stem cells and are candidate progenitors of luminal cells	Benign glands from TURP/RP for BPH, or cysto-prostatectomy for bladder cancer	Liu et al. (1997)
α2β1-integrin^{hi}	Represent ~1% of basal cells but are distinguishable from other basal cells by their ability to generate prostate-like glands *in vivo* with morphologic and immunohistochemical evidence of prostate-specific differentiation	Benign glands	Collins et al. (2001)
$\alpha_2\beta_1$-integrin^{hi} CD133^{+}	Possess high proliferative potential *in vitro*, and *in vivo* where they can reconstitute prostatic-like acini in immunocompromised nude mice	Benign glands	Richardson et al. (2004)
CD44^{+} $\alpha_2\beta_1$-integrin^{hi} CD133^{+}	Cells possess the capacity for self-renewal, and are capable of forming differentiated cell products, such as AR and PAP	Tumour cells from RRP specimens	Collins et al. (2005)
CK6a	Possess a high potential for proliferation and differentiation *ex vivo*	Benign glands	Schmelz et al. (2005)
CD44^{+} CD24^{-}	Cells form tumours when transplanted as xenografts and express genes known to be important in stem cell maintenance	LNCaP and DU-145 cell lines	Hurt et al. (2008)
Sca1+ CD49f^{hi} Trop2^{hi}	Sphere-forming assays were isolated from the human prostate using these markers identified in the mouse, suggesting conservation of interrelated progenitor markers between mouse and human	Benign glands	Goldstein et al. (2008)
Trop2^{hi} CD49f^{hi} CD44^{+}	This antigenic combination highlighted cells with enriched sphere-forming capability. Clonally derived prostaspheres could be dissociated and passaged for multiple generations and induce the formation of ductal/acinar-like structures in vivo.	Benign and malignant glands from RRP and cysto-prostatectomy specimens	Garraway et al. (2010)
Epcam^{+}CD44$^{+/-}$CD49f^{hi}	Epcam^{+}CD44^{+}CD49f^{hi} cells demonstrated self-renewal in 3D culture, but not differentiation in allografts; thus felt to represent the PC/TAs. However Epcam^{+}CD44^{-}CD49f^{hi} cells were non-sphere-forming but readily generated tubular structures when allografted (differentiation); felt to be SCs	Tumour cells from RRP specimens	Guo et al. (2012)
CD166^{hi}	CD166^{hi} human prostate cells have higher sphere forming capacity *in vitro* and more graft outgrowth *in vivo*, and up regulated in advanced PCa on gene expression and TMA analyses	Adult and foetal benign glands	Jiao et al. (2012)

Table 4: A summary of each reported human PrSC marker

1.4.6 Mouse prostate epithelial stem cell markers

Bcl2 is a proto-oncogene that, along with being anti-apoptotic, is often expressed in the proliferating zones of long-living cells (Hockenbery et al., 1991). This and other experiments have demonstrated how Bcl2 staining is confined to basal cells of the prostate epithelium (Bonkhoff and Remberger, 1996). Both the expression pattern in the prostate epithelium and its role in apoptosis contribute to Bcl2's potential for being a SC marker. Moreover, experiments using 2D colony-forming assays report that only 2-4% of cells display proliferation, and colonies derived from SCs co-express Bcl2 and CK5, further adding weight to the basal location of PrSCs.

As discussed in section 1.4.3, PrSCs responsible for populating epithelial compartments of the prostate express p63 (Signoretti et al., 2000), whereas p63-null mice fail to develop prostates. Recently the NH2-terminal truncated (ΔN) p63 isoform was studied by the generation of knock-in mice expressing Cre-recombinase under the control of an endogenous ΔNp63 promoter (Pignon et al., 2013). Genetic lineage tracing experiments concluded that ΔNp63-positive cells of the urogenital sinus were responsible for generating all epithelial lineages of the prostate and bladder, indicating that these cells represent the stem/progenitor cells of those epithelia during development (Pignon et al., 2013).

Shou et al. (2001) demonstrated that Notch1-expressing cells were associated with the basal epithelial cell population in the prostate. Furthermore, elegant experiments by Wang et al. (2004) revealed that elevated Notch1 expression during development suggests that Notch1-expressing cells define progenitors in the prostate epithelial cell lineage. These cells were shown to be of paramount importance in branching morphogenesis of the developing prostate in culture and in re-populating the prostate epithelia upon reintroduction of androgen after castration in a transgenic mouse model, concomitant with p63 and CK14 cells (Wang et al., 2004).

BrdU label-retaining experiments have previously suggested that slow-cycling PrSCs with high-proliferative potential are located in the proximal ducts of the mouse prostate (Tsujimura et al., 2002). These stem cells were prospectively isolated and purified based on their surface expression of stem cell antigen-1 (Sca-1), and shown to possess greater *in vivo* proliferative potential than cells expressing low levels of Sca-1 in a renal capsule allograft model (Burger et

al., 2005). Interestingly, the majority of Sca-1^+ cells co-expressed α6-integrin and Bcl-2, both known to be important when identifying SCs of other origins (Burger et al., 2005). Regeneration of Sca-1^+-enriched prostate regenerative cells (stem-like cells) that were transfected with lentivirus that mediated the expression of constitutively active AKT1, resulted in the initiation of prostate tumourigenesis (Xin et al., 2005). In this study, the Sca-1^+ subpopulation was shown to be largely quiescent (in G_0 on FACS) and able to display bipotency; both basal and luminal cell lineages were present in regenerated grafts.

Other papers have gone on to describe how prostate epithelial cells enriched for Sca-1 in combination with other cell surface markers, identifies groups of cells capable of displaying stem cell characteristics *in vivo* and *ex vivo*. These include Lawson et al. (2007), $CD45^+CD31^+Ter119^+[Lin^-]Sca\text{-}1^+CD49f^+$ (LSC^{hi}); Leong et al. (2008), $Lin^-Sca\text{-}1^+CD133^+CD44^+CD117^+$; Goldstein et al. (2008) and Lukacs et al. (2010), $LSC^{hi}Trop2^{hi}$; and Jiao et al. (2012), $LSC^{hi}CD166^{hi}$.

Finally, prominin (known as CD133 in humans) was identified as being a candidate SC marker in murine prostate epithelium for several reasons (Tsujimura et al., 2007). Firstly it is a cell surface marker that is widely used to identify and isolate SCs from various organs, including the hematopoietic system. Secondly, on cDNA microarray analysis, it was enriched greater than 20 times from the proximal mouse prostate when compared to most of the 4800 genes analysed. $CD133^+$ cells formed large glandular structures containing both basal and luminal cells in *in vitro* 3D culture that were significantly larger and more branched than $CD133^-$ cells, while in contrast, prominin-deficient cells from the proximal region did not form ductal structures.

Murine PrSC markers are summarised in table 5.

Mouse SC marker	Description	Evidence
Bcl-2	Anti-apoptotic protein expressed in long-living cells Expressed on basal cells	Hockenbery et al. (1991) Bonkhoff and Remberger (1996), Rizzo et al. (2005)
K5 & Bcl-2	Clonogenic cells demonstrated self-renewal and purification *in vitro*	Sawicki and Rothman (2002)
p63	p63-null mice fail to develop a prostate, hence p63 is essential for development of normal prostate cell populations Urogenital sinus cells positive for the NH2-terminal truncated p63 isoform generated all epithelial lineages of the prostate, suggesting that these cells represent the stem/progenitor cells	Signoretti et al. (2000) Pignon et al. (2013)
Notch	Receptor mapped to basal cells Ablation of Notch-1 cells in a transgenic mouse model severely affected morphogenesis, growth, and differentiation in prostate	Shou et al. (2001) Wang et al. (2004)
Sca-1 (stem cell antigen-1)	Cells from the proximal region displayed a 17-fold higher in vivo proliferative potential than Sca-1$^-$ cells Cells identified by FACS showed prostate-regenerating activity and oncogenic potential over Sca-1$^-$ cells	Burger et al. (2005) Xin et al. (2005)
Lin$^-$Sca-1$^+$ CD49f$^+$ (LSC)	LSC cells demonstrate self-renewal in vitro, in vivo (allograft) and differentiation upon administration of testosterone	Lawson et al. (2007)
CD133	CD133+ cells generated large-branched ducts in 3-D culture, whereas CD133- cells formed far fewer such structures	Tsujimura et al. (2007)
Lin$^-$Sca-1$^+$ CD133$^+$ CD44$^+$ CD117$^+$	Single cells were shown to generate a functional prostate after transplantation *in vivo*	Leong et al. (2008)
LSCTrop2^{hi} (LSCT)	Trop2 is expressed in the basal fraction. Trop2 exhibits enrichment for stem-like cells in 2-D and 3-D culture Trop2^{hi} cells were capable of forming spheres *in vitro,* over and above the efficiency of LSC cells	Goldstein et al. (2008) Lukacs et al. (2010)
LSC^{hi}CD166^{hi}	CD166 can be employed to further enrich stem/progenitor cells in *wild-type* murine prostate	Jiao et al. (2012)

Table 5: A summary of each reported PrSC marker in murine prostate

1.4.7 Cancer stem cells

Just as normal tissues can contain a mixture of dividing cells and cells at different stages of terminal differentiation, the same is true for many tumours. The observed heterogeneity of tumours underpins the CSC concept. The stochastic model opposes this explanation for tumour heterogeneity and both theories are depicted in figure 17.

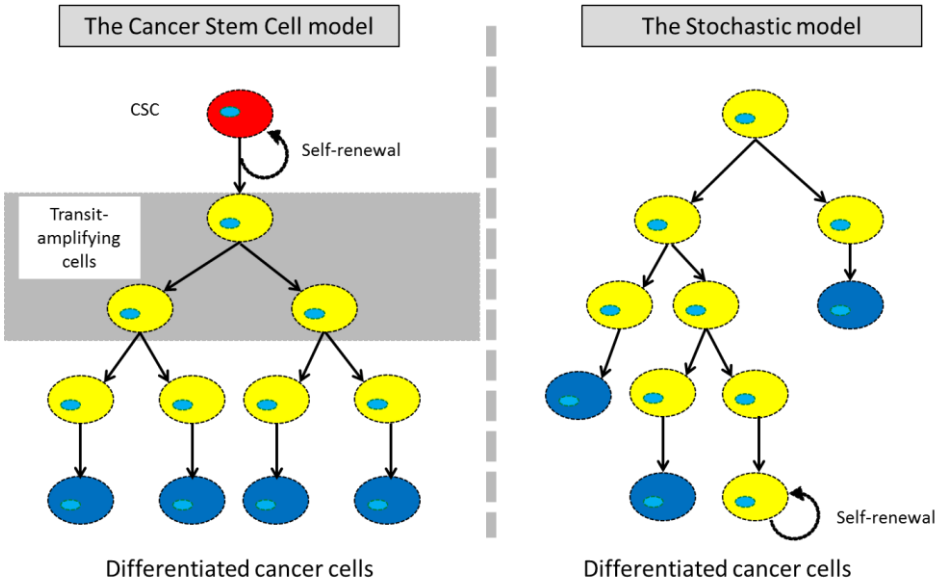

Figure 17: The Cancer Stem Cell model versus the Stochastic model of tumour heterogeneity. The stochastic model proclaims that tumour cells are biologically equivalent but the mutations that result in their malignant potential occurs at random and is therefore unpredictable. Thus, tumour-initiating cells/progenitor cells/PrSCs cannot be enriched for by sorting cells based on antigenic profile. In contrast, the hierarchical CSC model postulates the existence of classes of cells, biologically distinct from one another, with differing functional abilities and behaviour, whereby only a subset of cells has the ability to initiate tumour growth, the so-called CSC. These cells possess the ability to self-renew and give rise to progeny, which are not necessarily malignant, that make up the bulk of the tumour. This model predicts that tumor-initiating cells can be identified prospectively and purified from the rest of the tumour bulk, based on intrinsic characteristics. Adapted from Watt and Driskell (2010).

The CSC concept is an important one in PCa because it has been hypothesised that these cells are resistant to conventional ADT, which largely treat the bulk of the tumour only. Consequently, and in support of this, CRPC develops, which ultimately proves fatal. Figure 18 illustrates this hypothesis.

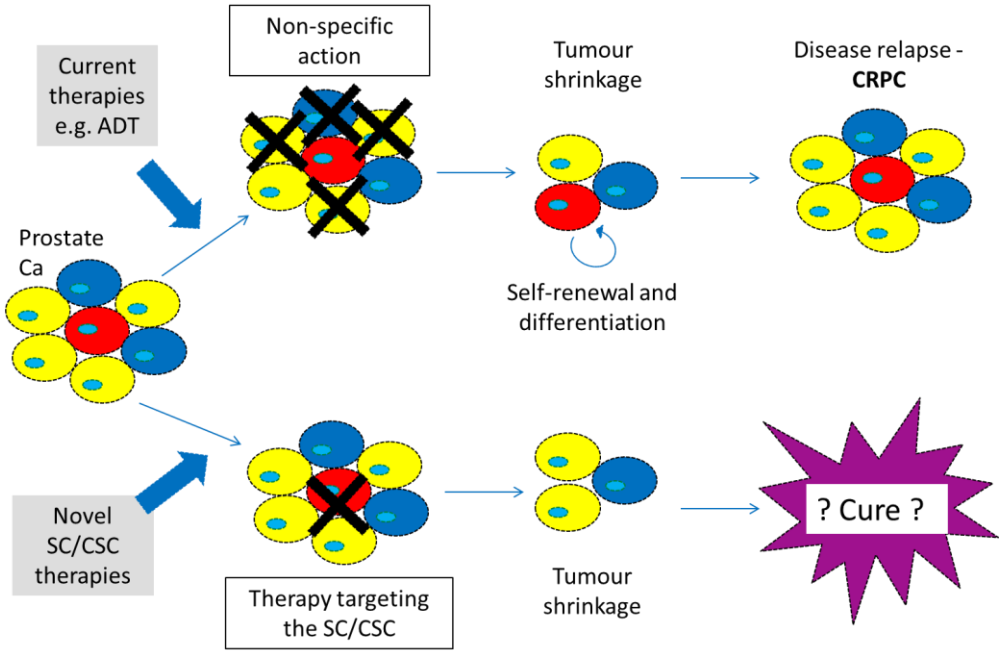

Figure 18: Cancer stem cells as drug targets in prostate cancer. Cancer stem cells often share antigenic profiles with normal PrSC/progenitor cells (Ginestier et al., 2007, Malanchi et al., 2008). This highlights the importance of identifying primitive cell populations in normal and malignant prostate tissue of both mice and humans to act as drug targets for novel therapies aimed at killing the CSC.

1.5 MODELLING PROSTATE CANCER IN VITRO

1.5.1 Cell lines

Immortalised cell lines are long established in the study of PCa. They have particularly been used to investigate genetic deregulation in support of *in vivo* findings. The important historical human prostate cancer cell lines such as DU-145 (Stone et al., 1978), PC-3 (Kaighn et al., 1979), and LNCaP (Horoszewicz et al., 1980), were originally cultured from metastatic sites, namely brain, bone, and supraclavicular lymph nodes respectively. Being from different sites, and possessing varying malignant potential, they have allowed rapid, prospective identification of genetic targets and molecular mechanisms in advanced disease. Perhaps one criticism of cell lines is that they preclude analysis of genetic alterations that are responsible for the transformation of normal prostate epithelium into adenocarcinoma. Furthermore, they lack the complex paracrine signalling of the tumour microenvironment (Hensley and Kyprianou, 2012).

1.6 MODELLING PROSTATE CANCER IN VIVO

There is no single mouse strain that fully models all stages of human prostate tumourigenesis. These are demonstrated in figure 19. The fundamental challenge that scientists have failed to overcome is the heterogeneity of both human and murine PCa. To date each mouse model has only characterised certain features or stages of the disease, but despite this, most models have contributed positively to our contemporary understanding of PCa.

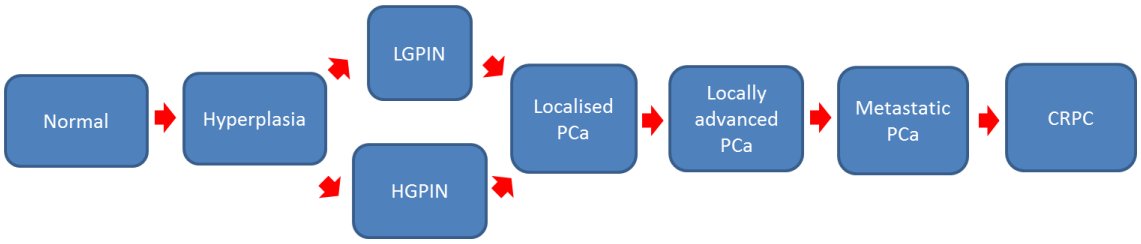

Figure 19: the stages of human prostate cancer. *LGPIN*, low-grade prostate intraepithelial neoplasia; *HGPIN*, high-grade PIN; *CRPC*, castrate-resistant prostate cancer.

Mouse models allow the important early and late phases of prostate tumourigenesis to be studied with set kinetics, in a stepwise fashion. Whether or not hyperplasia is a precursor to PIN, and whether or not low-grade disease is a precursor of high-grade disease, will not be deliberated here. The important mouse models of PCa are summarised in this section.

1.6.1 Xenograft models of prostate cancer

Immunodeficient mice have acted as recipients for human material, including cell lines, prostate cancer cells or cells from primary culture. Their genetic modifications render them unable to mount an immunological response, resulting in unabated tumour growth that facilitates the study of patient specific material. Xenograft models have been employed in assessing the efficacy of novel treatments, along with providing suitable conditions for *in vivo* passage when exploring SC/CSC properties. Specific xenograft models are countless, limited only by the genetic alterations and combinations of interest. The immunodeficient mice that are most commonly used for xenografts in the investigation of PCa are summarised in table 6.

Model	Description	Immunological deficiency	Specific features
Nude mice	Congenitally athymic	T-lymphocyte deficiency	Orthotopic injection may give a truer representation of tumour microenvironment than subcutaneous injection
Severe Combined ImmunoDeficient mice (SCID)	Autosomal recessive SCID mutation	B- and T-lymphocyte deficiency	Greater immunodeficiency than nude mice; NK cells and myeloid cells persist
Non-Obese Diabetic (NOD) – SCID mice	NOD mice crossed with SCID mice	Deficient in natural killer cells, complement and antigen presenting cells	Higher graft success rate due to greater immunodeficiency than SCID mice; NK cells persist
Renal capsule xenograft	PCa cells mixed with urogenital sinus mesenchyme injected under renal capsule	Usually NOD or SCID mice used	Used to determine the ability of putative PrSCs to generate prostatic tissue and ducts. Also used to determine the physiological significance of genes that cannot be studied via whole body knockouts due to embryonic lethality
Intrabone injection xenograft	Cells injected into tibia or femur under anaesthesia	Nude and SCID mice reported	Used to model the invasion and growth of PCa cells in bone. No mouse model of PCa spontaneously metastasises to bone

Table 6: The immunodeficient mice used in the study of PCa and the methods commonly used for xenografts

1.6.2 Constitutive/germline knockout models of prostate cancer

Traditional (whole body) knockout models have allowed the genetic modification of tumour suppressor genes felt to be important in PCa, thus enabling their roles in tumourigenesis to be defined. In this manner the whole gene, or a region of DNA essential to a maintain gene's integrity, can be excised. The major limitation precluding the widespread and continued use of this technique is embryonic lethality since many tumour suppressors play important roles in embryogenesis. Despite this, several knockout models have been well characterised, highlighting their importance in PCa.

PTEN (phosphatase and tensin homolog deleted from chromosome 10) is a tumour suppressor gene and negative regulator of the PI3K/Akt/mTOR pathway that has been implicated in many human cancers, including PCa. Germline mutations in the *PTEN* gene have been associated with Cowden syndrome whereby these patients develop hamartomas in various organs that have premalignant potential (Liaw et al., 1997, Marsh et al., 1999, Dahia, 2000). *PTEN* deregulation is strongly implicated in prostate tumourigenesis; *PTEN* deletions and/or mutations are found in 30% of primary PCa (Dahia, 2000) and up to 63% of mPCa (Suzuki et al., 1998). Indeed, *PTEN* mutations have likewise been implicated in the mechanisms of resistance to EBRT (Anai et al., 2006), and chemotherapy (Priulla et al., 2007), along with recurrence following RRP (Bedolla et al., 2007). Furthermore, *in vitro* analysis in mice has suggested a critical role for *Pten* in the progression of cancer cells to CRPC (Shen and Abate-Shen, 2007).

In mice *Pten* was found to be of paramount importance for early embryonic development, since $Pten^{-/-}$ mice are incompatible with life. In comparison, heterozygotes ($Pten^{+/-}$) survived up to 1 year and resulted in broad-ranging phenotypes in various tissues. These included tumours of the gonads, skin, uterus and endometrium, intestine, thyroid and adrenal glands. Prostatic lesions in these $Pten^{+/-}$ mice were classified as PIN, showing that *Pten* mutation was a critical molecular event in PCa development (Podsypanina et al., 1999). At least three other models describe knockouts in combination with *Pten* that have resulted in more aggressive phenotypes. These are outlined in table 7.

Constitutive double knockout model	Terminal stage of neoplasia	Other tissues affected	References
Pten x p27	Adenocarcinoma	Endometrium, intestine, thyroid, adrenal gland	Di Cristofano et al. (2001)
Pten x Nkx3.1	LN metastases	As for solitary $Pten^{+/-}$ model, including salivary, bulbourethral and adrenal gland hyperplasia/dysplasia	Abate-Shen et al. (2003) Gao et al. (2006)
Pten x p53	HGPIN	As for solitary $Pten^{+/-}$ model	Couto et al. (2009)

Table 7: Constitutive Pten double knockout mouse models and their consequences

To efficiently target deletion of genes within the prostate, and in so doing avoid embryonic lethality and multiple phenotypes, the prostate-specific promoter Probasin was exploited. Probasin (prostate basic protein, PB) is a prostate-specific gene, originally derived from the rat, and it is the most extensively used promoter in PCa research. It is a member of the lipocalin family and is found in the secretions and nuclei of prostate epithelial cells. It is reportedly regulated by androgens and zinc (Kasper and Matusik, 2000, Johnson et al., 2000), and although its precise function remains unknown, it is believed to be involved with transporting hydrophobic ligands into seminal fluid (Johnson et al., 2000).

Probasin contains two AR binding sites within the promoter (-236 to -223 and -140 to -117), referred to as the androgen responsive region (ARR), to enable full promoter activation (Kasper, 2005). Previous work has revealed that PB-driven expression occurred in all lobes of the prostate using both elements of the ARR (Gingrich et al., 1996). In an effort to increase the efficiency of the PB-promoter, the isolation and utilisation of a larger 12kb fragment (large PB promoter, LPB) resulted in higher expression of the transgene specific to luminal epithelium. This occurs because elevated androgen levels during prostate maturation facilitates increased activity in the LPB promoter (Yan et al., 1997). To further augment the specificity of PB, two ARRs were added to the LPB, thus creating the now widely used ARR_2PB promoter. This was employed to drive Cre-recombinase within the prostate (PBCre4), resulting in superior luminal epithelium-specific expression (Wu et al., 2001), which abrogates the neuroendocrine phenotype of its predecessor PB-Cre (Maddison et al., 2000, Wu et al., 2001). PBCre4 will be discussed in more detail later in section 1.6.5. Schematic representations of the ARR_2PB and ARR_2PBCre (PBCre4) constructs are illustrated respectively in figure 20.

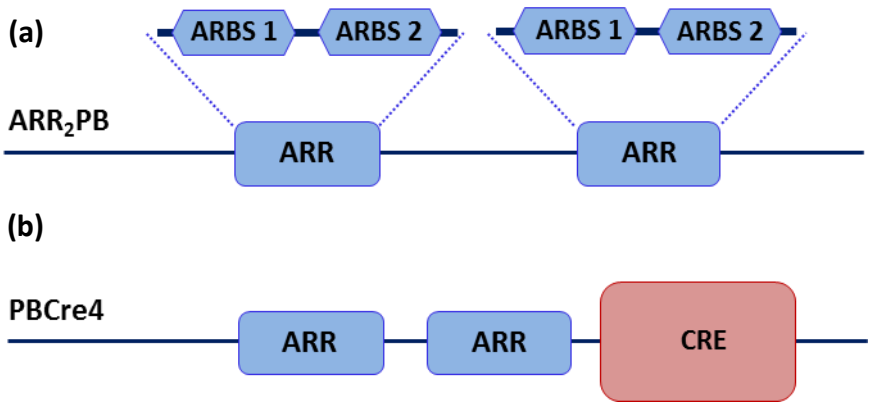

Figure 20: Structures of (a) the ARR_2PB construct and (b) the ARR_2PBCre (PBCre4) transgene. Each ARR contains two AR binding sites (ARBS) that results in higher transgene expression within the prostate epithelium than the outdated 1st generation PBCre construct (not shown), which comprised only one ARR. Adapted from Wu et al. (2001) and Kasper (2005).

1.6.3 Transgenic T-antigen models of prostate cancer

Early methods employed to genetically engineer mice involved the introduction of DNA constructs to induce the expression of oncogenes/oncoproteins under the control of tissue-specific promoters. To this effect, the first time PCa was modelled in this fashion was via the ectopic expression of simian virus 40 (SV40) Large T antigen (Tag) in the prostate. SV40 is defined as a DNA tumour virus. Its small genomic size prohibits it from encoding its own DNA polymerase and other proteins necessary for DNA replication. SV40 stimulates DNA synthesis through the expression of two viral proteins, the large-T and small-t antigens. Large-T binds to cell cycle 'gatekeeper' tumour suppressors within the host cell, such as p53 and pRb (retinoblastoma 1). The binding of T-antigen to both of these proteins, and their subsequent stabilisation, is required for the transforming ability of the virus (Chen and Paucha, 1990, Zhu et al., 1991) and leads to genetic and cell cycle instability. Small-t disrupts the activity of phosphatase 2A, resulting in constitutive MAPK activity and promoting tumour cell survival (Sontag et al., 1993). Overall, the SV40 antigen has been employed in many transgenic lines to promote prostate tumourigenesis, but the commonest two models to use this construct by far are the TRAMP and LADY models.

The transgenic adenocarcinoma of the mouse prostate (TRAMP) model is one of the most widely used transgenic mouse models to study PCa. Both the large and small SV40 tumour antigens (Tag/tag respectively) are controlled by the prostate-specific promoter, PB, to drive viral transgene expression solely within the prostate epithelium. TRAMP mice reportedly display prostate tumourigenesis with established kinetics (Gingrich et al., 1996): hyperplasia by 8-10 weeks, PIN by 18 weeks, and invasive carcinoma by 24 weeks. After 28 weeks all mice displayed lymphatic metastases (albeit rarely to the skeleton as seen in the advanced human disease), and of these approximately two-thirds displayed lung metastases (Gingrich et al., 1996). Furthermore when mice were castrated, 80% went on to develop prostate cancers that displayed more aggressive features and were more poorly differentiated (Gingrich et al., 1996), and interestingly were 2-fold more likely to metastasise than their un-castrated counterparts (Green et al., 1998) similar to patients with CRPC. Despite this the TRAMP model is not a panacea. The most frequent malignancy they predispose to is of a neuroendocrine phenotype (Chiaverotti et al., 2008), which does not parallel human PCa whereby cells are predominantly of epithelial origin. Regardless of its limitations, the TRAMP model is recognised as the best-characterised for PCa, having been used to study prevention, treatment, and progression to systemic disease.

The LPB promoter driving the large-T antigen (LADY) model is similar to the TRAMP model, but with two fundamental differences (Kasper et al., 1998). Firstly the LPB promoter was used to drive the large T-antigen, creating the LPB-Tag transgene rather than PB-Tag and PB-tag transgenes used in the TRAMP model. While the authors acknowledged that the PB promoter was sufficiently prostate specific, the transgene expression was variable between the founder cell lines, and thus this variability could be nullified and consistency restored by sole use of the LPB (Yan et al., 1997). Secondly, the LPB promoter was linked to a mutant SV40 T-antigen construct that had been erased of its small t-antigen. PIN develops by 10 weeks of age, and adenocarcinoma with neuroendocrine differentiation by 20 weeks. Metastasis to lymph nodes, liver and lungs was detected in several transgenic founder lines (Kasper et al., 1998).

Models utilising the PB promoter or part thereof, do not represent an ideal environment in which to investigate changes in hormone dependence (from androgen dependence to androgen independence/castration resistance) during tumour progression, since they employ androgen-responsive vectors fused to an oncogene. For example mice in the TRAMP model developed

fewer tumours when castrated at an early age, but this reduction in tumour incidence may be explained by the overall downregulation of PB, which resulted in a shorter duration of viral large-T antigen (Tag) driven expression. In other words, the tumours which arose in this model were androgen-independent from the beginning (Green et al., 1998). Tumours in the LADY model regressed upon castration and had their growth restored upon androgen replenishment, suggesting androgen dependency. Interestingly while no tumours recurred for up to 40 weeks in the face of castration, a small population of epithelial cells maintained their proliferative state which questioned the potential for castration-resistant growth in these cells (Kasper et al., 1998).

1.6.4 Cre-LoxP Technology

Before describing the evolution of conditional knockout models of PCa, it is important to consider the origin of Cre-LoxP technology. The Cre-LoxP system circumvents embryonic lethality, the major limitation of constitutive knockout models, as it is more specific to the organ of interest. 'Cre' is a gene that 'causes recombination', and catalyses site-specific DNA recombination in genes that are engineered with flanking 'LoxP' sites (locus of phage crossing over), which are synthetic 34-base pair sequences (Valkenburg and Williams, 2011). The system was first established after Cre recombinase was isolated from *E. coli* bacteria transfected with plaque-forming P1 phage (Sternberg et al., 1981, Sternberg and Hamilton, 1981). Eventually the technology was made more sophisticated for genetic recombination in eukaryotic cells; firstly yeast, and later in mice (Sauer and Henderson, 1989). Upon recombination, whereby floxed (flanked by LoxP sites) DNA is excised, a single LoxP site remains in the linear DNA. Meanwhile the process of reciprocal recombination produces a circular now redundant fragment of DNA containing the other LoxP site, which is rapidly degraded. These processes are depicted in figure 21.

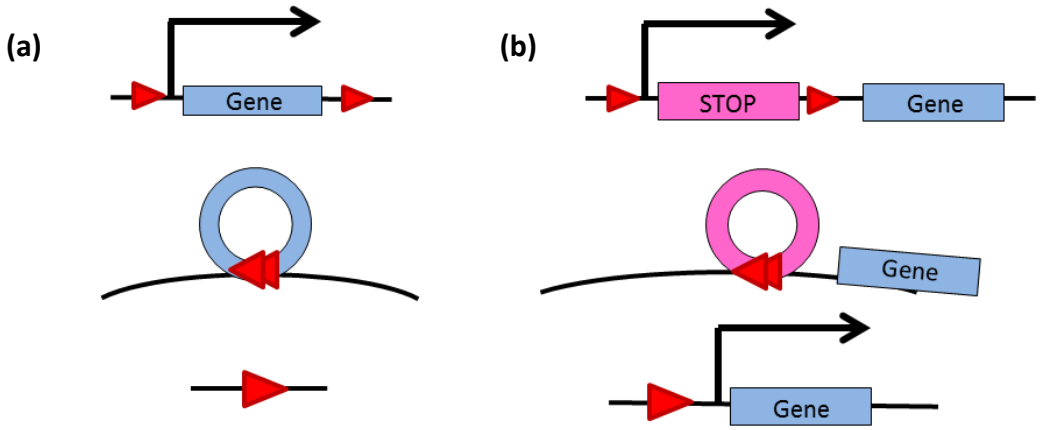

Figure 21: Schematic representation of the Cre-LoxP technology. Site-specific recombination through use of the Cre-LoxP technology can result in either (a) gene ablation or (b) gene activation. To this effect, exons essential for the normal functioning of a gene may be excised thus rendering it inactive, also known as a "conditional knockout". This is commonly used to silence tumour suppressor genes by flanking them with LoxP sites (floxing). Alternatively, signals that prevent gene expression, such as a "STOP" codon, may be silenced upstream of a target gene, resulting in transcription of a mutated proto-oncogene and thus its constitutively active protein. Adapted from Maddison and Clarke (2005)

The Rosa26 reporter construct has been widely used as a proxy of confirming the success (or otherwise) of endogenous recombination in the desired tissue (Soriano, 1999). The system employs a floxed NEO-STOP cassette located upstream of the LacZ reporter gene, and upon recombination, excision of the STOP codon results in transcription of β-galactosidase. Successful expression of Cre-recombinase is monitored thus by the appearance of a blue product in the tissue of interest after staining with X-gal (Soriano, 1999). The Rosa26 gene is constitutively expressed in every cell of the embryo and adult, but does not encode a functional LacZ product in the absence of recombination. Figure 22 is an illustrative representation of the Rosa26 reporter construct.

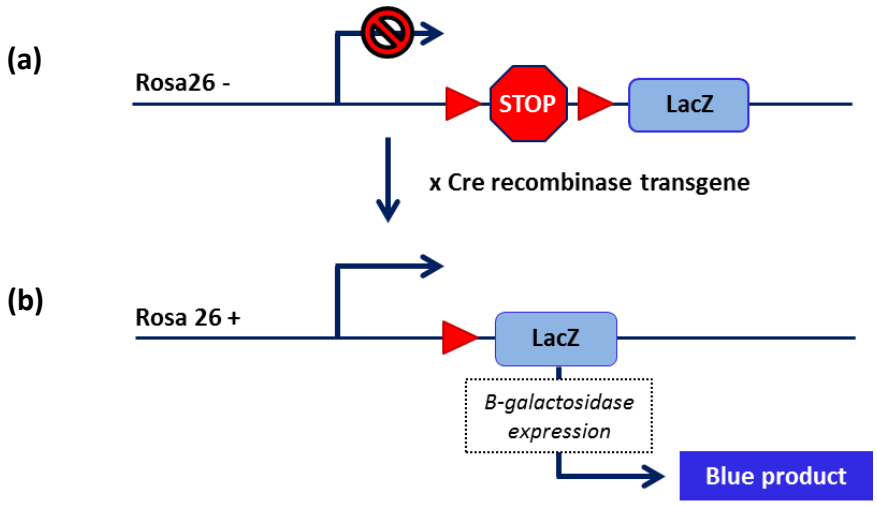

Figure 22: Mechanism of action of the Rosa26 reporter system. In (a) the absence of the Rosa26 locus, transcription will not occur due to the presence of the floxed STOP codon. Upon DNA recombination (via a tissue/site specific Cre recombinase), the STOP codon is excised (b) and LacZ is constitutively activated resulting in the expression of β-galactosidase and the formation of a blue product when stained with X-gal. Adapted from Soriano (1999). See mouse model chapter for utilisation of this technique.

DNA recombination that results from Cre-LoxP technology is typically under the control of a tissue-specific promoter, which serves to drive Cre recombinase expression either constitutively, or by induction. This enables the study of genes of interest in tissues of interest, which has led to the extensive search for powerful, specific promoters that minimise background recombination in other tissues.

1.6.5 Conditional knockout models of prostate cancer

Prostate-specific antigen has been employed as a promoter to drive Cre recombinase (PSA-Cre) expression in two important models of prostate tumourigenesis, namely conditional knockouts of Nkx3.1 (Abdulkadir et al., 2002) and Pten (Ma et al., 2005). Mice from the former model develop lesions consistent with hyperplasia and PIN thus supporting a role for Nkx3.1 in the early stages of PCa. Pten knockout mice also display hyperplasia to PIN transformation, and also progress to invasive carcinoma but with infrequent lymph node metastases.

The ARR_2PB-Cre (PBCre4) transgene is the most widely used promoter in PCa conditional knockout models. It has successfully facilitated recombination in all lobes of the murine

prostate but not in the embryo; >95% of the lateral lobe of the prostate, 50% of the ventral lobe, and about 10% and 5% of the epithelium of the dorsal and anterior lobes respectively (Wu et al., 2001). Many genes implicated in human PCa have been knocked out in this fashion and the important models driven by the PBCre4 transgene are shown in table 8 below. To date however, the only model reported to span the continuum from PCa initiation to locally invasive carcinoma and metastatic disease is the PBCre4PTEN^{flox} knockout model (Wang et al., 2003).

Conditional Knockout Model (PBCre4)	Terminal stage of neoplasia	Other tissues affected	References
Pten^{flox}	LN & lung metastases	None	Wang et al. (2003)
Rb^{flox}	Hyperplasia	None	Maddison et al. (2004), Zhou et al. (2006)
LSL-Ph15LO-1 (FLiMP)	PIN	None	Kelavkar et al. (2006)
p53^{flox} Rb^{flox}	LN, lung, liver, and adrenal metastases	None	Maddison et al. (2004), Zhou et al. (2006)
APC^{flox}	Locally invasive adenocarcinoma	None	Bruxvoort et al. (2007)
IGF-1^{flox}	Hyperplasia	None	Sutherland et al. (2008)
Catnb$^{+/lox(ex3)}$	Locally invasive adenocarcinoma	Metaplasia of G.U.T. accessory glands	
Kras$^{+/V12}$	LGPIN	None	Pearson et al. (2009)
Catnb$^{+/lox(ex3)}$Kras$^{+/V12}$	Locally invasive adenocarcinoma	As above	
Catnb$^{+/lox(ex3)}$	HGPIN	None	Yu et al. (2009), Francis et al. (2013)
BRCA2^{flox} p53^{flox}	HGPIN	None	Francis et al. (2010)
Pten^{flox} Kras$^{G12D/W}$	LN & lung metastases	None	Mulholland et al. (2012)
Catnb$^{+/lox(ex3)}$ Pten^{flox}	Locally invasive adenocarcinoma	None	Francis et al. (2013)

Table 8: The conditional knockout models of PCa governed by the PBCre4 transgene

The Pten gene is one of the most scrutinised in PCa, particularly in the pre-clinical setting since the creation of the conditional knockout mouse (Trotman et al., 2003, Wang et al., 2003). It has been shown that the degree of Pten knockdown on tumour progression is dose-related

(Trotman et al., 2003), given that Pten is a negative regulator of the PI3K/Akt pathway (see section 1.8.2). Loss of heterozygosity of Pten leads to a shortened latency of PIN formation, which is of higher grade when comparing the constitutively active heterozygote Pten mouse ($Pten^{+/-}$) with Pten hypomorphs ($Pten^{hy/-}$). Furthermore, conditional inactivation of Pten has complete penetrance, with the resulting carcinomas being poorly differentiated and diffuse. A separate group has reported how the *PBCre4Pten*^{flox} mouse progressed through stages of prostate tumourigenesis with set kinetics, eventually developing metastatic disease (Wang et al., 2003). In addition, evidence for castration resistant cells was strengthened in this model. Invasive Pten null prostate cancer cells responded to androgen ablation, as indicated by increased apoptosis, similar to most human PCa. However, even though the survival of Pten null prostate cancer cells was seen to be androgen sensitive, their proliferation continued in the face of castration (Wang et al., 2003). Thus the property of androgen-independent growth observed in Pten null prostate cancers may contribute to CRPC formation. Although prostate tumours in the PBCre4Pten^{flox} mouse do not metastasise to bone, it still continues to be one of the most useful models in the study and characterisation of PCa.

Two models have been created by knocking out tumour suppressors Rb and p53, alone or in combination. As a solitary knockout, the most severe prostate phenotype observed from solitary Rb deletion was hyperplasia and low-grade PIN, concluding that Rb loss alone was insufficient to cause progression to carcinoma (Maddison et al., 2004). A similar conclusion was drawn from the conditional p53 knockout (Zhou et al., 2006), but in combination, both Rb loss and p53 loss synergised to form metastatic PCa (Zhou et al., 2006) suggesting that they cooperate in the prostate during tumour progression and metastasis. Therefore, the *PBCre4p53*^{flox}*Rb*^{flox} mouse embodies a valuable model for studying PCa short of skeletal metastasis.

The Wnt pathway has also been identified as being important in PCa development. To investigate the effect of deregulated Wnt signalling on the prostate, a conditional APC (adenomatous polyposis coli) knockout mouse has been created. APC is a known negative regulator of the Wnt pathway, and hence its knockout will result in constitutively active Wnt signalling. Locally invasive adenocarcinoma was the terminal stage of disease seen in the *PBCre4APC*^{flox} model (Bruxvoort et al., 2007). In this model, that contained experiments analogous to those in the *PBCre4Pten*^{flox} paper (Wang et al., 2003), castration after the onset of

tumourigenesis resulted in retention of adenocarcinoma, indicating that although tumours are androgen dependent for their initiation, they may be androgen-independent during tumour maintenance and progression (Bruxvoort et al., 2007). Later, models to explore the role of Wnt signalling in PCa employed the β-catenin knock-in model (Pearson et al., 2009, Yu et al., 2009, Francis et al., 2013), whereby β-catenin is overexpressed in its constitutively active form (*PBCre4Catnb*$^{+/lox(ex3)}$). Due to the accumulating evidence that the Wnt pathway/β-catenin is upregulated in PCa, this model remains worthwhile. There is conflicting evidence between groups that have worked with the *PBCre4Catnb*$^{+/lox(ex3)}$ mouse on the highest stage of tumourigenesis. As a solitary mutation, this has been reported to display HGPIN (Yu et al., 2009, Francis et al., 2013) and invasive adenocarcinoma (Pearson et al., 2009).

T-antigen models have predominantly been utilised to overexpress activating mutations in *Ras* isoforms, principally *Hras*. In so doing, they have generated a variety of low-grade prostate phenotypes, including hyperplasia, low-grade PIN, and intestinal metaplasia, probably reflecting subtle differences in the transgenes and the genetic background used (Barrios et al., 1996, Scherl et al., 2004). Conditional knock-in models have focused on activating mutations of *Kras* due to the more recent discovery of its higher incidence in PCa. Similarly these support the notion that *Kras* activation is sufficient to drive the *RAS/MAPK* pathway but is insufficient to initiate cancer, amounting to LGPIN only. Together, these models show that activated *Ras* can facilitate prostate tumourigenesis and early stage tumour development. However, in combination with other alleles to form double mutants, *Kras* has demonstrated synergy to promote progression to invasive carcinoma in the *PBCre4Catnb*$^{+/lox(ex3)}$*Kras*$^{+/V12}$ mouse (Pearson et al., 2009), and even metastatic disease in the *PBCre4Pten*^{flox} *Kras*$^{G12D/W}$ model (Mulholland et al., 2012). This appears to parallel the findings displayed in human PCa that *RAS/MAPK* pathway activation contributes toward progression of advanced disease.

Figure 23 quantifies the incidence of some of the more important aberrations seen in human PCa, which further adds weight to the relevance of studying these mutations in conditional knockout mouse models.

RB signalling		PI3K signalling		MAPK signalling	
Primary	Metastatic	Primary	Metastatic	Primary	Metastatic
34%	74%	42%	100%	43%	90%

RB1		PTEN		KRAS	
5%	37%	4%	42%	8-10%	32%

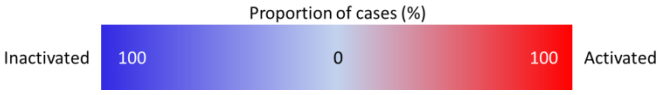

Figure 23: Three of the most commonly altered pathways in PCa: RB, PI3K, and RAS/RAF. Copy number alteration, transcriptome, and mutation data were combined to conduct analysis of core pathways. Alteration frequencies are shown for individual genes and the entire pathway in primary and metastatic tumours. The incidence of inactivation/downregulation highlighted shown in blue, whereas activation/upregulation is shown in red. Adapted from Taylor et al. (2010).

1.7 β-CATENIN

β-Catenin is a dual function protein, encoded by the CTNNB1 gene on chromosome 3 in humans and chromosome 9 in the mouse. It is a sub-unit of the cadherin complex and so plays a key role in regulating cell-cell adhesion, in addition to its role as an intra-cellular signal transducer in the Wnt signalling pathway where it is responsible for governing gene transcription.

1.7.1 The structure and function of β-catenin

The structure of β-catenin can be simplified into three main regions: an N-terminus, a central core, and a C-terminus. The N-terminal domain comprises of 130 amino acids and possesses phosphorylation sites that are targets of casein kinase 1α or 1ε (epsilon) (CK1α/ε), and GSK-3β, in addition to an α-catenin binding site (Kolligs et al., 2002). The N-terminus is also critical for β-catenin degradation owing to the conserved location of the short linear motif responsible for binding β-TrCP E3 ubiquitin ligase upon its phosphorylation. The central core is the best characterised of all three regions. It consists of 12 armadillo repeats, each being 42 amino acids long, which adopt a super-helical shape with a positively-charged groove running along its length (Clevers, 2006). This region interacts to form complexes with molecules such as axin,

APC, E-cadherin, and TCF (T-cell factor)/LEF (lymphoid enhancer factor) proteins, which all bind to this region in a mutually exclusive fashion (Clevers, 2006). The C-terminus appears to be a powerful transactivator of Wnt target genes when recruited into DNA, but it has also demonstrated interactions with transcriptional inhibitors, highlighting its importance in regulating the level of gene transcription (Xing et al., 2008). The C-terminal domain may also form interactions within the central armadillo repeat domain of its own β-catenin molecule to regulate ligand binding (Cox et al., 1999, Piedra et al., 2001, Castano et al., 2002, Solanas et al., 2004). The structure of the β-catenin molecule is depicted in figure 24.

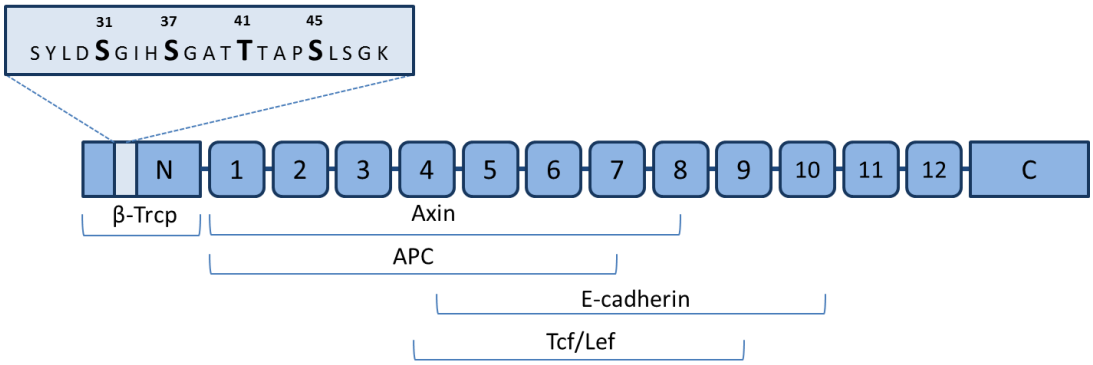

Figure 24: The molecular structure of β-catenin. The N and C termini of β-catenin serve as transcriptional activators. The central highly homologous armadillo repeats mediate most interactions with other proteins. Serine and threonine residues 33, 37 and 41 (see lighter insert) are the GSK-3 phosphorylation sites, whereas serine 45 is the CK1 phosphorylation site. Mutation of one of these residues prevents degradation of β-catenin. Adapted from Kolligs et al. (2002).

β-catenin is found in three distinct pools (Nollet et al., 1996) – at the membrane, along with cell adhesion molecules such as E-cadherin and α-catenin; in the cytoplasm; and in the nucleus, to where it translocates in response to Wnt signalling before driving gene transcription of downstream Wnt targets. Other well-known catenin molecules worthy of note are are α-, γ-catenin (or plakoglobin) and p120 catenin (p120ctn). β- and γ-catenin are members of the armadillo family and are mammalian orthologues of Armadillo (Arm), the historical name of the β-catenin gene found in the fruit fly Drosophila (Clevers, 2006). Both of these armadillo family proteins as well as p120ctn bind to E-cadherin in adherens junctions via their armadillo repeat sequences, while α-catenin binds to β-catenin to link the cadherin:catenin complexes to actin filaments (Niessen, 2007). The cadherin:catenin complexes are one of the two basic units of adherens junctions (along with nectin:afadin complexes) (Niessen, 2007), and it is well regarded

that β-catenin is critical to the maintenance of epithelial cell adhesion. Figure 25 demonstrates the spatial arrangement of the molecules that comprise a normal adherens junction.

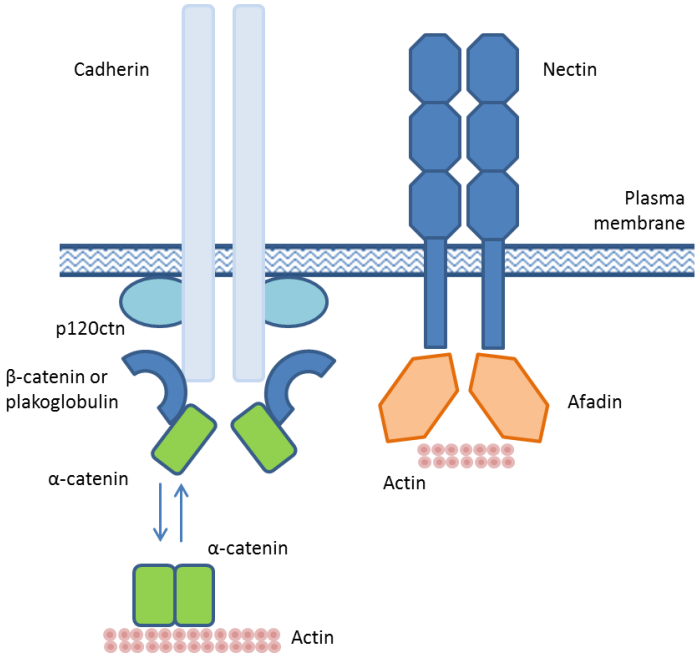

Figure 25: the structure of adherens complexes. Adapted from Niessen (2007)

β-catenin is the fundamental mediator of Wnt signalling. Three different Wnt pathways are in existence and are activated in the presence of Wnt ligand; the canonical Wnt pathway, the non-canonical planar cell polarity pathway (PCP) pathway, and the non-canonical Wnt/Ca^{2+} pathway. The canonical pathway is the best characterised of all three and will be explored in more detail here.

In the absence of Wnt ligand the degradation complex forms, comprising of APC, GSK3β and the important scaffold protein axin (Bienz and Clevers, 2000). CK1 is then recruited to the complex where it can phosphorylate β-catenin at Ser45 in preparation for further phosphorylation at Ser33, Ser37, and Thr41 by GSK3β (Hagen and Vidal-Puig, 2002). In turn, β-TrCP (a dedicated SCF-type (Skp, cullin, F-box) E3 ubiquitin ligase) joins the complex (Maniatis, 1999), which results in the ubiquitination and destruction of β-catenin by the proteosome (Aberle et al., 1997). GSK3β is a powerful phosphorylator, capable of also phosphorylating axin to regulate its stability (Yamamoto et al., 1999), and APC to maintain its binding efficiency to β-catenin (Rubinfeld et al., 1996). To ensure that TCF-mediated transcription does not occur in the

absence of Wnt ligand, the molecule Groucho binds TCF (Roose et al., 1998, Cavallo et al., 1998) and thereby recruits histone deacetylases to promote chromatin compaction (Chen et al., 1999) and inhibit transcription.

Wnt proteins are a diverse family of secreted cysteine-rich, lipid-modified signaling glycoproteins that are 350–400 amino acids in length, and highly conserved throughout most mammalian species (Cadigan and Nusse, 1997). Lipid modification is essential because it initiates targeting of the Wnt protein to the plasma membrane for secretion and it allows the Wnt protein to bind its receptor due to the covalent attachment of fatty acids. In Wnt signaling, these glycoproteins act as ligands to activate the different Wnt pathways via paracrine and autocrine routes (Nusse and Varmus, 1992, Komiya and Habas, 2008).

When present, extracellular Wnt ligand binds to Frizzled (Fz) a seven-pass transmembrane receptor, and in doing so it cooperates with co-receptors of the low density lipoprotein receptor (LRP) family, namely LRP-5 or LRP-6 (Clevers, 2006). Upon activation, Fz recruits dishevelled (Dsh) to the inner cell membrane by its phosphorylation (Axelrod et al., 1998, Lee et al., 1999b, Smalley et al., 1999, Boutros et al., 2000), which in turn activates axin by direct binding (Smalley et al., 1999, Kishida et al., 1999). Actin translocates to the membrane where it disintegrates the APC/Axin/GSK-3β complex by articulating with the LRP intracellular tail, resulting in the inhibition of GSK-3β-dependent phosphorylation of β- catenin and therefore its stabilisation (Kishida et al., 1999). Within the nucleus, β-catenin displaces groucho from its binding with TCF and takes its place to form a transcription complex (Behrens et al., 1996, Molenaar et al., 1996) that drives the expression of numerous Wnt target genes including CD44 (Wielenga et al., 1999), cyclin D1 (Shtutman et al., 1999), c-myc (He et al., 1998) and MMP-7 (Crawford et al., 1999). The mechanism of action in the Wnt signalling pathway is illustrated in figure 26.

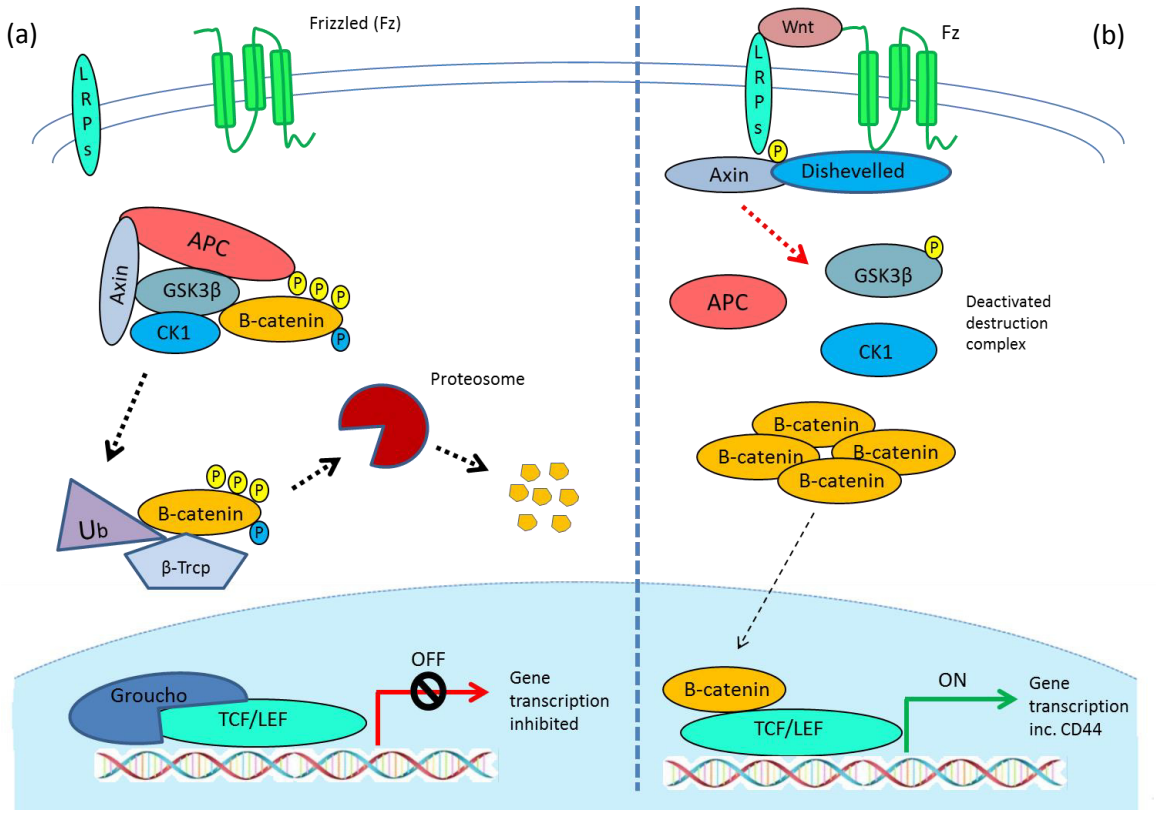

Figure 26: The Wnt pathway. In the absence of Wnt ligand (a) β-catenin is phosphorylated and therefore inactivated by the destruction complex. Following ubiquitination by β-Trcp it is targeted for rapid destruction by the proteasome. Meanwhile in the nucleus, groucho represses gene transcription. When Wnt ligand is present (b) the destruction complex is inhibited allowing β-catenin to accumulate in the cytoplasm. Upon its translocation into the nucleus, it binds Tcf/Lef to stimulate transcription of downstream Wnt targets. Adapted from MacDonald et al. (2009).

1.7.2 The role of β-catenin in cancer

Dysregulation of Wnt signalling is implicated in many types of cancer. Mutations in the proto-oncogene β-catenin specifically have been detected in around 5% of prostate cancers (Voeller et al., 1998), as well as cancers of the colon and rectum (Iwao et al., 1998), liver (Miyoshi et al., 1998), gallbladder (Yanagisawa et al., 2001), ovary (Wright et al., 1999) and melanocytes in the skin (Rimm et al., 1999). The most common mutation to be studied in these cancers occurs on exon 3 of the CTNNB1 gene that encodes for β-catenin. Other mutations of the CTNNB1 gene outside exon 3 that may result in altered Wnt signalling remain under investigation, such as the sequence encoding the section of β-catenin that interacts with a molecule responsible for its ubiquitination, Siah-1 (Yardy and Brewster, 2005). Generally speaking the role of stabilising

mutations of β-catenin in carcinogenesis could be attributed to a combination of one or more of the following mechanisms: (a) nuclear accumulation of β-catenin leading to over-expression of Wnt target genes responsible for driving proliferation, survival and cell migration, (b) interruption of the role β-catenin plays in cell to cell adhesion complexes with E-cadherin resulting in increased cell motility and possibly metastasis, and finally (c) the role of activated β-catenin in SC maintenance and/or differentiation.

1.8 PTEN

Pten has been discussed in some detail earlier in the "constitutive/germline models of PCa" section. Here we will talk about its structure and function, along with its role in the PI3K/Akt/mTOR pathway, and finally evidence for its role in carcinogenesis.

1.8.1 PTEN structure and function

PTEN is a 403-amino-acid-long phosphatase that can act on both polypeptide and phosphoinositide substrates (Song et al., 2012). Detailed insight into the complex three-dimensional folding of PTEN was demonstrated by crystallography (Lee et al., 1999a). Simplified, the important features of its structure are the phosphatase-binding domain, a phosphatase domain, and the C2 domain. The substrate-binding loop at the bottom of the active pocket, that is both deep and wide in shape and positively-charged, is important for the accommodation of phosphoinositide substrates (Song et al., 2012). This primitve PTEN-specific binding pocket is formed by folding of its β-sheet configuration, and appears to be evolutionarily conserved. It is the site of cancer-associated PTEN mutations that lead to a reduction of its phosphatase activity (Maehama and Dixon, 1998, Stambolic et al., 2000). Meanwhile the C2 domain binds the phospholipid membrane along its length, thus bringing the active site to the membrane-bound PIP_3 to de-phosphorylate it (Song et al., 2012).

As a participant in the PI3K/Akt/mTOR pathway, PTEN has many physiological roles in the normal cell including, (a) participation in glucose metabolism, cell motility and cell polarity, (b) induction and maintenance of cellular senescence, (c) involvement in the self-renewal capability of SC/CSCs, and (d) control of genomic stability and cell cycle progression within the nucleus (Song et al., 2012). PTEN also has effects independent of PI3K/Akt/mTOR signalling including activation of the JNK pathway in response to inflammation and UV radiation (Vivanco, 2007),

and activation of non-receptor tyrosine kinases that are important in immune system signal transduction (Zhang, 2011). The structure of PTEN is shown in figure 27.

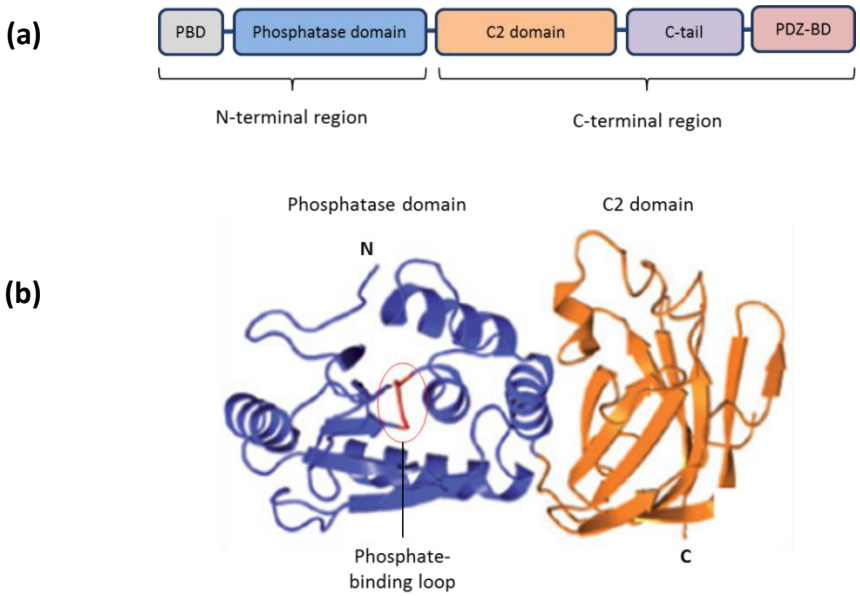

Figure 27: The structure of PTEN. (a) PTEN is a protein comprised of five domains; a PIP2 binding domain (PBD), a phosphatase domain, a C2 domain, a carboxy terminal tail, and a postsynaptic-density protein of 95 kDa, discs large, zona occludens-1 binding domain (a protein-interaction domain that often occurs in scaffolding proteins). (b) The overview of the PTEN protein structure allows spatial awareness of how the phosphate-binding loop (encircled red) is housed deep within the active pocket of the phosphatase domain (dark blue).N, N-terminal region; C, C-terminal region. Adapted from (Chalhoub and Baker, 2009) and Song et al. (2012).

1.8.2 *The role of PTEN in PI3K/Akt/mTOR signalling*

The powerful catalytic phosphatidylinositol (3,4,5)-triphosphate (PIP3) lipid phosphatase activity of PTEN makes it one of the most important tumour suppressors reported, as highlighted in figure 28. Following PTEN loss, excessive PIP3 recruits and activates Akt and PDK1 to cell membranes. Akt isoforms are activated by phosphorylation at two different residues: PDK1 phosphorylates Akt at Thr308 (Manning and Cantley, 2007), and Ser473 is phosphorylated by mammalian target of rapamycin complex 2 (mTORC2; composed of mTOR, DEP domain-containing mTOR-interacting protein (DEPTOR), mammalian lethal with SEC13 protein 8 (mLST8), stress-activated MAP kinase-interacting protein 1 (mSIN1; also known as MAPKAP1), Pro-rich protein 5 (PRR5; also known as PROTOR) and rapamycin insensitive companion of mTOR (RICTOR)) (Zoncu et al., 2011). Active Akt drives cell survival, proliferation

and cellular metabolism through inhibitory phosphorylation of downstream proteins, including glycogen synthase kinase 3 (GSK3), forkhead box O (FOXO), peroxisome proliferator-activated receptor-γ (PPARγ) co-activator 1α (PGC1) and p27, and through activatory phosphorylation of ectonucleoside triphosphate diphosphohydrolase 5 (ENTPD5), sterol-responsive element-binding protein 1C (SREBP1C), AS160 and S phase kinase-associated protein 2 (SKP2) (Manning and Cantley, 2007). AKT can also directly phosphorylate tuberous sclerosis protein 2 (TSC2; also known as tuberin), which in a complex with TSC1 largely inhibits the RAS-related small GTPase RAS homologue enriched in brain (RHEB). Phosphorylation of TSC2 by Akt results in the activation of RHEB, which then stimulates the phosphotransferase activity of mTOR (Guertin and Sabatini, 2007). Akt is capable of activating mTORC1 (composed of mTOR, DEPTOR, mLST8, 40 kDa Pro-rich AKT1 substrate 1 (PRAS40; also known as AKT1S1) and regulatory associated protein of mTOR (RAPTOR)) by inducing the inhibitory phosphorylation of PRAS40, which is a negative regulator of mTORC1 (Vander Haar et al., 2007, Zoncu et al., 2011). Active mTORC1 phosphorylates p70 ribosomal protein S6 kinase (S6K; also known as RPS6K) to activate protein translation in the ribosome (Ma and Blenis, 2009).

1.8.3 PI3K/Akt/mTOR signalling in cancer

The contribution of aberrant PI3K/Akt/mTOR signalling towards cancer development can be appreciated in three broad areas: firstly the cellular processes regulated by AKT, secondly characteristic cancer processes that exploit PI3K/Akt signalling, and finally the genetic alterations that can influence the pathway.

Akt impacts upon the function of numerous molecules involved in the regulation of cell survival, cell cycle progression and cellular growth, and their aberrant activation can result in a richly pro-tumourigenic environment (Fresno Vara et al., 2004). Abundant Akt induces various cell survival mechanisms; inactivation (by phosphorylation) of the pro-apoptotic factors Bcl-2 associated agonist of cell death (BAD) and caspase-9, as well as the Forkhead family of transcription factors that induce the expression of pro-apoptotic factors such as Fas ligand (Testa and Bellacosa, 2001). Other Akt targets such as GSK3β, mTOR, insulin receptor substrate-1 (IRS-1), the cyclin-dependent kinase inhibitors $p21^{CIP1/WAF1}$ and $p27^{KIP1}$, and Raf1, are all involved in protein synthesis, glycogen metabolism and cell cycle regulation (Blume-Jensen and Hunter, 2001).

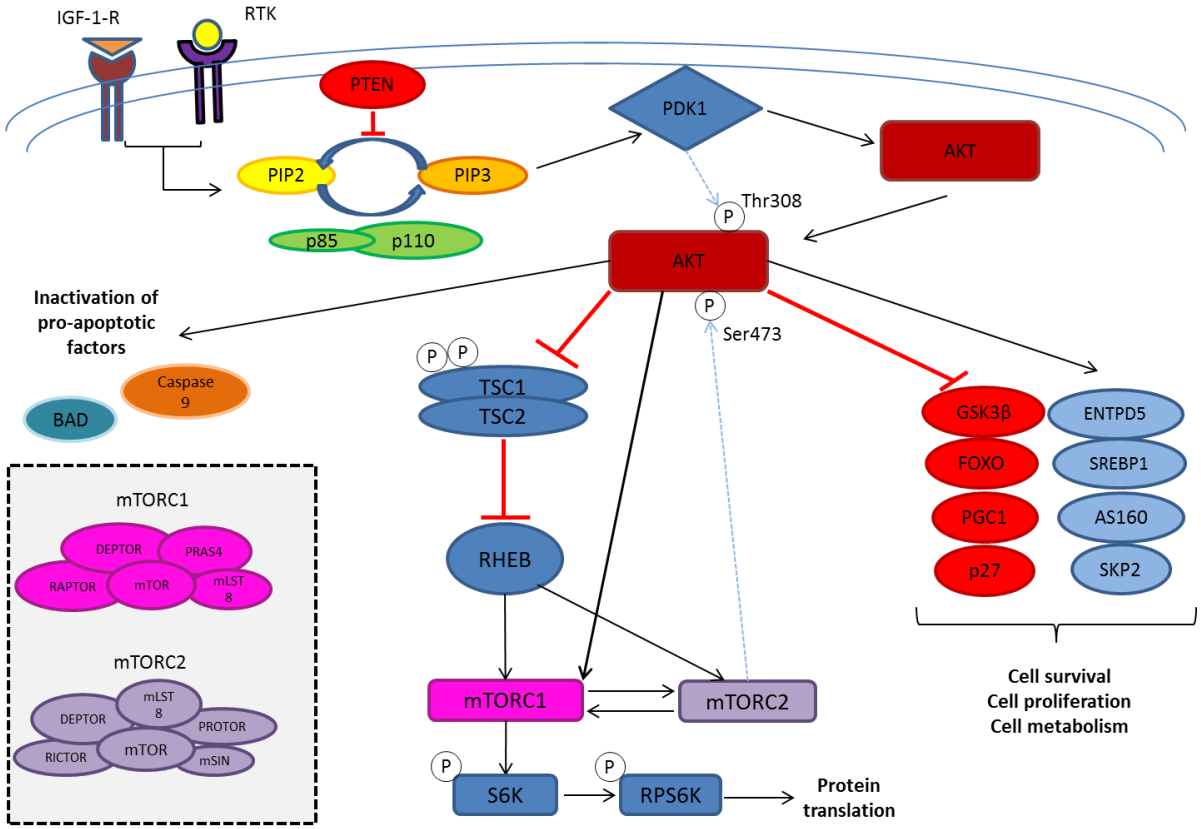

Figure 28: The PI3K/Akt/mTOR signalling pathway. Upstream activation of Akt by receptor tyrosine kinases (RTK) and insulin-like growth factor-1 receptor (IGF-1-R) trigger pathway signalling. Once activated, Akt phosphorylates a number of substrates in the cytoplasm and nucleus. Akt targets include: the pro-apoptotic Bcl-2 family member Bad, and procaspase-9; tuberous sclerosis complex 2 (TSC-2); glycogen systhesis kinase-3 (GSK3β), the forkhead family of transcription factors (FOXO), peroxisome proliferator-activated receptor-γ (PPARγ) co-activator 1α (PGC1) and the CDK inhibitor p27 through inhibitory phosphorylation; and through activatory phosphorylation ectonucleoside triphosphate diphosphohydrolase 5 (ENTPD5), sterol-responsive element-binding protein 1C (SREBP1C), AS160 and S phase kinase-associated protein 2 (SKP2). The p85 and p110 subunits are collectively known as PI3K. Black lines – direct activation, blue dotted lines – activation by phosphorylation, red lines – activation by inhibitory phosphorylation. Adapted from (Chalhoub and Baker, 2009) and Song et al. (2012).

Akt-regulated signalling plays a prominent role in numerous processes which are known to be characteristic of cancer (Fresno Vara et al., 2004). Akt overexpression may result in the following: increased ambient levels of growth factors causing growth autonomy, insensitivity of antiproliferative signals, heightened telomerase activity and thus greater replicative potential by phosphorylation of hTERT, stimulated angiogenesis through endothelial nitric oxide synthetase activation, secretion of matrix metalloproteinases and progression to metastasis by creation of tumour-permissive stroma (Trimboli et al., 2009).

Amplification is the major alteration described to occur in PI3KC (located in the chromosome 3q26), the gene that encodes for the p110a subunit of PI3K, and this alteration has been implicated in ovarian (Shayesteh et al., 1999) and cervical cancer (Ma et al., 2000). No mutations in the Akt gene have been discovered in humans but studies have reported amplifications in breast, ovarian, pancreatic, and stomach cancers (Bellacosa et al., 1995, Cheng et al., 1996).

1.9 RAS: THE PROTO-ONCOGENE

Ras is a small membrane-bound GTPase that is involved in cellular signal transduction ultimately leading to cellular proliferation. In this section the structure and function will be discussed, followed by the role of Ras in MAPK signalling, and finally its role in tumourigenesis.

1.9.1 The structure and function of Ras

In humans, three RAS genes encode four distinct Ras proteins of similar structure: HRAS (Harvey rat sarcoma viral oncogene homolog), NRAS (neuroblastoma RAS viral oncogene homolog), and KRAS (Kirsten rat sarcoma 2 viral oncogene homolog), where KRAS4A and KRAS4B are alternative splice variants of the KRAS gene (Pylayeva-Gupta et al., 2011). The four Ras isoforms are similar throughout the G domain (amino acids 1–165). The first 85 amino acids are identical in all four proteins and specify the guanosine diphosphate (GDP) and guanosine triphosphate (GTP) binding site. This includes the phosphate-binding loop (P loop), amino acids 10–16, responsible for binding the γ (gamma)-phosphate of GTP, and switches I (amino acids 32–38), and II (amino acids 59–67) which regulate binding to Ras regulators and effectors. Amino acids 85–165 show approximately 85–90% sequence homology, whereas the C-terminal hypervariable domain (amino acids 165–188/189) specifies membrane localisation unique to each isoform (Schubbert et al., 2007, Pylayeva-Gupta et al., 2011). An illustration of its structure can be seen in figure 29.

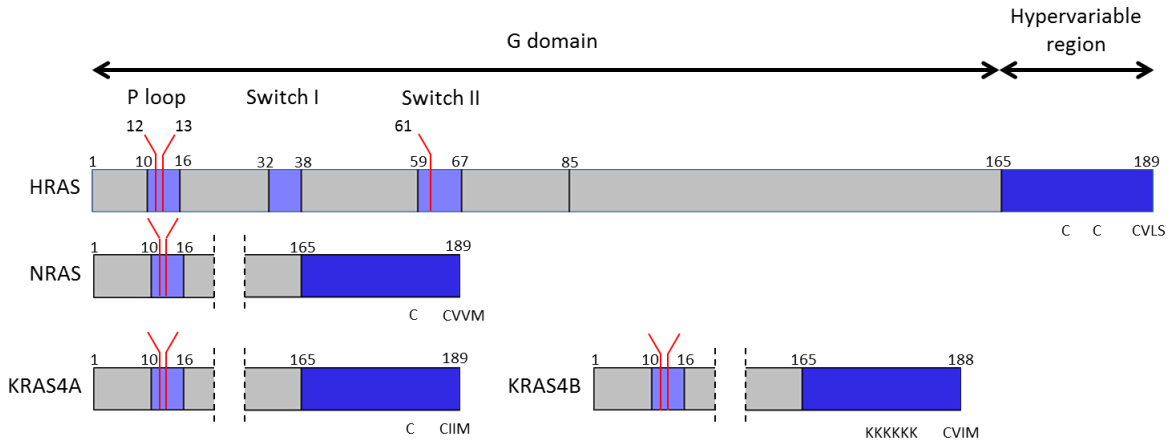

Figure 29: The structure of the four Ras isoforms. Given that a significant proportion of the G-domain (amino acids 85-165) is up to 90% homologous between isoforms, these sections have been truncated for Nras and Kras. Most somatic missense Ras mutations found in human cancers introduce amino acid substitutions at positions 12, 13 and 61. The P loop articulates with GTPase activating proteins (GAPs) that mediate the Ras-GTP hydrolysis reaction. Switches I and II are important for binding to Ras effectors. Amino acids in the hypervariable region: C, cysteine; I, isoleucine; K, lycine; L, Leucine; M, methionine; S, serine; and v, valine. Adapted from Pylayeva-Gupta et al. (2011) and (Prior et al., 2012).

Upon the binding of growth factors to membrane-bound receptor tyrosine kinases (RTKs) guanine nucleotide exchange factors (GNEFs) are free to activate GTPases. In this fashion GTPases (such as Ras proteins) can cycle between 'on' and 'off' conformations by the binding of GTP and GDP, respectively. Under physiological conditions GNEFs stimulate GDP for GTP exchange, whereas GTPase-activating proteins (GAPs) accelerate GTP hydrolysis back to GDP (Pylayeva-Gupta et al., 2011). In the case of Ras, activated RTKs stimulate the binding of intracellular proteins that possess SH2 (Src homology 2) domains such as SHC (SH2-containing protein), GRB2 (growth factor receptor-bound protein 2), and Gab (GRB2-associated binding), which when bound to activated RTKs, can recruit additional proteins. GRB2 binds a GNEF called SOS1 (son of sevenless) that is capable of activating Ras by stimulating it to release GDP in exchange for GTP. This process is depicted in figure 30.

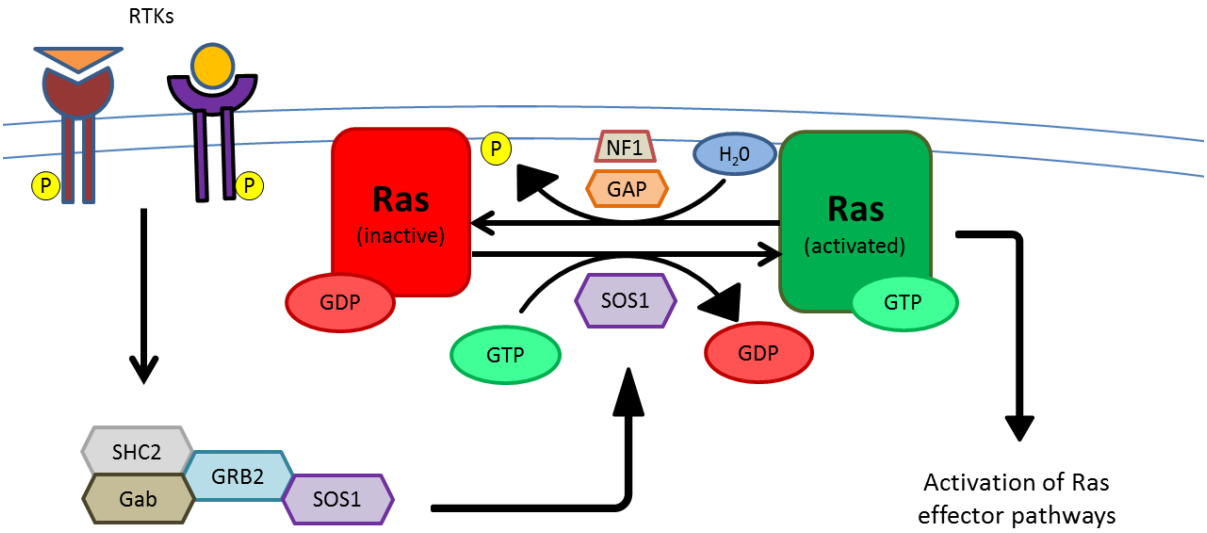

Figure 30: Schematic representation of Ras activation. SOS1 (a GNEF) functions to dissociate GDP from inactive Ras proteins and once released, GTP generally binds in its place because the cytosolic ratio of GTP to GDP is 10:1 (Bos et al., 2007). Formation of Ras-GTP releases SOS1 and thus renders it free to re-activate a new Ras protein. GAPs serve to inactivate GTPases by increasing their intrinsic rate of GTP hydrolysis, and neurofibromin (NF1) is one specific negative regulator of Ras signalling that is capable of exploiting this mechanism.

1.9.2 The role of Ras in MAPK signalling

Ras-GTP regulates a complex signalling network that modulates cell behaviour by binding to and activating many distinct classes of effector molecules. Perhaps the best described of these is the Raf–Mek–Erk signalling cascade (also known as the MAPK (mitogen activated protein kinase) pathway). There are three Raf serine/threonine kinases (ARAF, BRAF and RAF1) that can activate Mek, which in turn activates Erk by phosphorylation. Activation of these transcriptional regulators can lead to the expression of proteins responsible for control of cell-cycle progression, such as cyclin D1 (Pylayeva-Gupta et al., 2011).

1.9.3 The role of Ras in cancer

The COSMIC (Catalog of somatic mutations in cancer) dataset confirms that K-ras is the most frequently mutated isoform (Forbes et al., 2011). It was found to be present in 22% of all tumours analysed, compared with 8% for N-ras and 3% for H-ras (Prior et al., 2012).

The aberrant function of oncogenic Ras is typically associated with a single missense mutation at codon 12, 13, or 61. The predominant outcome of these somatic mutations is the attenuation of GTP hydrolysis by hindering the action of GAPs. The outcome of these substitutions therefore is the persistence of the GTP-bound state of Ras and, as a consequence, the constitutive activation of a multitude of *RAS*-dependent downstream effector pathways (Schubbert et al., 2007, Pylayeva-Gupta et al., 2011, Prior et al., 2012).

The extent to which specific mutations affect the biological behaviour of Ras remains to be established (Pylayeva-Gupta et al., 2011). In colorectal and lung cancers, $KRAS^{G12V}$ mutations have been associated with a poorer prognosis than $KRAS^{G12D}$ mutations, raising the possibility that particular amino acid substitutions might dictate specific transforming characteristics of oncogenic *Ras* alleles (Keohavong et al., 1996, Andreyev et al., 1998). However in studies on leukaemia (Perentesis et al., 2004), bladder cancer (Kompier et al., 2010), and pancreatic cancer (Burmer et al., 1991) failed to identify a correlation between the occurrence of specific *RAS* mutations and the aggressiveness of the disease, suggesting that the different *RAS* mutations may lead to a common pathophysiological end point in these tissues.

It is unsurprising that constitutive activation of *RAS* fuels cell proliferation because Ras proteins are mediators of mitogenic stimuli. Oncogenic Ras displays pro-survival features, such as independence from extracellular growth factors and growth inhibitors thereby promoting exit from the resting phase of the cell cycle, progression through G1 and entry into the S phase, before nullifying the effect of the G2 DNA damage checkpoint. Oncogenic *Ras* can result in replicative stress from the hyperproliferative state that results in DNA damage and entry into either a senescent or apoptotic state. Furthermore, inaccurate repair of DNA damage can lead to mutations and chromosome aberrations that escape the *p53* damage checkpoint and thereby contribute to tumourigenesis (Schubbert et al., 2007, Pylayeva-Gupta et al., 2011).

The effect of oncogenic *Ras* on apoptotic pathways and its role in carcinogenesis is well documented (Cox and Der, 2003). For example the elimination of inducible oncogenic $HRAS^{G12V}$ and $KRAS^{G12D}$ expression in mice resulted in the regression of melanomas and lung tumours respectively, as evidenced by massive tumour cell apoptosis (Chin et al., 1999, Fisher, 2001).

These experiments demonstrated the importance of Ras in tumour maintenance. Mechanistically also the PI3K and Raf effector pathways activated by oncogenic *Ras* can downregulate pro-apoptotic mediators or upregulate anti-apoptotic molecules. Other ways oncogenic Ras promotes and perpetuates tumourigenesis is by directly contributing to metabolic reactions that promote the use of glucose as an anabolic substrate for cellular growth (Jones and Thompson, 2009). Ras also effectively manipulates the cellular microenvironment to encourage tumour initiation and progression by upregulation of VEGFA, HIF1α and COX-2 (Tsujii, 1998, Blancher et al., 2001, Lee et al., 2002). Furthermore, oncogenic Ras is particularly sophisticated at evading the host adaptive immune response; it expresses reduced levels of antigen-presenting major histocompatibility complexes (MHC) on cancer cells (Maudsley et al., 1991, Lohmann et al., 1996, Seliger, 1996), and it recruits immunosuppressive regulatory T cells and myeloid-derived suppressor cells to the tumour site (Clark, 2007, Tran Thang, 2010).

Many metastatic tumours (such as lung, pancreas and colon tumours) contain *RAS* mutations, which has implicated *RAS* in the various complex processes that result in metastases. Therefore multiple experiments have been undertaken in these tissues aimed at better understanding how oncogenic *Ras* endows cells with metastatic potential. Steps in postulated mechanisms include: weakening of cell-cell adhesion by destabilisation of E-cadherin–β-catenin complexes and the nuclear translocation of β-catenin, and the upregulation of extracellular matrix (ECM) proteases (along with the downregulation of protease inhibitors) by *Ras* effectors to aid penetration of the ECM (Pylayeva-Gupta et al., 2011). It is likely however that solitary *RAS* mutations are rarely sufficient for the development of metastatic disease; instead it contributes to the overall genetic events crucial to the metastatic phenotype in combination with mutation(s) of other key signalling pathways. Evidence to support this notion exists for colorectal cancer (Janssen et al., 2006) and PCa (Pearson et al., 2009, Mulholland et al., 2012).

Chapter 2: Hypothesis, and Thesis Aims

2.1 *HYPOTHESIS*

Deregulation of the Wnt, PI3K/Akt/mTOR, and MAPK pathways are all sufficient to drive prostate cancer initiation and progression, and that there is synergy between these pathways in tumourigenesis. Furthermore it is thought that combinatorial mutants will more aggressive PCa with a metastatic phenotype. The profile of mutations used in the mouse model may be useful in both identifying aggressive disease and in stratifying risk in men with prostate cancer.

One mechanism by which these pathways may synergise is by altering either the pool of normal prostate epithelial stem cells (PrSCs) or the pool of cancer stem cells (CSCs). Conventional understanding suggests that deregulation of these pathways may alter the pool of 'cells of origin', whereas an alternative theory is that pathway synergy may drive expansion of the tumour initiating/SC/CSC population.

2.2 *THESIS AIMS*

The main aims of this thesis are three-fold:

1. To determine the extent of synergy between signal transduction pathways important in human PCa to afford better understanding of the molecular events that underpin the disease
    a. To employ Cre-LoxP technology to create novel conditional transgenic mouse models in which β-catenin, PTEN, and Kras are genetically modified in the prostate, alone and in combination, through action of the rat probasin promoter
    b. To characterise the phenotype of these mutations at different time points with immunohistochemistry
2. To evaluate the extent by which these observations are seen in human PCa
    a. To analyse deregulation of the PI3K/Akt/mTOR, Wnt and MAPK pathways in a human PCa tissue microarray by immunohistochemistry
3. To assess the capacity of stem cells or stem-like cells within both histologically normal prostate and pre-malignant prostates

a. To validate proposed SC/CSC markers in these models of prostate cancer by using immunohistochemistry
b. To optimise a primary, 3D tissue culture assay to explore the self-renewal capacity of histologically normal and pre-malignant prostates *in vitro*

Chapter 3: Materials and Methods

3.1 MOUSE COLONY

Mice with prostate epithelium-specific probasin-driven Cre recombinase were sourced from the National Cancer Institute Mouse Model for Human Cancer Consortium (NCI, Frederick). This line, named *PB-Cre4*, carries the Cre transgene under the control of a composite promoter, *ARR_2PB* which is a derivative of the rat prostate-specific probasin (PB) promoter (Wu et al., 2001). The conditional, constitutively active β-catenin mutant strain was created by Makoto M. Taketo (Harada et al., 1999). Mice with the conditional activating mutation of K-ras were derived by Mariano Barbacid (Guerra et al., 2003). PTEN was highlighted for LoxP-targeted homozygous deletion (Suzuki et al., 2001). The creation of these transgenic mice is depicted in figure 31:

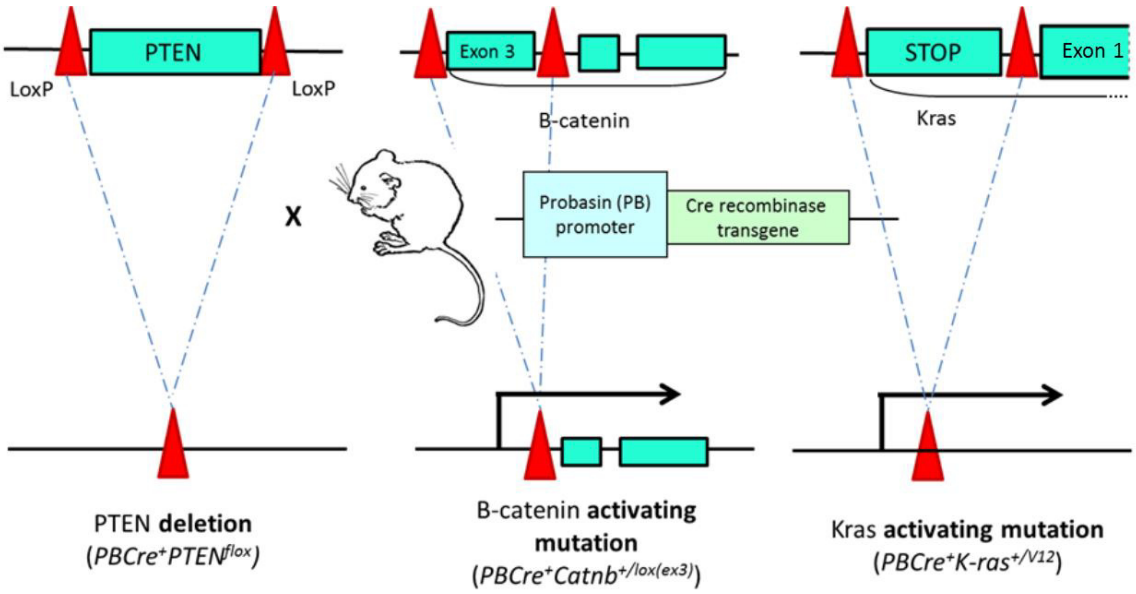

Figure 31: The technology used to facilitate prostate-specific genetic modification. PTEN is 'floxed out' upon recombination due to it being flanked by LoxP sites. Critical phosphorylation sites on exon 3 of β-catenin have been deleted, which does not halt its transcription albeit in mutated form. Similarly the excision of the 'STOP' codon upstream of exon 1 results in oncogenic Kras.

Including *wild-type* mice, the experimental cohorts studied in this thesis are outlined in table 9:

Single Mutants	Double Mutants	Triple Mutant
PBCre^{+}Catnb$^{+/lox(ex3)}$	*PBCre^{+}Catnb$^{+/lox(ex3)}$PTEN^{flox}*	*PBCre^{+}Catnb$^{+/lox(ex3}$PTEN^{flox}K-ras$^{+/V12}$*
PBCre^{+}PTEN^{flox}	*PBCre^{+}Catnb$^{+/lox(ex3)}$K-ras$^{+/V12}$*	
PBCre^{+}K-ras$^{+/V12}$	*PBCre^{+}PTEN^{flox} K-ras$^{+/V12}$*	

Table 9: Cohorts studied in this thesis

Mice were fed the Harlan standard diet (Scientific Diet Services) and water provided *al libitum*. All animal studies were conducted under the auspices of the UK Home Office (PPL 30/2737; PIL 30/9754).

3.1.1 Genotyping

Mice were genotyped by PCR using DNA extracted from ear biopsies at weaning, when deemed suitable size and age (usually ≥4 weeks). Genotypes were re-confirmed at necropsy.

3.1.2 Genotyping primers

Allele primer	Sequence (5'-3')	Product size (bp)
B-catenin (Primer3)	Ctnnb1: CTGCGTGGACAATGGCTACT Ctnnb2: TCCATCAGGTCAGCTGTAAAAA	WT: 324 HOM: 500
B-catenin recombined (Harada et al., 1999)	AS5: ACGTGTGGCAAGTTCCGTCATCC GF2: GGTAGGTGAAGCTCAGCGCAG	WT: 900 Rec: 700
Cre	CreA: TGACCGTACACCAAAATTTG CreB: ATTGCCCCTGTTTCACTATC	Cre: 1000
Kras^{V12} (Guerra et al., 2003)	510: AGGGTAGGTGTTGGGATAGC 3Ex1: CTCAGTCATTTTCAGCA 103rev-2: CTGTCCTTTACTGAAGGCTC	WT: 403 Floxed: 621 Rec: 669
LacZ	LacZa: CTGGCGTTACCCAACTTAAT LacZb: ATAACTGCCGTCACTCCAAC	LacZ: 500
PTEN (Suzuki et al., 2001)	Pten1: CTCCTCTACTCCATTCTTCCC Pten2: ACTCCCACCAATGAACAAAC	WT:228 HOM: 335

Table 10: Primers used to perform genotyping

3.2 TISSUE HARVESTING

3.2.1 For immunohistochemistry (paraffin)

The genitourinary tract, retroperitoneal lymph nodes, lungs, liver, and kidneys were harvested, and then placed into ice cold 10% neutral buffered formalin for 24 hours, before finally being submitted for sectioning in 70% ethanol at 4°C. They were embedded in paraffin wax using an automated tissue processor (Leica TP1050). Sections were cut (5-10µm thick) onto poly-*L*-lysine coated slides using a microtome. Samples adhered to the slides after placing onto a hot plate for up to 30 minutes, and then baked in an oven at 45-60°C for a minimum of 24 hours.

3.2.2 For primary tissue culture

The deceased mouse was submerged in 70% ethanol and pinned out onto a board that had likewise been cleaned with 70% ethanol. Sterile instruments, that had been autoclaved, were used each time, and stood up in 70% ethanol when not in use. The GU tract was excised as before, and placed immediately into ice cold D10 medium until mechanical digestion were to begin.

3.3 IMMUNOHISTOCHEMISTRY (PARAFFIN)

Formalin-fixed, paraffin-embedded sections were dewaxed in xylene (2 x 5 min), then dehydrated in decreasing concentrations of ethanol (2 x 5min 100%; 1 x 2min 95%; 1 x 2min 70%) before a 5min wash in dH_20. Once samples had been fully stained, dehydration in preparation for mounting took place in reverse order, finishing in xylene. All of the above took place in a fume extraction hood.

3.3.1 Primary antibodies

Antibody	Host	Manufacturer	Manufacturer code	Dilution	Method
Activated Notch1	Rabbit	Abcam	ab8925	1:300	A
p-Akt (Ser473) XP	Rabbit	Cell Signalling Technology (CST)	4060	1:50	B
p-Akt (Thr 308)	Rabbit	CST		1:50	B
AR	Rabbit	Labvision Neomarkers	RB -1358	1:100	A
B-catenin	Mouse	BD Transduction Laboratories	610154	1:200	D
Cleaved Caspase-3	Rabbit	CST	9661	1:200	A
CD44	Mouse	Pharmingen	550392	1:50	
CD44	Rat	Pharmingen	550538	1:50	D
CXCR4	Rabbit	Abcam	ab2074	1:100	A
EpCam	Rabbit	Abcam	ab71916	1:100	A
p-Erk (Thr202/Tyr204)	Rabbit	CST	4376	1:100	B
FRMD4a	Rabbit	c/o Prof Fiona Watt	N/A	1:500	A
Integrin B1	Goat	Santa Cruz	sc-9936	1:100	A
Keratin 5	Rabbit	Covance	PRB-160P	1:1000	B
Keratin 8	Chicken	Abcam	ab14053	1:500	E
Keratin 14	Rabbit	Covance	PRB-155P	1:1000	B
Keratin 18	Mouse	Progen	61528	1:50	D
Ki67	Mouse	Vector Labs	VP-K452	1:20	D
LRIG1	Rabbit	Abcam	ab36707	1:100	A
Notch4	Rabbit	Santa Cruz	sc-5594	1:200	A
p63	Mouse	Neomarkers	MS-1081-P1	1:50	C
p-Mek (Ser221)	Rabbit	CST	2338	1:75	B
p-mTOR (Ser2448) XP	Rabbit	CST	5536	1:100	B
Pten	Rabbit	CST	9559	1:100	B
p-Rps6 (Ser240/244) XP	Rabbit	CST	5364	1:200	B
p-S6k (Thr421/424)	Mouse	CST	2317	1:200	B
Trop2	Goat	R&D Systems	AF1122	1:200	B

Table 11: Primary antibodies utilised for IHC. FRMD4a antibody was kindly donated by Professor Fiona Watt, Wellcome Trust Centre for Stem Cell Research, University of Cambridge.

3.3.2 De-wax and rehydrate slides for immunohistochemistry

Selected slides were de-waxed in xylene for 2 x 5 min washes and then hydrated by washing in decreasing concentrations of alcohol; 2 x 3 min washes in 100%, 1 x 3 min wash in 95% and 1 x 3 min wash in 70% alcohol. Slides are then bathed in distilled H_20 (dH_20) prior to following primary antibody-specific staining protocol (see Methods A – D)

3.3.3 Method A: Rabbit polyclonal primary antibodies (Envision)

Antigen unmasking was performed by microwave heating slides on full power in 1X citrate buffer for 10mins before leaving to cool for 30mins and rinsing in dH_20. A border is drawn around the prostate tissue with a DAKO pen and slides are then covered for 20mins with Envision Kit Peroxidase Block to inhibit endogenous peroxidase activity. Slides were then washed for 3 x 5mins in 1X TBS/Tween and incubated with 10% normal goat serum (NGS) diluted in 1X TBS/T for 40mins to eradicate background staining. Rabbit polycloncal primary antibody (diluted to the desired concentration in NGS and TBS/T) was added for 2hours at room temperature followed by a further 3 x 5min washes in 1X TBS/T. Detection of primary antibody was achieved by horseradish peroxidase (HRP)-conjugated polymer (Rabbit Envision Kit, DAKO) for 1hour and washed in 1X TBS/T for 3 x 5mins to remove excess polymer. Visualisation of positive staining was identified by applying Diaminobenzidine (DAB) solution (K3467, DAKO) for 2-10mins and checking colour development regularly, until brown staining was visualised. Slides were then washed for 3 x 5mins in dH_20 before counterstaining in Meyer's haematoxylin for 30-60secs, rinsing in running tap water for 5mins, then dehydrating in increasing concentrations of alcohol before being mounted with DPX.

3.3.4 Method B: Rabbit polyclonal primary antibodies (Biotin)

Antigen unmasking was performed by microwave heating slides on full power in 1X citrate buffer for 15mins. Slides were then cooled for 30mins prior to drawing a border around the prostate tissue with a DAKO pen prior to inhibiting endogenous peroxidase activity with 1.5-3% H_20_2 (Sigma) in dH_20 for 20mins. Slides were then washed for 3 x 5mins in 1X TBS/Tween and incubated with 10% normal goat serum (NGS) diluted in 1X TBS/T for 40mins to eradicate background staining. Rabbit polycloncal primary antibody (diluted to the desired concentration in NGS and TBS/T) was applied overnight at 4°C. The following day slides were washed thoroughly for 3 x 5mins in 1X TBS/T. Detection of primary antibody was achieved by adding

biotinylated goat-anti-rabbit secondary antibody (E0432, DAKO) 1:200 in 10% NGS in 1X TBS/T for 30mins at room temperature then washed in 1X TBS/T for 3 x 5mins. Staining signal amplification was performed by using the Vectastain ABC (Avidin Biotin Complex) kit (Vector Labs, Burlingame, CA) for 30mins at room temperature before washing 3 x 5mins in 1X TBS/T. Visualisation of positive staining was identified by applying DAB solution (K3467, DAKO) for 2-10mins and checking colour development regularly, until brown staining was visualised. Slides were then washed for 3 x 5mins in dH_20 before counterstaining in Meyer's haematoxylin for 30-60secs, rinsing in running tap water for 5mins, then dehydrating in increasing concentrations of alcohol before being mounted with DPX.

3.3.5 Method C: Mouse monoclonal primary antibodies (Envision)

Antigen unmasking was performed by microwave heating slides on full power in 1X citrate buffer for 10mins before leaving to cool for 30mins and rinsing in dH_20. A border is drawn around the prostate tissue with a DAKO pen and slides are then covered for 20mins with Envision Kit Peroxidase Block to inhibit endogenous peroxidase activity. Slides were then washed for 3 x 5mins in 1X TBS/Tween and incubated with 10% normal rabbit serum (NRS) diluted in 1X TBS/T for 40mins to eradicate background staining. Mouse monoclonal primary antibody (diluted to the desired concentration in NRS and TBS/T) was added for 2hours at room temperature followed by a further 3 x 5min washes in 1X TBS/T. Detection of primary antibody was achieved by adding horseradish peroxidase (HRP)-conjugated polymer (Mouse Envision Kit, DAKO) for 1hour and washed in 1X TBS/T for 3 x 5mins to remove excess polymer. Visualisation of positive staining was identified by applying DAB solution (K3467, DAKO) for 2-10mins and checking colour development regularly, until brown staining was visualised. Slides were then washed for 3 x 5mins in dH_20 before counterstaining in Meyer's haematoxylin for 30-60secs, rinsing in running tap water for 5mins, then dehydrating in increasing concentrations of alcohol before being mounted with DPX.

3.3.6 Method D: Mouse/Rat polyclonal (Biotin)

Antigen unmasking was performed by microwave heating slides on full power in 1X citrate buffer for 15mins. Slides were then cooled for 30mins prior to drawing a border around the prostate tissue with a DAKO pen prior to inhibiting endogenous peroxidase activity with 1.5-3% H_20_2 (Sigma) in dH_20 for 20mins. Slides were then washed for 3 x 5mins in 1X TBS/Tween and incubated with 10% normal rabbit serum (NRS) diluted in 1X TBS/T for 40mins to eradicate

background staining. Mouse (or rat for anti-CD44) polycloncal primary antibody (diluted to the desired concentration in NRS and TBS/T) was applied overnight at 4°C. The following day slides were washed thoroughly for 3 x 5mins in 1X TBS/T. Detection of primary antibody was achieved by adding rabbit-anti-mouse biotinylated secondary antibody (E0464, DAKO), or for anti-CD44 rabbit-anti-rat biotinylated secondary antibody (E0468, DAKO), 1:200 in 10% NRS in 1X TBS/T for 30mins at room temperature then washed in 1X TBS/T for 3 x 5mins. Staining signal amplification was performed by using the Vectastain ABC (Avidin Biotin Complex) kit (Vector Labs, Burlingame, CA) for 30mins at room temperature before washing 3 x 5mins in 1X TBS/T. Visualisation of positive staining was identified by applying DAB solution (K3467, DAKO) for 2-10mins and checking colour development regularly, until brown staining was visualised. Slides were then washed for 3 x 5mins in dH_20 before counterstaining in Meyer's haematoxylin for 30-60secs, rinsing in running tap water for 5mins, then dehydrating in increasing concentrations of alcohol before being mounted with DPX.

3.3.7 Method E: Chicken polyclonal primary antibody (Biotin)

Antigen unmasking was performed by microwave heating slides on full power in 1X citrate buffer for 15mins. Slides were then cooled for 30mins prior to drawing a border around the prostate tissue with a DAKO pen prior to inhibiting endogenous peroxidase activity with 1.5-3% H_20_2 (Sigma) in dH_20 for 20mins. Slides were then washed for 3 x 5mins in 1X TBS/Tween and incubated with 10% normal rabbit serum (NRS) diluted in 1X TBS/T for 40mins to eradicate background staining. Chicken polycloncal primary antibody (diluted to the desired concentration in NRS and TBS/T) was applied overnight at 4°C. The following day slides were washed thoroughly for 3 x 5mins in 1X TBS/T. Detection of primary antibody was achieved by adding rabbit-anti-chicken biotinylated secondary antibody (12-341, Upstate) 1:200 in 10% NRS in 1X TBS/T for 30mins at room temperature then washed in 1X TBS/T for 3 x 5mins. Staining signal amplification was performed by using the Vectastain ABC (Avidin Biotin Complex) kit (Vector Labs, Burlingame, CA) for 30mins at room temperature before washing 3 x 5mins in 1X TBS/T. Visualisation of positive staining was identified by applying DAB solution (K3467, DAKO) for 2-10mins and checking colour development regularly, until brown staining was visualised. Slides were then washed for 3 x 5mins in dH_20 before counterstaining in Meyer's haematoxylin for 30-60secs, rinsing in running tap water for 5mins, then dehydrating in increasing concentrations of alcohol before being mounted with DPX.

3.4 HISTOPATHOLOGICAL CHARACTERISATION

3.4.1 Haematoxylin and eosin staining

Slides were immersed in Meyer's haematoxylin for 1 min and rinsed in water for 5 mins, before counterstaining with 1% aqueous eosin for 30sec.

3.4.2 LacZ stain of prostate wholemounts

Male mice were euthanised and the GU tract was dissected out and washed in 1X PBS. The GU tract was fixed for 40min in whole mount fixative (0.2% Glutaraldehyde, 5mM EGTA, and 2mM $MgCl_2$ in 0.1M phosphate buffered saline [pH 7.3]) on ice. The specimen was rinsed 3 x 15 min in detergent rinse (0.02% Igepal, 0.01% sodium deoxycholate, and 2mM $MgCl_2$ in 0.1M PBS [pH 7.3]) and stained by immersion in 1mg/ml X-gal staining solution (0.02% Igepal, 0.01% Sodium Deoxycholate, 5mM Potassium Ferricyanide, 5mM Pottassium Ferrocyanide, and 2mM $MgCl_2$ diluted in 0.1M phosphate buffer [pH 7.3]) overnight at 37°C in the dark. The X-gal staining solution was prepared ahead of time, stored at room temp in the dark, and 1mg/ml X-Gal in N,N-dimethylformamide (Promega) added immediately prior to use. The GU tract was washed in 1X PBS for 15mins, and post-fixed in 4% paraformaldehyde in 1X PBS at 4°C. The wholemount was then ready to bephotographed and submitted in 70% ethanol for sectioning as required.

3.4.3 Characterisation of murine prostate tumours

All histopathological analysis and tumour grading was undertaken with Dr David Griffiths, Consultant Histopathologist, University Hospital of Wales, Cardiff.

3.4.4 Scoring proliferation

The percentage of positive cells for AR, Caspase-3, H&E (apoptosis and mitosis), Ki67, and p63 were scored by dividing the number of positively-stained cells by the total number of cells counted (positive and negatively-stained cells) from 20 acini, or in prostate lesions (PIN and tumours) 20 random 2500μm^2, and a running mean calculated. Photographs were taken using Motic Images Plus 2.0 software at 40x magnification, and all counting performed in ImageJ (Schneider et al., 2012). A minimum of 1000 cells/mouse were counted (n=3). The median score for each genotype at each time point underwent statistical analysis using the non-

parametric Mann-Whitney U test (95% confidence interval, $p<0.05$), using SPSS 20 software (IBM).

3.5 3D PRIMARY PROSTATE EPITHELIAL STEM CELL CULTURE

The technique for prostate sphere assay was adapted from Lukacs et al. (2010).

3.5.1 Creation of a prostate epithelial single cell suspension

The GU tract (bladder, seminal vesicles, prostate and urethra) of male mice aged 90 – 100 days was harvested under sterile conditions, and quickly placed into an un-skirted 15ml centrifuge tube containing 10ml dissecting medium. Micro-dissection to isolate only the prostate was performed in a tissue culture hood on a clean 10cm Petri dish. Two pairs of fine non-toothed forceps were used to separate all 4 prostate lobes intact from the seminal vesicles, bladder and urethra. Prostates were minced into paste after undergoing 3-4 passes through a tissue chopper. The tissue paste was then placed into a clean 50ml centrifuge tube containing dissection medium (see box below for reagent setup) and collagenase (Life Technologies; cat no 17018-029) in a ratio of 1:9:1 per prostate (e.g. 3 prostates, 27ml of dissecting medium, along with 3ml of collagenase solution), and incubated on a *gentle* orbital shaker at 37°C overnight.

Dissecting medium: *to 500 ml Dulbecco's modified Eagle's medium (DMEM; Invitrogen/Gibco, 12100-061), add 50 ml fetal bovine serum (Sigma; F7524) (10% (vol/vol), 5 ml 100X GlutaMAX (Invitrogen/Gibco, 35050-038) (1X final concentration), and 5 ml 100X penicillin-streptomycin(Invitrogen/Gibco;* 15140-122) *(1X final concentration). Stored at 4 °C and used within 1 month.*

The following morning, the tissue was spun down at 1300rpm for 5 minutes at room temperature; the supernatant was discarded before 5mls of warm trypsin/0.05% EDTA (Invitrogen/Gibco; 25300-062) was added to dissociate the cell pellet. The mixture was thoroughly mixed using with a P1000 pipette and placed in an incubator at 37°C for 5 minutes.

Next, the cell suspension was mixed with a P1000 pipette and 3ml dissecting media containing 500U (25µl of 10mg/ml) DNase I (Roche; 10 104 159 00) added to inactivate the trypsin and break up any DNA released from dead cells. The suspension was then *gently* passed through an 18-G needle 5 times. If any chunks of prostate tissue were to remain, then 1ml (10mg/ml) collagenase was added for 1 hour and the process up to this point was repeated. If the cell

suspension appeared well digested and cells were fully in suspension, then the trypsin/EDTA stage was repeated again, to maximise cellular yield.

Next, the mixture was filtered through a 40µm nylon mesh filter into a 50ml centrifuge tube, and the 15ml centrifuge tube washed out with dissection media. This was spun down at 1300rpm for 5 minutes at room temperature and the pellet re-suspended in 2ml dissecting media for counting by trypan blue exclusion on a haemocytometer. 10µl of suspended cells was mixed with 10µl trypan blue in a 1.5ml Eppendorf tube. 10µl of this sample was taken and placed on haemocytometer, at which point live and dead cells were counted and recorded.

3.5.2 Unsorted prostate epithelial cells

Unsorted cells were diluted to 2.5×10E5 cells per ml in PrEGM. 40µl cell mixture (10E4 cells) was thoroughly mixed with 60µl cold Matrigel (BD Biosciences; 354234) and the 100 µl mix pipetted around wells of a 12-well plate. Plates were swirled to evenly distribute the mixture around the rim and once complete they were incubated for 30minutes at 37°C to allow the Matrigel to solidify. Once time had lapsed and the Matrigel was solidified, 1ml of warm PrEGM (see box below for reagent setup) was added to each well by aiming the pipette at the centre of the well in order to not disturb the Matrigel ring. Plates were checked daily for infection and spheres monitored for 7-10days depending on their destiny. A media change was performed every 3rd day by tilting the plate to 45 degrees and replacing half of the spent PrEGM with 500µl of fresh, warm PrEGM.

Spheres were counted using an inverted microscope by following the rim of Matrigel around the wells. When many spheres were present, a single field was counted, and the whole well total estimated by multiplying by 14.5 if viewed at 4X or multiplying by 36 if viewed at 10X.

PrEGM™: *a commercial preparation (Lonza Walkersville, Inc.; CC-3166) that requires addition of the inclusive SingleQuots™ growth supplements (Lonza; CC-4177) (Bovine pituitary extract, 2 ml; hydrocortisone, 0.5 ml; human epidermal growth factor, 0.5 ml; epinephrine, 0.5 ml; transferrin, 0.5 ml; insulin, 0.5 ml; retinoic acid, 0.5 ml; triiodothyronine, 0.5 ml; gentamicin-amphotericin-B 1000, 0.5 ml) to a 500 ml bottle of prostate epithelial cell basal medium (Lonza; CC-3165).*

3.5.3 FACS enrichment: sorted prostate epithelial cells

FACS was facilitated and supervised by Dr Kirsty Richardson PhD, FACS manager, School of Biosciences, Cardiff University on a BD FACS Aria cell sorter.

3.5.4 Sorted cells

Five hundred microlitres of dissecting medium was aliquoted into five Eppendorf tubes and 5×10E4 cells added to each tube; these were used to set up the compensation for sorting. The remaining cells are divided into new Eppendorf tubes up to 3×10E6 cells per tube in a 1 ml total volume; these are stained for sorting.

For compensation, FMO (Fluorescence-Minus-One) compensation was carried out when calibrating gates for the first time. The following antibodies were added to individual compensation tubes:

1. Unlabelled cells
2. 1µl CD49f–PE-Cy5 (BD Pharmingen; cat no 551129)
3. 1µl Sca-1–PE–Cy7 (BioLegend; 122514)
4. 2µl Trop2–biotin (R&D Systems; AF1122)
5. 1µl CD31-FITC (eBioscience; 11-0311-85)
6. 1µl CD45–FITC (eBioscience; 11-0451-85)
7. 1µl Ter119–FITC (eBioscience; 11-5921-85)
8. 1µl each of CD31-FITC, CD45–FITC and Ter119–FITC to the fifth tube
9. 1 µl DAPI (Invitrogen; D21490)

To the sample tube(s) for sorting, the following were added together:

- 3µl CD49f–PE
- 2µl Sca-1–PE–Cy7
- 10µl Trop2–biotin
- 4µl each of CD31–FITC, CD45–FITC and Ter119–FITC
- 2µl DAPI

All tubes are then wrapped in aluminium foil and placed on a shaker at 4°C for 20min.

Cells were pelleted in a bench top centrifuge at 2,300rpm for 2min at room temperature. Media were aspirated off and cells were re-suspended in 500µl of fresh dissecting medium for

the compensation cells and 1 ml for the sorting sample cells. All samples were kept on ice where possible throughout.

1µl SA–APC (BD Biosciences; cat no 554067) secondary antibody was added to its own compensation tube, with 1µl SA–APC to the Trop2-APC compensation tube (now 10 compensation tubes in total), and 5µl SA–APC antibody to each of the sample tubes. Tubes were wrapped in aluminium foil and placed on a shaker at 4°C for 15min. Cells were then pelleted in a bench top centrifuge at 2,300rpm for 2min at room temperature. Media were aspirated off and cells re-suspended in 500µl fresh dissecting medium for the compensation cells and 1ml for the sorting sample cells. Cells were transferred back to the tissue culture hood in either 0.3% BSA in 1X PBS or dissecting medium on ice.

After completing the compensation, the following populations were sorted using the FACS Aria cell sorter and cells collected into 15 ml centrifuge tubes containing 5ml FACS collection medium:

1. FITC^{-}PE-Cy7^{+}PE-Cy5^{+}APC^{hi} (Lin^{-}CD49f^{+}Sca-1^{+}Trop2^{hi}; **Trop2^{Hi}**)
2. FITC^{-}PE-Cy7^{+}PE-Cy5^{+}APC^{lo} (Lin^{-}CD49f^{+}Sca-1^{+}Trop2^{lo}; **not Trop2^{Hi}** or **Trop2^{lo}**)
3. FITC^{-}PE-Cy7^{-}PE-Cy5^{-} (Lin^{-}CD49f^{-}Sca-1^{-}; **not CD49f/Sca-1^{+}**)

Upon return to the tissue culture suite, cells were pelleted at 1,300rpm for 5min at room temperature, re-suspended in 500µl PrEGM, and again counted using a haemocytometer. At this point cells were ready for *in vitro* culture.

The 3 cell populations were diluted to 2.5×10E5 cells per ml in PrEGM. 40µl cell mixture (10E4 cells) was thoroughly mixed with 60µl cold Matrigel and the 100 µl mix pipetted around wells of a 12-well plate, identical to that used to plate unsorted cell as above. Each population was plated in triplicate at 1x10E4/well and the rest of the cells plated at 10E5/well in bulk.

3.5.5 Passage of prostate epithelial stem cells in vitro

After 7 days, the prostate spheres were ready to be dissociated into single cell suspension and re-cultured to assess self-renewal.

PrEGM was aspirated from each well and 1ml Dispase (Invitrogen/Gibco; 17105-041) added. The plate was incubated at 37°C for 1 hour to digest the Matrigel. Spheres were collected into a 15ml centrifuge tube and pelleted at 1300rpm for 5mins at room temperature. The sphere pellet was re-suspended in 1ml trypsin/0.05% EDTA and transferred into a 1.5ml Eppendorf tube and incubated at 37°C for 5 minutes. Spheres were gently passed through a 1ml syringe with a 27-G needle five times to dissociate cells and then centrifuged at 2300rpm for 2minutes at room temperature.

The Trypsin/0.05% EDTA was aspirated off and the pellet re-suspended in 1ml PrEGM before again passing cells through a 1ml syringe with a 27-G needle five times, then centrifuging again at 2300rpm for 2 minutes at room temperature. Cells were finally re-suspended in 0.5ml fresh PrEGM. Cells were counted on a haemocytometer and plated as before at 1x10E4 and bulk to maximise passage success through further generations.

3.5.6 Quantifying self-renewal

The size of 50 spheres per well, chosen at random, were measured and recorded at days 1, 4, and 7 after primary plating and each re-plating following passage. When assessing prostate organoid size, a cut-off of 40µm was set – the growth of structures smaller than this ceased at or around day 5 and so not counted as PrSC organoids. Similarly, sphere number was counted on day 7 and averaged. Photographs were taken on AnalySIS software on an inverted light microscope, measurements and counts performed in ImageJ (Schneider et al., 2012), all results were collated in Microsoft Excel 2010, and all statistical analysis performed in SPSS20 (IBM). The median score for each population (n=4) at each time point underwent statistical analysis using the non-parametric Mann Whitney U-test (95% confidence interval, $p<0.05$), using SPSS 20 software (IBM).

Sphere-forming units (SFU) were calculated at each generation by using the following formula:

SFU = number of spheres formed per well / number of cells plated per well X 100%

Chapter 4: Investigating the interactions between the Wnt, PI3K/Akt/mTOR, and MAPK pathways in prostate tumourigenesis

4.1 INTRODUCTION

Several important molecular lesions have been associated with human prostate cancer, including deregulation of the Wnt pathway (Yang et al., 2006, Wang et al., 2008, Kypta and Waxman, 2012, Lee et al., 2013), the PI3K/Akt/mTOR pathway (Mulholland et al., 2006, Sarker et al., 2009, Elfiky and Jiang, 2013), and the MAPK pathway (Weber and Gioeli, 2004, Prior et al., 2012). Given that there is extensive evidence for crosstalk between these pathways in both tumour development and resistance to therapy, the interplay between them remains largely unmodelled and poorly characterised in the pre-clinical setting. This chapter explores the interplay between the Wnt, PI3K/Akt/mTOR, and MAPK pathways in mouse models of prostate tumourigenesis.

4.1.1 PTEN is implicated in human prostate cancer

PTEN (phosphatase and tensin homolog deleted from chromosome 10) is a potent tumour suppressor and negative regulator of the PI3K/Akt/mTOR pathway. *PTEN* deregulation is strongly implicated in prostate tumourigenesis and therefore it is one of the most interrogated molecular lesions in prostate cancer. *PTEN* deletions and/or mutations are found in approximately 30% of primary prostate cancers (Dahia, 2000) and up to 63% of metastatic prostate cancers (Suzuki et al., 1998).

PTEN loss of function is well described in both localised and metastatic prostate cancers and includes homozygous deletions, loss of heterozygosity (LOH), and inactivating somatic mutations. However, the reported frequency and mode of inactivation at different stages of prostate cancer vary, along with the techniques employed to identify the prevalence of the loss of function within the tumour. Examples are given in table 12.

Reference	Tumour type	Finding	Prevalence in tumour	Techniques used
Yoshimoto et al. (2007)	Primary PCa	Homozygous deletion	5%	FISH
		Heterozygous deletion	39%	
		Somatic mutation	70%	
Verhagen et al. (2006)	Locally-advanced PCa	Homozygous deletion	30-38%	PCR-SSP, IHC
		Heterozygous deletion	20%	
Cairns et al. (1997)	Localised Pca and lymph node metastases	Homozygous deletion	7.5%	DNA sequencing, PCR, FISH
		Heterozygous deletion	21%	
Dong et al. (1998)	Primary T2, and T3 PCa	Homozygous deletion	15%	DNA sequencing, PCR
		Heterozygous deletion	0%	
		Somatic mutation	2.5%	
Yoshimoto et al. (2006)	Primary PCa from RRP specimens	Homozygous deletion	6%	FISH, IHC
		Heterozygous deletion	63%	
Dong et al. (2001)	Primary PCa	Somatic mutation	16%	PCR-SSP, DNA sequencing
	Metastatic PCa	Somatic mutation	33%	
Feilotter et al. (1998)	Primary PCa	Heterozygous deletion	49%	PCR-SSP, DNA sequencing
		Somatic mutation	2%	
Halvorsen et al. (2003)	Primary PCa from RRP specimens	Absence of PTEN expression	27%	IHC
McMenamin et al. (1999)	Primary PCa from RRP and TURP specimens	Absence of PTEN expression	20%	IHC
Suzuki et al. (1998)	Metastatic PCa	Homozygous deletion	11%	DNA sequencing, PCR-SSP, FISH
		Heterozygous deletion	56%	
		Somatic mutation	63%	

Table 12: The frequency of PTEN loss of functions are outlined to include the type of mutation, and the techniques used for investigation. *FISH*, fluorescence in situ hybridisation; *PCR-SSP*, Polymerase chain reaction – Sequence-specific amplification; *IHC*, immunohistochemistry.

PTEN mutations have likewise been implicated in the mechanisms of resistance to radiotherapy (Anai et al., 2006), and chemotherapy (Priulla et al., 2007), along with recurrence following prostatectomy (Bedolla et al., 2007).

4.1.2 The PI3K/Akt/mTOR pathway and human prostate cancer

Further to the incapacitation of PTEN, the PI3K/Akt/mTOR pathway has been identified as playing important other roles in the genetics and pathophysiology of prostate cancer.

The p110β subunit of PI3K in particular has been identified as a critical molecule in prostate tumourigenesis. Both p85α and p110β appear to influence androgen-induced AR transactivation and impact on cell proliferation and tumour growth (Zhu et al., 2008). Studies of p110β conditional knockout mice evaluated the impact of its deletion. Prostates were normal upon p110β loss but had universal high-grade PIN in the anterior lobe by 12 weeks in the absence of PTEN alone. However, ablation of p110β prevented the tumourigenesis caused by PTEN loss; this led to increased Akt phosphorylation in the prostate, whereas ablation of p110β had the opposite effect (Jia et al., 2008). These changes were p110β-specific because p110α knockout did not abrogate tumour formation or Akt phosphorylation, supporting a potential avenue for p110β inhibitors in prostate cancer treatment to be explored.

Proteins of the ETS family are related signal-dependent transcriptional regulators that mediate cellular proliferation, differentiation and tumourigenesis (Seth and Watson, 2005). In human prostate cancer, genomic alterations of ETS-related genes (principally *ERG*), as a result of a fusion between an androgen receptor–regulated gene promoter of *TMPRSS2* and ETS transcription factors, is present in approximately 50-70% of prostate cancers (Tomlins et al., 2005, Sarker et al., 2009). Thus, overexpression of ETS factors may represent a crucial event in prostate tumourigenesis. However, important details of the biological role of aberrant ETS expression in prostate cancer initiation and progression have yet to be elucidated.

Data have shown that loss of *PTEN* cooperates with *TMPRSS2:ERG* activation in both human and murine prostate cancer in dose-dependent fashion. Transgenic mice expressing *TMPRSS2:ERG* in the prostate failed to develop PIN or invasive prostate cancer (King et al., 2009). However, when these were crossed either with $PTEN^{+/-}$ mice, or prostate-specific Akt transgenic mice, PIN but not invasive cancer developed. In another strain of transgenic mouse overexpressing *ERG*, both PIN and invasive cancer developed only when crossed with *PTEN*-deficient mice (Carver et al., 2009). In addition, this study showed that prostate cancer specimens containing the *TMPRSS2:ERG* rearrangement (~40%) are significantly enriched for *PTEN* loss. These data implicate *PTEN* loss and *ERG* rearrangements as associated events that act in tandem to promote prostate cancer progression, potentially by inducing transcription of downstream checkpoint genes involved in promoting cell proliferation, senescence, and survival.

Reports suggest that PI3K/Akt/mTOR signalling may play a critical role in the development of CRPC (Mulholland et al., 2006). The transgenic mouse models that recapitulate features of PI3K/Akt/mTOR-dependent PCa (Shen and Abate-Shen, 2007), demonstrated an initial response to androgen deprivation therapy, and eventual tumour growth despite castration (Wang et al., 2003). Thus PI3K/Akt/mTOR signalling may contribute to continued AR gain-of-function despite reduced steroid ligand levels (Mulholland et al., 2006), by triggering a downstream cascade of events that are likely to interact with AR transcriptional activity e.g. Wnt pathway/β-catenin (Sarker et al., 2009).

Chemokines have been associated with prostate carcinogenesis, by impacting cancer cell proliferation, survival, adhesion, and invasion (Balkwill, 2004) through their stimulation of transmembrane-spanning receptors involved in the PI3K/Akt/mTOR pathway and the resultant activation of downstream p110β signalling (Richter et al., 2005). Chemokines such as CCL2 (monocyte chemo-attractant protein) have also been reported to stimulate monocyte/macrophage migration into tumours, potentially fuelling tumour growth, propagation of angiogenesis, and the inhibition of autophagy (Roca et al., 2008).

4.1.3 Beta-catenin is implicated in human prostate cancer

The observation that β-catenin is a target for mutation in PCa originated from a study of 104 PCa samples, of which 5 were found to harbour specific mutations in exon 3 of the *CTNNB1* gene (Voeller et al., 1998). This 5% mutation rate was later corroborated by another study (Chesire et al., 2000), but smaller studies contradict this prevalence and reported differing frequencies ranging from 0% in eight CRPC samples (de la Taille et al., 2003), to 33% (2/6) in locally-advanced tumours (Gerstein et al., 2002). Thus mutations that directly activate Wnt/β-catenin signalling are reportedly rare in PCa, suggesting that other mechanisms may account for its over-expression (Kypta and Waxman, 2012). These may include mutations in *APC* and *AXIN1*, which are likewise rare in PCa. Whilst occurring in 25% of xenograft cell lines derived from bone metastases (Gerstein et al., 2002), mutant *APC* alone was not seen in 49 samples of advanced PCa, but mutation of the APC-binding domain of axin-1 was seen in 4% (Yardy et al., 2009). Furthermore *APC* is frequently hypermethylated in PCa progression (Jeronimo et al., 2011), which may result in increased Wnt signalling by reduction of APC expression (Kypta and Waxman, 2012).

The low frequency of β-catenin mutations is at odds with reports that aberrantly-expressed or localised β-catenin is commonly found in PCa. Table 13 summarises the frequencies and expression patterns reported.

Participants (n) and PCa grade/stage	Expression	Change in localisation	Reference
122 T2 **90 CRPC**	Increased	Increased nuclear and cytoplasmic in 30% PCa overall	de la Taille et al. (2003)
232 T2 **26 metastatic**	Decreased	Decreased membranous and nuclear expression but cytoplasmic expression unchanged in men with metastatic PCa	Horvath et al. (2005)
73 T2 **25 T3/4** **3 metastatic**	No change	88% diffuse membranous expression, and 12% negative	Bismar et al. (2004)
80 BPH **35 Gleason 6** **33 Gleason 7** **77 Gleason 8-10**	Increased	Increased intensity in all membranous, cytoplasmic, and nuclear compartments Nuclear expression: 37% BPH, 14% Gleason<7, 9% Gl 7, 5% Gl>7	Whitaker et al. (2008)
47 T2 **65 T3/4 or metastatic**	Decreased	Decreased overall expression was observed in 4% PCa, and commoner with high grade PCa	Kallakury et al. (2001)
49 T2 **18 T3/4 or metastatic**	Increased	Cytoplasmic and nuclear staining in 43% Gl 6 and 7, and 78% Gl>7 Staining density correlated with stage and grade	Chen et al. (2004b)

Table 13: The prevalence and expression patterns seen for β-catenin at IHC. *Gl*, Gleason grade (6-10).

There is no clear conclusion as to the prevalence of nuclear localisation of β-catenin in PCa, nor its clinical relevance. Hypotheses to account for the dissimilarities in reports could include intra- and inter-tumoural heterogeneity (Chesire et al., 2000, Chesire et al., 2002), and variance in immunohistochemical staining protocols (Whitaker et al., 2008). Nevertheless, expression at all stages of prostate tumourigenesis suggests that β-catenin activation plays an important role in disease progression.

Synergy between AR and β-catenin pathways has been well documented (Lee et al., 2013), whereby β-catenin and AR regulate one another. AR binds β-catenin directly to stimulate AR-mediated gene transcription (Song and Gelmann, 2005), and the AR gene itself is a transcriptional target of β-catenin (Yang et al., 2006).

Recent studies have revealed that Wnt signalling is a significantly deregulated pathway in the lethal phase of PCa (Grasso et al., 2012). Furthermore, enhanced crosstalk between AR and β-catenin has been observed in mouse models of CRPC (Wang et al., 2008). CSCs may resist androgen deprivation therapy, and recent studies have identified Wnt/β-catenin signalling as being highly active in CSCs (Chen et al., 2007, Woodward et al., 2007, Vermeulen et al., 2010, Wang et al., 2010), perhaps further identifying a role for β-catenin in an androgen-independent environment.

4.1.4 The Wnt pathway and human prostate cancer

Genetic changes alone may not be necessary for the activation of Wnt signalling. Variation in the expression of Wnt ligands could also have an effect. When Wnt/β-catenin signalling is activated (see figure 26 in chapter 1.7.1), Wnt ligands induce LRP phosphorylation and recruitment of axin and Dvl proteins to the plasma membrane. This disrupts the β-catenin ubiquitination complex, thus enabling β-catenin stabilisation and its translocation to the nucleus. Studies have demonstrated upregulation Wnt-1 (Chen et al., 2004b), and Wnt-7b (Li et al., 2008), in both primary tumours and metastases and their prevalence correlate with disease progression. More recently, expression of Wnt-16b in PCa was shown to mitigate the effects of cytotoxic chemotherapy *in vivo*, promoting tumour cell survival and disease progression (Sun et al., 2012). Furthermore, the down regulation of secreted Wnt antagonists has also been identified as a contributing factor toward β-catenin stabilisation, however their influence has proven to be complex and their involvement in PCa formation remains unknown (Kypta and Waxman, 2012). In view of these data, Wnt ligands play an important albeit largely unclear role in β-catenin/Wnt pathway signalling during prostate tumourigenesis.

4.1.5 KRAS and MAPK pathway signalling are implicated in human prostate cancer

Ras proteins are proto-oncogenes that are frequently mutated in many human cancers (Prior et al., 2012), but *RAS* mutations have long been identified as rare in PCa (Carter et al., 1990). Indeed in human PCa the incidence of *RAS* isoform mutations overall in contemporary genomic studies is 15%; 8-10% of which occur in *KRAS* (Taylor et al., 2010, Forbes et al., 2011, Pylayeva-Gupta et al., 2011, Prior et al., 2012). Paradoxically, aberrations that result in upregulated MAPK pathway signalling are among the commonest seen in PCa (Taylor et al., 2010, Selvaraj et al., 2014), suggesting that Ras effectors represent a convergence point for numerous diverse

extracellular signals (Gioeli et al., 2008) particularly in metastatic disease and CRPC development.

Data from mouse models suggest that Ras mutations is necessary to initiate the early stages of prostate tumourigenesis and to maintain the phenotype, whereas progression to invasive PCa requires a second hit from synergistic mutations. Transgenic mice expressing activated H-Ras from the human T24 human bladder carcinoma cell line (Ha-RasT24) under control of the PB promoter developed atypical hyperplasia (AH) of the prostate before 12 months (Barrios et al., 1996). Later, Scherl and colleagues (2004) showed that mice expressing a G12V point mutation in cH-Ras (termed H-Ras^{V12}), under the control of the minimal PB promoter, developed low-grade prostate intraepithelial neoplasia (LG-PIN) that displayed intestinal metaplasia by 3 months. At 12 months, the H-Ras^{V12} transgene was not detected in this model, coinciding with a decrease in PIN incidence.

Thus to summarise, the Wnt, PI3K/Akt/mTOR, and MAPK pathways have been implicated in prostate cancer, but the interplay between them in prostate tumourigenesis remains poorly modelled and poorly understood.

4.2 CHAPTER AIMS

Following on from previous discoveries regarding the activation of the Wnt and MAPK pathways in murine prostate epithelium (Pearson et al., 2009), it was hypothesised that the additional over-activation of the PI3K/Akt/mTOR pathway by PTEN knockout, would initiate metastatic disease.

The aims of this chapter were therefore:

1. To employ Cre-LoxP technology to create conditional transgenic mouse models in which β-catenin, Pten, and Kras are genetically modified in the prostate alone and in combination through action of the rat probasin promoter
2. To subsequently investigate the impact of mutating these critical lesions within the Wnt, PI3K/Akt/mTOR, and MAPK pathways respectively, to define the interplay between them in prostate tumourigenesis
3. To employ immunohistochemistry to characterise the phenotype of these mutations at different stages of tumourigenesis
4. To explore whether the same pathway deregulations and/or synergy are seen in human PCa to substantiate its usefulness as a pre-clinical model of the human disease

4.3 RESULTS

4.3.1 The probasin-Cre (PBCre4) transgene mediates DNA recombination of target alleles within the prostate epithelium

In order to decipher the pattern of PBCre4-mediated recombination in the murine GU tract, wholemounts and frozen sections of wild-type mice with and without both the PBCre4 transgene and the Rosa26 reporter locus underwent staining with Xgal (see figure 32).

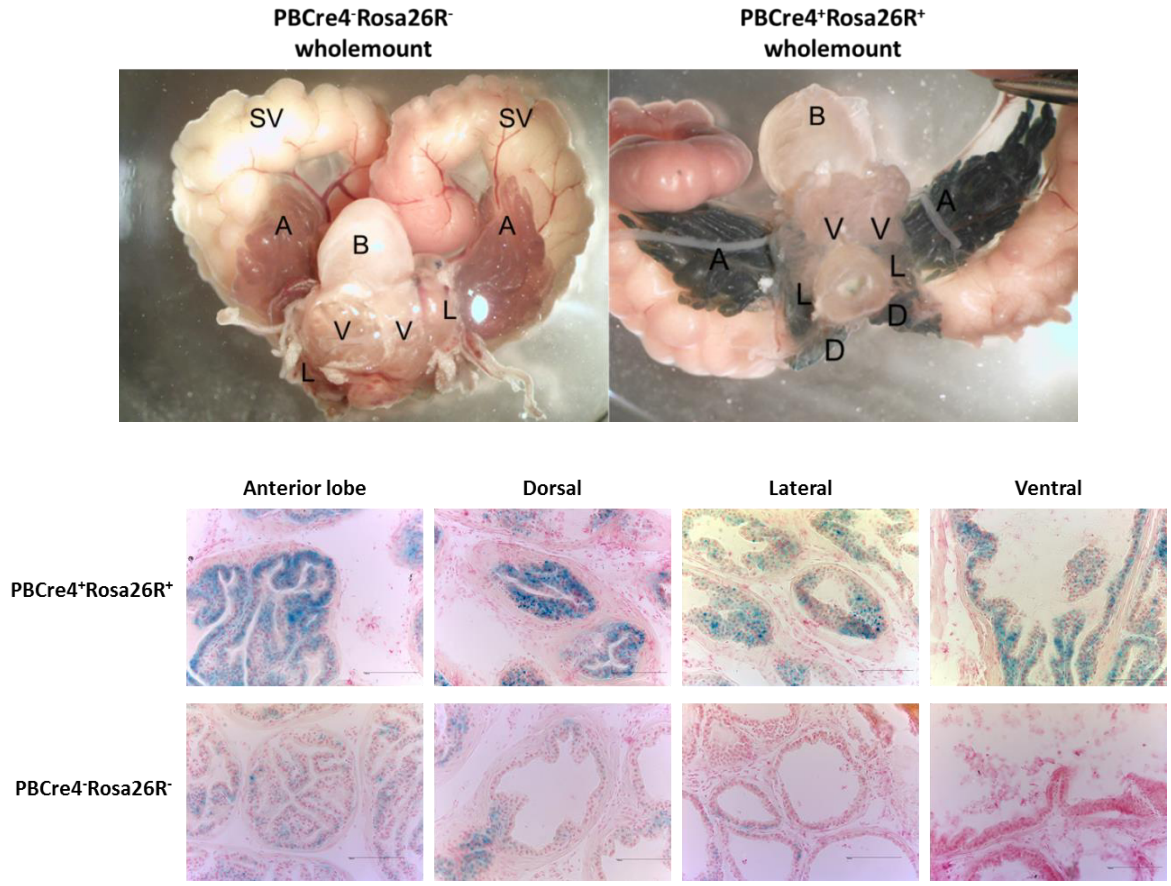

Figure 32: Wholemounts and their sections were used to assess for LacZ staining/recombination in the murine prostate. The Rosa26 reporter locus permits staining with Xgal to assess gross recombination. Note that in PBCre4+Rosa26R+ mice, the appearance of a blue product signifies successful DNA recombination. On wholemount the ventral lobe appears spared but recombination is confirmed in all four lobes on frozen sections. PBCre4-Rosa26R- mice demonstrated occasional non-specific staining for ß-galactosidase. All images were taken at 40x magnification, and scale bars represent 100µm.

Expression of ß-galactosidase (blue product), a surrogate marker of recombination at the Rosa26 reporter locus was detected in the luminal epithelial cells of all four lobes of the prostate in PBCre+Rosa26+ mice, with sparing of the basal cells. Elsewhere in the GU tract, recombination was detected in the testis and epididymis, whereas no recombination was seen in the seminal vesicles or bladder (photographs not shown). In contrast, PBCre-Rosa26- mice demonstrate rare, non-specific expression of ß-galactosidase. These findings are consistent with those of Wu et al. (2001).

To allow monitoring of disease progression, mice were dissected at 100 days (n=6), while the majority (n=12) were aged in survival cohorts until their terminal endpoint or 500 days,

whichever was sooner. The prevalence with which they developed prostate phenotypes is shown in table 14.

Prostate phenotype	100 days n=6					Endpoint (death or 500 days) n=12-15				
	Normal	Hyperplasia	PIN	Low grade PCa	High grade PCa	Normal	Hyperplasia	PIN	Low grade PCa	High grade PCa
Genotype										
WT	100%					100%				
$Catnb^{+/lox(ex3)}$	33%		67%			27%			73%	
$Pten^{flox}$	33%		67%			71%			29%	
$Kras^{+/V12}$	83%	17%				100%				
$Catnb^{+/lox(ex3)}$ $Pten^{flox}$	33%		33%		33%	92%				8%
$Catnb^{+/lox(ex3)}$ $Kras^{+/V12}$			50%		50%	60%				40%
$Pten^{flox}$ $Kras^{+/V12}$			50%		50%	77%				23%
Triple						80%				20%

Table 14: Prevalence of disease stage seen in each mouse model at both time points. Note that due to rapid progression to lethal PCa in the triple mutant (mean survival 76 days), any alive at 100 days were found to be 'mosaic males' with normal prostates and discounted. Apart from *wild-type* males, all other genotypes that exhibited normal prostates at endpoint were also due to mosaicism. See below for full explanation of mosaic male phenotype development.

4.3.2 Beta-catenin and Pten single mutant mice display reduced survival, whereas Kras single mutant mice do not

To investigate the potential for cooperation between the pathways of interest, an appreciation of the outcomes of single mutations first had to be established. To this end, cohorts of single mutant mice were generated (n=12-15); heterozygous for activating mutations of β-catenin (*PBCre4*$^{+}$*Catnb*$^{+/lox(ex3)}$) or Kras (*PBCre4*$^{+}$*Kras*$^{+/V12}$), or homozygously-deleted PTEN (*PBCre4*$^{+}$*Pten*^{flox}). Mice were aged and sacrificed using schedule 1 methods when symptomatic of disease.

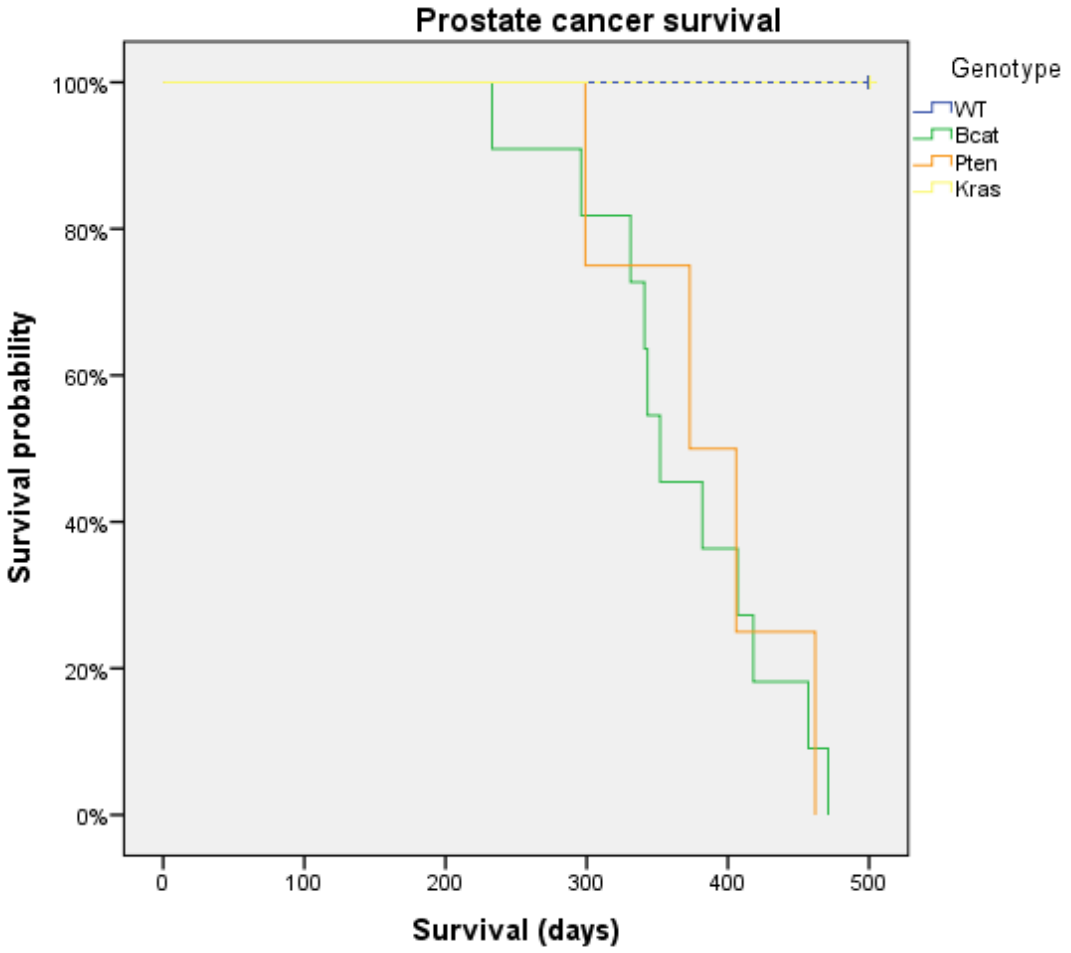

Figure 33: Kaplan-Meier survival estimates comparing normal controls vs single mutant mice. Note that β-catenin (PBCre4^{+}Catnb$^{+/lox(ex3)}$) and Pten (PBCre4^{+}Pten^{flox}) single mutants and mice develop lethal prostate tumours, whereas controls (*wild-type* and PBCre4^{-} mice) and Kras single mutant mice (PBCre4^{+}Kras$^{+/V12}$) do not. Statistical analysis was performed in SPSS 20 (Armonk, NY: IBM Corp).

Controls (true *wild-type* and PBCre4^{-} mice) and Kras single mutants (PBCre4^{+}Kras$^{+/V12}$) mice were censored at the 500d endpoint as they did not succumb to PCa. As previously reported (Pearson et al., 2009), Kras single mutant mice develop PIN thereby implicating Kras in the early stages of prostate tumourigenesis. Therefore Kras mutants will not be discussed in further detail as a single mutation here. Beta-catenin (PBCre4^{+}Catnb$^{+/lox(ex3)}$) and Pten (PBCre4^{+}Pten^{flox}) single mutants survived to median 352 and 389 days respectively, as seen in figure 33.

4.3.3 Dominant, stablilised β-catenin results in progression from HGPIN to invasive adenocarcinoma associated with keratinised squamous metaplasia

When compared to *wild-type*, β-catenin single mutant mice (PBCre4^{+}Catnb$^{+/lox(ex3)}$) develop a diffuse, HGPIN in all lobes of the prostate by 100 days that is associated with keratinising squamous metaplasia. Lesions demonstrated nuclear atypia, with occasional apoptotic bodies, active mitosis, and keratin deposition. At endpoint, lesions had progressed to bulky locally-invasive, non-metastatic adenocarcinomas akin to human Gleason pattern 3, also with keratinising squamous metaplasia. Tumours were macroscopically found to be large and solid in nature, with associated enlargement of bulbourethral glands (BUGs), which were also found to be globally infiltrated with keratinising squamous metaplasia (photographs not shown). Lesions from β-catenin single mutants can be seen in figure 34.

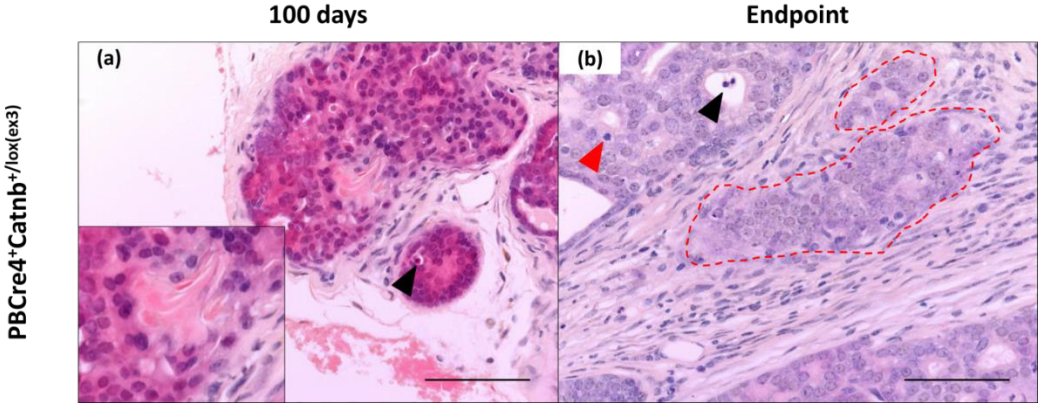

Figure 34: Dominant stabilisation of β-catenin governed by PBCre4 mimics human disease progression to locally-advanced PCa. Histological analysis of formalin-fixed, paraffin-embedded sections of prostate stained with H&E from mice aged 100 days and at endpoint. Early lesions (a) are comparable with human HGPIN, but with keratin formation within squamous metaplastic foci (inset). Lesions are confined to the basement membrane and occasional apoptotic bodies are seen within (black arrow head). When mice succumb to disease (b), lesions can be seen to invade the stroma (red broken lines) in gland-forming fashion, which is pathognomonic of Gleason pattern 3. Tumours contain frequent mitosis (red arrow head), and apoptotic bodies (black arrow head), along with squamous metaplasia (not shown here). Nuclei are pleomorphic and contain large, prominent nucleoli. All images were taken at 40x magnification, and scale bars represent 100µm.

4.3.4 Homozygous loss of Pten results in progression from HGPIN to invasive adenocarcinoma

When compared to *wild-type*, Pten single mutants (PBCre4^{+}Pten^{flox} mice) develop diffuse HGPIN in all four prostate lobes by 100 days. Lesions are phenotypically distinct from those seen in β-catenin single mutants (PBCre4^{+}Catnb$^{+/lox(ex3)}$) at 100 days, in that they do not display squamous metaplasia. However, Pten-deficient HGPIN displays regular mitoses and apoptotic bodies, along with considerable cellular atypia compared with normal prostate epithelium. Upon loss of Pten at endpoint, locally-invasive, non-metastatic tumours develop, often with large dilated glands containing secretions. Often mice were noted to have turbid urine prior to deterioration in their health. In further contrast with β-catenin single mutants, there is no bulbourethral gland enlargement in Pten-deficient mice at endpoint. The lesions that arose within the prostates of Pten single mutants are shown in figure 35.

4.3.5 Combinatorial mutations in β-catenin and/or Kras, with/without Pten loss, accelerates prostate tumourigenesis to lethal locally-advanced adenocarcinoma

When compared with single mutant mice, those bearing combinatorial oncogenic mutations displayed dramatically reduced survival due to PCa. Both double and triple mutant combinations developed lethal high grade, locally invasive adenocarcinomas; β-catenin/Pten mutants (PBCre4^{+}Catnb$^{+/lox(ex3)}$Pten^{flox} mice) survived to 140 days; β-catenin/Kras mutants (PBCre4^{+}Catnb$^{+/lox(ex3)}$K-ras$^{+/V12}$) survived to 251 days; Pten/Kras mutants (PBCre4^{+}Pten^{flox}K-ras$^{+/V12}$) survived to 185 days; while triple mutants (PBCre4^{+}Catnb$^{+/lox(ex3)}$Pten^{flox}K-ras$^{+/V12}$) survived to 76 days. This acceleration in prostate tumourigenesis is demonstrated in figure 36.

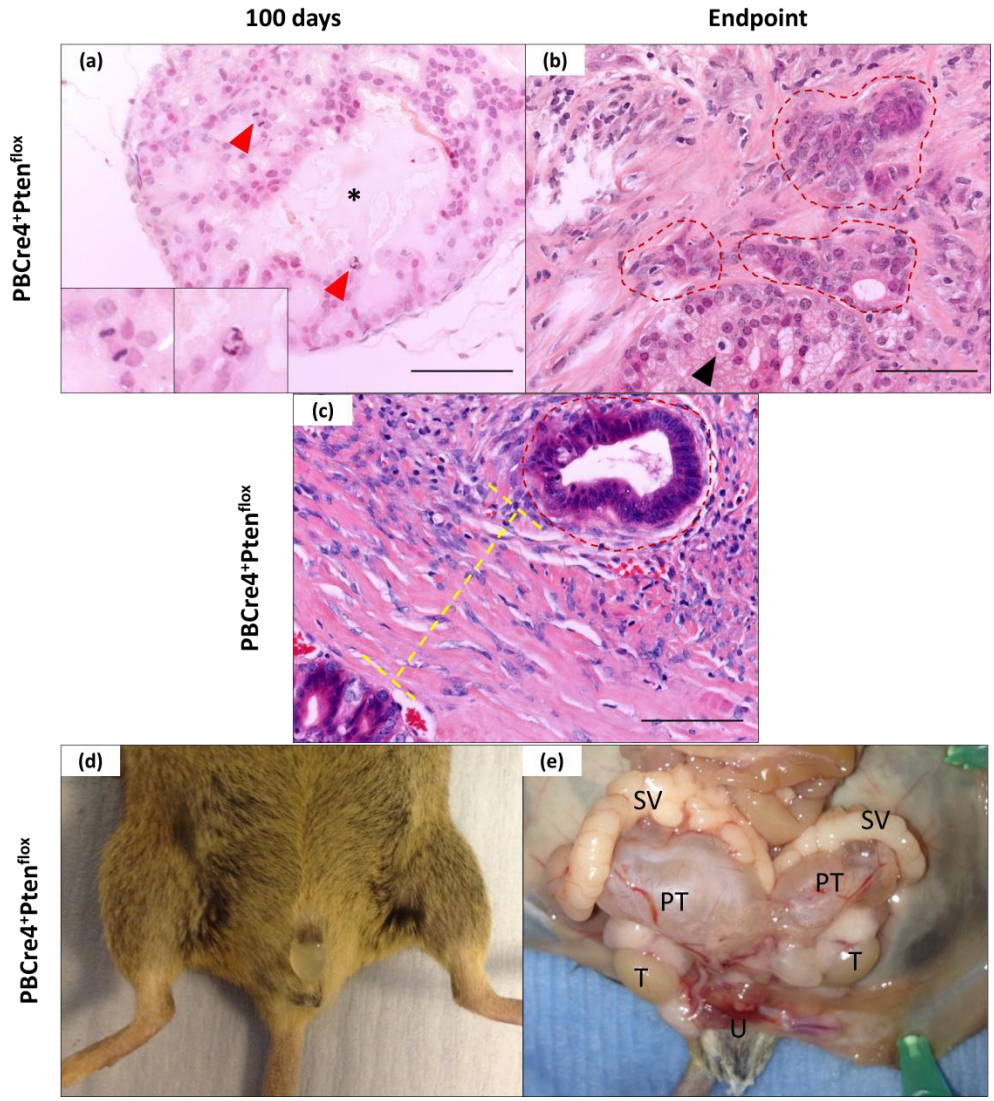

Figure 35: Pten-deletion, within murine prostate, leads to adenocarcinoma when governed by the PBCre4 transgene. HGPIN lesions (a) demonstrate diffuse nuclear atypia with prominent mitoses (red arrow heads) and the presence of protein-rich secretions (*). Invasive adenocarcinoma (broken red lines) at endpoint (b) is consistent with Gleason pattern 3, with occasional apoptotic bodies (black arrow head). Pten-deficient invasive adenocarcinoma (c) is associated with a marked fibroblastic stromal reaction as evidenced by the abundant spindle-shaped cells with pale nuclei suggestive of myelofibroblasts (broken yellow lines); this is a common response to tumour (broken red line). Tumours can be suspected clinically in Pten-null prostates by the presence of turbid urine (d), and tumours appear to consistently be cystic in nature and contain copious protein-rich secretions (e); *PT* prostate tumour, *SV* seminal vesicles, *T* testes, and *U* cut end of urethra. Images a-c were taken at 40x magnification, and scale bars represent 100µm. Images d-e were taken with an Olympus digital camera following necropsy (Olympus, Japan).

(a)

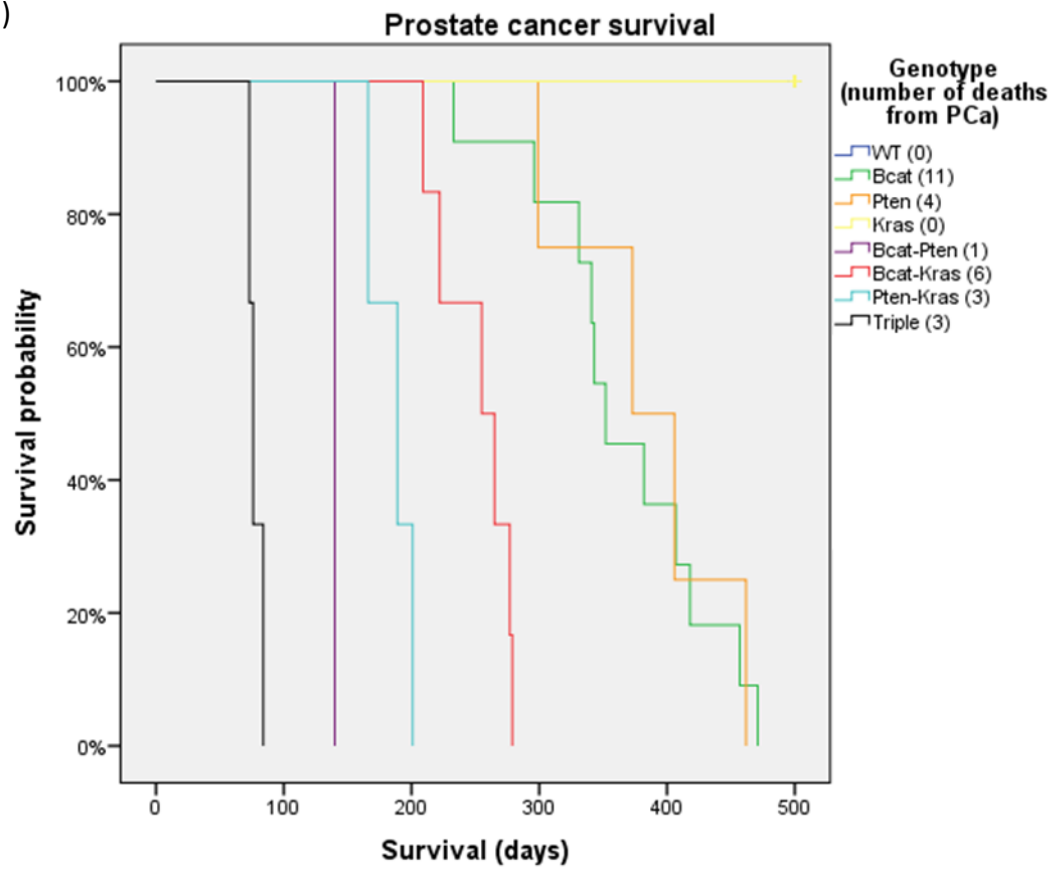

(b)

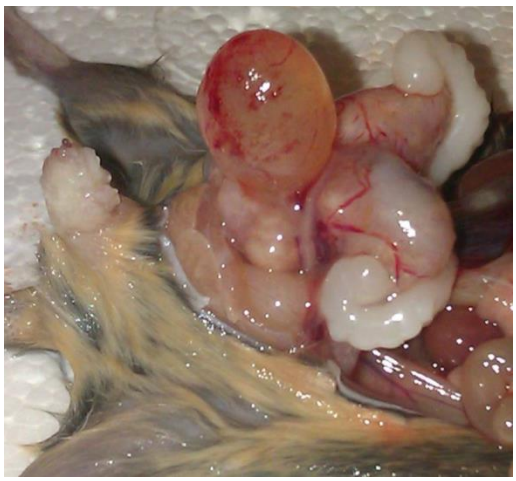

Figure 36: (a) Kaplan-Meier survival estimates for all cohorts of mutant mice for comparison, and (b) a locally-advanced lethal prostate tumour causing obstructive uropathy. Compound mutant mice display reduced survival compared to single mutants and/or *wild-type* mice. Numbers of mice that died for each genotype are shown in brackets. Compound mutants develop aggressive locally-advanced, non-metastatic prostate tumours from which the causes of death tend to be either from general tumour burden probably with significant cytokine release, or obstructive uropathy as in (b). Note the distended bladder and prolapsed penile lesion here. Statistical analysis was performed in SPSS 20 (Armonk, NY: IBM Corp). Image (b) was taken with an Olympus digital camera following necropsy (Olympus, Japan).

No metastatic lesions were identified in the major organs of compound mutant mice, however all combinatorial mutants displayed reactive retroperitoneal lymphadenopathy (see figure 37).

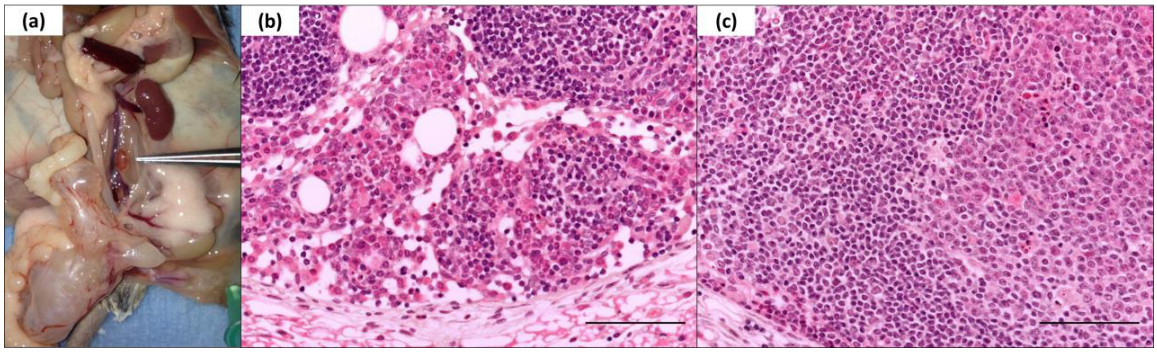

Figure 37: All combinatorial mutants develop reactive retroperitoneal lymphadenopathy. Enlarged lymph nodes were readily identifiable in the retroperitoneum, as identified by forceps in (a). Histological analysis of formalin-fixed, paraffin-embedded sections of lymph nodes stained with H&E was performed (b and c). Normal lymph nodes possess two zones: the cortex and medulla. Here (b) the medulla displays discrete germoid centres and prominent lymphoid follicles within. Peripheral sinuses are evident in the cortex (not shown). By comparison, enlarged lymph nodes from compound mutant mice (c) are seen to demonstrate loss of nodular architecture and cortico-medullary differentiation. The node is infiltrated with a mixed population of small and large lymphocytes, with an appearance similar to that of human lymphoma. Image (a) was taken with an Olympus digital camera following necropsy (Olympus, Japan), while images (b) and (c) were taken at 40x magnification, and scale bars represent 100µm.

4.3.6 Double and triple mutant mice model rapid disease progression from HGPIN to high-grade prostate cancer

At the 100 day time point, all double mutant mice display either HGPIN or a combination of early/low-volume invasive carcinoma of high-grade (see figure 38) with HGPIN. Here HGPIN is the most prevalent lesion at 100 days regardless of genotype. By endpoint, mice develop locally-advanced high-grade adenocarcinomas analogous to Gleason pattern 4 in the human.

It is worthy of not that all prostate lesions, whether HGPIN or invasive adenocarcinoma, contain keratinised squamous metaplasia if their genotype contains a dominant stabilising mutation of β-catenin. This can be seen from the photographs in figure 38.

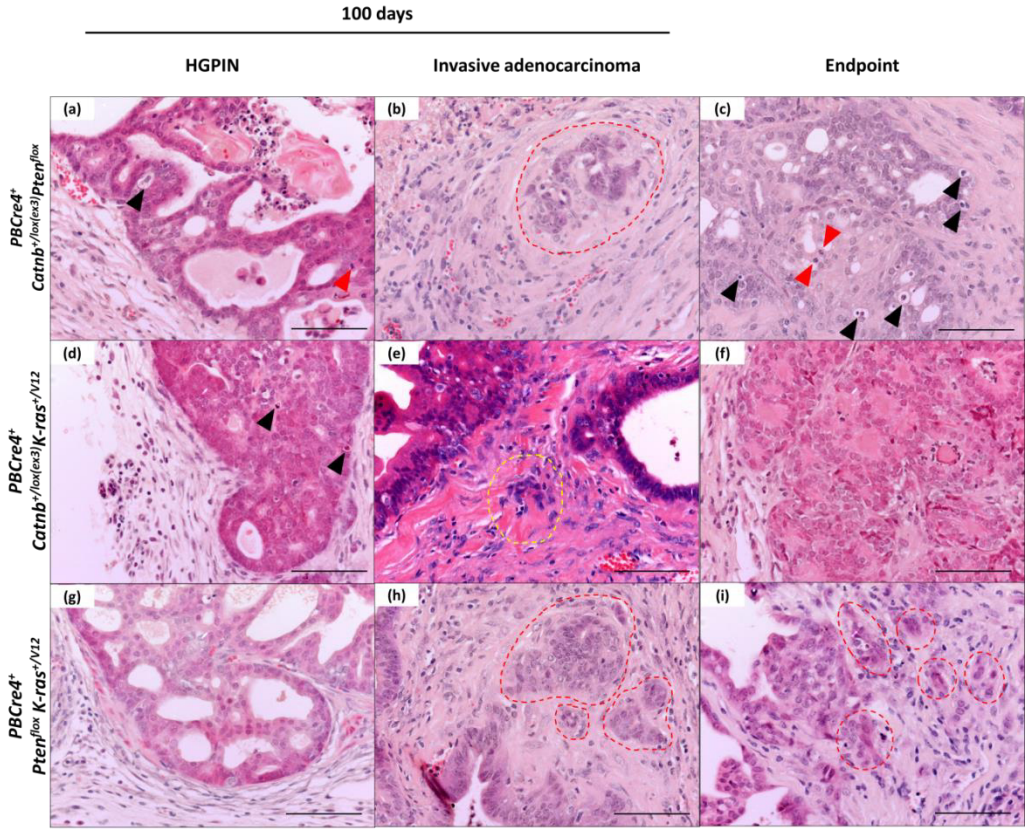

Figure 38: Double mutation of β-catenin and/or Kras, with/without Pten loss promotes the promotes the progression to high grade PCa from HGPIN. Histological analysis of formalin-fixed, paraffin-embedded sections of prostate stained with H&E from mice aged 100 days and at endpoint. At 100 days double mutant mice display a large volume of HGPIN (see a, d, g) with evidence of focal invasive PCa (see b, e, h); broken red/yellow lines highlight early but high-grade, invasive adenocarcinoma. HGPIN demonstrates obvious nuclear atypia that fills duct lumens with cribriform patterning (best seen in a, and g), and occasional apoptotic bodies (black arrowheads) and mitoses (red arrowheads). Such is the bulk of HGPIN here that there is bulging with surrounding stromal distortion. At endpoint (see images c, f, and i), high-grade PCa has no demonstrable glandular architecture due to gland fusion; instead there are irregular nests of cells in cribriform arrangement or sheets of pleomorphic carcinoma cells with prominent hyperchromatic nucleoli, increased angiogenesis, and frequent mitoses and apoptotic bodies. All images were taken at 40x magnification, and scale bars represent 100µm.

Prostate tumours that arose in triple mutant mice ($PBCre4^{+}Catnb^{+/lox(ex3)}Pten^{flox}K\text{-}ras^{+/V12}$) can likewise be seen to be bulky, locally-advanced, and high-grade. It is important to note that because triple mutant mice survive to median 76 days, none survived to the 100 day time point. Thus no PIN was analysed in these mice. Characterisation of triple mutant tumours is described in figure 39.

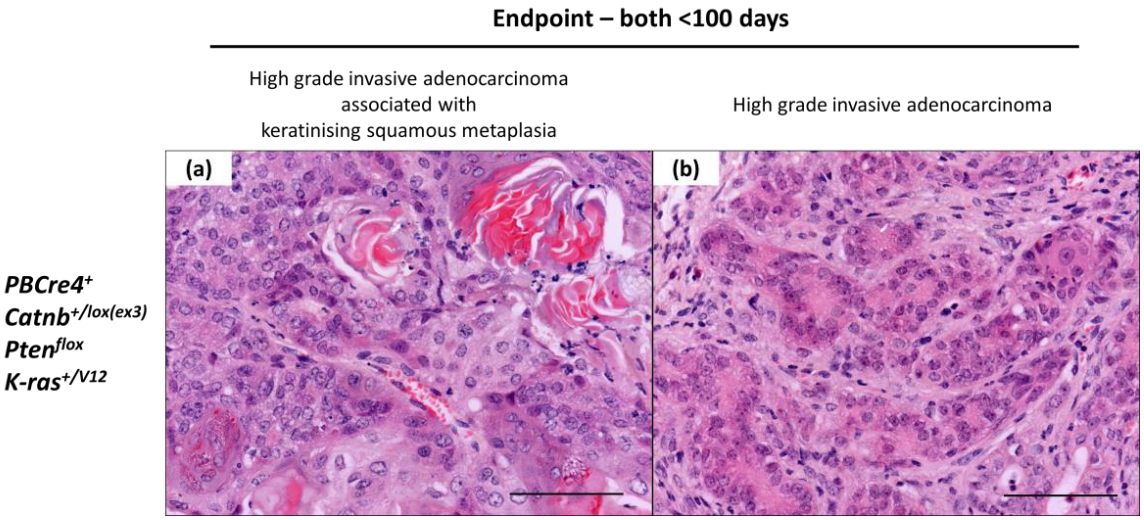

Figure 39: Mutations in all three alleles synergistically promotes the rapid development of high-grade adenocarcinoma. Note that these tumours contain discreet pockets of keratinising squamous metaplasia (a). The tumours formed are morphologically similar to human Gleason pattern 4 (b) in that there are irregular nests of cells in cribriform arrangement with occluded gland lumens, and pleomorphic cells with prominent hyperchromatic nucleoli. All images were taken at 40x magnification, and scale bars represent 100µm.

4.3.7 The probasin-Cre transgene exhibits mosaic genetic deletion when transmitted maternally

When transmitted paternally, probasin-Cre (PBCre4) is expressed exclusively in the male prostate epithelium, leading to intended prostate-specific phenotypes. However it was noted that when transmitted maternally, recombination of loxP-flanked alleles arose in a variety of tissues in both male and female offspring, termed “mosaic” recombination. The effects of mosaic PBCre4 activity can be seen in the survival cohorts (as shown in figure 40) leading to adversely prolonged survival in all genotypes. The effect on the prostate phenotype was similarly unreliable as outlined in table 14.

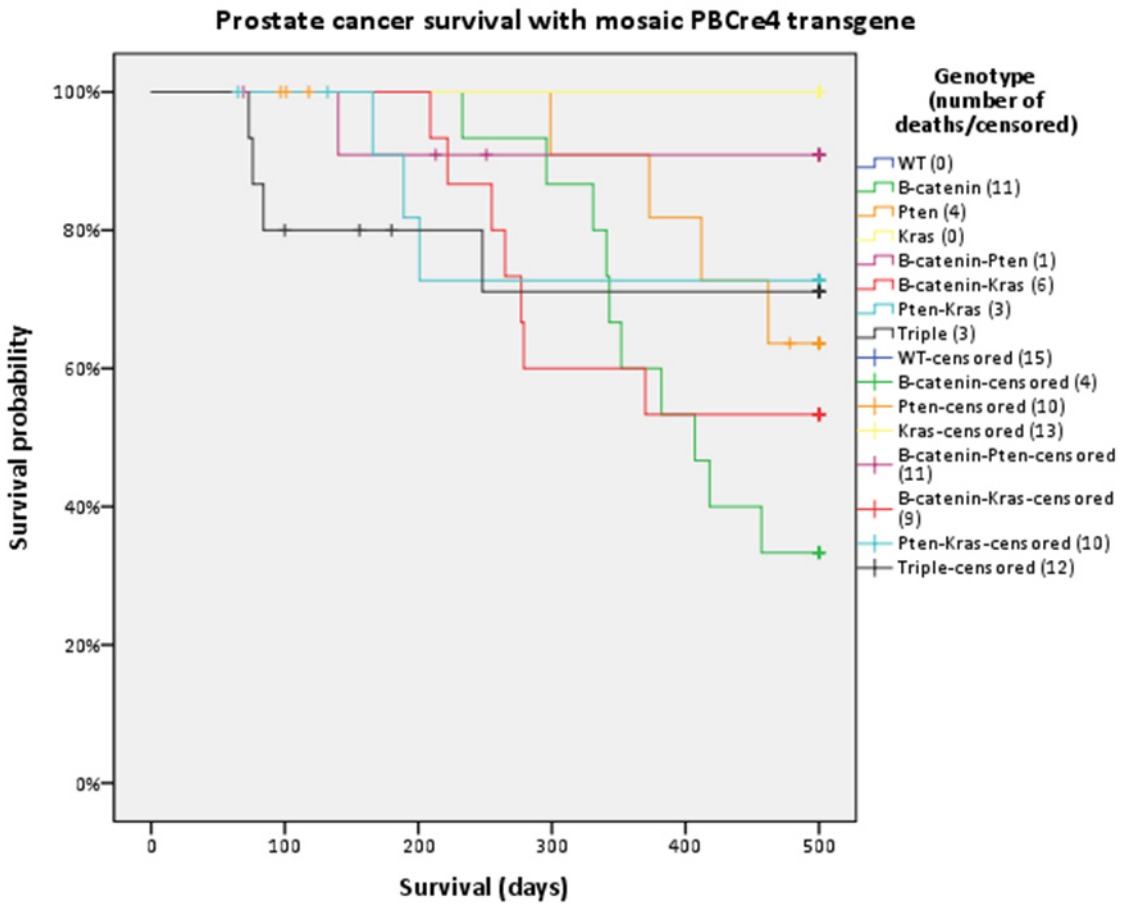

Figure 40: Kaplan-Meier curves demonstrate the effect of pronged survival in all cohorts when PBCre4 is transmitted maternally. Upon closer inspection the PBCre4 transgene was functioning incorrectly, and so all mosaic males were censored from final survival analyses, dramatically reducing the size of some most cohorts; the result of this can be seen in figure 36(a). Statistical analysis was performed in SPSS 20 (Armonk, NY: IBM Corp).

Given that there was substantial variation between the prostate tumours observed compared with those expected, a Chi-square cross tabulation analysis was performed as shown in figure 41. This ultimately supported the hypothesis that the PBCre4 transgene is not transmitted equally between parents (χ^2 = 39.37, $p<0.001$). Taken together these data suggest that paternally inherited loxP-flanked alleles are inefficiently recombined by maternal PBCre4, giving rise to mosaic expression patterns in the offspring. These findings have since been corroborated (Birbach, 2013).

	Value	♂ PBCre4+ ♀ PBCre4-	♂ any PBCre4 ♀ PBCre4+	♂ PBCre4+ ♀ unknown	Total
Tumour	Observed	24	2	2	28
	Expected	11.27	9.72	7	28
No tumour	Observed	5	23	16	44
	Expected	17.72	15.27	11	44
Total		29	25	18	72

H0: no difference in PBCre4 transmission between parents
H1: there is a true difference in PBCre4 transmission between parents

Tumour * Parentage Crosstabulation

Count

		Parentage			
		Father PBCre4+; Mother PBCre4-	Father any PBCre4; Mother PBCre4+	Father PBCre4+; Mother unknown	Total
Prostate tumour	Y	24	2	2	28
	N	5	23	16	44
Total		29	25	18	72

Chi-Square Tests

	Value	df	Asymp. Sig. (2-sided)
Pearson Chi-Square	39.366[a]	2	.000
Likelihood Ratio	43.069	2	.000
Linear-by-Linear Association	28.756	1	.000
N of Valid Cases	72		

a. 0 cells (.0%) have expected count less than 5. The minimum expected count is 7.00.

$\chi^2 = 39.37$, $p<0.001$ therefore **reject** H0

Figure 41: Chi-square cross-tabulation analysis to determine whether or not the PBCre4 transgene is equally transmitted both maternally and paternally. Pairings that resulted in prostate tumours were compared with those that led to absent prostate tumourigenesis and/or unwanted phenotypes. From the original 111 mice allocated to 8 cohorts, 39 were excluded from the Chi-square test; 15 were *wild-type*, 13 Kras, 1 mouse was lost to follow-up, and 10 were found dead with no cause. Analysis was performed in SPSS 20 (Armonk, NY: IBM Corp).

No evidence of tumourigenesis was visible within the prostate of mosaic males (photographs not shown). However, some male mice developed rapidly-growing tumours from within the mammary gland which attenuated their survival. Photographs of mosaic male mammary tumours are shown in figure 42.

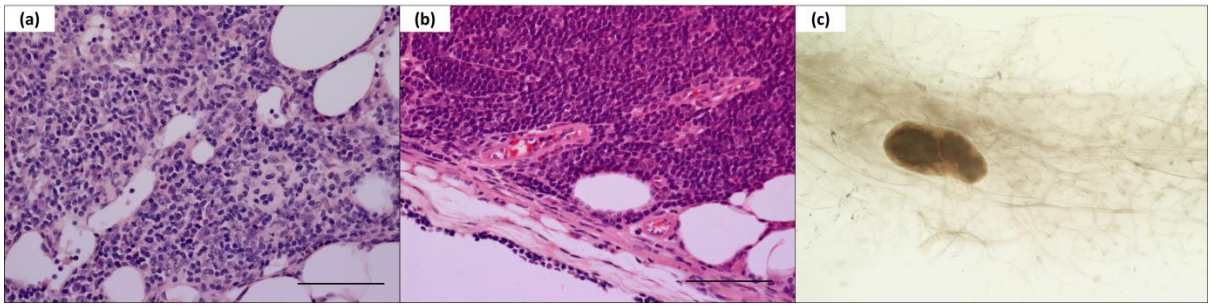

Figure 42: Maternal transmission of the PBCre4 transgene leads to unwanted lymphoid phenotypes in male offspring. In the absence of prostate tumourigenesis, rapid enlargement of mammary gland lymph nodes can be detected when assessing the health of mosaic males. Upon histological analysis of formalin-fixed, paraffin-embedded sections, it can be seen that lymph nodes (a) and (b) are flooded with a mixed population of small and large lymphocytes. The mammary wholemount photograph (c) demonstrates the location of the central lymph node within the gland that stained with Xgal, whereas staining is absent from the ducts. Images (a) and (b) were taken at 40x magnification, and scale bars represent 100µm. Image (c) was taken with an Olympus digital camera (Olympus, Japan).

4.3.8 Progression of prostate tumourigenesis in these mouse models correlates with Ki67 expression

Ki67 is a marker of cellular proliferation; it is present during all active phases of the cell cycle (G_1, S, G_2, and mitosis), but absent from resting cells (G_0). Figure 43 demonstrates proliferation within murine prostate tumours of various stages.

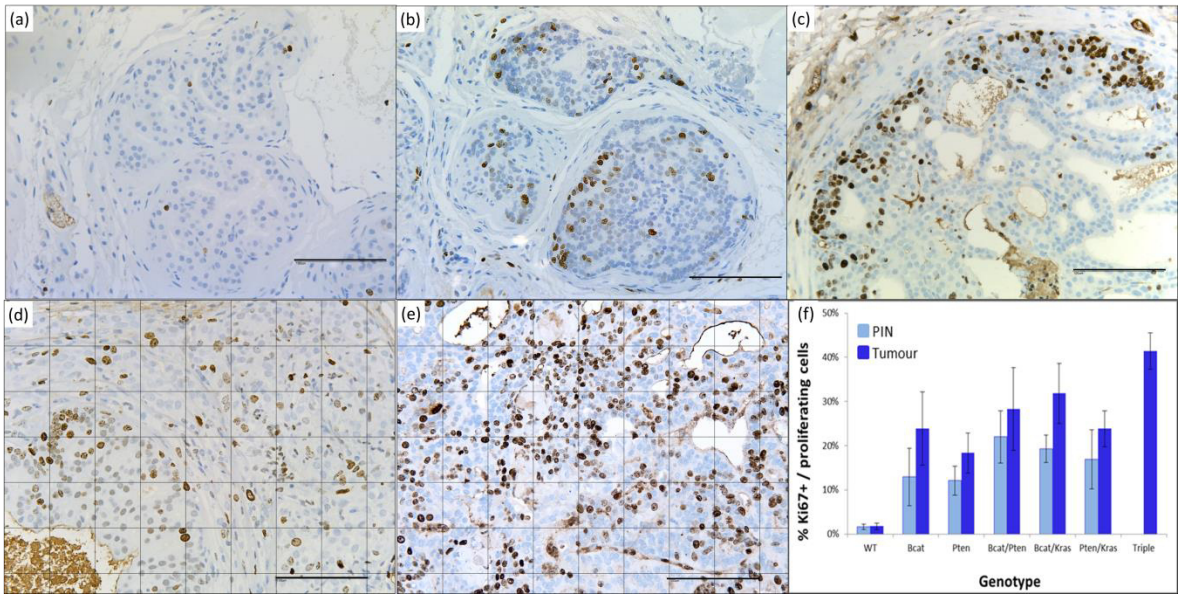

Figure 43: Immunohistochemistry to detect cellular proliferation by Ki67 expression in prostate lesions. It can be seen from IHC that Ki67 staining is rare in normal wild-type epithelium (a). In both low-grade (b), and high-grade PIN (c), cells nearer the basement membrane stain avidly for Ki67. In both low-grade (d) and high-grade adenocarcinoma (e), the distribution of Ki67+ cells is more random, with the greatest level of expression being in the high-grade tumours. The percentage of Ki67+ prostate epithelial cells were scored for PIN and adenocarcinomas of each genotype (f), n=3 mice. Columns depict median, while error bars represent SD; statistical analysis was carried out using the non-parametric Mann-Whitney U test, $p<0.05$ (95% confidence interval). Analysis was performed in SPSS 20 (Armonk, NY: IBM Corp).

It can be seen in figure 43(a) that physiological levels of Ki67 expression in *wild-type* mice are low, with little change between 100 days (light blue – PIN) and the 500 day endpoint (dark blue – tumour) seen in 43(f). Expression levels are increased significantly in PIN lesions of all genotypes compared to *wild-type*, see 43(b), (c), and (f). Moreover, upon progression from PIN to adenocarcinoma there is further elevation in Ki67 expression among all genotypes. As seen in figure 43(d), and (e), Ki67 also appears to correlate with adenocarcinoma grade: high grade adenocarcinoma (from double and triple mutants) reveals a significantly greater level of Ki67

expression than low-grade adenocarcinoma (in single mutant tumours), p=0.011. Triple mutant tumours express significantly more Ki67 than single β-catenin (p=0.0404, Mann Whitney U test, n=3) and PTEN (p=0.404, n=3) mutants but not more than double mutant combinations. This suggests that Ki67 correlates with tumour grade.

4.3.9 Progression of prostate tumourigenesis in these mouse models correlates with AR expression

AR is expressed by differentiated luminal epithelial cells that appear to comprose the tumour bulk. This is highlighted in figure 44.

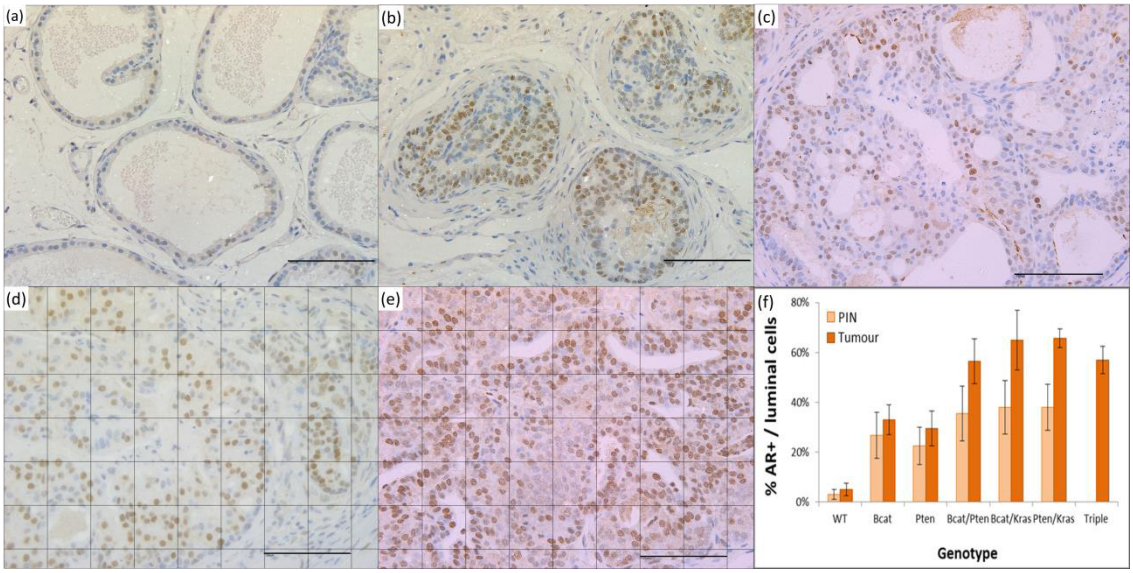

Figure 44: Immunohistochemistry to detect AR expression in prostate lesions. It can be seen from IHC that AR staining is infrequent in normal wild-type epithelium (a). In both low-grade (b), and high-grade PIN (c), cells located centrally stain avidly for AR, while thos located basally are relatively spared. The level of AR positivity increases from low-grade (d) to high-grade adenocarcinoma (e). The percentage of AR+ prostate epithelial cells were scored for PIN and adenocarcinomas of each genotype (f), n=3. Columns depict median, while error bars represent SD; statistical analysis was carried out using the non-parametric Mann-Whitney U test, p<0.05 (95% confidence interval). Analysis was performed in SPSS 20 (Armonk, NY: IBM Corp).

Baseline levels of AR expressed in *wild-type* prostate on IHC are low, as seen in figure 44(a). These levels are significantly increased in PIN across all genotypes which does not statistically differ between them (Mann-Whitney U test, n=3 mice), as seen in 44(b), (c), and (f). Furthermore it can be seen in figure 44(f) that disease progression in β-catenin and PTEN single mutants causes a non-significant rise in AR expression, whereas disease progression in double

mutants from PIN to high-grade adenocarcinoma is associated with a significantly elevated rate of AR expression (p=0.0404 for all combinations). Triple mutant tumours revealed a non-significant decrease in level of AR expression compared to double mutants, possibly reflecting their androgen-independent state. AR also appears to correlate positively with tumour grade given that level of AR expression is significantly greater in combinatorial mutants (high-grade adenocarcinoma, n=12) compared with single mutants (low-grade adenocarcinoma, n=6), p=0.001, Mann-Whitney U test.

4.3.10 Progression of prostate tumourigenesis in these mouse models negatively correlates with p63 expression

Tumour protein p63 is a member of the tumour-suppressor p53 gene family, and is expressed by basal cells in both human and mouse prostate. The levels of p63 expression seen in prostate lesions are evident in figure 45.

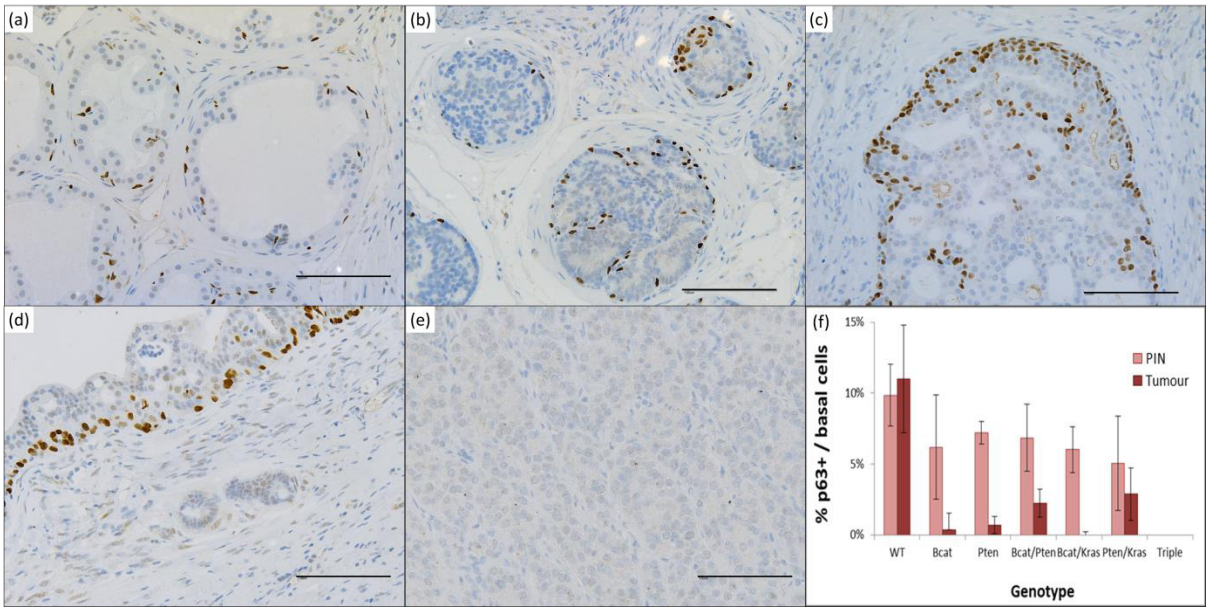

Figure 45: Immunohistochemistry to detect p63 expression in prostate lesions. It can be seen from IHC that p63 reliably stains basal cells in normal *wild-type* epithelium (a). In both low-grade (b), and high-grade PIN (c), there is an upsurge in p63+ cells but the overall percentage decreases due to a greater proliferation of p63- (luminal) cells. In low-grade adenocarcinoma (d), invasive disease lacks p63 expression, which is further corroborated in high-grade adenocarcinoma (e). The percentage of p63+ prostate epithelial cells were scored for PIN and adenocarcinomas of each genotype (f), n=3. Columns depict median, while error bars represent SD; statistical analysis was carried out using the non-parametric Mann-Whitney test, $p<0.05$ (95% confidence interval). Analysis was performed in SPSS 20 (Armonk, NY: IBM Corp).

Physiological levels of p63 expression range from 10 to 15% in *wild-type* mice. Universally in murine PIN the rate of p63 positivity appears to drop non-significantly to between 5 and 8% across all genotypes; this can be seen in figure 45(e). Progression from PIN to adenocarcinoma negatively correlates with p63 expression for all genotypes individually ($p=0.0404$ except Pten/Kras double mutants, $p=0.05$) and when all PIN lesions ($n=15$) are compared with adenocarcinoma ($n=18$), $p<0.001$. The absence of p63 staining is a hallmark of prostate cancer in humans. Beta-catenin/Kras double mutants and triple mutants do not express p63, perhaps reflecting greater differentiation into p63- luminal cells. However adenocarcinomas of other genotypes express p63 at low level. In mice, basal cell markers can be retained by cancer cells so the presence of such staining does not exclude PCa (Ittmann et al., 2013). Likewise complete loss of p63 in a focus that is histologically compatible with prostate cancer supports this diagnosis.

4.3.11 Caspase-3 staining correlates with the number of pathways activated and disease progression, but not tumour grade

Caspase-3 is an antigen expressed by cells undergoing apoptosis. An alternative method of quantifying apoptosis would be to count apoptotic bodies after H&E staining. One disadvantage of this latter technique is that usually only end-stage apoptotic cells can be observed; pre-apoptotic cells are very difficult to detect unless caspase-3 is utilised (Eckle et al., 2004). In addition, counting apoptotic bodies after H&E staining is both time-consuming and more prone to bias. Demonstration of the Caspase-3 expression patterns in both normal murine prostate and tumour is provided in figure 46.

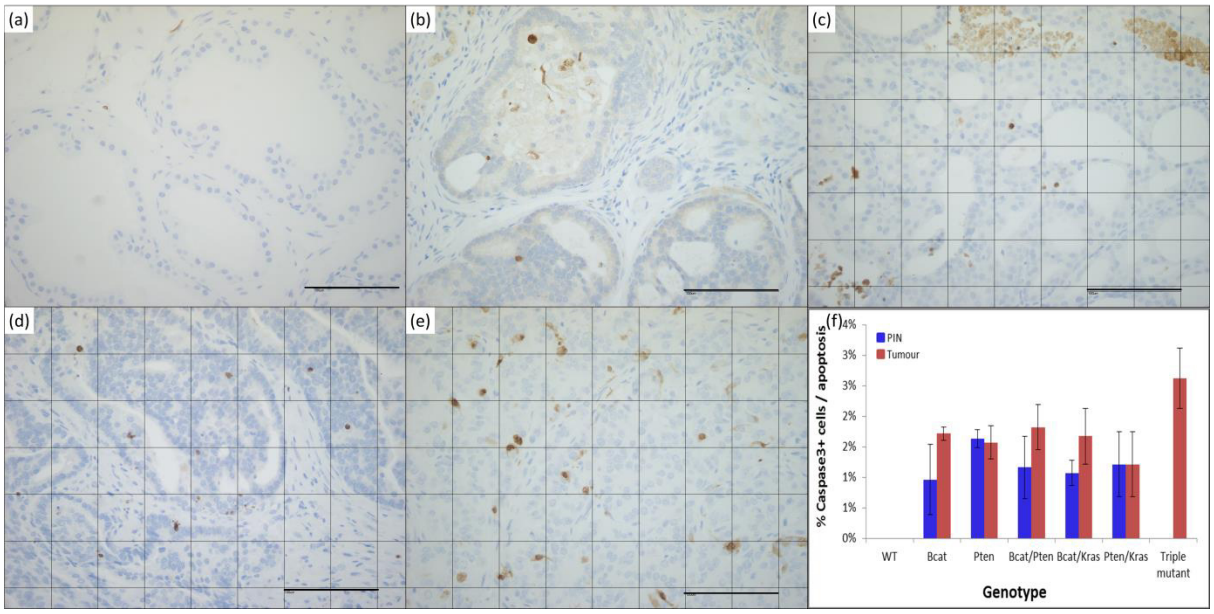

Figure 46: Immunohistochemistry to detect for the presence of apoptotic bodies by Caspase-3 expression in prostate lesions. It can be seen from IHC that apoptosis in normal wild-type prostate epithelium is uncommon (a). In both low-grade (b), and high-grade PIN (c), caspase-3^+ cells are notably more prevalent, but there is little difference according to the severity of PIN. Apoptosis occurs more regularly in adenocarcinoma than PIN but this is not dose dependent when comparing low-grade adenocarcinoma (d), with high-grade disease (e). The percentage of caspase-3^+ apoptotic cells were scored for PIN and adenocarcinomas of each genotype (f), n=3 mice. Columns depict median, while error bars represent SD; statistical analysis was carried out using the non-parametric Mann-Whitney test, $p<0.05$ (95% confidence interval). Analysis was performed in SPSS 20 (Armonk, NY: IBM Corp).

When all three pathways are activated in the triple mutant (n=3), caspase-3 expression levels were significantly increased compared with double (p=0.013, n=9), or single pathway activation (p=0.020, n=6). The rate of apoptosis also correlated with disease progression from PIN (n=18) to adenocarcinoma (p=0.003, n=15) across all genotypes. However the increased level of apoptosis observed between low-grade (n=6) and high-grade (n=12) adenocarcinoma as per caspase-3 positivity was not significant (p=0.349), shown in figure 46(f).

4.3.12 The pattern of expression of cytokeratins corroborates the expression of AR and p63 in each stage of prostate tumourigenesis

Upon the stepwise progression from normal prostate to PIN to invasive adenocarcinoma, a progressively more luminal phenotype develops, reflecting the human disease. Cytokeratins (CK) 8 and CK18 are markers of differentiated luminal epithelial cells, while CK5 and CK14 stain

undifferentiated basal cells. Figure 47 highlights this change, which further supports the findings of figures 44 and 45, wherein AR expression was upregulated and p63 downregulated in parallel with disease progression respectively, confirming a tendency towards luminal differentiation.

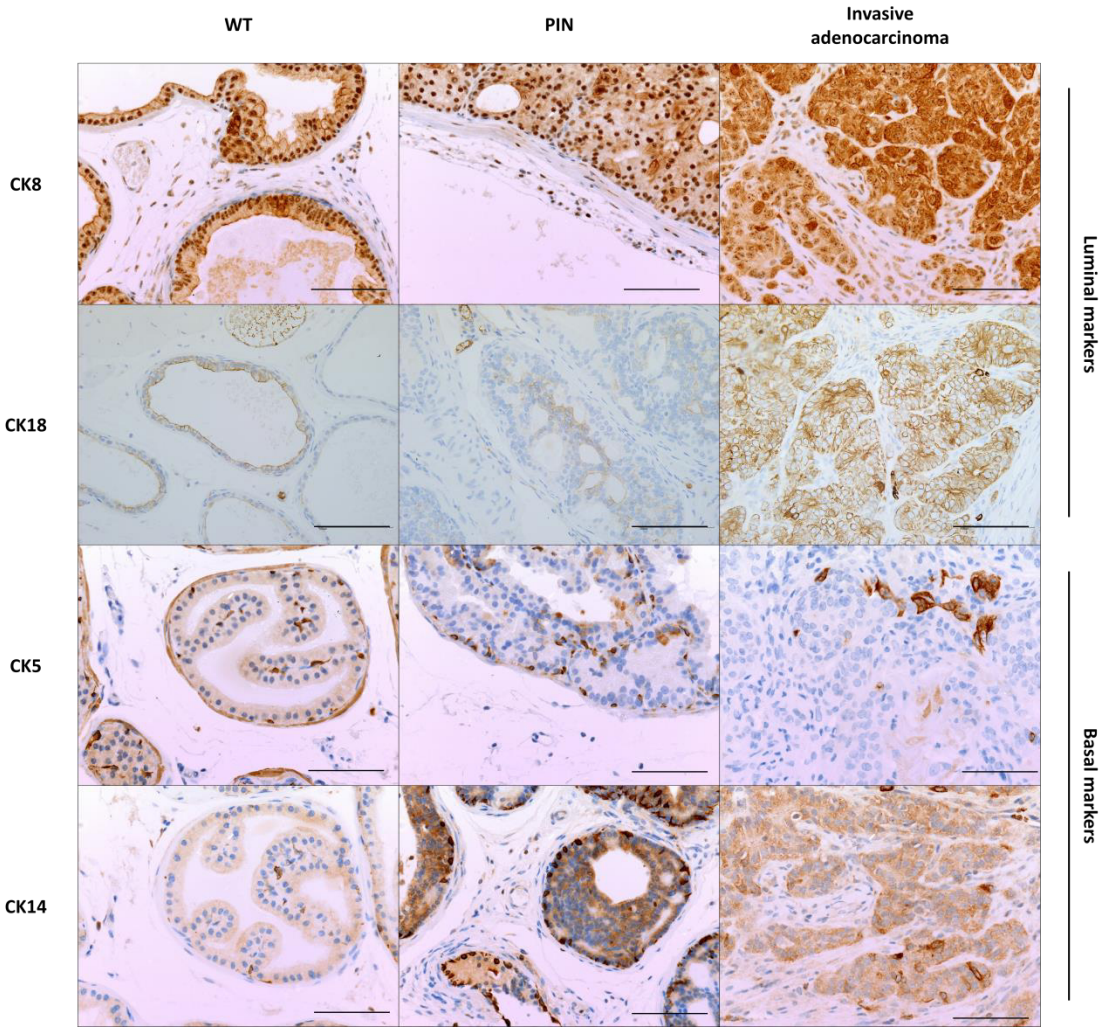

Figure 47: Immunohistochemistry for cytokeratins enables further characterisation of prostate lesions. Histological analysis of formalin-fixed, paraffin-embedded sections of *wild-type*, PIN, and invasive adenocarcinoma was performed to assess differentiation. It can be seen that upon progression from normal prostate to invasive disease there is over-expression of CK8 and 18, clearly highlighting the proliferation of terminally differentiated luminal cells. Conversely there is a trend towards loss of the basal undifferentiated phenotype, but note the increase in the number of CK5 and 14+ cells in both PIN lesions, prior to a clear reduction in basal cells in invasive adenocarcinoma. Also note the high background staining in the CK5 WT, CK14 PIN, and CK14 invasive adenocarcinoma photographs. All images were taken at 40x magnification, and scale bars represent 100µm.

4.3.13 Beta-catenin single mutant mice display simultaneous activation of the Wnt, PI3K/Akt/mTOR, and MAPK pathways

As expected (and demonstrated in figure 48.1) β-catenin single mutant mice were shown to activate the Wnt pathway; recognisable by over-expression of nuclear β-catenin (48.1(c)) and its downstream counterpart CD44 (48.1(d)) when compared to wild-type (48.1(a)) and (48.1(b)). Surprisingly, dominant stabilised β-catenin, resulting in its constitutive activation, appears to demonstrate concurrent over-expression of proteins from both the PI3K/Akt/mTOR (48.2(h-j) and (n-p)), and MAPK pathways (48.3(s&t)). This suggests that there is synergy between these pathways in prostate tumourigenesis.

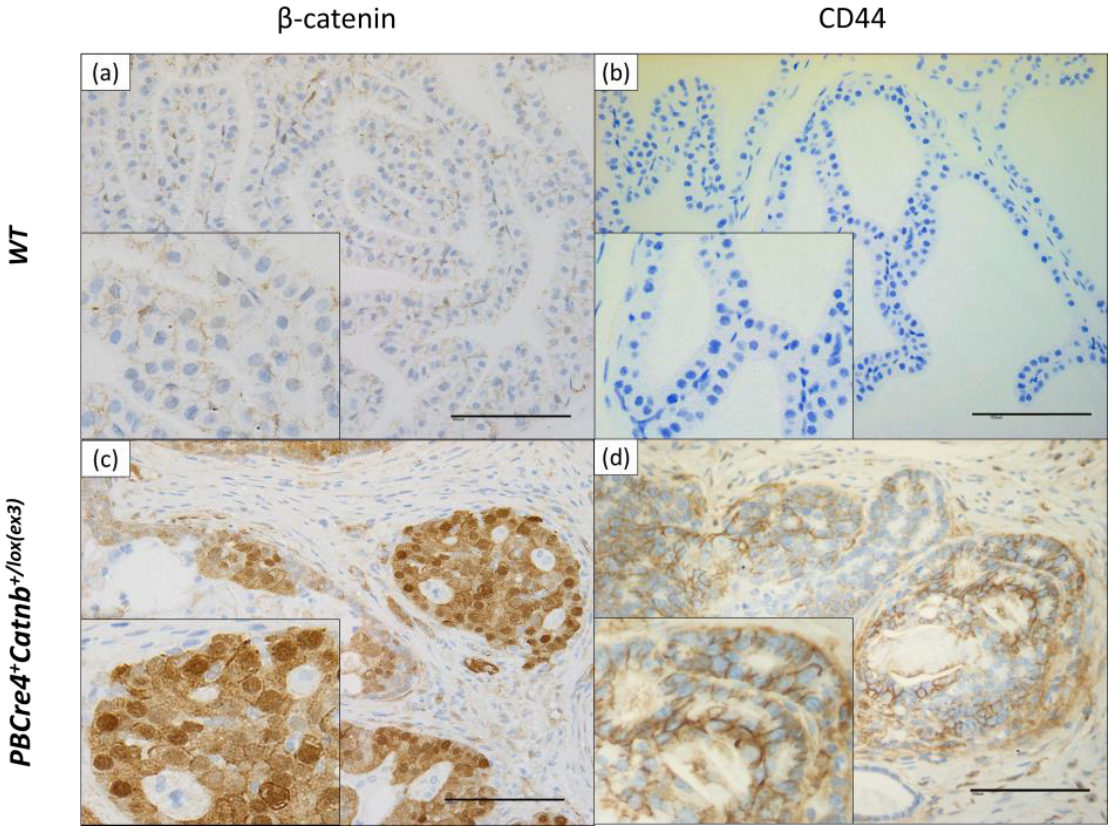

Figure 48.1: Beta-catenin single mutant prostate tumours demonstrate activated Wnt signalling. IHC to detect nuclear β-catenin and CD44 was performed, which indicates deregulation of the Wnt pathway in β-catenin single mutants (PBCre4^{+}Catnb$^{+/lox(ex3)}$). *Wild-type* β-catenin (a) exhibits membranous localisation, whereas activated β-catenin, resulting from the monoallelic deletion of exon 3 and its subsequent stabilisation, is recognisable by nuclear localisation (c). CD44+ cells are rare in wild-type epithelium (b), but over-expression of CD44 demonstrates strong membranous localisation (d). All images were taken at 40x magnification, and scale bars represent 100µm.

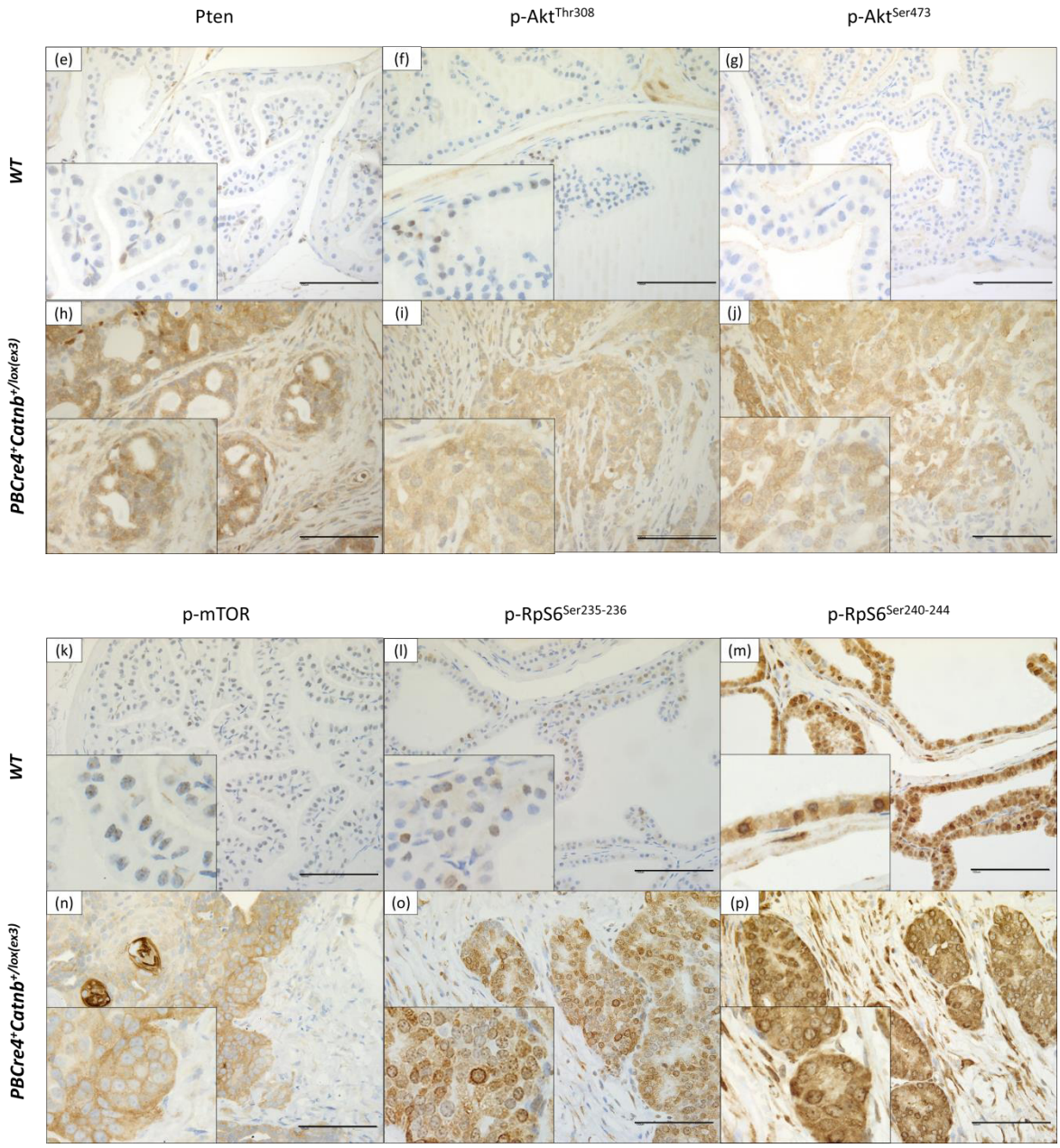

Figure 48.2: Beta-catenin single mutant prostate tumours demonstrate activated PI3K/Akt/mTOR signalling. IHC to detect Pten and its downstream targets was performed, which indicates deregulation of the PI3K/Akt/mTOR pathway in β-catenin single mutant mice (PBCre4^{+}Catnb$^{+/lox(ex3)}$). Despite intact Pten (h), p-Akt is over expressed with cytoplasmic localisation (i and j), in addition to p-mTOR (n), and downstream p-RpS6 (o and p) suggesting β-catenin-dependent activation of the PI3K/Akt/mTOR pathways. All images were taken at 40x magnification, and scale bars represent 100µm.

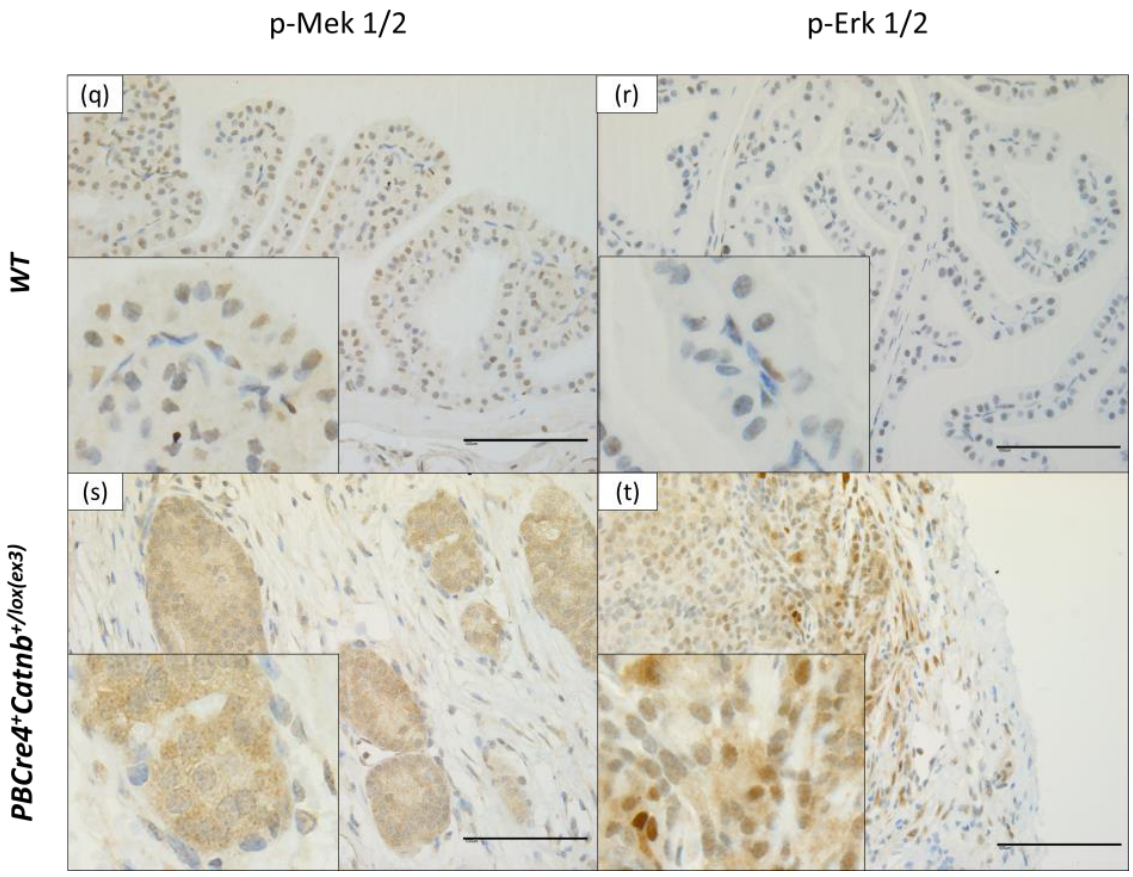

Figure 48.3: Beta-catenin single mutant prostate tumours demonstrate activated Ras/MAPK signalling. Compared to *wild-type* mice where there is little expression of activated Mek (q) and Erk (r), dominant, stabilised β-catenin results in over-expression of these important Ras/MAPK signalling proteins in cytoplasmic and cytoplasmic/nuclear fashion respectively. All images were taken at 40x magnification, and scale bars represent 100µm.

4.3.14 PTEN single mutant mice display simultaneous activation of the Wnt, PI3K/Akt/mTOR, and MAPK pathways

Upon homozygous loss of PTEN, as anticipated, there is confirmatory loss of Pten expression at IHC (see figure 49.1(d)) with concurrent over-expression of its downstream counterparts p-Akt (49.1(e&f)), and p-mTOR (49.1(j)). There is also evidence of activated MAPK signalling as shown by the upregulation of Mek and Erk expression (see figure 49.2(o&p)).

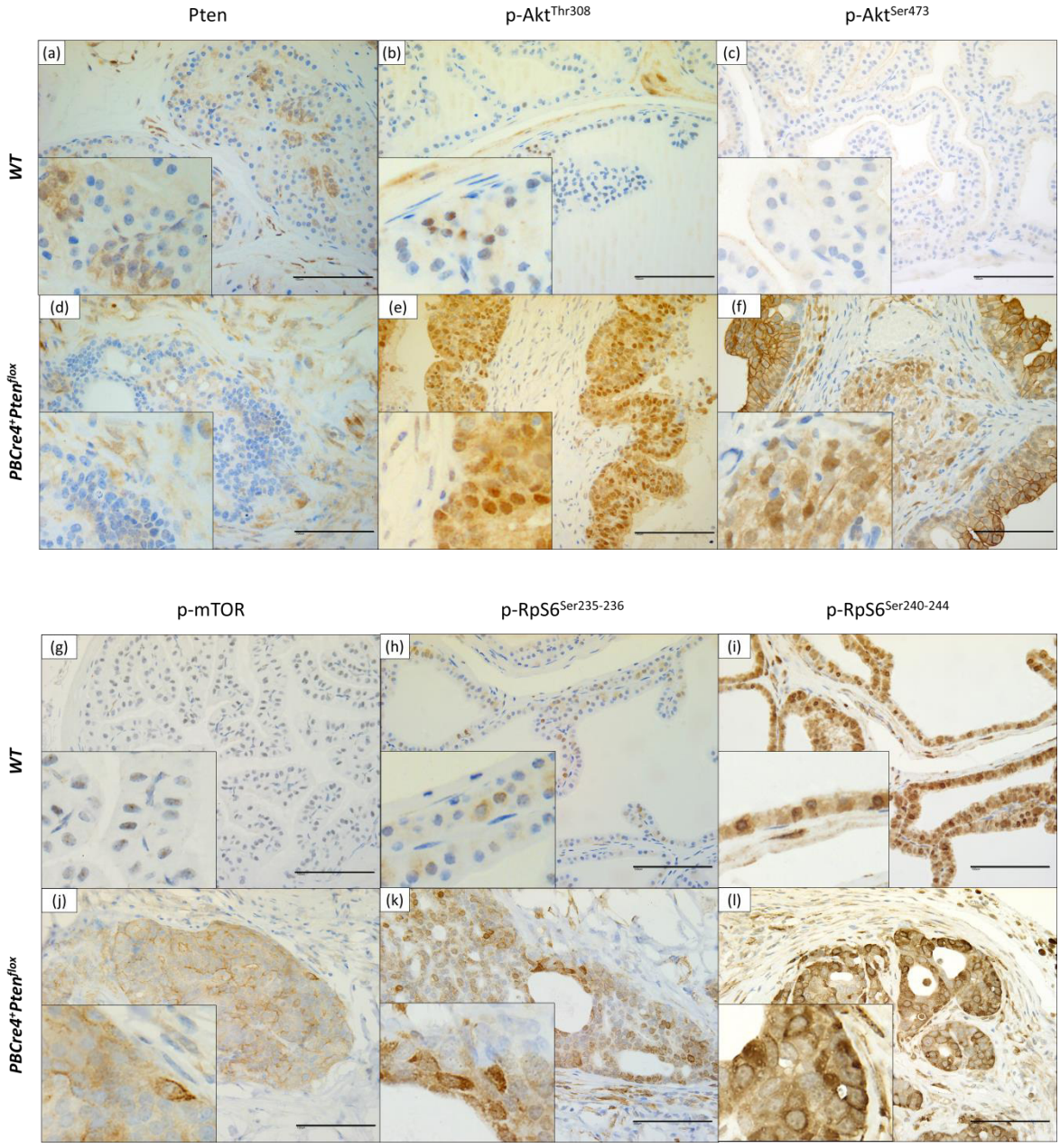

Figure 49.1: PTEN-null prostate tumours demonstrate activated PI3K/Akt/mTOR signalling. IHC to detect Pten and its downstream targets was performed, which indicates deregulation of the PI3K/Akt/mTOR pathway in Pten-null prostate lesions. Upon loss of Pten (d), a negative regulator of the PI3K/Akt/mTOR pathway, p-Akt is dramatically over expressed (e and f), in both a nuclear and cytoplasmic fashion. This is in contrast to the solely cytoplasmic staining seen in β-catenin mutants (see figure 48.2(i) and (j)). Expression of p-mTOR (j) and p-RpS6 (k and l) are also increased to further add weight to this notion. Note that IHC for p-RpS6$^{Ser240-244}$ (i and j) displays significant background signal. All images were taken at 40x magnification, and scale bars represent 100µm.

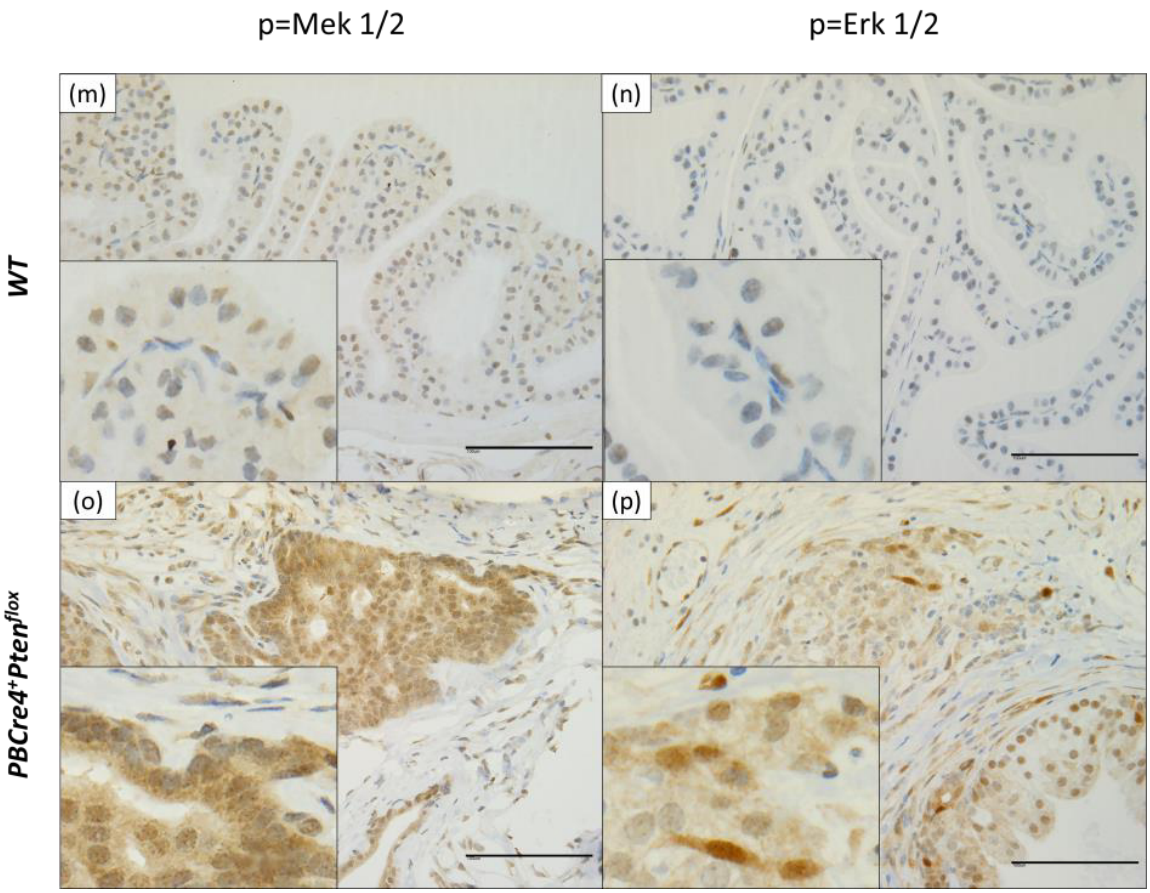

Figure 49.2 PTEN-null prostate tumours demonstrate activated Ras/MAPK signalling. Compared to *wild-type* mice, where there is little evidence of activated Mek and Erk (m and n respectively), PTEN single mutant mice display up-regulation of Ras/MAPK pathway signalling proteins in both cytoplasmic and cytoplasmic/nuclear expression respectively. Pten-loss-dependent Ras/MAPK pathway activation is most likely to occur through the metabolically-active p-Akt, but substantiation of this claim requires further investigation. All images were taken at 40x magnification, and scale bars represent 100µm.

It can also be seen in figure 49.3 that Pten loss results in elevated Wnt signalling, by the upregulation of nuclear β-catenin (49.3(s)) and CD44 (49.3(t)).

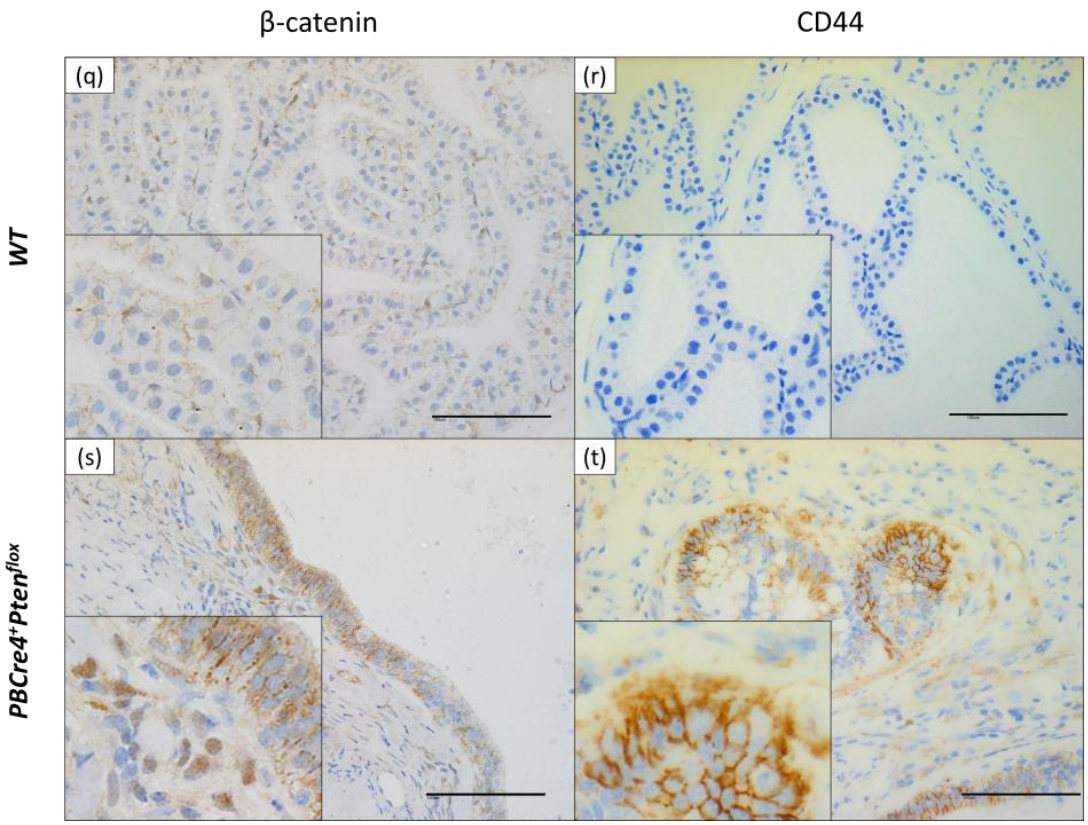

Figure 49.3: PTEN-null prostate tumours may demonstrate activated Wnt signalling. IHC to detect nuclear β-catenin and CD44 was performed, which suggests deregulation of the Wnt pathway in Pten-null prostate lesions. *Wild-type* β-catenin expression (q) is exhibited in the localised disease in (s), but the focus of invasive PCa (inset) clearly exhibits nuclear localisation to suggest Wnt activation. This is supported by over-expression of its downstream transcriptional target CD44 in (t). All images were taken at 40x magnification, and scale bars represent 100µm.

Taken together, data in this thesis suggest that in the presence of Pten loss, crosstalk between the three pathways is mediated by a molecule downstream of Pten, such as p-Akt, or mTOR. However it remains unconfirmed whether or not Pten deletion truly results in over-expression of β-catenin because findings at IHC were inconsistent in this thesis. Two out of three (66%) tumours appeared to demonstrate upregulation of nuclear (activated) β-catenin, whereas the other displayed membranous (*wild-type*) staining. Furthermore there was even heterogeneity within individual tumours, and examples of intra-tumour variability are shown in figure 50.

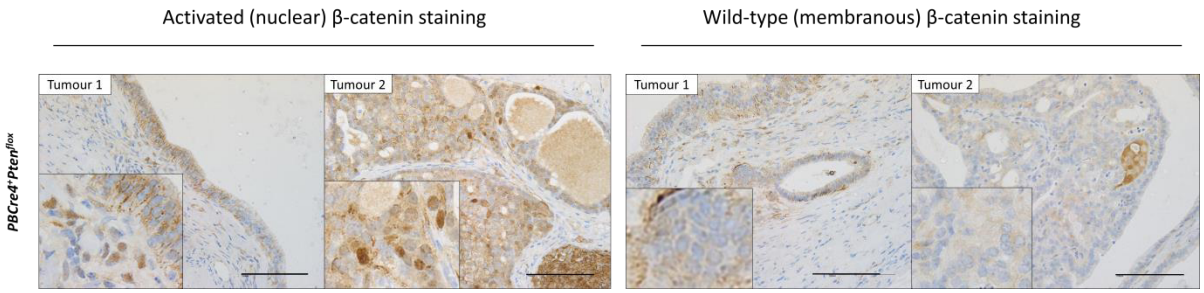

Figure 50: PTEN-null prostate tumours display intra-tumoural heterogeneity for nuclear β-catenin expression. It can be seen that there is evidence of variable staining for nuclear β-catenin within the same tumours from Pten single mutants (compare tumours 1 and 2 above). Whether or not Pten loss truly results in synergistic activation of nuclear β-catenin should be explored further using PCR and/or western blot analysis. This may only be accurately addressed by the use of laser-capture microdissection to select areas for comparison within the same tumour if expression of nuclear β-catenin remains heterogeneous in ongoing experiments. All images were taken at 40x magnification, and scale bars represent 100µm.

4.3.15 Activated Wnt, PI3K/AKt/mTOR and Ras/MAPK pathways synergise to accelerate prostate cancer progression

It was hypothesised that simultaneous oncogenic transformation of the Wnt, PI3K/Akt/mTOR, and/or the MAPK pathways would result in synergistic hyperactivation of their downstream transcriptional targets. To address this, IHC was performed on all double and triple mutant combinations to compare the expression of important molecules within each signalling pathway of interest. The fact that survival is reduced upon deregulation of more than one pathway suggests there is cooperation between these signalling pathways resulting in accelerated prostate tumourigenesis.

In this section, figures 51(a) and (b) demonstrate the synergistic outcomes identified at IHC.

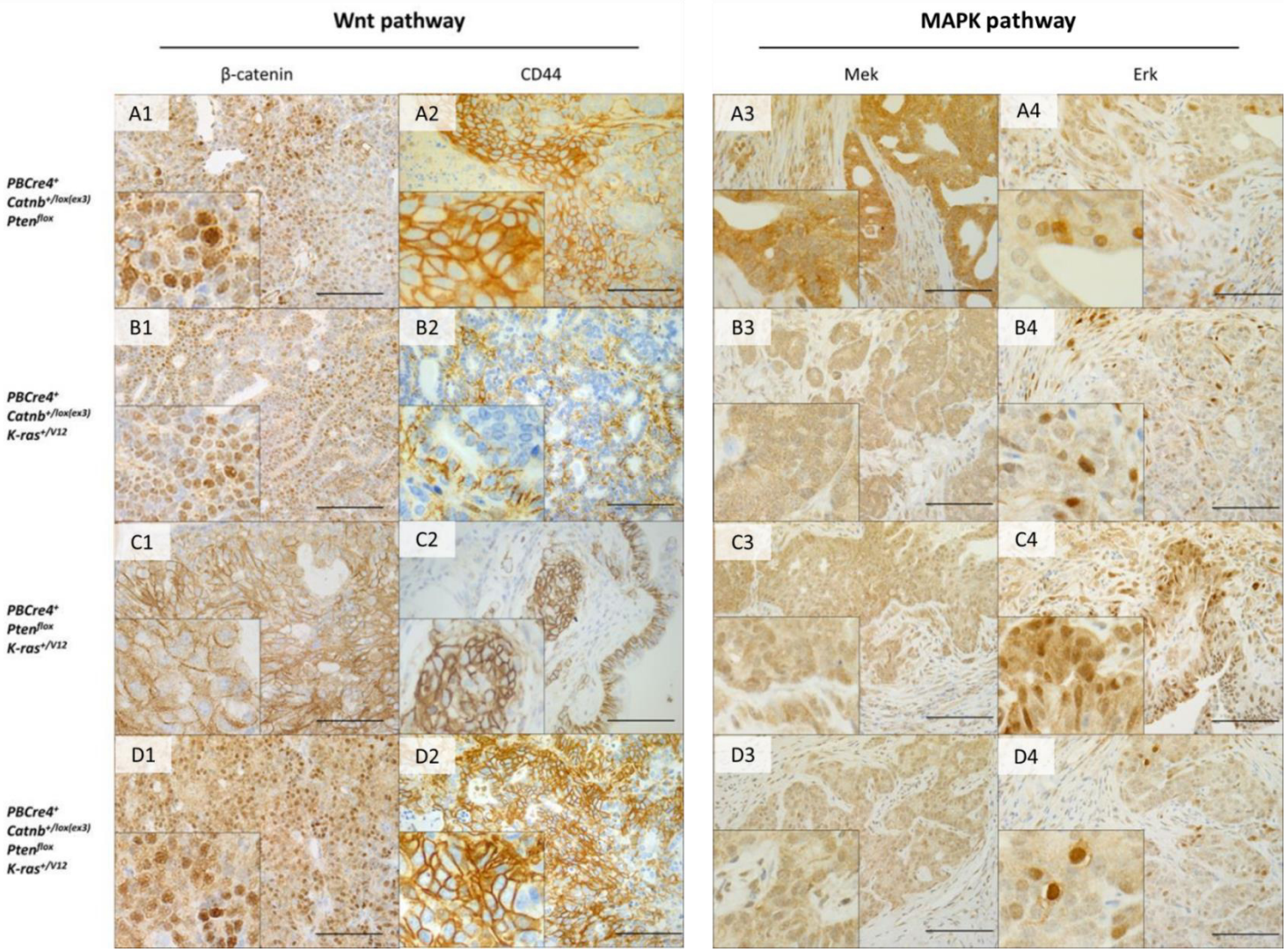

Figure 51(a): Immunohistochemistry in compound mutant prostate tumours. Images were taken at 40x magnification, scale bars represent 100µm.

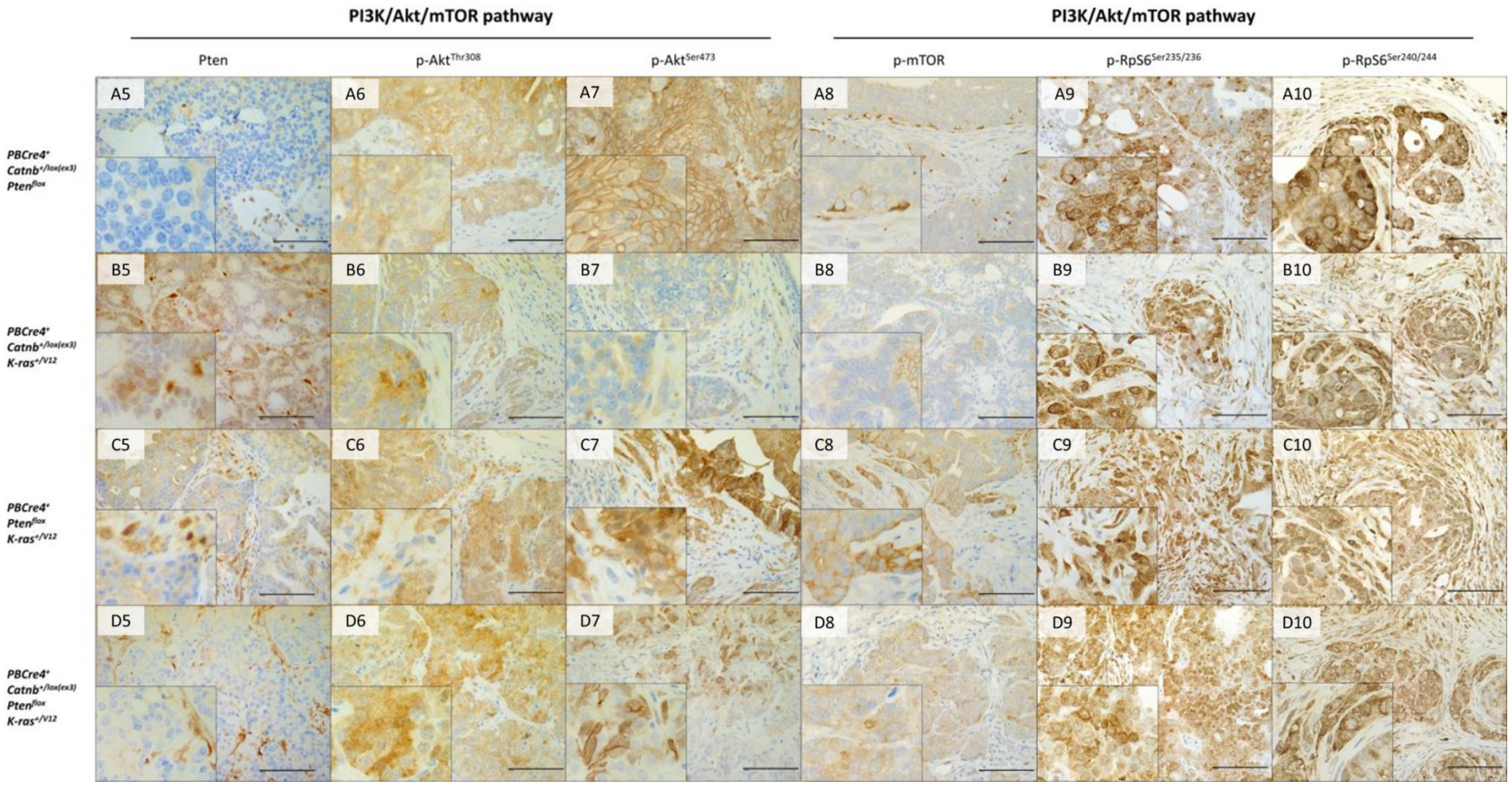

Figure 51(b): Immunohistochemistry in compound mutant prostate tumours. All images were taken at 40x magnification, and scale bars represent 100µm.

Beta-catenin/PTEN double mutants (PBCre4+Catnb+/lox(ex3)Ptenflox) develop higher grade PCa than either of its component single mutants (see figure 36). Nuclear localisation of β-catenin (figure 51(a), A1) and elevated levels of its downstream transcriptional target CD44 (A2) confirm that activation of the Wnt pathway is contributory to these invasive carcinomas. Likewise over-expression of p-Akt (A6&7) and p-RpS6 (A9&10) confirm that PI3K/Akt/mTOR signalling is enhanced. Furthermore these lesions unexpectedly demonstrated elevated expression of p-Mek1/2 and p-Erk1/2 (A3-A4). These activated proteins suggest that Ras/MAPK signalling has also been switched on by Wnt and PI3K/Akt/mTOR cooperation.

In β-catenin/Kras double mutant mice (PBCre4+Catnb+/lox(ex3)K-ras+/V12) there is confirmatory over-expression of activated Wnt signals nuclear β-catenin and CD44 (B1-B2). There is also activation of the MAPK cascade through upregulation of p-Mek and p-Erk, albeit at a lower intensity than seen in Beta-catenin/PTEN double mutants (PBCre4+Catnb+/lox(ex3)Ptenflox mice). Interestingly there was retained staining of the Pten antigen (a negative regulator of Akt), alongside p-Akt staining that was upregulated at Thr308 but absent at Ser473. Expression of mTOR was suppressed in the presence of upregulated downstream p-RpS6. This supports synergistic Wnt and MAPK-dependent PI3K/Akt signalling that serves to activate Akt (at Thr308) independent of mTOR. See chapter discussion for explanation of this mechanism.

PTEN/Kras double mutant mice (PBCre4+PtenfloxK-ras+/V12) display co-activation of all three pathways. Firstly Mek and Erk are greatly over-expressed signifying active Ras/MAPK signalling (C3-C4). Secondly, while there is up-regulation of PI3K/Akt/mTOR signalling (C6-C10), there also appears to be some residual nuclear Pten expression (C5) of either irregular invasive carcinoma cells or stromal cells.

When analysing the staining pattern of the triple mutant mouse (PBCre4+Catnb+/lox(ex3)PtenfloxK-ras+/V12), it can be seen that there is activation of all pathways, but some molecules are not as strongly over-expressed as might have been expected. For example, Mek and Erk signalling is somewhat suppressed at IHC in the triple mutant, whereas Wnt signalling is greatly overexpressed.

A summary of the expression profile identified at IHC for each genotype is provided in table 15.

Pathway	Genotype / Stain	WT	*Catnb*$^{+/lox(ex3)}$	*PTEN*^{flox}	*Catnb*$^{+/lox(ex3)}$ *PTEN*^{flox}	*Catnb*$^{+/lox(ex3)}$ *Kras*$^{+/V12}$	*PTEN*^{flox} *Kras*$^{+/V12}$	*Catnb*$^{+/lox(ex3)}$ *PTEN*^{flox} *Kras*$^{+/V12}$
Wnt	β-catenin	-	++	+	++	++	-	++
	CD44	-	++	+	++	+	++	++
PI3K/ Akt/ mTOR	Pten	+	-/+	-	-	+/++	+	-
	p-Akt^{Ser473}	-	+/++	++	++	-	++	+
	p-Akt^{Thr308}	-	+	+/++	++	-/+	+/++	+
	p-mTOR	-	-/+	-/+	-/+	-/+	+/++	+
	p-RpS6$^{Ser240/244}$	+	++	++	++	++	++	++
	p-RpS6$^{Ser235/236}$	-	++	++	++	++	++	++
MAPK	p-Erk	-/+	+	+/++	+/++	+	+/++	+
	p-Mek	-/+	++	++	++	++	++	+

Table 15: A summary of the expression profile for each tumour genotype at immunohistochemistry. Legend: - absent staining; -/+ heterogeneous expression with areas of absent and positive staining; + universally low level of expression; +/++ heterogeneous expression with areas of both low and high staining intensity; ++ high or intense level of expression; n=3 for each genotype analysed.

4.4 CHAPTER CONCLUSION

4.4.1 Dominant, stabilisation of β-catenin in murine prostate epithelium predisposes to adenocarcinoma and keratinising squamous metaplasia formation

Given that aberrant Wnt signalling has been identified as having a role in prostate tumourigenesis, this thesis aimed to investigate the consequences of mutating β-catenin alone and in combination with mutations in other key pathways identified as also playing important roles in the human disease. A conditional transgenic mouse model was created leading to the dominant stabilisation of β-catenin in prostate epithelium that resulted in oncogenic transformation. Male mice demonstrated reduced longevity due to overwhelming tumour burden, in the absence of metastatic disease (median 352 days). Tumours were characterised by the upregulation of activated β-catenin, which localised to the nucleus, and subsequent over-expression of its downstream transcriptional target, CD44. These results support previous work using the PBCre4 transgene model (Pearson et al., 2009), however these findings are disputed by others who claim that β-catenin single mutants (PBCre4^{+}Catnb$^{+/lox(ex3)}$ mice) at worst develop PIN (Yu et al., 2009, Francis et al., 2013). Regardless of this understandably subjective staging, the use of transgenes under the influence of other promoters have further supported the notion that dominant, stabilisation of β-catenin plays an important role in progression from PIN to invasive adenocarcinoma (Gounari et al., 2002, Bierie et al., 2003, Yu et al., 2011), using MMTV-Cre (Cre transgene under control of the mouse mammary tumour virus), MMTV-LTR-Cre (Cre transgene under control of the mouse mammary tumour virus-long terminal repeat), and LPB-Tag (large probasin promoter directed SV40-large T-antigen) respectively.

Even though squamous metaplasia is rarely associated with human PCa, monoallelic deletion of exon 3 and subsequent stabilisation of β-catenin results in the prominent development of keratinising squamous metaplasia. This finding has been widely reported in mouse models of prostate tumourigenesis, therefore in the human disease it is hypothesised that other events need to take place to allow β-catenin to drive disease progression without squamous formation. These events are yet to be identified or modelled in the mouse. It has been shown in the present study that even when combined with other mutations, an intrinsic property of high levels of activated β-catenin drives squamous transdifferentiation (Francis et al., 2013).

The mechanisms by which activated β-catenin co-activates both the PI3K/Akt/mTOR and Ras/MAPK pathways are poorly reported in the literature, and remain unclear following work in this thesis. Beta-catenin-dependent activation of PI3K/Akt/mTOR signalling may result from the upregulation of Wnt effectors c-myc and cyclinD1, both of which are capable of triggering the cell cycle and metabolic reprogramming (see figure 52). The metabolic activation in cancer cells leads to the production of reaction oxygen species (ROS), which activate the forkhead box protein O (FoxO), responsible for carbohydrate metabolism by insulin signalling. FoxO is the transcription factor of RICTOR, one of the key components of mTORC2 recognised as the kinase that phosphorylates Akt on Ser473 (Vadlakonda et al., 2013). This may result in elevated PI3K/AKT/mTOR signalling at, or downstream of, p-Akt. This hypothesis could be addressed with further IHC for other Wnt effectors such as c-myc, cyclinD1, MMP-7, Foxa1, and COX-2, along with qRT-PCR and western blotting for the respective molecules.

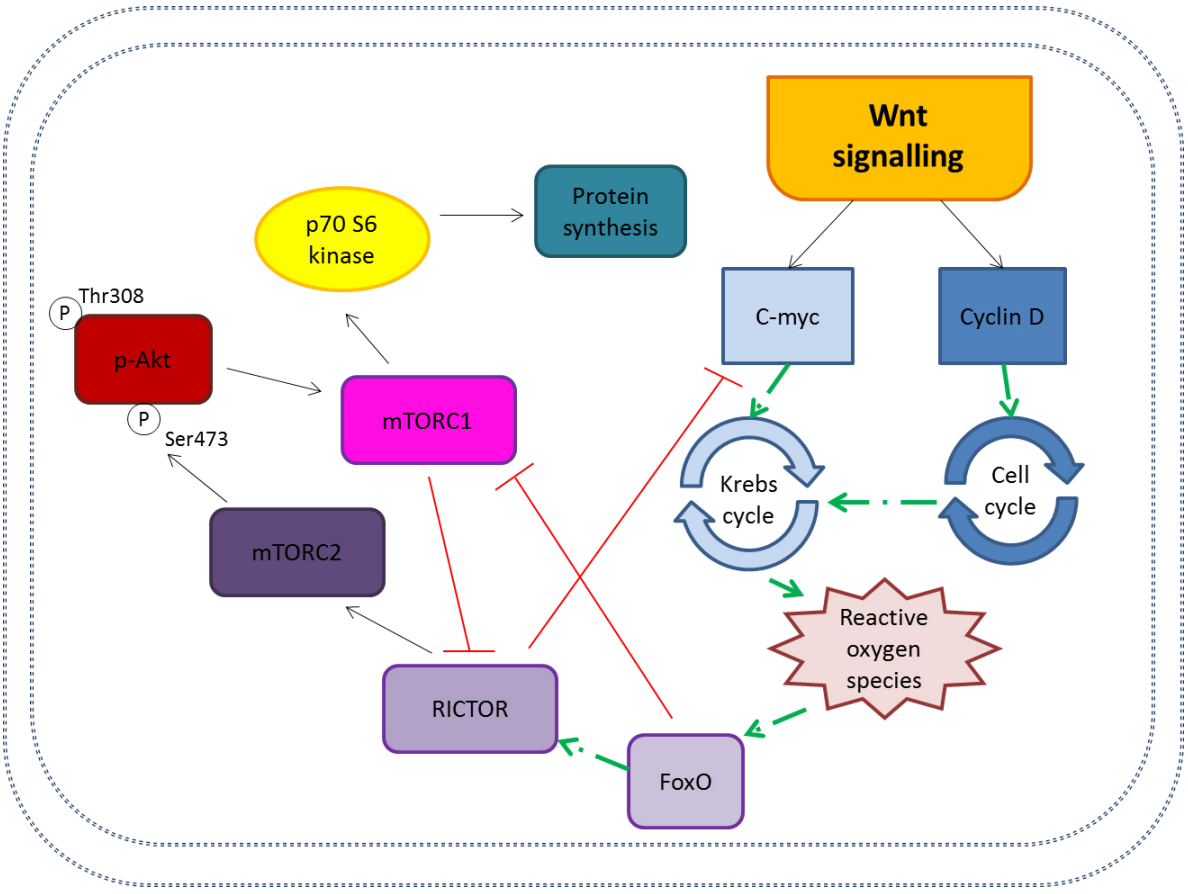

Figure 52: A schematic representation of the synergy that results in Wnt-dependent activation of PI3K/Akt/mTOR pathway. Note that broken green lines represent hypothesised cooperation, whereas black lines represent known activation, and red lines depict inhibition. Adapted from Vadlakonda et al. (2013).

Previous studies have linked Wnt pathway activation to increased MAPK signalling in colorectal cancer cell lines and Cre-virus-induced Apc knockout in primary $Apc^{flox/flox}$ mouse embryonic fibroblasts (Park et al., 2006), and in NIH3T3 fibroblast cells transfected with either murine β-catenin or Erk1 siRNA (Yun et al., 2005). The former study concluded that MAPK activation by β-catenin was reduced by co-expression of APC, indicating that APC inhibits the ERK pathway by an action on β-catenin. RAS-induced activation of the MAPK pathway was reduced by the dominant negative form of Tcf4, indicating that the MAPK pathway regulation by Wnt signalling is caused by effects on β-catenin/Tcf4-mediated gene expression (Park et al., 2006). The latter study suggests that MAPK pathway activation by Wnt signalling could occur at multiple levels. These include β-catenin-independent direct signalling resulting from increased Wnt 3a ligand levels, and β-catenin/Tcf-4-dependent post-gene transcriptional events (Yun et al., 2005). Given that Wnt ligand 3a is not over-expressed in the dominant, stablilised β-catenin model used in this thesis (PBCre4+Catnb+/lox(ex3) mice), a post-transcriptional point of synergy is more likely. This synergistic interaction is demonstrated in figure 53. These findings are contrary to previous results (Pearson et al., 2009), whereby activated MAPK signalling proteins p-Mek1/2 and p-Erk1/2 were expressed at wild-type levels in β-catenin single mutant prostate tumours.

It is known that exogenous oestrogen promotes the formation of squamous metaplasia in male mice by inducing aberrant proliferation in the basal layer (Risbridger et al., 2001), and this is usually reversible upon its removal (Cunha et al., 2004). Two oestrogen receptors (ERs) have been identified in existence, ERα and ERβ, which are predominantly expressed in the prostatic stroma and epithelium respectively (Chang and Prins, 1999), while induction of prostatic squamous metaplasia is mediated through the former (Cunha et al., 2004). In the murine uterus, ER signalling has been linked to elevated Wnt signalling by the upregulation of Wnt ligands, and Wnt receptors that collectively promote uterine growth (Hou et al., 2004). Taken together the evidence suggests that the keratinising squamous metaplasia exhibited in β-catenin mutant mice ($PBCre4^{+}Catnb^{+/lox(ex3)}$) may be the result of disruption in the homeostatic mechanisms that control AR and ER signalling in prostate epithelium (Risbridger et al., 2007).

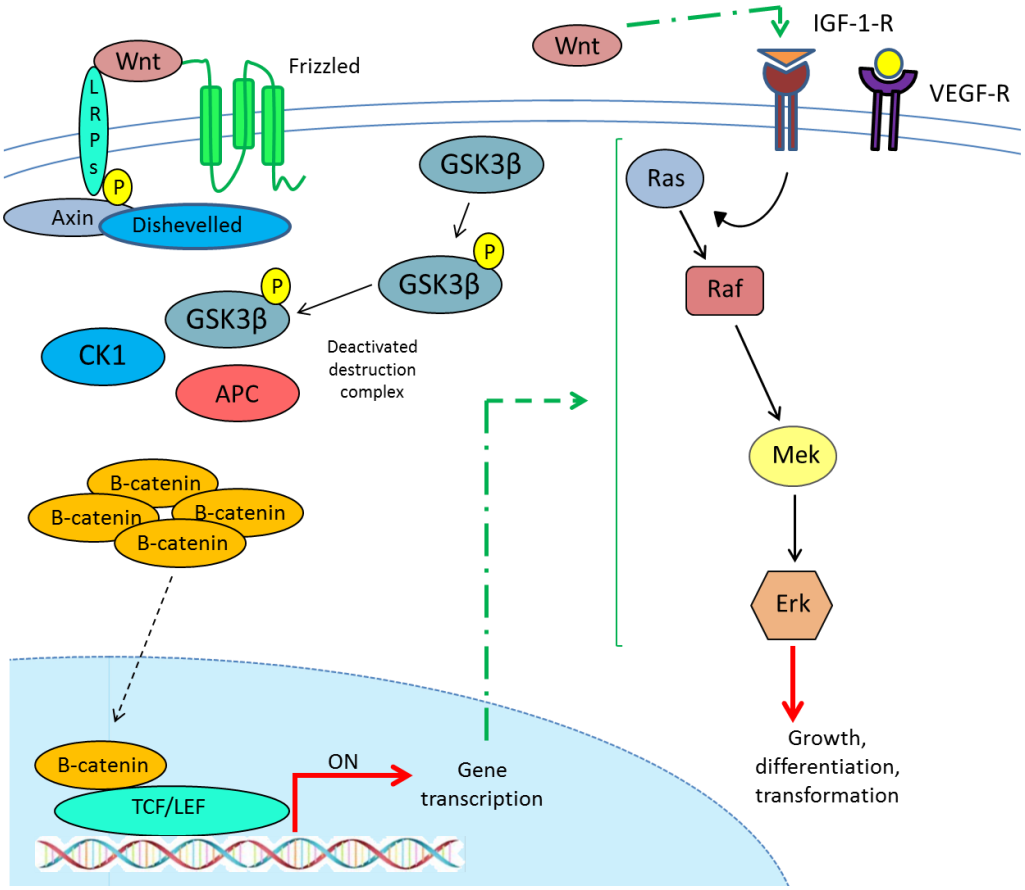

Figure 53: A schematic representation of the mechanism by which Wnt signalling may synergise with the Ras/MAPK pathway. A β-catenin/Tcf-4-dependent post-transcriptional event is the likely trigger for cooperation with the Ras/MAPK pathway, but the level at which this occurs in the latter is unknown. Ras/MAPK signalling may also result from binding Wnt ligand. Broken green lines represent hypothesised cooperation, whereas black lines represent known activation, and red lines depict inhibition.

Accepting that ERα signalling stimulates proliferation of basal cells, intuitively these cells express p63. Ectopic expression of p63 resulted in squamous metaplasia transdifferentiation in an inducible transgenic mouse model of lung tumourigenesis (Romano et al., 2009). Furthermore, elevated expression of p63 has been associated with the early stages of squamous cell carcinoma (SCC) and β-catenin has been shown to regulate this protein in oesophageal SCC (Hu et al., 2002) and HCC (Ruptier et al., 2011). One study claims that dominant, stabilised β-catenin induces high levels of p63 to drive the transdifferentiation process towards a squamous fate (Francis et al., 2013), however there is evidence to both support and refute this. Beta-catenin/Kras mutants (PBCre4+Catnb+/lox(ex3)Kras+/V12) examined in this thesis had no demonstrable p63 expression at IHC, in the presence of small

foci of squamous metaplasia (as shown in figure 38). One paper reported that these tumours do not display squamous metaplasia (Pearson et al., 2009). In addition, tumours in β-catenin single mutants (PBCre4+Catnb+/lox(ex3)) express very low levels of p63 but contain copious keratinising squamous metaplasia. Moreover triple mutant mice display abundant squamous metaplasia but very little p63 expression. In contrast, β-catenin/PTEN double mutants (PBCre4+Catnb+/lox(ex3)Ptenflox mice) display increased expression of p63 in metaplastic foci but at levels lower than wild-type due to the concurrent increased number of luminal p63- cells. In light of these conflicting views future analysis of tumours from mice entered into these aforementioned survival cohorts should seek to clarify the association of p63 and the presence of squamous metaplasia.

4.4.2 Homozygous loss of PTEN predisposes mice to invasive adenocarcinoma of the prostate

Pten-deficient prostate tumours were non-metastatic in contrast to findings by others (Wang et al., 2003), however they were consistent with locally-advanced adenocarcinoma. Reasons to account for this discrepancy could include the different genetic background of mice, and the use in outbred rather than inbred mice in this thesis, and/or contaminated surroundings leading to poorer health status and predisposition to infection. Mice displayed reduced median survival due to tumour burden at 359 days. Tumours were characterised by the expected over-expression of the PI3K/AKt/mTOR signalling but the unexpected over-expression of the Wnt, and MAPK signalling cascades. It is interesting to note that the pattern of p-Akt expression in PTEN-null prostate tumours was both nuclear and cytoplasmic, in contrast with cytoplasmic only staining in β-catenin mutant mice. In thyroid cancer (Vasko et al., 2004) and non-small cell lung cancer (Shah et al., 2005), nuclear-localisation of p-Akt was a feature of poor prognostic outcome. Meanwhile in PCa, it has been demonstrated that the degree of nuclear p-Akt increased according to disease progression (Van de Sande et al., 2005). Furthermore, the extent of Akt nuclear localisation correlated with the Gleason grade, the most powerful predictor of disease progression after RRP (Montironi et al., 2005). This observation suggested that nuclear Akt could be used as biomarker for PCa prognosis. Additional signs of PI3K/Akt/mTOR signalling were highlighted in this thesis by the over-expression of p-mTOR, and its downstream substrate p-RpS6 (see figure 49.1).

In the present study, PTEN-null PCa demonstrated evidence for activation of Wnt signalling by the upregulation of nuclear β-catenin, and its downstream transcriptional target CD44, albeit in heterogeneous fashion. However, not all Pten-null tumours reviewed demonstrated nuclear localisation of β-catenin, which could be attributable to inconsistent fixation times in formalin resulting in variable antigen preservation or truly heterogeneous expression. Further work needs to be done to confirm the cellular localisation of β-catenin in PTEN-null prostate tumours, along with complimentary IHC of other downstream post-transcriptional targets, such as c-myc, cyclinD1, MMP-7, Foxa1, and COX-2. Analysis of these tumours by qRT-PCR and/or western blotting should be interpreted carefully because of the regional variation in antigen expression possibly reflecting heterogeneous recombination. To better understand the mechanism that underpins PTEN-loss-mediated Wnt signalling, a technique such as laser-capture microdissection to isolate areas of nuclear (activated) β-catenin localisation for comparison with areas of membranous (wild-type) localisation in PBCre4+Ptenflox tumours would be helpful.

Deletion of PTEN activates the PI3K/Akt/mTOR pathway, which in turn inhibits GSK3β through phosphorylation at Ser9 by p-Akt (Mulholland et al., 2006). As such it is widely accepted that inactivated GSK3β results in a disabled ubiquitination complex and aberrant translocation of β-catenin to the nucleus occurs (Kypta and Waxman, 2012). This is schematically demonstrated in figure 54. Studies in PCa cell lines support this notion (Persad et al., 2001, Sharma et al., 2002) but the belief is not universally held. It has been reported in another study that utilised PC3 PCa cells, that the axin-bound pool of GSK3β was distinct and protected from the pool activated by Akt (Ng et al., 2009). Also 'knock-in' mice in which the Akt inactivating-phosphorylation sites on both GSK3α (Ser21) and GSK3β (Ser9) were mutated, did not display elevated Wnt signalling (McManus et al., 2005). In a mouse model of bladder cancer PTEN loss alone was insufficient to activate Wnt signalling (Ahmad et al., 2011), suggesting that perhaps it is a tissue-specific phenomenon only seen in prostate. However some human bladder cancers have been found to express high levels of nuclear β-catenin in conjunction with absent Pten and over-expressed Akt, implying there are important interactions between these pathways in human tumourigenesis (Ahmad et al., 2011). Thus it is important to explore GSK3β staining with IHC to investigate whether its Akt-dependent deactivation is apparent upon PTEN deletion and important in PCa development. In any event, β-catenin reportedly possesses an Akt

phosphorylation site at Ser552 to allow its activation by Akt directly, independent of GSK3β (Verheyen and Gottardi, 2010).

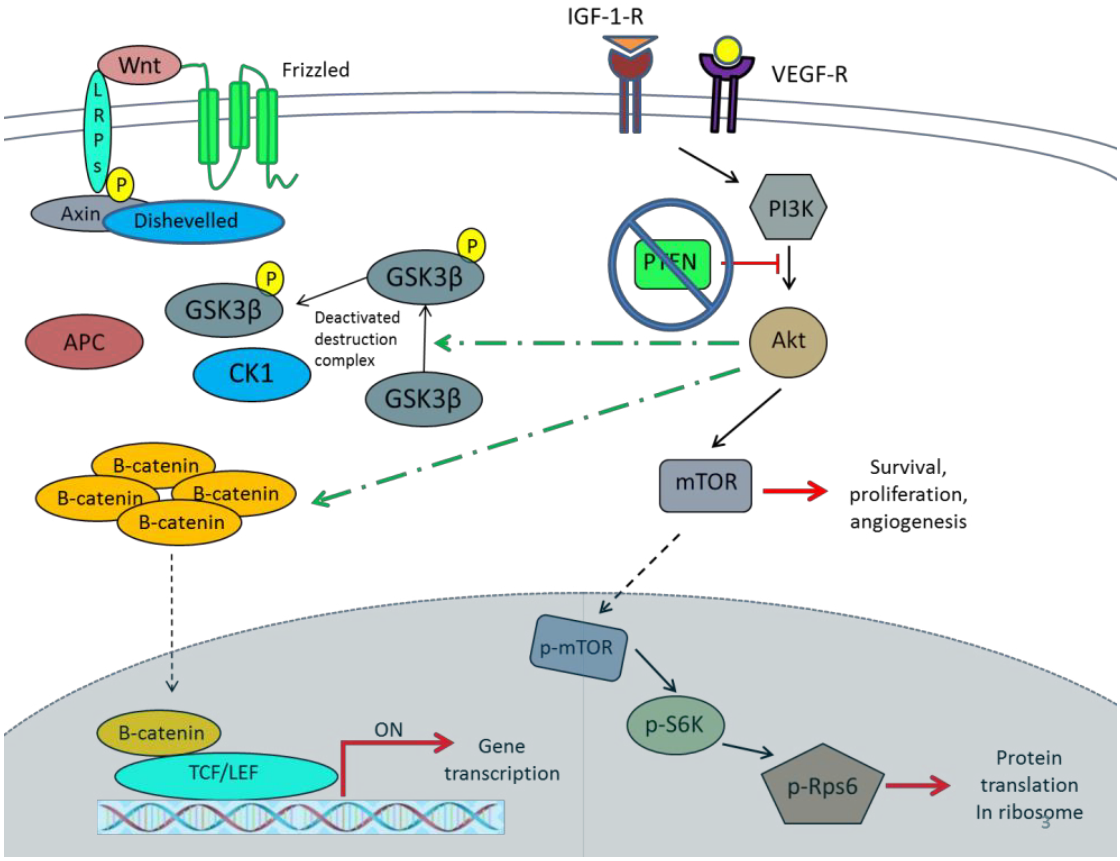

Figure 54: A schematic representation of PTEN-loss-dependent activation of the Wnt pathway. Activation of Wnt signalling and nuclear translocation of β-catenin remains contentious and may be tissue-specific. Several points of synergy with p-Akt have been suggested. Broken green lines represent hypothesised cooperation, whereas black lines represent known activation, and red lines depict inhibition.

The importance of PTEN-loss-dependent activation of MAPK signalling on PCa development has not previously been described, however purported mechanisms to account for this interaction in other tissues are complex (Castellano and Downward, 2011). Firstly this synergy has been demonstrated in human red blood cell progenitors, stimulated by erythropoietin (Schmidt et al., 2004), which highlights the importance of PI3K/Akt/mTOR in connecting to and regulating Ras signalling. Secondly these findings were corroborated in a zebrafish model, wherein the PI3K/Akt/mTOR pathway was found to regulate Ras signalling during both hematopoiesis and angiogenesis (Liu et al., 2008). Together these data support the notion that crosstalk between the PI3K/Akt/mTOR and MAPK pathways exists. The MAPK pathway through Ras is

PI3K/Akt/mTOR-dependent, and aberrant PI3K/Akt/mTOR signalling drives Raf/Mek/Erk activation through Raf by an uncharacterised mechanism (Wandzioch et al., 2004).

4.4.3 Combinatorial activating mutations of β-catenin and/or Kras with/without Pten deletion cooperate to accelerate prostate tumourigenesis

The survival of compound mutant mice is notably poorer than single mutants or wild-type mice, irrespective of their genotype. Triple mutant mice appear to have the poorest outcome due to overwhelming tumour burden; however numbers in each double and triple cohort were too small to draw definitive conclusions on survival. Histological analysis revealed the development of invasive adenocarcinoma as the primary cause of reduced longevity, illustrating that Wnt, PI3K/Akt/mTOR, and Ras/MAPK signalling do synergise in the prostate to promote tumourigenesis and disease progression.

High grade tumours seen in compound mutant mice were comparable to the human Gleason pattern 4. They were large solid tumours, microscopically displaying sheets of cells with widespread invasion of the surrounding stroma, often in cribriform pattern with marked pleomorphism. High nuclear:cytoplasmic ratio with irregular nuclear borders and prominent nucleoli with cellular overlapping was seen. Areas of necrosis were identifiable in addition to frequent mitoses and apoptotic bodies. Mice bearing activating mutations of β-catenin were associated with keratinising squamous metaplasia, whereas those with Pten-loss were seen to have markedly thickened, and fibrous stroma. Unfortunately no mice succumbed to metastatic disease as hypothesised; instead lymph nodes were prolifically infiltrated by lymphocytes.

Beta-catenin/PTEN double mutant mice (PBCre4+Catnb+/lox(ex3)Ptenflox) clearly demonstrate upregulated PI3K/Akt/mTOR and Wnt signalling, which synergise to accelerate prostate tumourigenesis. The low expression of p-mTOR seen in figure 51 (A8-D8) may represent less than complete activation, or that its level of expression is constitutionally low, or that the antibody used to target the p-mTOR antigen was weak, requiring longer or more concentrated incubation with the primary antibody or greater signal amplification. If the first notion is true, Akt may be preferentially phosphorylated and activated at Thr308, in a PI3K/PDK1-dependent manner, at the expense of phosphorylation at Ser473 (and hence the mTOR avenue). Subsequent activation of p70S6k by PDK1 is sufficient to phosphorylate RpS6k independent of mTOR (Alessi et al., 1998, Pullen et al., 1998, Kozma and Thomas, 2002, Castellano and Downward, 2011). MAPK signalling through Erk1/2 has also been shown to positively control

the activation of p70S6k (Babchia et al., 2010, Sunayama et al., 2010). These mice also demonstrate upregulated MAPK signalling, which reflects cooperation between these pathways. Hypotheses for how activated β-catenin and Pten-loss alone may activate MAPK signalling have been outlined above in their respective sections in this discussion. It can be seen that the abundant expression of p-Mek1/2 and p-Erk1/2 here suggests that synergistic interaction triggers MAPK signalling in the absence of an activating mutation in Kras.

β-catenin/Kras mutants (PBCre4+Catnb+/lox(ex3)K-ras+/V12) overexpress both Wnt and MAPK signalling, which demonstrates synergy in accelerating the onset of PCa. Interestingly intact PTEN is insufficient to abrogate Wnt signalling in the presence of dominant, stabilised β-catenin mutation. CD44 does not appear to be expressed as avidly as when activating mutations of β-catenin or Kras are combined with Pten loss. Preserved Pten expression is concomitant with mild upregulation of p-Akt Thr308, but absent Ser473, reduced mTOR expression, and overexpressed p-RpS6k. Upregulation of mutant Kras is sufficient to aberrantly activate the p110α subunit of PI3K, which in turn activates PDK1 resulting in Akt phosphorylation at Thr308 (Castellano and Downward, 2011). PDK1 and Erk1/2 can activate p70S6k and ultimately its substrate p-RpS6k (Babchia et al., 2010, Sunayama et al., 2010). Furthermore nuclear Pten is capable of inhibiting mTOR activation independent of interference with Akt (Liu et al., 2005). Taken together, these data support the synergistic Wnt and MAPK-dependent PI3K/Akt signalling that serves to activate Akt independent of mTOR. The mechanism of this synergistic interaction is illustrated in figure 55.

Tumours from PTEN/Kras mice (PBCre4+PtenfloxK-ras+/V12) display co-activation of all three signalling pathways. However the expression profile seen in these mice to some extent opposes the notion that (at least on an IHC level) in the presence of PTEN deletion, Wnt signalling is dependent on nuclear β-catenin. Here it can be seen that on a compound background of activated Kras and PTEN loss, activation of downstream Wnt effectors may occur independent of β-catenin activation. This could be implied by the absence of nuclear localisation of β-catenin in the presence of CD44 over-expression. With this in mind, perhaps the appearance of cytoplasmic β-catenin staining, due to its accumulation (as seen here in figure 51, C1), which does not conform to the classical description of membranous staining (as seen in *wild-type*), may indicate that nuclear translocation is occurring at a level too low to detect with IHC.

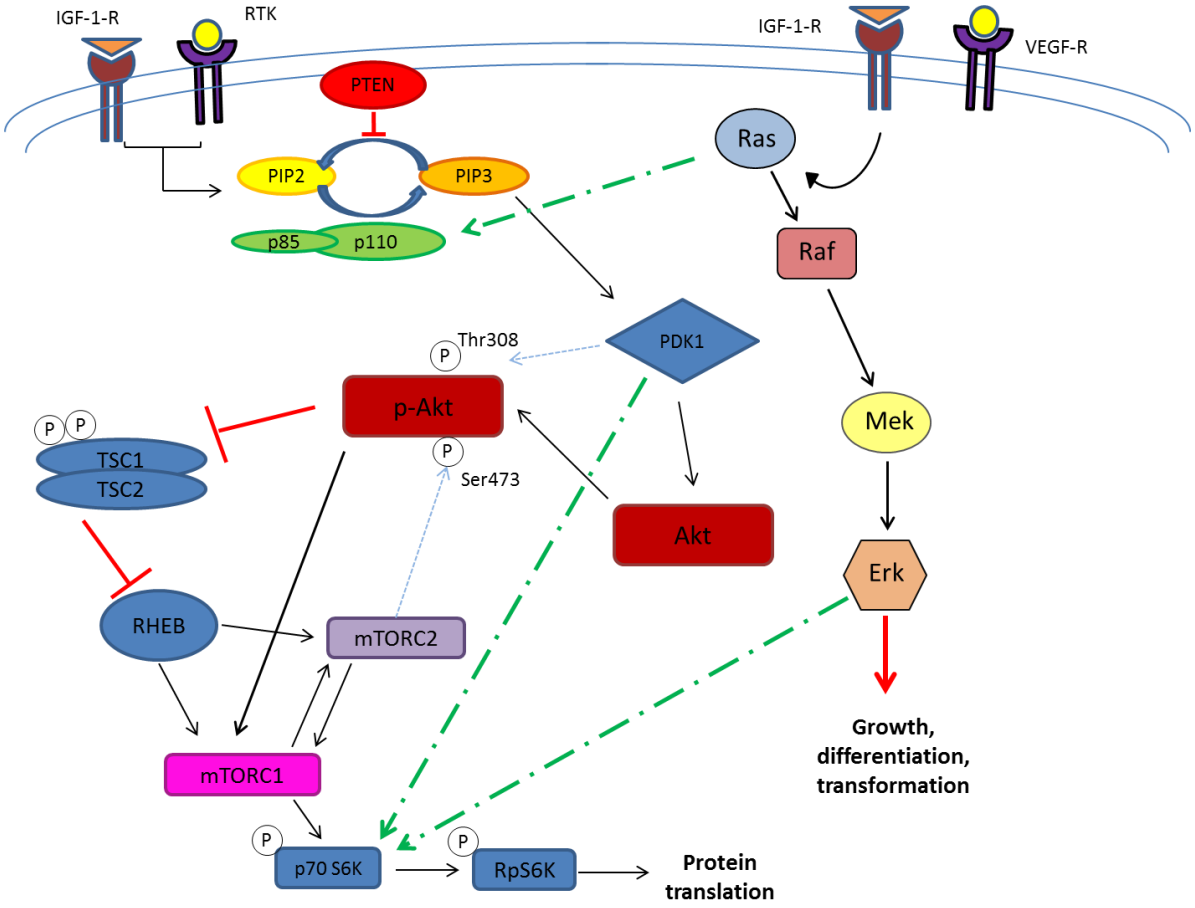

Figure 55: A schematic representation of the mechanism by which PI3K/Akt signalling is activated by dominant, stabilised Kras in β-catenin/Kras double mutants (PBCre4^{+}Catnb$^{+/lox(ex3)}$K-ras$^{+/V12}$). It is felt that Ras/MAPK signalling cooperates with the PI3K/Akt pathway independent of mTOR in the presence of intact PTEN. Broken green lines represent hypothesised cooperation, whereas black lines represent known activation, and red lines depict inhibition.

Alternatively enhanced CD44 expression in PTEN/Kras mice could be the result of an expanded pool of PrSCs. In addition to its role in Wnt signalling, CD44 is known to be a transmembrane glycoprotein involved in cell-cell adhesion, inflammation, and cell migration (Zoller, 2011, Guo et al., 2012) that avidly stains basal cells in benign human prostate (Palapattu et al., 2009). Studies have shown that CD44+ prostate epithelial cells in combination with other cell surface antigens and/or integrins select for stem/progenitor cells (see tables 4 and 5 in general introduction; human and murine PrSC markers respectively). Moreover it is has been shown that the number of prostatic stem/progenitor cells are increased in Pten-null mice (Wang et al., 2006) leading to tumour initiation. Therefore it is conceivable that because formation of a

compound PTEN/Kras mutant increases the severity of PCa, one mechanism by which this could occur would be to expand the pool of SC/CSCs, and increase CD44 expression. This question will be addressed by future work on culturing PrSCs from the prostates of these mouse models *in vitro*.

In PTEN/Kras double mutants, there also appears to be occasional residual nuclear Pten expression (see figure 51 (C5)). One theory for this could be that accelerated tumourigenesis, and thus poorer survival, has a negative impact on the time available for DNA recombination to occur, resulting in reduced PTEN deletion. This may in part be supported by the fact that in PTEN single mutants (see figure 56), Pten expression negatively correlates with disease progression from PIN to invasive carcinoma.

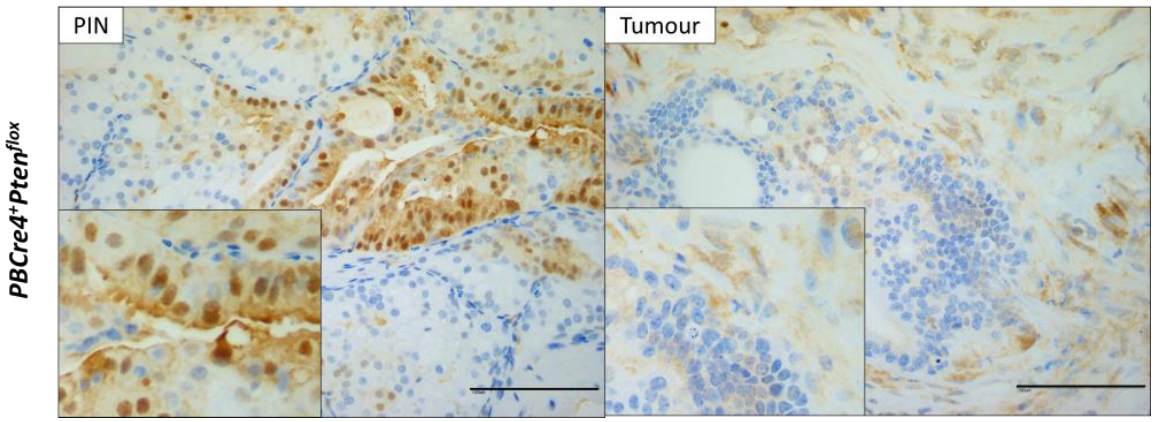

Figure 56: Pten expression negatively correlates with disease progression in the PTEN single mutant model. The above PIN lesion displays residual Pten expression, which is absent from invasive adenocarcinoma (Tumour) but still retained by the surrounding stroma. Images were taken at 40x magnification, and scale bars represent 100µm.

Triple mutant mice demonstrated more severe, lethal high-grade PCa. Lesions were locally-advanced and non-metastatic. The IHC expression profile exhibited by these mice has led to the belief that with increasing DNA damage i.e. when all 3 pathways are activated, there is selection of dominant pathways with/without deselection of other pathways in clonal expansion. This concept may be further supported by the finding that triple mutant mice displayed abundant foci of squamous metaplasia throughout the prostate tumour and the urethra, suggesting that the Wnt pathway was most dominant in this model.

In human cancers, the impact of a given mutation will depend on the position and relative importance of the affected protein within the signalling pathway. Although genetic heterogeneity between tumours is known to be widespread, it has long been appreciated that phenotypic heterogeneity may not be as extensive, with the same cellular pathways often repeatedly affected (Burrell et al., 2013). The selection of dominant signalling cascades is often dictated by environmental pressures, such as progression to metastatic disease, or following treatment, whereby heterogeneity is wiped out; so-called clonal sweep (Greaves and Maley, 2012). The dominant signalling cascades that result thus dictate the clonal landscape resulting in a more homogeneous cell population. These processes are far-removed from the tighter spatial regulation in the mouse models observed in this thesis, but it provides an insight into the selection/deselection of certain signalling transduction pathways in triple mutant mice resulting in rapid tumourigenesis.

4.4.4 AR correlates positively with prostate cancer aggressiveness

Synergistic activation of two or more pathways results in a PCa similar to the human disease. Previous work has demonstrated that Wnt (Truica et al., 2000), PI3K/Akt/mTOR (Carver et al., 2011), and Ras/MAPK (Carey et al., 2007) signalling are all capable of regulating AR. It has been shown here that *in vivo* cooperation between these pathways when mutated in combination demonstrate synergistic overexpression of AR compared with single mutants, which in turn express a significantly higher level of AR expression than *wild-type* prostate.

The development of CRPC is not commonly associated with the loss of AR expression. Instead, evidence points to the accumulation of molecular changes that reduce the threshold of AR ligand required for proliferation and survival (Isaacs and Isaacs, 2004). To this effect, a 2- to 5-fold increase in AR mRNA is both necessary and sufficient for progression to CRPC in mouse models, and subsequently, cells can become supersensitive to androgens rather than being independent of them (Chen et al., 2004a). This discovery led to the introduction of novel anti-androgen therapies in the fight against the human disease, namely abiraterone, and enzalutamide (Karantanos and Thompson, 2013). As a whole this evidence raises the possiblity that overexpression of AR in all single and combinatorial PCa models used in this thesis may be sufficient to promote androgen-independent prostate growth, a poorly modelled area *in vivo*. Validation by castration studies could contribute important information to the landscape of CRPC development and provide platforms for therapeutic testing.

4.4.5 p63 correlates negatively with prostate cancer aggressiveness

Expression of p63 was shown to diminish with disease progression in tumours of all genotype when compared with their respective PIN lesions. This mimics human prostate cancer whereby progression to a luminal phenotype is pathognomonic. Given that p63+ basal cells are more proliferative, and that secretory cells originate from p63+ basal cells, the reduction of p63 is felt to reflect the withdrawal of differentiated malignant cells from the stem cell/progenitor compartment. The presence of p63+ cells does not prevent tumours being classified as malignant, as basal cell markers can be retained by murine cancer cells (Ittmann et al., 2013). Linear stem cell theory dictates that luminal cells arise from basal cells, therefore differentiated cancer cells in mice could feasibly retain p63 expression. The progressive loss of p63 in parallel with tumour progression may reflect elevated MAPK signalling (Pearson et al., 2009). MAPK is postulated to be a negative regulator of p63 since Src and MEK were activated in the luminal cells of $p63^{-/-}$ prostate (Kurita et al., 2004). Therefore, it is likely that loss of basal cells disturbs the interaction between stromal cells and epithelial cells, and causes activation of Src, and hence Ras/MAPK signalling, in luminal cells.

Activated β-catenin and PI3K/Akt/mTOR signalling are also reportedly regulators of p63, and so might explain why tumours arising in β-catenin/PTEN double mutants (PBCre4+Catnb+/lox(ex3)Ptenflox) and PTEN/Kras mice (PBCre4+PtenfloxK-ras+/V12) express higher levels of p63 than others, but significantly less than *wild-type* prostate. βeta-catenin is known to induce high levels of p63, which in turn drives differentiation towards a squamous cell fate, and so foci of keratinising squamous metaplasia in β-catenin/PTEN mice (PBCre4+Catnb+/lox(ex3)Ptenflox) could thus account for increased p63 expression. In addition, PI3K/Akt/mTOR signalling has been shown to regulate p63 in keratinocytes; treatment of immortalised keratinocytes with EGF resulted in activation of both the MAPK and PI3K pathways. Subsequent pharmacological inhibition of PI3K/Akt/mTOR but not MAPK signalling nullified the increase in ΔNp63 expression (Barbieri et al., 2003). This could also account for the increased incidence of $p63^{+}$ cells in β-catenin/PTEN and PTEN/Kras tumours.

4.4.6 Ki67 correlates positively with prostate cancer aggressiveness

The Gleason grading system for human PCa makes no reference to the proliferation rate of cells, but the addition of Ki67 status could provide additional prognostic information at

diagnosis. In humans studies Ki67 accurately predicts overall survival for patients undergoing watchful waiting (non-curative management) (Berney et al., 2009); time to radical treatment for men on active surveillance (deferred curative management) (Kristiansen, 2012); time to biochemical relapse in men treated with radical prostatectomy (Laitinen et al., 2008, Gunia et al., 2008, Miyake et al., 2010); and disease progression in patients undergoing external beam radiotherapy (Khor et al., 2009). In these mouse models, compound dysregulation of Wnt, PI3K/Akt/mTOR, and/or MAPK signalling results in the synergistic increase in Ki67 expression that clearly correlates with grade and stage progression. The triple mutant tumours displayed the greatest degree of proliferation due to deregulated cell cycle kinetics. It will be interesting to find out whether these findings are corroborated in a human prostate cancer tissue microarray.

4.4.7 Probasin-Cre demonstrates unwanted mosaic genetic deletion when inherited maternally

Cohorts for both 100day and endpoint in all genetic combinations were incomplete at the end of the period of study in this thesis due to the previously unappreciated phenomenon that maternal transmission of probasin-Cre leads to loss of transgene efficacy, and mosaic genetic deletion in target males. Ongoing efforts at the time of writing have since rectified this, and re-established a mouse colony with correctly functioning probasin-Cre. Future work aims to fully recruit to all incomplete cohorts to ensure that characterisation of each genetic combination is robust, and capable of withstanding statistical analysis for publication.

4.5 CHAPTER SUMMARY

Utilisation of conditional mouse models through Cre-loxP technology allows activation of the Wnt, PI3K/Akt/mTOR, and Ras/MAPK pathways to initiate prostate tumourigenesis. These signalling transduction pathways are not closed loops functioning in isolation; it has been shown here that both dominant stabilisation of β-catenin, and PTEN loss trigger activation of their own pathways and the ectopic activation of neighbouring pathways clearly demonstrating synergy. Furthermore combinatorial, synergistic pathway activation drives rapid disease progression from PIN to high-grade locally invasive adenocarcinoma. These models accurately mimic features of the human disease and provide a platform for the pre-clinical testing of novel therapeutic agents aimed at curing high-grade prostate cancer.

Chapter 5: Establishing a 3D primary tissue culture assay to explore self-renewal in murine adult prostate epithelial stem cells (PrSCs)

5.1 INTRODUCTION

Adult epithelial stem cells are of interest due to their ability to facilitate organ homeostasis and for their potential role in tumourigenesis. Throughout the life span of an adult organ, stem cells operate to replace lost or damaged tissue to ensure proper function (Blanpain et al., 2007), such as in the blood, skin, and intestine. Owing to their longevity and inherent self-renewal capacity, adult stem cells are potential cells of origin for certain cancers (Barker, 2009). Prospective isolation of these cells and investigation into their properties will allow better understanding of their basic biological processes when designing and/or testing novel therapeutic agents.

The rodent prostate is a suitable model system to investigate the properties of adult epithelial stem cells due to the proven ability of the rodent gland to undergo seemingly unlimited cycles of involution after castration and subsequent organ replenishment upon androgen reintroduction (English et al., 1985, English et al., 1987). Perhaps the most important reason to study prostate stem cells (PrSCs) is that they too are androgen independent (or castration resistant, Montpetit et al., 1988), and therefore similar to the subpopulation of prostate cancer cells capable of initiating CRPC, the lethal phase of the disease (Antonarakis and Eisenberger, 2011). Identifying critical self-renewal pathways in PrSCs may provide new therapeutic targets against the SC that would be of use as adjuncts to current therapies, which for the most are only effective against differentiated tumour cells.

5.1.1 Cancer stem cell theory

Cancer stem cells (CSCs) are SCs that are capable of populating all cell types within a malignant neoplasm, but the precise derivation of CSCs remains elusive. Theoretically, a CSC could evolve from any one of the following mechansims: (a) an oncogenic mutation within a developing stem- or progenitor cell, (b) an oncogenic mutation within an adult stem- or progenitor cell, or (c) de-differentiation of a mutated tumour cell that acquires stem-like properties.

Strictly speaking the CSC model postulates for hierarchical organisation of tumours with cancer stem cells at the top of the lineage hierarchy, capable of indefinite self-renewal, unlike their

progeny, which undergo terminal differentiation and loss of tumourigenicity (Isaacs and Coffey, 1989). Note that prostate CSCs may not display features of the cell of origin in this model (Wang and Shen, 2011). In contrast, the stochastic (clonal) model proposes that the majority of cancer cells within a tumour are tumourigenic and possess varying genetic or epigenetic properties (Marotta and Polyak, 2009, Rosen and Jordan, 2009, Shackleton et al., 2009). Clones with distinct growth advantages and/or therapy resistance that are capable of withstanding these selection pressures survive, and drive tumour progression. Thus, in the clonal evolution model, it is essential to eliminate differentiated cancer cells in bulk to achieve therapeutic efficacy, whereas in the CSC model, tumour eradication ought to require dual therapy against both the CSC and the tumour bulk. In theory, these two models do not need to be mutually exclusive (Wang and Shen, 2011). Cancers that follow the CSC model may simultaneously undergo clonal evolution if more than one type of CSC coexists, or CSCs are under environmental selection (Marotta and Polyak, 2009). Similar to other solid tumours, it is presently unclear whether prostate cancers are organised hierarchically and follow the CSC model exclusively, which suggests that cancer-initiating mutations could occur in different cells of origin within the prostate epithelium. Indeed this notion has recently been supported by claims that prostate cancer can initiate from both the basal and luminal cell lineages (Choi et al., 2012), and furthermore these separate entities display distinct molecular signatures that are predictive of human patient outcomes (Wang et al., 2013). During prostate cancer progression, clonal progeny of the resulting TICs are constantly under selection, from such factors as environmental and treatment pressures. Some of these clones may gain additional growth and survival advantages and become the driving force of tumour malignancy, ultimately acquiring the properties of CSCs.

5.1.2 The origin of human cancer stem cells

Cancer stem cells often share antigenic profiles with normal tissue stem/progenitor cells (Ginestier et al., 2007, Malanchi et al., 2008), and as CSCs may originate from oncogenic transformation of a normal tissue SC, many studies have focused on the identification of normal PrSCs as a starting point for subsequent studies to determine whether genetic alterations of these SCs may confer tumour-initiating properties (Wang and Shen, 2011). Distinctive methodologies have been established to identify and investigate prostate epithelial cells with stem-like capabilities in both humans and mice. As discussed in the introduction, many of these

purported SC populations are non-overlapping. The identification of candidate SCs has led to the consideration of whether these populations in the mouse, or their analogous populations in humans, can serve as cells of origin for prostate cancer.

5.1.3 In vitro and in vivo experiments have provided evidence for PrSC/CSCs

To date, no one assay is capable of displaying all characteristics of SC/CSCs, and therefore three main assays have been employed to satisfy this brief in both humans and mice. These include, (a) 2D culture for proliferation and differentiation *in vitro*, (b) 3D culture to display self-renewal *in vitro*, and (c) for reconstitution of the primary tissue in allografts, be it normal or malignant (termed xenografts if human cells are transplanted into mice).

To facilitate study of human prostate CSCs methods usually include, fresh frozen, primary tumour cells (usually from RRP samples) or established cell lines for 2D culture *in vitro* (also known as colony-forming assays), or cell line xenografts using immunodeficient mice. One group has employed magnetic bead cell sorting to isolate $CD44^{+}\alpha2\beta1\text{-integrin}^{hi}CD133^{+}$ cells from primary human cancers, and showed that this subpopulation displayed high proliferative potential in 2D culture, as well as the ability to differentiate to a luminal phenotype in culture following treatment with dihydrotestosterone (Collins et al., 2005). A subsequent collaborative paper involving the same group reported how $CD44^{+}\alpha2\beta1\text{-integrin}^{hi}CD133^{+}$ cells can initiate prostate cancer, which displays a luminal phenotype, following xenotransplantation (Lawrence et al., 2013). This technique however is complex, and is limited by low yield of graft success (27% when transplanted with mouse UGS mesenchyme, 0% when cultured alone), occasional absence of PCa cells in the graft, and because immunodeficient mice are used, grafts are often infiltrated with host immune cells with unknown impact on the graft (Lawrence et al., 2013). Attempts to develop 3D tissue culture assays to enrich for human SCs have failed as it appears that these cells are unable to form spheres, instead preferring to proliferate in 2D monolayer (Garraway et al., 2010, Guo et al., 2012).

Other studies claim to have isolated CSCs from long-established human PCa cell lines, using similar combinations of cell-surface markers. For example, $CD44^{+}\alpha2\beta1\text{-integrin}^{hi}CD133^{+}$ cells were isolated from the DU145 cell line (Wei et al., 2007), $CD133^{hi}$ cells were identified from the human telomerase reverse transcriptase-immortalised primary tumour-derived prostate epithelial cell lines (Miki et al., 2007), and $CD44^{+}CD24^{-}$ cells were isolated from the LNCaP cell

line (Hurt et al., 2008), and $CD44^{+}CD133^{+}$ cells in the PC3 and DU145 cell lines (Dubrovska et al., 2009). The CSC properties of these cell populations were demonstrated by colony formation assays and tumour reconstitution following subcutaneous injection, whereas other studies demonstrated tumour formation using allografts under the renal capsule (Gu et al., 2007).

Cell lines were long preferred to primary PCa cells because the latter are notoriously difficult to culture (Peehl, 2005). However in the former, extensive passaging is likely to alter the genetic properties of cell lines compared to the precursor human primary tumours from which they were established (Wang and Shen, 2011). Assays employed to demonstrate prostate CSC properties may be fundamentally flawed. In particular, 2D colony formation assays in culture may selectively favour cells that are better adapted to the culture conditions, and may not accurately model micro-environmental conditions in vivo (Quintana et al., 2008). Similar concerns apply to in vivo assays, as many studies have employed flank or sub-renal capsule injection of CSCs to assess tumour-initiation ability, and thus are not conducted within a prostate microenvironment. A recent publication showed how basal cells, both in vivo and in vitro, can exhibit substantial plasticity when removed from their endogenous tissue microenvironment (Wang et al., 2013). Moreover their work supports the notion that genetic lineage tracing in vivo, and not transplantation-based assays, represents a gold standard for identification of SCs/CSCs (Snippert and Clevers, 2011).

The specificity of the cell-surface markers utilised in CSC studies is also questionable and their biological function is often unknown. Although CD44 and CD133 have been implicated as CSC markers in a variety of tissues, such as brain/CNS (Uchida et al., 2000, Singh et al., 2004), breast (Al-Hajj et al., 2003), and prostate (Richardson et al., 2004), proving their specificity to the CSC is difficult. To highlight one example, CD133 is broadly expressed in luminal cells of colon, lung and pancreas, and appears to display little specificity for colon cancer-initiating cells (Shmelkov et al., 2008). Furthermore another study noted that $CD133^{+}$ cells from the DU145 cell line were no more clonogenic than $CD133^{-}$ cells, while CD133 was not expressed in other prostate cell lines including DuCaP, LAPC-4, 22Rv1, LNCaP, and PC-3 (Pfeiffer and Schalken, 2010). Finally, mouse CD133 was shown to be widely expressed by prostate luminal cells, whereas human CD133 is less broadly expressed in benign tissue, but is upregulated in regions of inflammation within tumours, suggesting a lack of correlation with CSCs (Missol-Kolka et al., 2011). Thus, the utility of current putative CSC markers for identification of prostate CSCs remains unclear.

5.1.4 Why use mouse models to study the function of PrSC/CSCs?

Difficulties associated with human prostate CSC culture can be circumvented by the use of mouse prostate in similar tissue culture experiments. Mouse models are advantageous as they can largely evade host cross-species transplantation reactions, and candidate CSCs can be analysed from genetically defined tumours in vivo.

Mouse prostate cancer models have not as yet been extensively exploited to identify candidate CSCs by way of tumour-reconstitution/allograft assays. However, the $Lin^{-}Sca\text{-}1^{+}CD49f^{hi}$ subpopulation from constitutive Pten-null mice displayed tumour-initiating properties in both 3D culture and following reconstitution of malignant glands in renal grafts *in vivo* (Mulholland et al., 2009). A similar approach was later used to isolate $Lin^{-}Sca\text{-}1^{+}$ cells from tumours in a conditional Pten deletion model. This paper went on to report how cancer-associated fibroblasts enhanced the pro-tumourigenic effects of candidate CSCs in renal grafts over and above normal fibroblasts (Liao et al., 2010).

Given that one theory for CSC provenance postulates for oncogenic transformation of a PrSC, many studies using mouse tissue have focused on this to determine whether genetic alterations in PrSCs may confer tumour-initiating properties. As previously mentioned, the reporting of non-overlapping candidate SC populations between groups has understandably raised controversy as to their precise biological roles and whether they truly serve as cells of origin for PCa.

5.1.5 FACS enables prospective identification of purported PrSCs/CSCs

FACS has been integral to the identification and isolation of candidate PrSCs, to allow assays challenging their function to be undertaken. The prostate reconstitution/allograft assay involves culturing PrSCs with embryonic urogenital sinus mesenchyme (EUSM), and this method has shown Sca-1+ cells to be more efficient at regenerating prostatic tissues than Sca-1- cells (Burger et al., 2005, Xin et al., 2005). Other studies have successfully displayed features of stem cells *in vivo* and *in vitro* that expressed cell surface markers CD49f and Trop2 (Lawson et al., 2007, Goldstein et al., 2008). Furthermore, 1 in 10 $Lin^{-}Sca\text{-}1^{+}CD133^{+}CD44^{+}CD117^{+}$ cells have been reported to be capable of prostate reconstitution in the renal allograft assay (Leong et al., 2008).

Several studies have also utilised FACS to isolate candidate human prostate epithelial stem cells. Cells expressing high levels of α2β1-integrin were more proliferative in 2D and xenograft culture than the total basal population (Collins et al., 2001). Further enrichment of prospective these candidate PrSCs can be carried out using the marker CD133 (Richardson et al., 2004). Similarly, the Trop2 marker can be used in combination with CD49f to enrich for sphere-forming cells from the human prostate consistent with the findings seen in mice (Goldstein et al., 2008).

5.1.6 Trop2 is a candidate PrSC marker

Tumour-associated calcium signal transducer 2 (Trop2) has been recognised as a candidate stem cell marker from prostate-specific microarray analysis, because it was 20-fold enriched in the murine prostate after castration (Wang, 2007), and 12-fold enriched in prostate sphere cells compared with the total epithelium (Goldstein et al., 2008). Trop2 has no known function or ligand (Fornaro et al., 1995, Tsujikawa, 1999), and is a type I transmembrane protein akin to EpCAM, a family of transmembrane glycoproteins that mediate calcium-independent epithelial cell-cell adhesion. Trop2 expression has been reported in normal and/or malignant tissue from kidney, lung, ovary, testis (El Sewedy et al., 1998), colon and rectum (Ohmachi, 2006), pancreas (Fong, 2008), and breast (Huang, 2005).

This chapter reports the successful identification and isolation of a subpopulation of prostate epithelial basal cells from histologically normal tissue, which displays the ability to self-renew *in vitro,* consistent with a stem-like phenotype. The steps taken to optimise this 3D sphere-forming assay are also described here.

5.2 CHAPTER AIMS

The aims of this chapter are:

1. To evaluate a panel of postulated CSC markers as readouts of disease progression from normal prostate to invasive tumour in autochthonous mouse models of prostate cancer
2. To identify potential markers at immunohistochemistry that could be used to identify stem cells at FACS
3. To optimise a tissue culture assay to allow maintenance and expansion of primitive prostate cells that display stem cell characteristics in vitro
4. To demonstrate the ability of prostate epithelial stem cells identified prospectively at FACS in normal murine prostate to act as stem cells in 3D culture
5. To determine whether alteration of the genetic background of murine prostate epithelium to create a pro-oncogenic environment, alters the pool of stem cells

5.3 RESULTS

5.3.1 Validation of proposed stem cell markers in autochthonous mouse models of human prostate cancer

Cancer stem cells may arise from normal stem/progenitor cells that have undergone malignant transformation (Jordan et al., 2006). As such, markers of normal prostate stem/progenitor cells may also be markers of prostate CSCs/initiating cells. Given that PrSCs are felt to reside in the basal layer, one might also expect a number of luminal cells in normal prostate to express SC markers if luminal cells are believed to not arise from a separate luminal progenitor (see figure 13, in General Introduction).

The expression of postulated CSC markers was examined by IHC in formalin-fixed, paraffin-embedded sections of both normal mouse prostate and prostate tumours. The cellular antigens tested for are included in table 16, along with proportion of positive staining.

Putative CSC markers CXCR4 (Miki et al., 2007), EpCam (Guo et al., 2012), Integrin-β1 (Collins et al., 2001), Lrig1 (Powell et al., 2012), Sca-1 (Burger et al., 2005, Xin et al., 2005), and CD133 (Collins et al., 2005) were not expressed in either normal prostate or prostate tumours at immunohistochemistry (photographs not shown), and so will not be discussed further.

CSC marker	Intensity in normal prostate	Proportion of normal prostate	Localisation in normal prostate	Intensity in tumour	Proportion of tumour	Localisation in tumour
CD44	-	-	-	++	+++	C and M
CXCR4	-	-	-	-	-	-
EpCam	-	-	-	-	-	-
FRMD4a	+	+	Nuc	+++	+++	C and M
Integrin-β1	-	-	-	-	-	-
Lrig1	-	-	-	-	-	-
Notch1	++	+++	C	+++	+++	C and Nuc
Notch4	+	+++	C	++	+++	C
Trop2	++	++	Nuc	+++	+++	C and M
Sca1	-	-	-	-	-	-
CD133	-	-	-	-	-	-

Table 16: Putative markers of prostate SC/CSCs tested by immunohistochemistry. Staining intensities and proportion were scored and the pattern of expression noted. Intensity scores: - absent expression; + low intensity; ++ moderate intensity; +++ high intensity. Proportion scores: - absent expression; + 1-5% expression; ++ up to 50% expression; +++ 51-100% expression. Localisation: C, cytoplasmic; M, membranous; Nuc, nuclear. N=3 for all stains.

5.3.1.1 CD44

CD44 is a cell surface glycoprotein involved in cell–cell interactions, cell adhesion and migration. In addition to these cellular functions, CD44 is extensively used as a surface marker for isolating CSCs from breast, prostate, pancreas, ovarian, and colorectal cancers (Jaggupilli and Elkord, 2012). However, the usefulness of CD44 as CSC marker remains uncertain (Slomiany et al., 2009). CD44 has been assigned roles in cancer initiation (Leung et al., 2010), and metastasis (Visvader and Lindeman, 2008), but its association has been opposed in breast (Lopez et al., 2005) and prostate cancer (Gao et al., 1997) because its high expression failed to differentiate areas of normal tissue from cancer (Naor et al., 2002). CD44 is found to be ubiquitously expressed in most normal and cancer cells, which has limited its widespread use as a lone CSC marker. However in combination with other surface markers, it serves to purify populations that have displayed SC traits *in vitro* and *in vivo* (see tables 4 and 5 for summaries of human and mouse PrSC markers respectively – General Introduction).

As shown in figure 57, CD44 was not expressed in normal prostate but was heterogeneously overexpressed in tumours, where it stained strongly in a cytoplasmic/membranous fashion.

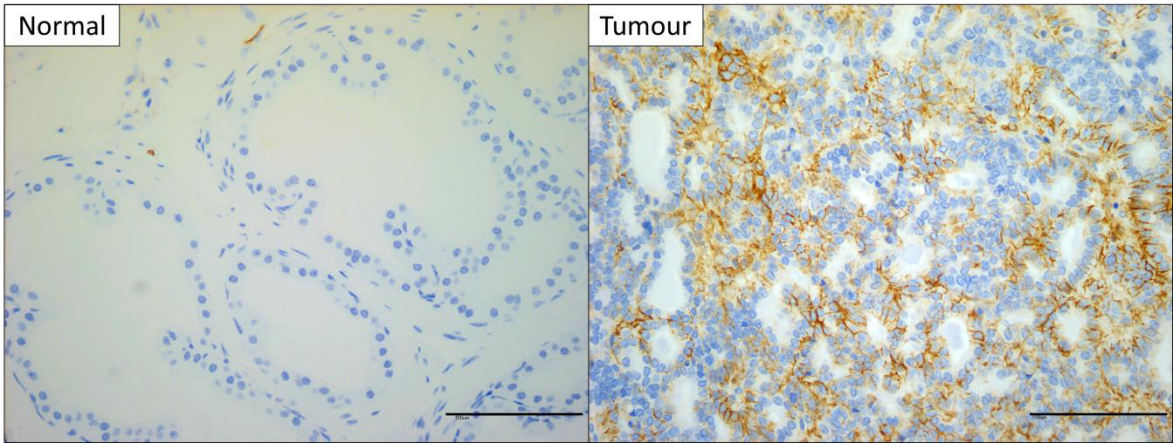

Figure 57: Expression of CD44 in normal prostate and prostate tumour. Error bars 100µm.

5.3.1.2 FRMD4a

FRMD4a is a human epidermal SC marker upregulated in squamous cell carcinoma (Jensen and Watt, 2006), and in this regard it has been implicated in cell polarity (Ikenouchi and Umeda, 2010) and metastasis (Goldie et al., 2012).

Infrequent luminal cells in normal prostate demonstrated nuclear avidity for FRMD4a while tumours ubiquitously exhibit strong cytoplasmic staining (see figure 58). This does not satisfy the description of a SC/CSC marker.

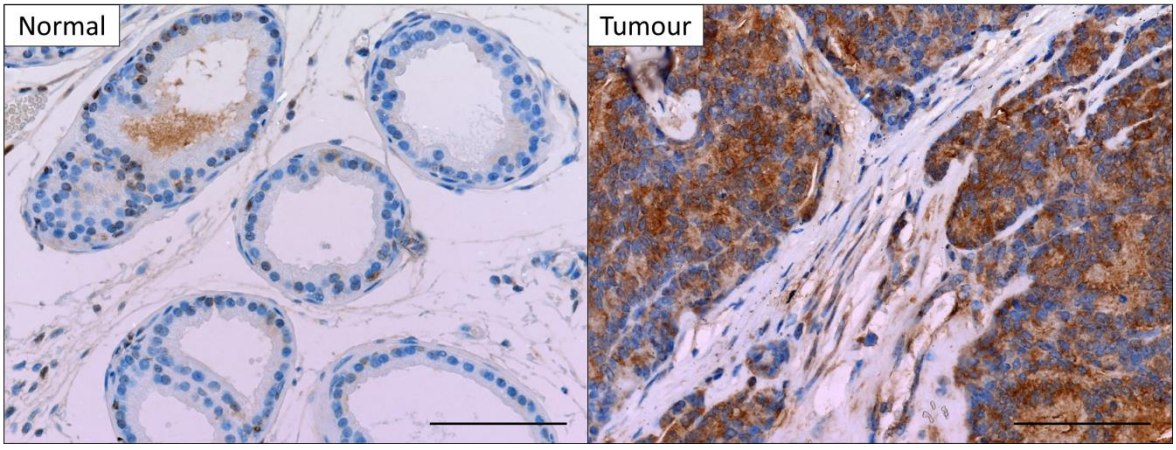

Figure 58: Expression of FRMD4a in normal prostate and prostate tumour. Error bars 100µm.

5.3.1.3 Notch1

NOTCH1 encodes for a member of the notch family of single pass transmembrane receptors. The Notch pathway is a short-range communication system that regulates cell fate (Leong and Gao, 2008), and inappropriate Notch activation stimulates proliferation, restricts differentiation, and/or prevents apoptosis (Pannuti et al., 2010). Mammals have four paralogs that essentially vary in the number of EGF repeats in the extracellular domain (Pannuti et al., 2010). Mouse models have unearthed a direct role for Notch signalling in the regulation of various stem/progenitor cells, including the hematopoietic system, skin, hair, inner ear, skeletal muscle, and intestine (Chiba, 2006). In normal mouse prostate, Notch1 mRNA expression was upregulated following castration and down-regulated following hormone replacement (Wang et al., 2004), providing evidence for its role as a normal SC marker. Recently its importance in mediating chemoresistance in PCa has also identified it as a potential CSC marker (Liu et al., 2014), but more data are required from both animal and human studies to prove its value in either role.

In normal prostate Notch1 expression can be seen to stain both luminal and basal prostate epithelial cells, whereas it is expressed ubiquitously in tumour cells and surrounding stroma. It appears to localise to the cytoplasm in normal prostate, and is over-expressed in both the cytoplasmic and nuclear compartments in tumour. When associated with tumour, stroma exhibits cytoplasmic localisation. This does not fit the SC/CSC phenotype, as demonstrated in figure 59.

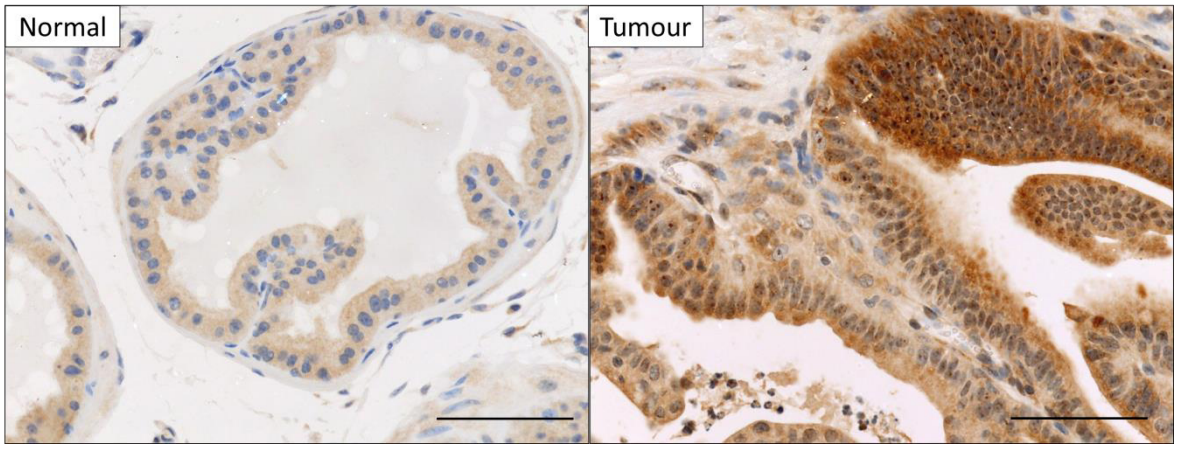

Figure 59: Expression of Notch1 in normal prostate and prostate tumour. Error bars 100µm.

5.3.1.4 Notch4

There is good evidence for the role of Notch in CSC regulation in breast cancer, which has provided the basis to question whether the same function can be extrapolated to prostate (Pannuti et al., 2010). In breast ductal carcinoma in situ (DCIS), the ability to culture SCs into spheroids (called "mammospheres") is dramatically decreased by co-culture with a Notch-4 monoclonal antibody (Farnie et al., 2007). This intimates cooperation between epidermal growth factor receptor and Notch4 in DCIS SC maintenance.

Notch4 stains only luminal epithelial cells in normal prostate with low intensity, and it is widely expressed in all tumour cells with higher intensity. Both display cytoplasmic staining, which is overall reduced compared with Notch1. Stromal cells do not stain for Notch4. These findings are not in-keeping with a stem cell phenotype, and can be seen in figure 60.

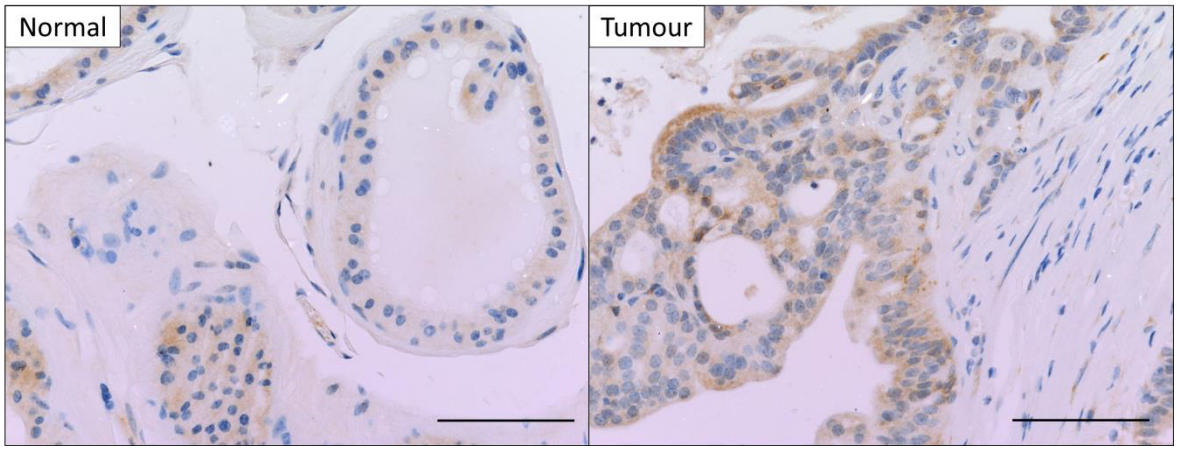

Figure 60: Expression of Notch4 in normal prostate and prostate tumour. Error bars 100µm.

5.3.1.5 Trop2

Trop2 was found to be enriched after castration and in the basal prostate epithelium (Goldstein et al., 2008). Both its location within the mouse prostate and demonstration of its function *in vitro* and *in vivo* satisfy the stem cell brief in the mouse.

A minority of normal prostate luminal cells and a significant proportion of basal cells display nuclear staining with Trop2 antibody. Conversely, prostate tumours exhibit cytoplasmic and membranous staining in the vast majority of cells in a heterogeneous fashion. A subset of cells

is seen to stain with greater intensity than the bulk of tumour cells. Given that Trop2 is a transmembrane glycoprotein member of the EpCam family, these findings support those of others that Trop-2 is a regulator of cell-cell adhesion in PCa (Trerotola et al., 2012). Interestingly Trop2 is also expressed in the stroma. The expression pattern seen here satisfies cancer stem cell theory, whereby there is upregulation of Trop2 expression on malignant transformation.

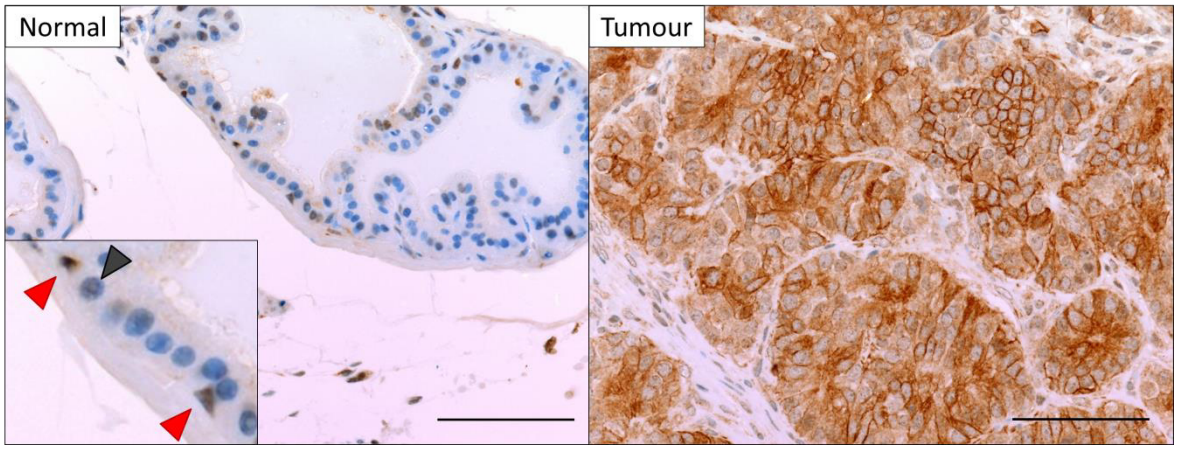

Figure 61: The expression pattern of Trop2 in normal prostate and prostate tumour is consistent with cancer stem cell theory. Trop2 is seen to stain a significant proportion of triangular basal cells (inset – red arrowheads), and a small minority of luminal cells (inset – black arrowheads), in normal prostate. There is massive upregulation of Trop2 expression seen in tumour in-keeping with a CSC phenotype that has undergone malignant transformation from a normal SC. Error bars 100µm.

5.3.2 Optimisation of PrSC 3D tissue culture assay

Single unsorted prostate epithelial cells from 100-day old mice were plated in Matrigel at varying densities in 12-well plates to determine the optimal density for (a) accurate counting of prostate organoids, and (b) bulk passage of cells (see figs (a) and (b) below).

Plated cell densities ranged from 1000 cells/well to 10E6cells/well and the average numbers of prostate organoids grown out and counted are shown for each.

When accurately quantifying the organoid-forming efficiency (or the sphere-forming unit) a plated density of 10E4cells/well was deemed to be optimal (see (a) and (c) below). Furthermore in order to maintain sphere-forming cells (PrSCs) through numerous rounds of

passage, plating cells at a density of 10E5 was employed as it appeared to consistently maximise the yield of organoids (see (b) and (d) below). Beyond this density there is toxicity to sphere-forming cells thereby inhibiting organoid-formation (see (d-f) below).

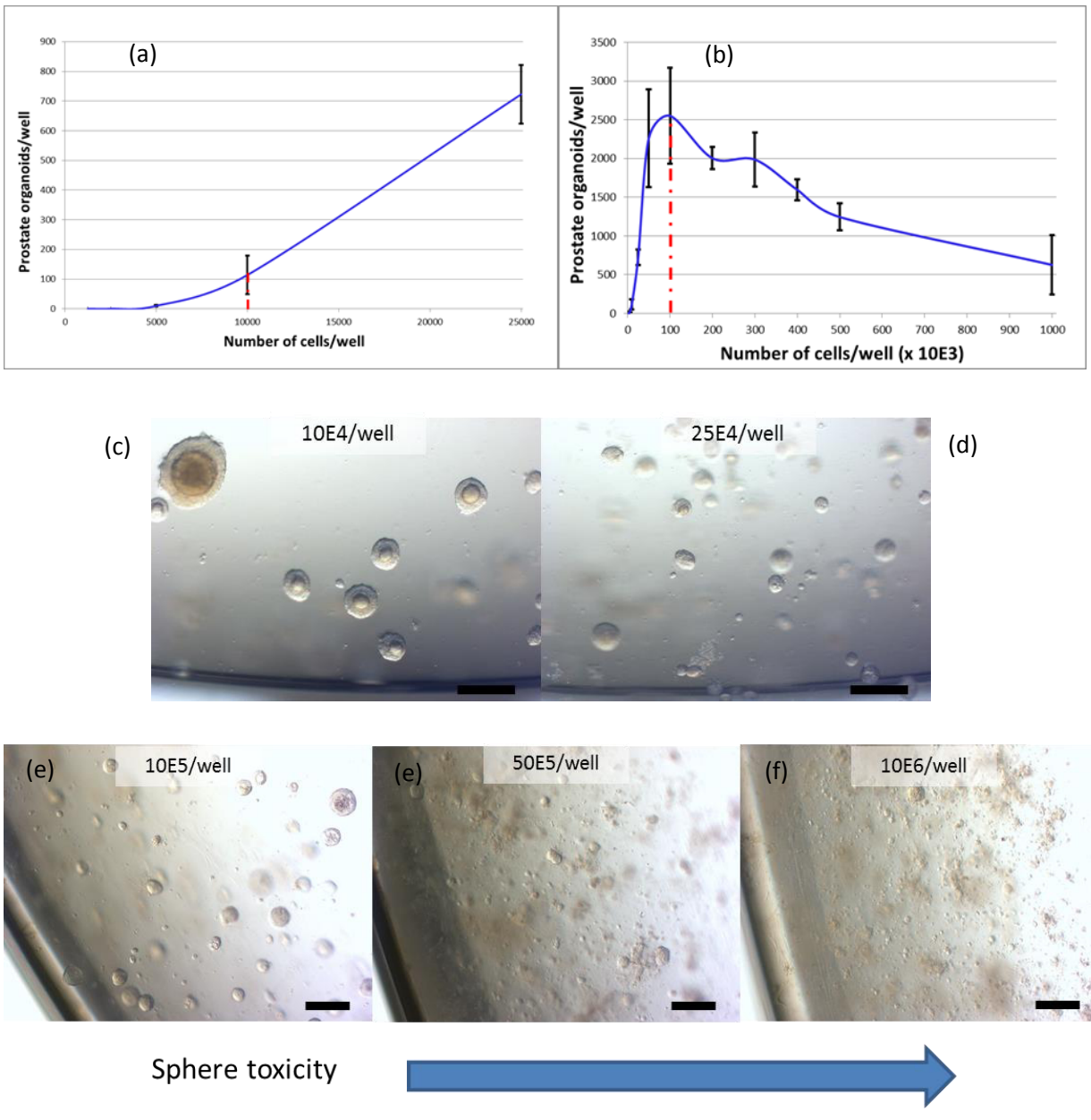

Figure 62: Assay optimisation to determine optimal plating density. Experiments to ensure the optimal plating densities for (a) accurately counting prostate spheres, and (b) to maximise yield of sphere cells, where performed. Counting of spheres was best done at 10E4/well (c), as it can be seen that increasing seeding density to 25E4/well could introduce bias when counting spheres (d). At higher densities, sphere growth is impaired (e & f). Error bars 200µm. Photographs taken on inverted brightfield microscope.

The live cellular yield from each 100-day old wild-type prostate ranged from 1.25x10E6 to 2x10E6 (mean 1.6x10E6, median 1.4x10E6 cells) when stained with trypan blue (n=5).

It was noted that the ratio of live:dead cells counted by trypan blue exclusion varied according to genotype, as depicted in the box and scatter plots below. This suggests that genomic instability negatively correlates with cell fate. Possible explanations for this finding include: 1. combinatorial pro-oncogenic mutations result in abnormal cell signalling, which in turn trigger activation of pro-apoptotic pathways, and/or 2. the increased number of dead cells seen may be a consequence of necrosis.

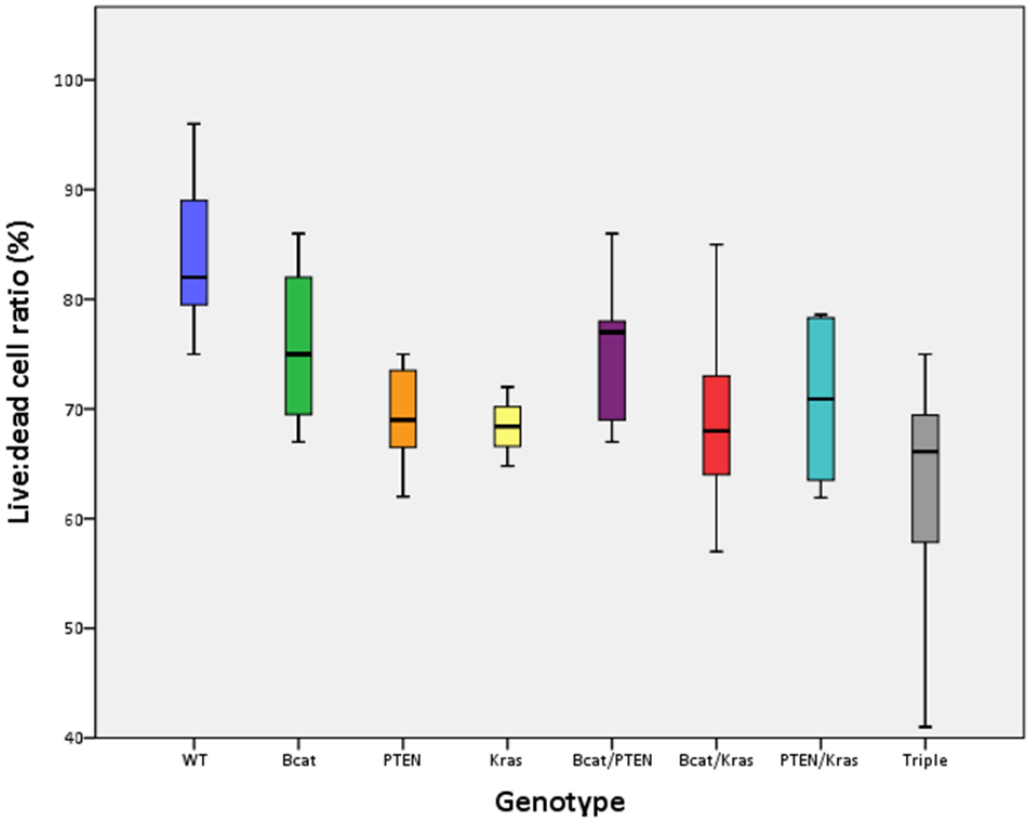

Figure 63: The proportion of dead cells correlates with the degree DNA mutation. The ratio of live:dead cells were counted by trypan blue exclusion of single prostate epithelial cells. It can be seen from the box plots that the proportion of dead cells counted from mutant prostates is higher than *wild-type*, and this is greatest in combinatorial mutants compared with single mutants or *wild-type*; n=3 for all genotypes.

Unsorted prostate epithelial cells from 100 day-old wild-type mice are incapable of self-renewal. To determine the self-renewal capacity of unsorted cells, prostate epithelial cells were digested into single cell suspension and passaged to finality in triplicate. It can be seen that unsorted cells possess restricted self-renewal capacity; being capable of a maximum 2 rounds of passage only (n=4), with a median 128 spheres formed in the 1st generation (1/72 cells). In the 2nd generation, this diminished to median 32 spheres per well (p=0.083), hence a ratio of 1/167 1st generation sphere cells were capable of self-renewal. No 2nd generation sphere cells were capable of forming spheres in the 3rd generation, thus demonstrating attenuated 'stemness'.

Cohort	1st Generation	2nd Generation	3rd Generation
1	140	63	-
2	136	-	-
3	120	60	-
4	64	3	-
Median	**128**	**31.5**	-

Table 17: Unsorted prostate epithelial cells are incapable of self-renewal in vitro. None of these cells was able to passage to generation 3, and the median number of spheres formed in the 2nd generation was significantly less than the 1st.

To enable the function of normal PrSCs to be evaluated, techniques to enable their prospective isolation *in vitro* were explored.

5.3.3 Prostate epithelial stem cells possess the antigenic profile Lin^{-}CD49f^{+}Sca1^{+}Trop2^{Hi}

To enable the isolation and cultivation of PrSCs, a single cell suspension of prostate epithelial cells was sorted by FACS, cultured to permit sphere formation, then passaged and re-plated to allow direct comparison of their self-renewal capacity with unsorted prostate epithelial cells. The flow-diagram in figure 64 illustrates this process.

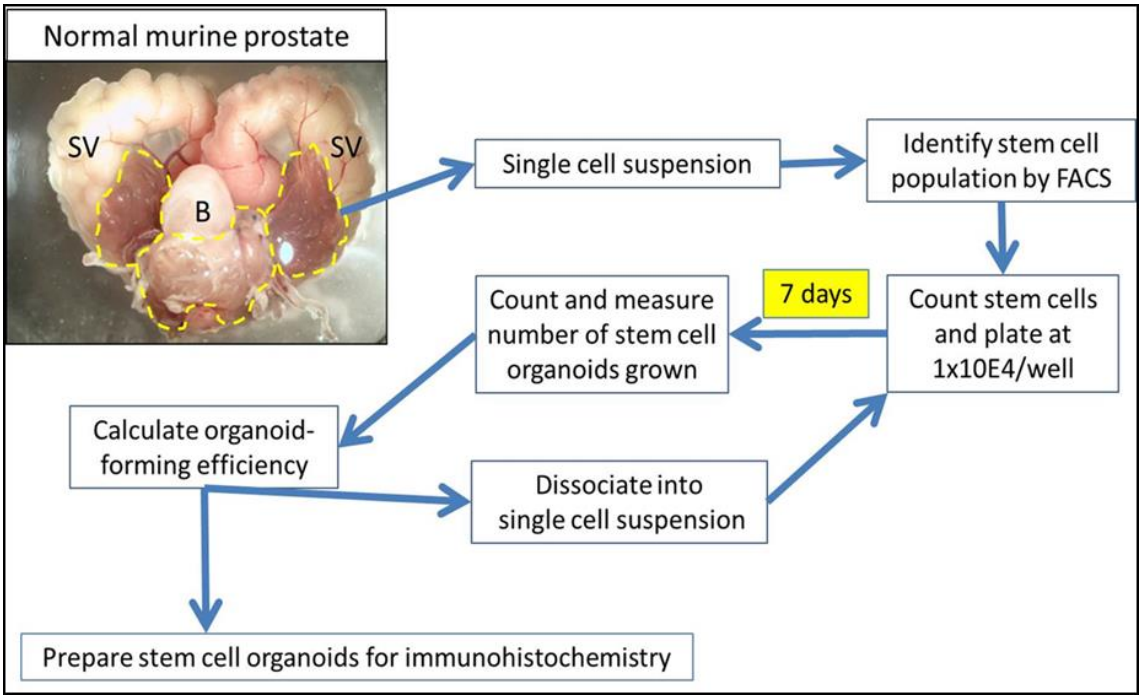

Figure 64: Normal mouse prostates were digested and sorted to extract PrSCs for 3D primary culture. The above flow diagram depicts the abbreviated version of the methods of culture and passage. For a more detailed explanation, please refer to section 3.5 in methods and materials.

In order to quantify the stemness of *wild-type* PrSCs in vitro, the number and proportion of stem cells formed at each generation after passage were established, along with PrSC organoid size. When assessing prostate organoid size, a cut-off of 40µm was set because these small structures seemed to cease growing at or around day 5 and so were not counted as PrSC organoids.

A typical FACS plot would yield the following proportions for each subpopulation (as a percentage of total cell number), and each experimental FACS plot is shown thereafter:

- **Trop2^{Hi}:** median 7.6% (IQR 5.7 – 11.4)
- **Not CD49f/Sca1^{+}:** median 27.5% (IQR 22.8 – 32)
- **Not Trop2^{Hi}:** median 5.7% (IQR 4.6 – 7.1)

Experiment 1

Experiment 2

Experiment 3

Experiment 4

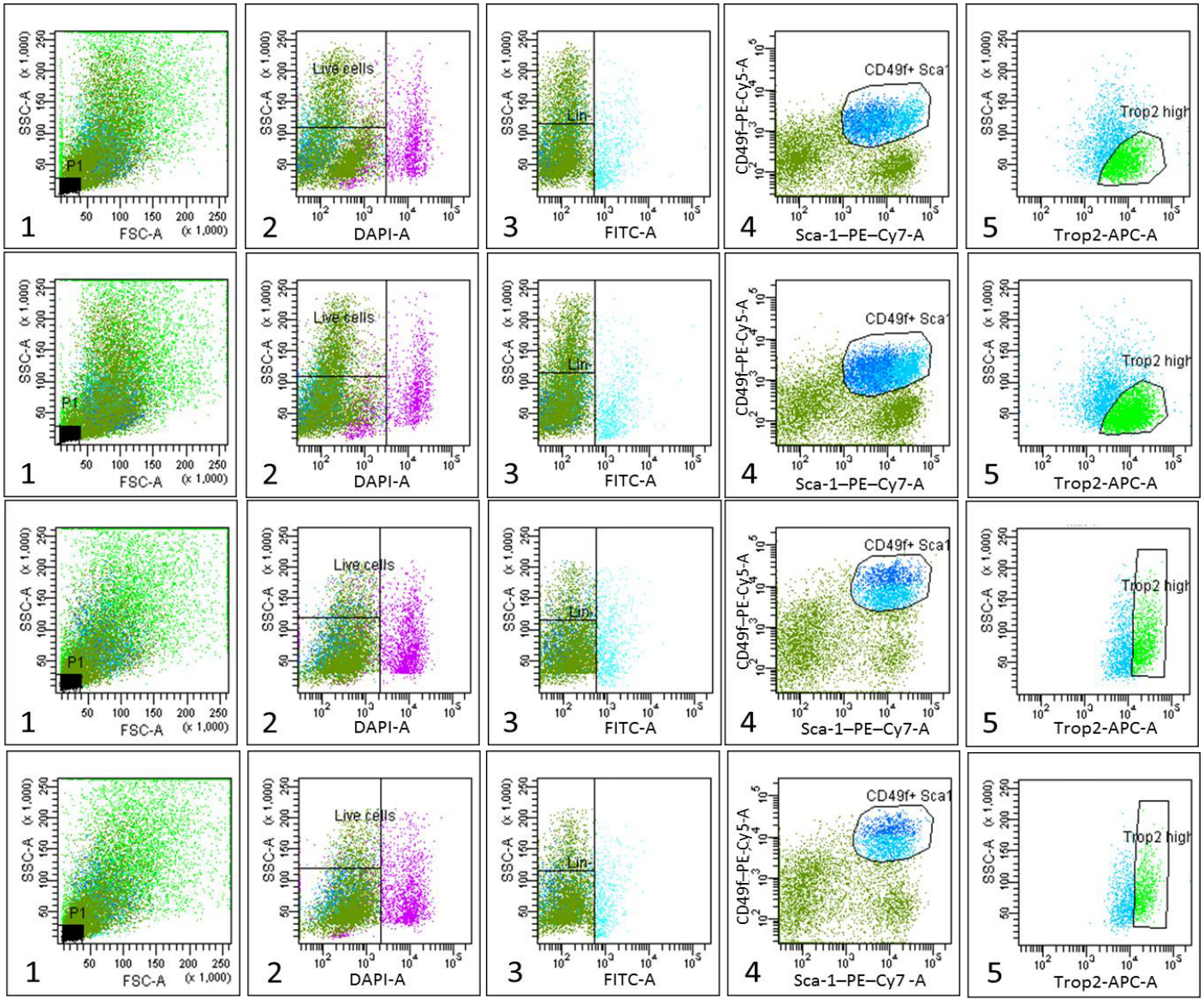

Figure 65: FACS plots from each experiment used to utimately select out the Trop2^{Hi} subpopulation in five gated phases

The FACS plots from each of 4 experiments are shown in figure 65 in 5 gated phases. Following digestion into single cell suspension (gate 1), all cells are shown in the forward scatter vs side scatter plot, in which cell debris (labelled P1) and cell clumps were excluded. In gate 2, live cells only were selected using DAPI exclusion (seen here as dark green), before all Lin- cells were gated for (seen as dark green in gate 3). In gate 4 all cells expressing high levels of CD49f–PE-Cy5 and Sca-1–PE–Cy7 were chosen (blue population), and finally of these shown in gate 5, cells expressing high levels of Trop2-APC were defined (light green). The large green population in gate 4 represents the "not CD49f/Sca1+" population, and the light blue population in gate 5 represents the "not Trop2Hi" population.

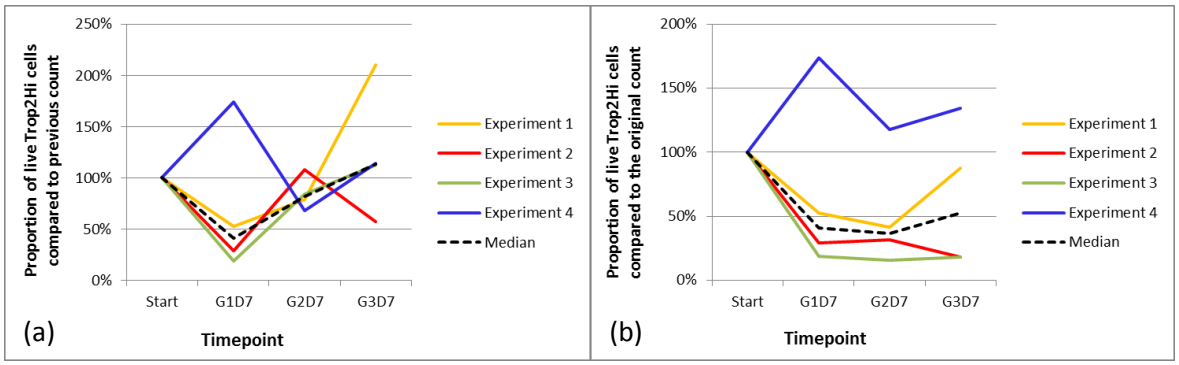

Figure 66: The proportions of live PrSCs counted prior to re-plating demonstrate variability in each generation, and with each experiment. The number of live Trop2^{Hi} PrSCs cells was compared with the previous generation's count (a), and with the original number of PrSCs at the beginning of each experiment (b). Prefix *G*, denotes the generation after plating and passage, whereas *D*, denotes the number of days elapsed since cells were plated, i.e. G1D7 is the 7th day of the 1st generation. Prostate spheres were always passaged on day 7. It is worth noting that experiments were terminated at day 7 of G4, and so spheres were fixed in formalin for IHC, rather than re-dissociating back to single cells for counting.

After FACS in each culture experiment, the remaining number of live Trop2^{Hi} PrSCs was determined by Trypan blue exclusion before plating. It can be seen that while there was variability amongst experiments, comparison of the proportion of live cells to the previous generation (figure 66a) shows that from the end of the 1st generation (G1D7) the Trop2^{Hi} cell population is expanded *in vitro* as illustrated by the median plot (black broken line). Perhaps the reason for the initial dip in cell number at G1 is that progenitor cells lose their self-renewal capacity and undergo apoptosis, while the stress of passage stimulates PrSCs to replicate. When compared to the number of cells at the beginning of each experiment (figure 66b), the

median cell number at the termination of all but experiment 4 is decreased. This suggests that Trop2^{Hi} cells can be maintained *in vitro* despite repeated rounds of passage. In reality cells are inevitably lost each time the cells are re-dissociated back to single cells and passaged. Furthermore in figure 66(b), the median Trop2^{Hi}PrSC number is lower at the end of generation 3 than at the starting point of each experiment. Despite this it can be seen from the graph that the median number of PrSCs begins to increase and thus perhaps at this point, progenitors are exhausted and PrSCs are becoming more purified.

5.3.4 PrSC organoids demonstrate self-renewal in vitro

Murine prostate epithelial cells expressing the antigenic profile Lin$^-$Sca-1$^+$CD49f$^+$Trop2^{Hi} (Trop2^{Hi}) were capable of self-renewal in vitro (n=4), whereas both Lin$^-$Sca-1$^-$CD49f$^-$ (not CD49f/Sca-1$^+$) and Lin$^-$Sca-1$^+$CD49f$^+$Trop2^{Lo} (not Trop2^{Hi}) were incapable of sustained self-renewal.

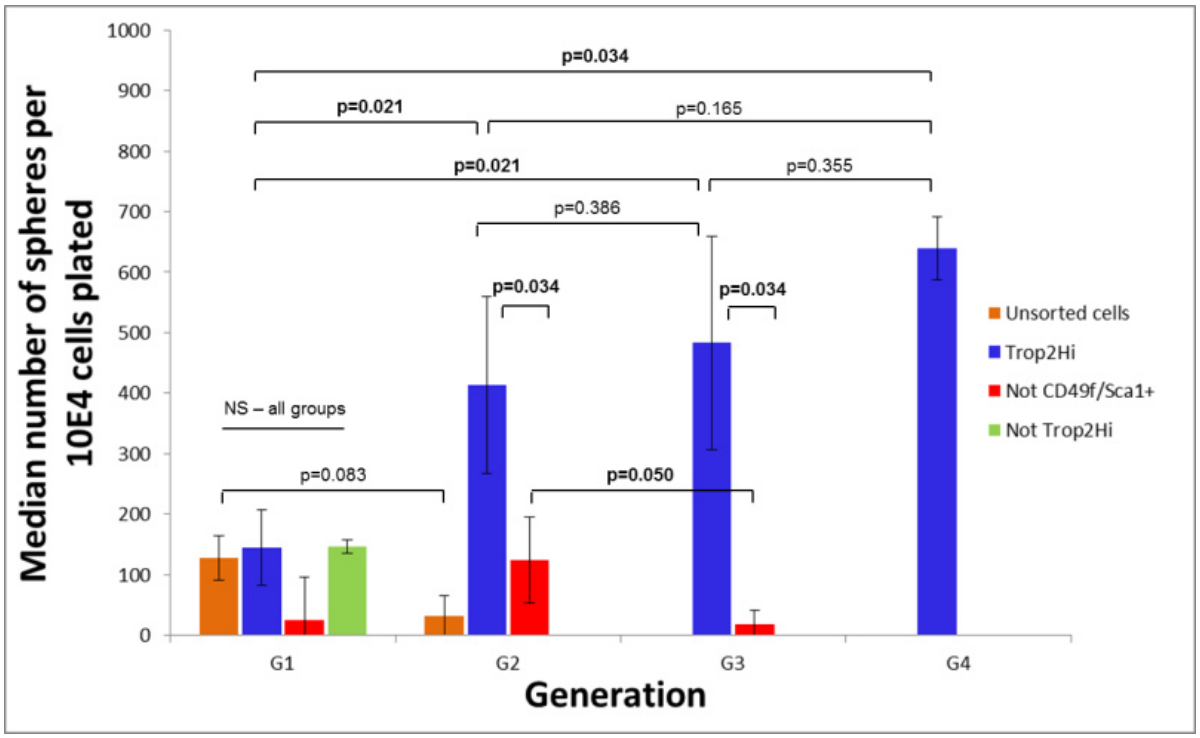

Figure 67: PrSCs are increasingly purified through at least three rounds of passage whereas other prostate epithelial cells are not. Columns depict median, while error bars represent SD; significance was tested using the non-parametric Mann-Whitney test, p<0.05 (95% confidence interval), n=4. Analysis was performed in SPSS 20 (Armonk, NY: IBM Corp).

Figure 67 plots the median number of prostate spheres formed per generation (n=4) in each of the 4 prostate cell populations. It was shown earlier (see table 17) that unsorted prostate cells lose the ability to form spheres beyond G2. In a similar manner, cells that are not Trop2^{Hi} lack the ability to undergo self-renewal. The ability of cells that do not express CD49f^{+}Sca1^{+} to self-renew declines significantly from G2 to G3 (p=0.050). Trop2 enriches for sphere-forming cells from the mouse prostate that display self-renewal *in vitro*. Second, 3rd, and 4th generation Trop2^{Hi} cells form significantly more spheres than 1st generation cells (p=0.021, 0.021, and 0.034 respectively), but apparent increases in the sphere-forming efficiency from 2nd to 3rd, and 3rd to 4th are not statistically significant (p=0.386, and 0.355 respectively).

SFU (%)	G1	G2	G3	G4
Unsorted cells	1.28	0.32	0.00	-
Trop2^{Hi}	1.46	4.14	4.83	6.39
Not CD49f^{+}Sca1^{+}	0.26	1.25	0.19	0.00
Not Trop2^{Hi}	1.46	0.00	-	-

Ratio of sphere forming cells	G1	G2	G3	G4
Unsorted cells	1/78	1/313	-	-
Trop2^{Hi}	1/69	1/24	1/21	1/16
Not CD49f^{+}Sca1^{+}	1/392	1/80	1/526	-
Not Trop2^{Hi}	1/68	-	-	-

Table 18: PrSCs become more efficient at forming spheres than other prostate epithelial cells through multiple rounds of passage. The proportion of Trop2^{Hi} cells capable of forming spheres rises from 1/69 to 1/16 from G1 to G4 respectively wheras the ability of other populations diminishes. SFU = number of spheres/number of cells plated x 100%

The Trop2^{Hi} subpopulation can be purified through at least 4 rounds of passage, and thereby increasing the proportion of Trop2^{Hi} cells capable of forming spheres from approximately 1/69 in the 1st generation (G1) to around 1/16 in the 4th generation (G4). In contrast, cells that are not Trop2^{Hi} are incapable of self-renewal, whereas both unsorted cells, and not CD49f^{+}Sca1^{+} cells, are capable of limited self-renewal *in vitro* as illustrated by their diminishing sphere-forming ability in table 18.

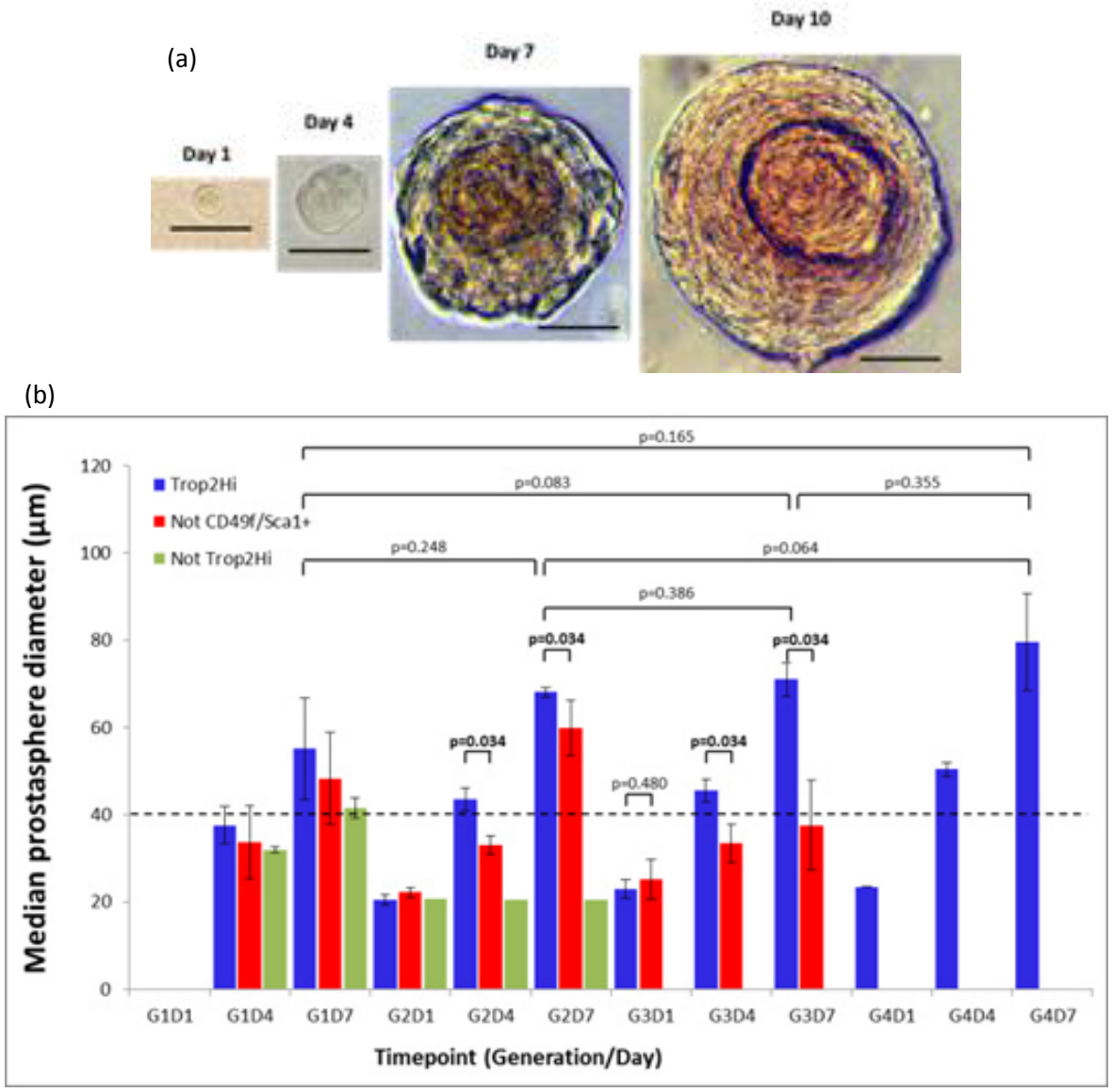

Figure 68: PrSCs consistently form large spherical structures *in vitro*, whereas other prostate epithelial cells do not. The appearance of prostaspheres at each time point on an inverted brightfield microscope are shown (a); scale bars depict 50µm. The size of prostate spheres formed in each generation at days 1, 4, and 7 after plating are shown for each group (b). Only spheres greater the 40µm in size were counted. Columns depict median, while error bars represent SD; significance was tested using the non-parametric Mann-Whitney U test, $p<0.05$ (95% confidence interval), n=4. Analysis was performed in SPSS 20 (Armonk, NY: IBM Corp).

By day 4 of G2, $Trop2^{Hi}$ spheres are significantly larger than those that do not express $CD49f^{+}Sca1^{+}$ (p=0.034). Moreover in G3, $Trop2^{Hi}$ spheres grow faster and larger than not CD49f/Sca1+ cells (p=0.034). As such no sphere that lacked $Trop2^{Hi}$ expression met the size criteria for counting in G2 (see figure 68(b)), and neither did the vast majority of those not expressing CD49f/Sca1+ in G3. Spheres from unsorted cells are not included in figure 68.

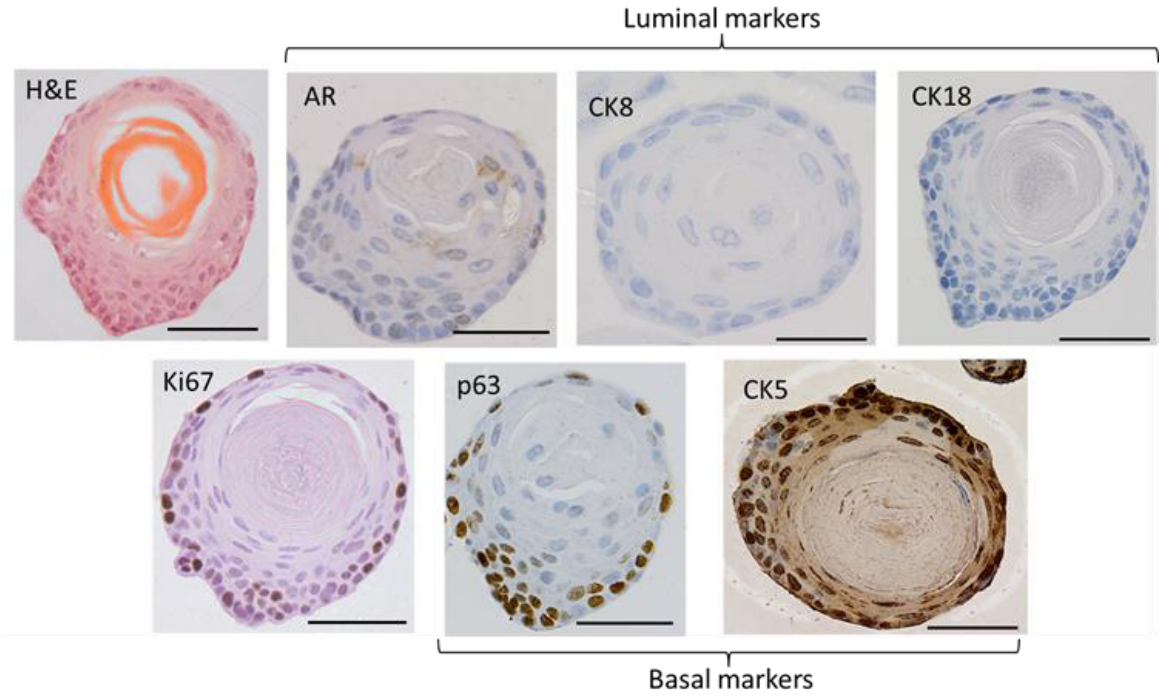

Figure 69: Prostaspheres display a basal phenotype. Formalin-fixed, paraffin-embedded prostaspheres were sectioned for IHC analysis. They demonstrate signs of early squamous differentiation and keratin deposition centrally. Error bars depict 50µm.

Prostate spheres can either be solid in appearance, or display an organised bi-laminar structure with a central lumen and secretions within it. When stained with H&E, secretions appear consistent with keratin suggesting squamous differentiation centrally. However they predominantly consist of a primitive basal phenotype, as highlighted by p63 and CK5 staining, thus their constituent cells remain largely undifferentiated. Furthermore they appear to lack CK8 and CK18, markers of terminally differentiated luminal cells. Interestingly, cells located centrally display weak AR^{+} expression (luminal cell marker), perhaps indicating that they may be in the early stages of differentiation here. Proliferating cells reside in the periphery, as indicated by avid Ki67 expression.

5.3.5 Assay optimisation

This technique posed several quality control issues during its inception. These are outlined below along with the approaches for addressing and solving these problems.

Problem: How to determine the optimal number of prostates to use in order to extract sufficient numbers of PrSCs for each experiment
Solution: Perform number reduction experiments to discover the minimum number of prostates acceptable

Optimisation of an assay to analyse the biological properties of PrSCs may eventually be useful as a baseline comparator for CSCs isolated from transgenic mouse models of human PCa. One hypothesis to be explored in future experiments is that CSCs are more difficult to prospectively identify and culture than PrSCs from wild-type mice if earlier findings hold true (see unsorted cell live:dead ratios), whereby genomic instability (i.e. increasing the number of pro-oncogenic mutations) reduces cell survival. Ultimately this will impact upon the yield of SC/CSCs, thus the minimum number of prostates that allows a complete experiment needed to be determined, all the while remaining mindful of the guidance outlined by the National Centre for the Replacement, Refinement and Reduction of Animals in Research (NC3Rs). Thus the minimum number of prostates acceptable was defined as, *'the number of glands sufficient to allow development of at least 4 generations of prostate spheres in vitro'*.

Given that firstly the PrSC population is hypothesised to comprise ≤1% of murine prostate epithelium, and because secondly wild-type murine prostates are small, sorting of a single prostate was not attempted.

The following table outlines the results from experiments performed to determine the minimum number of prostates required for 3D PrSC culture:

Number of prostates	Number of experiments performed	Sphere generation attained	Adequacy for PrSC culture
10	1	4	Inadequate
4	4	-*	Inadequate
3	4	4	Adequate
2	4	3	Inadequate

Table 19: Digestion of three prostates per experiment is shown to be optimal

While 10 prostates provided ample material for tissue culture, it would not be feasible to continue this usage due to unacceptably high expenditure in animal fees, and it would also be insensitive to NC3Rs guidance. Conversely using only 2 prostates per culture experiment was found to be insufficient because obtaining 4th generation prostate spheres were not feasible. When attempts were made with 4 prostates, experiments suffered due to poor digestion; this can be seen in table 19 (*). However using 4 prostates per experiment was felt to be unacceptably high both for reasons already stated, in addition to the fact that even the most efficient breeding will form triple mutants at a rate of 1 in 16. Ultimately 3 prostates were deemed to be an appropriate number to use whilst enabling a full experiment to be completed.

Problem: How to make the technique more manageable and maximise the cellular yield obtained for each experiment
Solution: Perform experiments with different digestion times

If performed in a single day, the technique from dissection to plating can be thought of in the following steps:

1. Dissection and mechanical dissociation 1 hour
2. 1st stage of enzymatic digestion 2 hours
3. Formation of single cell suspension 0.5 hours
4. Enrichment of PrSCs 4 hours
5. Counting and plating cells 2 hours

Total **9.5 hours**

The arduousness of this technique should not be understated, and to make this more manageable without compromising the cellular yield, the following questions were explored:

1. Could prostate epithelial cells be safely digested overnight?
2. Does the duration of digestion affect cell viability?
3. Does the duration of digestion affect cell yield?

To answer these questions, wild-type mouse prostates were digested in identical conditions for 2 hours and overnight (n=4). Representative FACS plots from these experiments are shown in figure 70 for comparison, along with median values for key readouts in table 20:

Digestion	**Debris [P1]** (% of total)	**Live cells** (% of parent population)	**Live cells** (% of total)	**Lin- fraction** (% of total)	**Trop2^{Hi} cells** (% of total)
2 hour	23.6	75.5	39.8	36.7	8.8
Overnight	18.3	91.8	56.5	53.2	13.7

Table 20: Overnight enzymatic digestion does not adversely affect epithelial cell viability and maximises cellular yield

It appears that prostate epithelial cells can withstand overnight digestion; in fact the median proportion of total live cells was greater in the overnight group than the 2 hour group, 56.5% vs 39.8% (p=0.018 Mann-Whitney test). Furthermore the overnight digestion appears not to affect the total percentage yield of PrSCs when compared with 2 hour digestion; the median proportion of Trop2^{Hi} cells in the overnight group was 13.7% whereas it was 8.8% in the 2 hour group (p=0.237, Mann-Whitney test). However given that the proportion of live cells when digested overnight is greater, the total number of Trop2^{Hi} (PrSCs) in real terms is truly larger. These facts combined mean that using overnight digestion is feasible, and increases cellular yield.

Two hour digestion

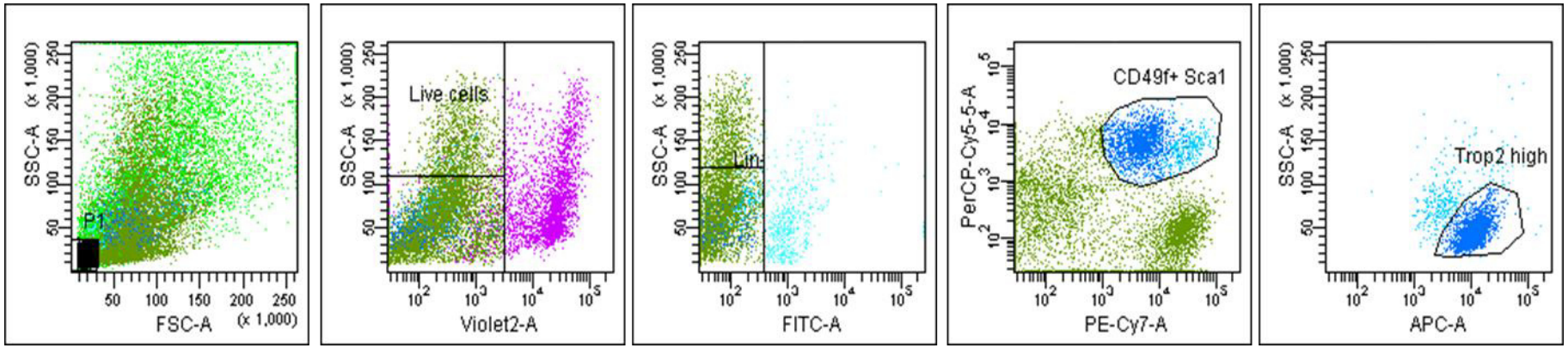

Overnight digestion

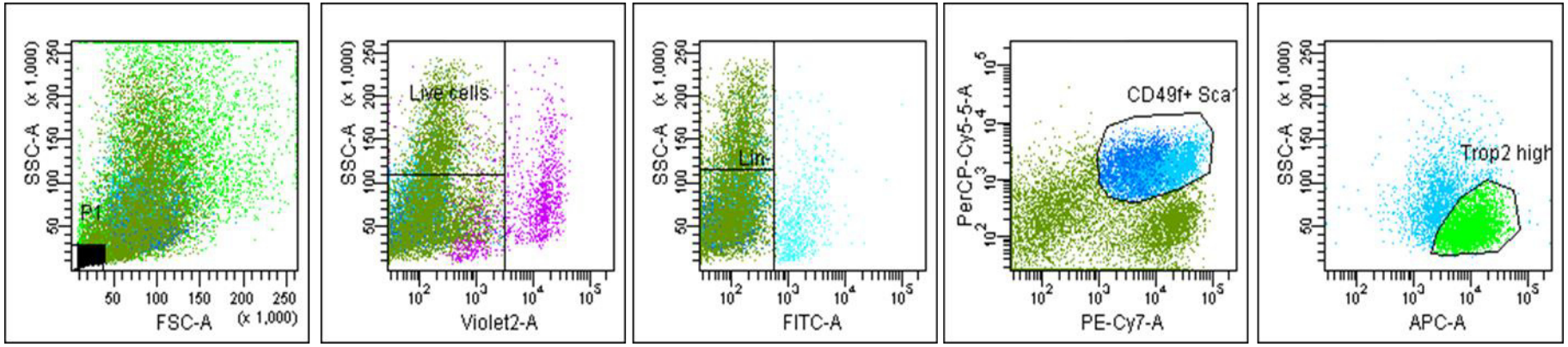

Figure 70: Representative FACS plots highlighting the effect of the duration of digestion on cellular yield

Occasionally it would be evident at FACS that poor digestion had occurred, despite efforts throughout to keep the volume of media and enzymatic concentrations constant. Three examples of tissue that underwent inadequate digestion are shown in figure 71. In all 3 examples shown, there are significant proportions of debris demonstrated (P1 on FACS plots), resulting in fewer live cells, and ultimately few $Trop2^{Hi}$ cells (PrSCs). This point is further highlighted in table 21, along with a subsequent breakdown of the different fractions obtained from FACS.

Example	**Debris [P1]** (% of total)	**Live cells** (% of parent population)	**Live cells** (% of total)	**Lin^- fraction** (% of total)	**$Trop2^{Hi}$** cells (% of total)	**$Trop2^{Hi}$ cells** (Hand counted)
1	63.2	88.6	21.6	15.8	0.1	5,000
2	54.7	78.9	21.3	9.6	0.2	17,500
3	34.0	70.8	30.3	29.9	0.5	35,000

Table 21: Digestion of prostates into single cell suspension is critical to a successful experiment

If and when tissue chunks remained following overnight digestion, this was remedied by performing a further hour-long round of digestion with fresh collagenase and dispase on a shaking platform at low speed prior to the trypsin stage, rather than forcing tissue chunks through a needle and syringe under pressure. If upon performing FACS the proportion of debris was > 1/3 and/or the proportion of total live cells was <1/3, then samples were discarded as these features appeared to represent inadequate digestion that was difficult to overcome, and sorted cells were unlikely to contain a satisfactory proportion of PrSCs.

Poor digestion Example 1

Poor digestion Example 2

Poor digestion Example 3

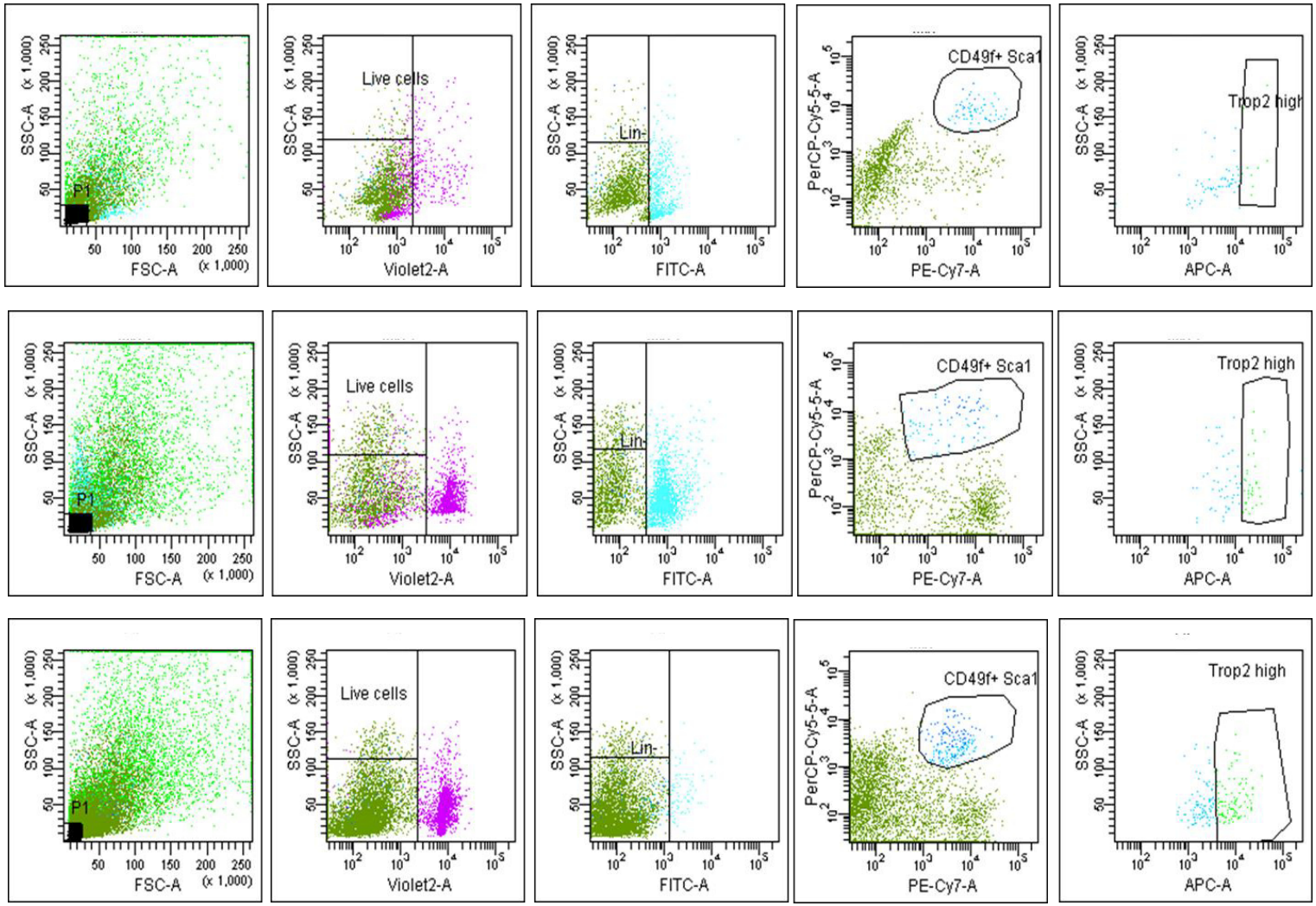

Figure 71: Three examples of inadequate digestion leading to poor cellular yield.

5.4 CHAPTER CONCLUSION

5.4.1 Primitive prostate epithelial cells that possess the antigenic profile Lin$^-$ CD49f$^+$Sca1$^+$Trop2^{Hi} display stem cell characteristics in vitro

Using the assay described here, PrSCs that display self-renewal can be isolated prospectively from wild-type murine prostate, and can be expanded and purified in 3D culture, whilst largely circumventing differentiation. These findings verify those published by others (Goldstein et al., 2008, Lukacs et al., 2010).

Self-renewal is defined as the ability of stem cells to maintain their undifferentiated state, and this attribute was investigated to determine whether Trop2Hi murine prostate cells could demonstrate the potential to act as PrSCs *in vitro*. Three main readouts were reported to quantify stemness in each of the 3 subpopulations. Firstly, the number of spheres grown out at each generation, secondly sphere-forming units (number of spheres as a ratio of cells plated), and thirdly sphere size at the end of each generation. It has been shown that Trop2^{Hi} cells form significantly more prostate spheres than each of the other subgroups by the end of G2. This equates to sphere-forming units of approximately 1/69 in G1, with efficiency improved to 1/16 in G4, further highlighting that cells exhibiting Trop2^{Hi} can be maintained and purified *in vitro*. Additionally Trop2^{Hi} cells formed significantly larger prostate spheres *in vitro*. Midway through G3, Trop2^{Hi} spheres grow significantly larger and faster than those not expressing CD49f/Sca1+. Taken together, Trop2Hi cells display an important distinguishing feature of PrSCs, namely, the ability to self-renew *in vitro*.

5.4.2 PrSC organoids are shown to be spherical and largely undifferentiated by IHC

Overall, the IHC expression profile of p63+ CK5+ AR- CK8- CK18- suggests that PrSCs originate from the basal layer within prostate epithelium. Prostaspheres do however display early signs of squamous differentiation at their core by the presence of weak AR+ staining (luminal differentiation), and keratin (squamous differentiation), which has been reported in 3D culture assays from other tissues e.g. epithelial SCs from tongue papillae (Hisha et al., 2013). This is likely to be a consequence of upregulated Wnt signalling in Trop2^{Hi} cells (Stoyanova et al., 2012), because it is known that dominant stabilised β-catenin induces high levels of p63 to drive cells into a transdifferentiated squamous cell fate (Francis et al., 2013). Basal cells that express unopposed p63 outside their niche, and thus AR:ER homeostatic environment, are likely to

create dysregulated ERα, which is linked to keratinising squamous metaplasia formation, and in turn encourages basal cells to proliferate (Risbridger et al., 2007).

Non-adherent or free-floating 3D culture assays for the investigation of neuronal stem cells have been in use for over 20 years. However, they were noted to suffer from differentiation when plated on an adherent surface. Differentiation was avoided in this assay by the use of the semisolid mimic of the extracellular matrix (ECM)-rich basement membrane, Matrigel. By artificially re-creating the ECM, cell signalling truly representative of the stem cell microenvironment is promoted, thus maintaining basal cells, that express high levels of ECM-binding integrins, in an undifferentiated state (Pontier and Muller, 2009).

5.4.3 Trop2 is co-expressed in both human and mouse prostate

The amount of Trop2^{Hi} cells from normal murine prostate represents 7.6% (IQR 5.7 – 11.4) of total prostate cells, consistent with other reports in mice (Goldstein et al., 2008). We know that the PrSC subpopulation in humans equates to 1 – 15% (defined by confocal microscopy and FACS respectively) of total basal cells. Using the technique described in this chapter, the proportion of Trop2^{Hi} PrSCs as a proportion of basal cells (CD49f/Sca1+) is approximately 45%. Clearly it is difficult to make direct comparisons between the size of PrSC populations in mice with and humans firstly because of the difference in anatomy, and secondly due to the lack of a PrSC marker that is consistently retained in both species. The basal layer in mice is discontinuous whereas in humans it constant, and thus PrSCs in humans should intuitively represent a smaller proportion of basal cells than in mice. One method that may facilitate direct comparison between the 2 species would be to perform FACS on normal prostate from both human and mouse, and to select the high expression of an agreed PrSC marker that is proven in both species as a proportion of the the p63-expressing basal cells.

One such marker that is conserved between species is tumour-associated calcium signal transducer 2 (Trop2). Trop2 was recognised as a candidate stem cell marker from prostate-specific microarray analysis when found to be 20-fold enriched in the murine prostate after castration (Wang, 2007), and 12-fold enriched in prostate sphere cells compared with the total epithelium (Goldstein et al., 2008).

Another marker that enriches for the *in vitro* sphere-forming ability of normal prostate from both human and mouse PrSCs is $CD166^{Hi}$ (Jiao et al., 2012). Also known as activated leukocyte cell adhesion molecule (ALCAM), it is highly upregulated in human and murine CRPC samples. Compared to $CD166^{Lo}$ cells, one of the distinguishing features of $CD166^{Hi}$ cells is their higher expression of Trop2.

5.4.4 Trop2 poses a therapeutic target for the treatment of prostate cancer

Identifying pathways that are critical to PrSC survival and self-renewal may provide new therapeutic targets for the treatment of PCa. Although Trop2 serves as a putative PrSC marker and is upregulated in various epithelial cancers, its functional role in self-renewal, transformation, and signal transduction has remained unclear until recently. Trop2 consists of two biologically distinct domains, and is activated by regulated intramembrane proteolysis. It is ultimately cleaved within the transmembrane domain, leading to expulsion of the extracellular domain (ECD) and translocation of the intracellular domain (ICD) to the nucleus (Stoyanova et al., 2012). Nuclear ICD is found in human prostate cancer but not in benign tissue, implicating Trop2 cleavage in cancer development. The ICD promotes self-renewal, initiates prostatic intraepithelial neoplasia (PIN), and is involved in a β-catenin-dependent signalling cascade. Overexpression of Trop2 leads to up-regulation of the β-catenin downstream targets cyclin D1 and c-myc, demonstrating that Trop2 signals via β-catenin (Stoyanova et al., 2012). Moreover, nuclear β-catenin co-localises with the nuclear ICD of Trop2 in human prostate cancer. Furthermore, loss of β-catenin abolishes Trop2-driven self-renewal and transformation activity. If Trop2 cleavage is impaired by blockage of important cleavage sites, its self-renewal and transformation capacity is abrogated, demonstrating that RIP is essential for Trop2 activity.

5.4.5 Novel primary tissue culture techniques are valuable but subject to criticism

While $Trop2^{Hi}$ cells are hypothesised to consist predominantly of PrSCs, within this subpopulation there may be contamination from progenitors such as transit-amplifying cells; these also possess self-renewal capability, albeit to a lesser extent. The definition of what constitutes $Trop2^{Hi}$ is undeniably subjective. In order to therefore minimise bias, the two pairs of experiments (n=2 x 2) were consistent in selecting the $Trop2^{Hi}$ subgroups relative to one another. The process of passage aims to mitigate progenitor cell contamination of the PrSC

population by exhausting their attenuated self-renewal capacity, however it is not known how many passages are required for this to occur completely.

Other limitations of 3D primary tissue culture assays were considered throughout this work. It currently remains unknown whether all Trop2^{Hi} cells are capable of forming prostate spheres. For neurospheres it has been reported that aggregation of cells into spheres occurred even at low plating densities (Mori et al., 2006, Singec et al., 2006). By employing time lapse photography it has been shown that sphere aggregation is enhanced by the spontaneous locomotion of neurospheres (Singec et al., 2006), and by experimenter-induced aggregation during plate movement (Coles-Takabe et al., 2008). In contrast several studies (albeit from the same group) report that prostate spheres demonstrate clear clonality (Lawson et al., 2007, Xin et al., 2007, Lukacs et al., 2008), as authenticated by co-culturing prostate cells with fluorescent lineage tracing markers (GFP+ and dsRED+), and no spheres containing both cells were observed. Presumably Matrigel culture also favours clonal outgrowth because cells are immobilised and cannot merge together. Following on from the findings in this thesis, work has already begun to modify this method to plate very low seeding densities in 384 well plates by incorporating new technology. The claim that Trop2^{Hi} prostate spheres are truly clonal can be further substantiated by passaging spheres formed at lower density in order to perform linear regression analysis. The plating of single cells would be extremely challenging using this current technique but is theoretically possible using FACS.

A sticking point for many stem cell assays is that stem cells possess the innate ability to shuttle between quiescent and activated states (Li and Clevers, 2010) and that even more committed progenitors can revert back to a more primitive state (Davies and Fuller, 2008). This feature likely prevents their depletion *in vivo* and minimises the possibility of mutagenesis during replication. It could be argued that this assay, as a readout of PrSC function, only selects for more physiologically active cells, whereas stem cells are felt to be predominantly quiescent and remain in phase G0 of the cell cycle. Bearing this in mind, the process of passage may represent the stress stimulus required to reintroduce PrSCs back into the active phase of the cell cycle.

It is not the intention to claim that this *in vitro* 3D sphere forming assay gives an accurate readout of *in vivo* PrSC activity, rather it reflects the ability of Trop2^{Hi} cells to exhibit self-renewal, an important stem cell trait. To complete the whole picture as to their biological

attributes, future experiments will aim to further satisfy the assertion that Trop2^{Hi} cells are PrSCs. A 2D colony-forming assay to explore proliferation and differentiation (in the presence of dihydrotestosterone) is being trialled, whereby Trop2^{Hi} cells will be co-cultured with feeder (STO) cells. Secondly an allograft assay for the *in vivo* regeneration of prostate tubule has been the subject of recent grant proposals to Prostate Cancer UK, and The Urology Foundation. Transplantation of purified PrSCs back into their endogenous niches can complement *in vitro* assays in evaluating their *in vivo* potential. Although envisioned to be challenging, serial passage studies could help determine the self-renewal capacities of these cells *in vivo*, arguably the best indicator of the presence of PrSCs. Xenograft assays of CD133^{+} human prostate cells transplanted under the renal capsule of immunocompromised mice only successfully formed grafts in 27% when co-cultured with mesenchymal tissue and never successful when cultured alone (Lawrence et al., 2013). It is anticipated therefore that adopting this technique will be both timely and expensive.

5.4.6 Optimisation of this 3D primary tissue culture assay provides a baseline standard with which to compare the function of SC/CSCs in mouse models of tumourigenesis

By performing similar experiments on Cre-LoxP transgenic mouse models of prostate cancer, future experiments will aim to discover how mutations of Pten, K-ras and β-catenin alone and in combination within the prostate epithelium impacts on the pool of CSCs. In particular, the influence of these pathways upon the putative CSC population will be interrogated to address the hypothesis that deregulation of these pathways drives both tumour growth and progression by directly expanding the CSC population.

5.4.7 The technical demands of this 3D primary cell culture assay may prevent its widespread adoption

The inception of any assay poses many technical considerations and this was no different. It was deemed that 3 prostates per experiment would be most suitable when looking to perform the same experiments on the prostates of transgenic pro-tumourigenic mice in future. Taking into account the finding (stated earlier in the chapter) that cells with genomic instability are less likely to survive the digestion process, more mice would ideally be needed. However when aiming to use double and triple mutant mice, the likelihood of obtaining more than 3 genotypically identical mice of similar age is low. It is also currently being investigated whether fresh prostate tissue can be frozen and later thawed successfully without affecting cell viability. It is understood that the enzymatic digestion of primary tissue can affect cell surface antigen

survival thereby influencing marker expression (Pastrana et al., 2011). Despite this, results here show that marker expression was preserved using overnight digestion, and indeed cellular yield was improved.

5.5 CHAPTER SUMMARY

The successful isolation and cultivation of prostate epithelial cells with stem-like attributes will allow their unique biological properties to be explored further. These experiments provide a baseline standard with which to compare the function of prostate cancer stem cells from mouse models of tumourigenesis in due course.

Chapter 6: General Discussion

The generation of mouse models that accurately mimic the molecular interactions in human prostate cancer are valuable for studying PCa initiation and disease progression. They also provide platforms for *in vivo* testing of novel therapeutic agents. With this in mind, this thesis aimed to evaluate the roles of the Wnt, PI3K/Akt/mTOR, and Ras/MAPK pathways, all important signal transduction pathways in human PCa, in prostate tumourigenesis. Furthermore, the identification of biomarkers to stratify PCa risk or select for personalised therapeutic strategies is an ultimate aim.

The rodent prostate provides an ideal model system to explore the properties of PrSCs, due to the persistence of androgen-independent cells upon castration, and these cells may contribute to treatment failure and the development of CRPC. The use of primary tissue culture allows the prospective isolation and purification of prostate epithelial cells that can demonstrate stem-like properties *in vitro* and *in vivo*. By developing an understanding of PrSC biology and the mechanisms that govern self-renewal, it is hoped that new therapeutic agents targeted at killing the PrSC can prevent CRPC, the fatal form of disease.

Beta-catenin ($PBCre4^{+}Catnb^{+/lox(ex3)}$) and PTEN ($PBCre4^{+}Pten^{flox}$) single mutant mice demonstrated activation of their own and other cell signalling pathways, highlighting the importance of synergy between them in prostate tumourigenesis. Previous studies have shown that Kras single mutant ($PBCre4^{+}Kras^{+/V12}$) mice develop non-lethal PIN lesions, and do not progress to adenocarcinoma (Pearson et al., 2009, Mulholland et al., 2012); therefore these mice were not studied further in this thesis.

Work in this thesis demonstrates that dominant stabilisation of β-catenin promotes progression from HGPIN with keratinising squamous metaplasia at 100 days, to lethal prostate tumours consistent with adenocarcinoma. As expected, these tumours demonstrate activated Wnt signalling, as shown by the upregulation of nuclear β-catenin, and CD44. They also reveal simultaneous activation of the PI3K/Akt/mTOR, and Ras/MAPK signalling pathways. Mechanisms for β-catenin-dependent upregulation of PI3K/Akt/mTOR and Ras/MAPK signalling are not well understood, and the manner by which this may occur has been speculated in this study following a review of the literature.

Activation of PI3K/Akt/mTOR signalling in β-catenin mutants may result from the upregulation of Wnt effectors c-myc and cyclinD1, both of which are capable of triggering the cell cycle and metabolic reprogramming. This postulated mechanism is expanded upon in figure 52, however it may ultimately result in elevated PI3K/AKT/mTOR signalling at, or downstream of, Akt. This hypothesis will be addressed with further IHC for other Wnt effectors such as c-myc, cyclinD1, MMP-7, Foxa1, and COX-2, along with qRT-PCR and western blotting for the respective molecules in both pathways.

Previous studies in colorectal cancer have linked Wnt pathway activation to increased Ras/MAPK signalling *in vitro* and *in vivo*, with evidence of synergy at the β-catenin/Tcf4-mediated gene expression level (Park et al., 2006), and multiple levels including β-catenin-independent direct signalling resulting from increased Wnt 3a ligand levels and β-catenin/Tcf-4-dependent post-gene transcriptional events (Yun et al., 2005). This has been corroborated by findings in this thesis, wherein the MAPK proteins Mek and Erk were over-expressed in the presence of dominant stabilisation of β-catenin. These findings however contrast with those of others (Pearson et al., 2009), whereby MAPK signalling was detected at normal levels in the prostate tumours of β-catenin single mutant mice.

Pten-deficient prostate tumours were characterised by the upregulation of PI3K/Akt/mTOR signalling, and the unexpected synchronous activation of Wnt, and MAPK signalling.

Prostate tumours in which PTEN was deleted (PBCre4^{+}Pten^{flox}) demonstrated evidence of upregulated nuclear β-catenin and CD44 expression. This suggests activated Wnt signalling but expression of these proteins was inconsistent and possible reasons why have been discussed. Further work to clarify whether synergy occurs at the level of GSK3β, or β-catenin, is ongoing at the time of writing. In addition to analysing more PTEN-null prostate tumour samples, future experiments should include IHC for GSK3β if a suitable primary antibody is commercially available, along with IHC of downstream post-transcriptional targets to verify upregulated Wnt signalling. They include c-myc, cyclinD1, MMP-7, Foxa1, and COX-2. As antigen expression may be heterogeneous in these tumours (as already identified), a technique such as laser-capture microdissection may allow qRT-PCR and/or western blotting to compare areas of nuclear (activated) β-catenin localisation or activated Wnt signalling, with areas of membranous (wild-type) β-catenin localisation or inactive Wnt signalling in PTEN-null (PBCre4^{+}Pten^{flox}) tumours.

These tumours also demonstrated Pten-loss-dependent activation of MAPK signalling, which has not previously been reported. Again given that numbers were low, it is hoped that this notion will be strengthened when current cohorts of PBCre4^{+}Pten^{flox} mice age. Mechanisms to explain this synergy have not been explored in this work, but evidence for crosstalk is supported by other animal models, claiming that the MAPK pathway through Ras is PI3K/Akt/mTOR-dependent and that aberrant PI3K/Akt/mTOR signalling drives Raf/Mek/Erk activation. Despite these findings, the manner by which these interactions occur is complex and remains uncharacterised in the scientific literature.

Simultaneous cooperating mutations in the Wnt, PI3K/Akt/mTOR, and Ras/MAPK pathways were seen to significantly reduce survival due to PCa. Upon constitutive activation of all three pathways, mice failed to survive beyond three months due to high grade, locally-advanced non-metastatic tumours. Mice bearing double mutations demonstrate reduced survival, but for reasons outlines earlier, more mice will need to be investigated to address whether or not these findings are statistically significant. In spite of this obvious limitation, this thesis provides sufficient evidence to conclude that Wnt, PI3K/Akt/mTOR, and Ras/MAPK signalling synergise in the prostate to promote tumourigenesis and disease progression.

This thesis demonstrates that the molecular profile of PCa progression in these mouse models parallels the human disease. There is upregulation of AR, and Ki67, along with down-regulation and eventual loss of p63 concomitant with tumour grade.

The *in vivo* cooperation between the Wnt, PI3K/Akt/mTOR, and Ras/MAPK pathways, when mutated in combination, demonstrates synergistic overexpression of AR compared with single mutants, which in turn express a significantly higher level of AR expression than wild-type prostate. The development of CRPC is not commonly associated with the loss of AR expression, and so these models may also in time be shown as a sound platform through which to investigate CRPC, given that only a modest increase in AR mRNA is both necessary and sufficient for progression to CRPC in mouse models (Chen et al., 2004a).

Data in this thesis provide evidence for the inclusion of Ki67 when diagnosing PCa due to its clear correlation with DNA damage, and disease stage and grade. However its adoption as a diagnostic adjunct has suffered from badly designed studies that have hampered its widespread clinical adoption.

Loss of p63 expression is a hallmark of human PCa, which is associated with luminal cell differentiation. Total loss of p63 expression was seen in high grade tumours in these mouse models, with very low levels in low grade tumours and PIN, reflecting the human disease.

When transmitted paternally, the PBCre4 transgene reliably demonstrated genetic manipulation of target alleles in murine prostate epithelium. The data published in this thesis supports the work of others (Wu et al., 2001, Birbach, 2013), wherein paternally inherited loxP-flanked alleles are inefficiently recombined by maternal PBCre4. The introduction of mosaic genetic deletion led to contamination of the mouse colony with dilution and eventual loss of the PBCre4 transgene. As such, experiments deemed essential to this thesis were unfortunately delayed, and as a result prevented full population of survival cohorts, and similarly prevented FACS of mutant prostates to evaluated SC/CSC biology as outlined in the thesis aims and objectives (see chapter 2).

Tumours in combinatorial mutants appeared morphologically similar to Gleason pattern 4, when compared with lower-grade tumours from single mutant mice, which appeared largely akin to Gleason pattern 3. However, there were limitations identified during histological characterisation that limit the widespread use of Gleason grading in mouse models; for some lower-grade lesions, the Gleason pattern was seen to be evolving, rather than the cytological morphology. A lesion was deemed to be PIN in the absence of invasion, but when stromal invasion was evident, irrespective of the degree of invasion, one was obliged to grade the invasive element rather than the bulk of *in situ* tumour. As explained earlier in the general introduction, murine prostate lobes are encased in thin stroma that is not comparable to the dense fibromuscular stroma of the human. All cases were reviewed by Dr David Griffiths, a consultant histopathologist, and in several cases single cells were seen to be invading the surrounding scanty stromal tissue in the absence of high grade *in situ* tumour. The presence of high grade *in situ* tumour with single cells invading stroma is pathognomonic of Gleason pattern 5. Only descriptions of invasive pattern 3 or 4 (low- or high grade) were used in this thesis, but herein lies the difficulty in extrapolating Gleason pattern 5 to mouse models of prostate cancer.

Deregulation of the Wnt, PI3K/Akt/mTOR and Ras/MAPK pathways have all been identified as playing important roles in human prostate cancer, but the interplay between them has been

largely unmodelled. This thesis is the first to explore crosstalk between these three influential signal transduction pathways simultaneously in mouse models of prostate tumourigenesis.

Appreciating the molecular consequences of critical mutations in human PCa will prove valuable for tailoring treatment depending on a tumour's genetic background. This principle forms the basis of personalised medicine; a priority for the management of solid cancers such as breast, bowel, lung, prostate, ovary and melanoma through many worldwide strategies. The Medical Research Council/National Institute of Health Research-funded Stratified Medicine Initiative is one example of such a programme in the UK. To this end, and following on from experiments in this thesis, a human PCa tissue microarray (TMA) has been created from a tissue repository at the Wales Cancer Bank to determine whether or not the consequences of mutations in the Wnt, PI3K/Akt/mTOR and Ras/MAPK pathways seen in these mouse models are relevant to the human disease. The oncogenomics of archived PCa samples will be explored using either standard pyrosequencing or next generation DNA sequencing, and pathway expression profiles will be determined using IHC as in this study. Findings can then be analysed against disease-specific clinical outcomes to define any correlation, in the hope of identifying further biomarkers for PCa that may help to identify men with aggressive disease, or stratify risk. It is currently not known whether or not activating mutations of *CTNNB1*, *KRAS*, and/or *PTEN* occur in combination in human PCa, but future work will aim to address this research question.

Drugs used in combination with ADT are increasingly being investigated in an effort to circumvent the adaptive capacity of PCa cells, and the failure of current regimen to overcome CRPC. Different approaches include targeting the same pathway at different levels (vertical combinations) or aiming for different pathways synchronously (horizontal combinations). If studies following on from this thesis similarly identify that the Wnt, PI3K/Akt/mTOR and Ras/MAPK are synchronously deregulated in human PCa, future experiments could be aimed at targeting PCa *in vivo* using the horizontal approach. The data contained in this thesis emphasise that multiple signalling pathways synergise within the same prostate tumour, and for this reason, current strategies for the treatment of PCa may be fundamentally flawed.

The primary tissue culture assay verified in this thesis allows a population of cells with stem-like characteristics that can be isolated using the antigenic profile $Lin^{-}CD49f^{+}Sca1^{+}Trop2^{Hi}$, to be maintained and expanded through multiple rounds of passage *in vitro*. In contrast, other

subpopulations defined by FACS, namely not CD49f/Sca1^{+}, and Trop2^{Lo} cells, demonstrated notably attenuated self-renewal. Furthermore, Trop2^{Hi} PrSCs were seen to possess a basal expression profile at IHC (i.e. p63^{+} CK5^{+} AR^{-} CK8^{-} CK18^{-}), suggesting they remain largely undifferentiated following multiple rounds of passage. Further proof that Trop2^{Hi} cells remain undifferentiated following passage will be addressed by re-staining single cells post-passage for the same antigenic profile and re-sorting them using FACS. It is anticipated that cells will tightly cluster in the Trop2^{Hi} region if they retain stem-like characteristics, similar to the appearance of immortalised cell lines that are truly clonal.

Despite these promising results, further data to verify the notion that Lin^{-}CD49f^{+}Sca1^{+}Trop2^{Hi} prostate epithelial cells are PrSCs are required. Ideally, evidence demonstrating the ability of these cells to differentiate and repopulate all cell types of the normal prostate, along with the ability to self-renew *in vivo*, would be confirmatory.

If CSCs originate from malignant transformation of a normal PrSC, then it stands to reason that they may share antigenic profiles (Ginestier et al., 2007, Malanchi et al., 2008). To this end, this thesis aimed to determine whether alteration of the genetic background of a prostate tumour, by utilising the mouse models of PCa outlined in chapter 4, altered the size of the pool of PrSCs, or enhanced their ability to display self-renewal *in vitro*. Unfortunately due to time constraints, and eventual loss of the PBCre4 transgene, experiments thought to be achievable at the outset were not performed. However, the initial data reported in this study have formed the basis of successful grant awards from Prostate Cancer UK, and The Urology Foundation, which will enable future work to continue.

Primary 3D tissue culture proved to be technically challenging due to time constraints, the size of the murine prostate and thus the low yield of PrSCs, and the expense of failed experiments. In spite of this, efforts were made to increase efficiency where possible. For example, rather than performing the whole technique in one day, it was noted that survival was not adversely affected by overnight digestion, and furthermore cellular yield was actually improved. It will be interesting to discover how genetically modified prostate epithelial cells stand up to the stresses of this assay, given that the cell viability of combinatorial mutant mice after digestion into single cells was significantly reduced prior to sorting (see figure 63). Intuitively both the

length of time and the cost of each experiment improved alongside operator experience, and should continue to do so in future.

To date, the main criticism of stem cell assays has been that many have failed to avoid differentiation. It is felt that this phenomenon may be alleviated by culturing SCs in 3D using Matrigel, as utilised in this thesis, because this method more accurately mimics the tumour microenvironment in support of clonal outgrowth (Sato et al., 2011, Pastrana et al., 2011). Further experiments using time lapse photography may allow visualisation of developing prostate spheres in order to determine whether they occur due to cellular aggregation, or whether they are truly clonal, capable of growth from single cells. There is evidence to support both notions, but this question may be answered by linear regression analysis when PrSCs are plated at lower densities, and as single cells. The resultant prostate spheres can then be quantified using automatic plate readers with parameters set to detect only spheres of agreed dimensions, rather than counting by hand.

Thesis Summary

Mouse models continue to play a pivotal role in the study of the molecular events that surround PCa initiation, as well as providing pre-clinical platforms for testing novel therapeutic agents tailored to a tumour's genetic background. Models such as those developed in this thesis, which reflect features of the human disease, may prove valuable if the same profile of mutations and their molecular consequences are validated in human PCa. The discovery of biomarkers aimed at identifying aggressive disease and stratifying PCa risk may be achievable following these experiments.

In opposition to the conventional stochastic model of tumour development, there is evidence to support the CSC theory in PCa. Indeed given that CSCs are hypothesised to survive in a castrate environment they may be resistant to ADT, which remains the cornerstone of treatment for advanced PCa, and responsible for treatment failure and ultimately CRPC. As such, efforts to culture PrSCs/CSCs and learn of their self-renewal properties may aid development of more sophisticated treatments for advanced PCa. This thesis goes some way to appreciating the function of normal PrSCs as a baseline comparator of CSCs from mouse models of prostate tumourigenesis that display deregulation of the Wnt, PI3K/Akt/mTOR, and/or Ras/MAPK pathways in due course.

References

ABATE-SHEN, C., BANACH-PETROSKY, W. A., SUN, X., ECONOMIDES, K. D., DESAI, N., GREGG, J. P., BOROWSKY, A. D., CARDIFF, R. D. & SHEN, M. M. 2003. Nkx3.1; Pten mutant mice develop invasive prostate adenocarcinoma and lymph node metastases. *Cancer Res,* 63**,** 3886-90.

ABDULKADIR, S. A., MAGEE, J. A., PETERS, T. J., KALEEM, Z., NAUGHTON, C. K., HUMPHREY, P. A. & MILBRANDT, J. 2002. Conditional loss of Nkx3.1 in adult mice induces prostatic intraepithelial neoplasia. *Mol Cell Biol,* 22**,** 1495-503.

ABERLE, H., BAUER, A., STAPPERT, J., KISPERT, A. & KEMLER, R. 1997. beta-catenin is a target for the ubiquitin-proteasome pathway. *EMBO J,* 16**,** 3797-804.

AHMAD, I., MORTON, J. P., SINGH, L. B., RADULESCU, S. M., RIDGWAY, R. A., PATEL, S., WOODGETT, J., WINTON, D. J., TAKETO, M. M., WU, X. R., LEUNG, H. Y. & SANSOM, O. J. 2011. beta-Catenin activation synergizes with PTEN loss to cause bladder cancer formation. *Oncogene,* 30**,** 178-89.

AL-HAJJ, M., WICHA, M. S., BENITO-HERNANDEZ, A., MORRISON, S. J. & CLARKE, M. F. 2003. Prospective identification of tumorigenic breast cancer cells. *Proc Natl Acad Sci USA,* 100**,** 3983-3988.

ALBERTSEN, P. C., HANLEY, J. A. & FINE, J. 2005. 20-year outcomes following conservative management of clinically localized prostate cancer. *JAMA,* 293**,** 2095-101.

ALESSI, D. R., KOZLOWSKI, M. T., WENG, Q. P., MORRICE, N. & AVRUCH, J. 1998. 3-Phosphoinositide-dependent protein kinase 1 (PDK1) phosphorylates and activates the p70 S6 kinase in vivo and in vitro. *Curr Biol,* 8**,** 69-81.

AMIN, M. B., SCHULTZ, D. S. & ZARBO, R. J. 1994. Analysis of cribriform morphology in prostatic neoplasia using antibody to high-molecular-weight cytokeratins. *Arch Pathol Lab Med,* 118**,** 260-4.

ANAI, S., GOODISON, S., SHIVERICK, K., ICZKOWSKI, K., TANAKA, M. & ROSSER, C. J. 2006. Combination of PTEN gene therapy and radiation inhibits the growth of human prostate cancer xenografts. *Hum Gene Ther,* 17**,** 975-84.

ANDREYEV, H. J., NORMAN, A. R., CUNNINGHAM, D., OATES, J. R. & CLARKE, P. A. 1998. Kirsten ras mutations in patients with colorectal cancer: the multicenter "RASCAL" study. *J Natl Cancer Inst,* 90**,** 675-684.

ANTONARAKIS, E. S. & EISENBERGER, M. A. 2011. Expanding treatment options for metastatic prostate cancer. *N Engl J Med,* 364**,** 2055-8.

AUS, G., ABRAHAMSSON, P. A., AHLGREN, G., HUGOSSON, J., LUNDBERG, S., SCHAIN, M., SCHELIN, S. & PEDERSEN, K. 2002. Three-month neoadjuvant hormonal therapy before radical prostatectomy: a 7-year follow-up of a randomized controlled trial. *BJU Int,* 90**,** 561-6.

AXELROD, J. D., MILLER, J. R., SHULMAN, J. M., MOON, R. T. & PERRIMON, N. 1998. Differential recruitment of Dishevelled provides signaling specificity in the planar cell polarity and Wingless signalling pathways. *Genes Dev,* 12**,** 2610-2622.

AZIM, A. A., FAYAD, S., FATTAH, A. A. & HABEIB, M. 1978. Immunologic studies of male infertility. *Fertil Steril,* 30**,** 426-9.

BABCHIA, N., CALIPEL, A., MOURIAUX, F., FAUSSAT, A. M. & MASCARELLI, F. 2010. The PI3K/Akt and mTOR/P70S6K signaling pathways in human uveal melanoma cells: interaction with B-Raf/ERK. *Invest Ophthalmol Vis Sci,* 51**,** 421-9.

BAERT, L. V., GOERTHUYS, H. J. & DERIDDER, D. J. 1998. Neo-adjuvant treatment before radical prostatectomy decreases the number positive surgical margins in CT2-T3 but has no impact on PSA progression or survival in CT2-T3. *J Urol,* 159**,** 61.

BALKWILL, F. 2004. Cancer and the chemokine network. *Nat Rev Cancer,* 4**,** 540-50.

BARBIERI, C. E., BARTON, C. E. & PIETENPOL, J. A. 2003. Delta Np63 alpha expression is regulated by the phosphoinositide 3-kinase pathway. *J Biol Chem,* 278**,** 51408-14.
BARBIERI, C. E. & PIETENPOL, J. A. 2006. p63 and epithelial biology. *Exp Cell Res,* 312**,** 695-706.
BARKER, N., ET AL. 2009. Crypt stem cells as the cells-of-origin of intestinal cancer. *Nature Cell Biol,* 457**,** 608-611.
BARRIOS, R., LEBOVITZ, R. M. & WISEMAN, A. L., ET AL. 1996. RasT24 driven by a probasin promoter induces prostatic hyperplasia in transgenic mice. *Trangenics,* 2**,** 23-8.
BARTHELEMY, C., KHALFOUN, B., GUILLAUMIN, J. M., LECOMTE, P. & BARDOS, P. 1988. Seminal fluid transferrin as an index of gonadal function in men. *J Reprod Fert,* 82**,** 113-118.
BEDOLLA, R., PRIHODA, T. J., KREISBERG, J. I., MALIK, S. N., KRISHNEGOWDA, N. K., TROYER, D. A. & GHOSH, P. M. 2007. Determining risk of biochemical recurrence in prostate cancer by immunohistochemical detection of PTEN expression and Akt activation. *Clin Cancer Res,* 13**,** 3860-7.
BEERLAGE, H. P., THUROFF, S., MADERSBACHER, S., ZLOTTA, A. R., AUS, G., DE REIJKE, T. M. & DE LA ROSETTE, J. J. 2000. Current status of minimally invasive treatment options for localized prostate carcinoma. *Eur Urol,* 37**,** 2-13.
BEHRENS, J., VON KRIES, J. P., KUHL, M., BRUHN, L., WEDLICH, D., GROSSCHEDL, R. & BIRCHMEIER, W. 1996. Functional interaction of beta-catenin with the transcription factor LEF-1. *Nature Methods,* 382**,** 638-642.
BELLACOSA, A., DE FEO, D. & GODWIN, A. K. E. A. 1995. Molecular alterations of the AKT2 oncogene in ovarian and breast carcinomas. *Int J Cancer,* 64**,** 280-5.
BERARDI, A. C., WANG, A., LEVINE, J. D., LOPEZ, P. & SCADDEN, D. T. 1995. Functional isolation and characterization of human hematopoietic stem cells. *Science,* 267**,** 104-8.
BERNEY, D. M., GOPALAN, A., KUDAHETTI, S., FISHER, G., AMBROISINE, L., FOSTER, C. S., REUTER, V., EASTHAM, J., MOLLER, H., KATTAN, M. W., GERALD, W., COOPER, C., SCARDINO, P. & CUZICK, J. 2009. Ki-67 and outcome in clinically localised prostate cancer: analysis of conservatively treated prostate cancer patients from the Trans-Atlantic Prostate Group study. *Br J Cancer,* 100**,** 888-93.
BERRY, P. A., MAITLAND, N. J. & COLLINS, A. T. 2008. Androgen receptor signalling in prostate: effects of stromal factors on normal and cancer stem cells. *Mol Cell Endocrinol,* 288**,** 30-7.
BIENZ, M. & CLEVERS, H. 2000. Linking colorectal cancer to Wnt signaling. *Cell,* 103**,** 311-320.
BIERIE, B., NOZAWA, M., RENOU, J. P., SHILLINGFORD, J. M., MORGAN, F., OKA, T., TAKETO, M. M., CARDIFF, R. D., MIYOSHI, K., WAGNER, K. U., ROBINSON, G. W. & HENNIGHAUSEN, L. 2003. Activation of beta-catenin in prostate epithelium induces hyperplasias and squamous transdifferentiation. *Oncogene,* 22**,** 3875-87.
BIRBACH, A. 2013. Use of PB-Cre4 mice for mosaic gene deletion. *PLoS One,* 8**,** e53501.
BISMAR, T. A., HUMPHREY, P. A., GRIGNON, D. J. & WANG, H. L. 2004. Expression of beta-catenin in prostatic adenocarcinomas: a comparison with colorectal adenocarcinomas. *Am J Clin Pathol,* 121**,** 557-63.
BLANCHER, C., MOORE, J. W., ROBERTSON, N. & HARRIS, A. L. 2001. Effects of ras and von Hippel-Lindau (VHL) gene mutations on hypoxia-inducible factor (HIF)-1αl, HIF 2α, and vascular endothelial growth factor expression and their regulation by the phosphatidylinositol 3 kinase/Akt signaling pathway. *Cancer Res,* 61**,** 7349-7355.
BLANPAIN, C., HORSLEY, V. & FUCHS, E. 2007. Epithelial stem cells: turning over new leaves. *Cell,* 128**,** 445-458.
BLUME-JENSEN, P. & HUNTER, T. 2001. Oncogenic kinase signalling. *Nature,* 411**,** 355-65.
BOLLA, M., COLLETTE, L., BLANK, L., WARDE, P., DUBOIS, J. B., MIRIMANOFF, R. O., STORME, G., BERNIER, J., KUTEN, A., STERNBERG, C., MATTELAER, J., LOPEZ-TORECILLA, J., PFEFFER, J. R., LINO-CUTAJAR, C., ZURLO, A. & PIERART, M. 2002. Long-term results with immediate androgen suppression and external irradiation in patients with locally advanced prostate cancer (an EORTC study): a phase III randomised trial. *Lancet,* 360 103 - 6.

BOLLA, M., GONZALEZ, D., WARDE, P., DUBOIS, J. B., MIRIMANOFF, R. O., STORME, G., BERNIER, J., KUTEN, A., STERNBERG, C., GIL, T., COLLETTE, L. & PIERART, M. 1997. Improved survival in patients with locally advanced prostate cancer treated with radiotherapy and goserelin. *N Engl J Med,* 337**,** 295 - 300.

BOLLA, M., VAN POPPEL, H., COLLETTE, L., VAN CANGH, P., VEKEMANS, K., DA POZZO, L., DE REIJKE, T. M., VERBAEYS, A., BOSSET, J. F., VAN VELTHOVEN, R., MARECHAL, J. M., SCALLIET, P., HAUSTERMANS, K., PIERART, M., EUROPEAN ORGANIZATION FOR, R. & TREATMENT OF, C. 2005. Postoperative radiotherapy after radical prostatectomy: a randomised controlled trial (EORTC trial 22911). *Lancet,* 366**,** 572-8.

BOLLA, M., VAN POPPEL, H., TOMBAL, B., VEKEMANS, K., DA POZZO, L., DE REIJKE, T. M., VERBAEYS, A., BOSSET, J. F., VAN VELTHOVEN, R., COLOMBEL, M., VAN DE BEEK, C., VERHAGEN, P., VAN DEN BERGH, A., STERNBERG, C., GASSER, T., VAN TIENHOVEN, G., SCALLIET, P., HAUSTERMANS, K., COLLETTE, L., EUROPEAN ORGANISATION FOR, R., TREATMENT OF CANCER, R. O. & GENITO-URINARY, G. 2012. Postoperative radiotherapy after radical prostatectomy for high-risk prostate cancer: long-term results of a randomised controlled trial (EORTC trial 22911). *Lancet,* 380**,** 2018-27.

BONKHOFF, H., FIXEMER, T. & REMBERGER, K. 1998. Relation between Bcl-2, cell proliferation, and the androgen receptor status in prostate tissue and precursors of prostate cancer. *Prostate,* 34**,** 251-8.

BONKHOFF, H. & REMBERGER, K. 1993. Widespread distribution of nuclear androgen receptors in the basal cell layer of the normal and hyperplastic human prostate. *Virchows Arch A Pathol Anat Histopathol,* 422**,** 35-8.

BONKHOFF, H. & REMBERGER, K. 1996. Differentiation pathways and histogenetic aspects of normal and abnormal prostatic growth: a stem cell model. *Prostate Cancer Prostatic Dis,* 28**,** 98-106.

BONKHOFF, H., STEIN, U. & REMBERGER, K. 1994. The proliferative function of basal cells in the normal and hyperplastic human prostate. *Prostate,* 24**,** 114-8.

BONKHOFF, H., STEIN, U. & REMBERGER, K. 1995. Endocrine-paracrine cell types in the prostate and prostatic adenocarcinoma are postmitotic cells. *Hum Pathol,* 26**,** 167-70.

BONKHOFF, H., WERNERT, N., DHOM, G. & REMBERGER, K. 1991. Relation of endocrine-paracrine cells to cell proliferation in normal, hyperplastic, and neoplastic human prostate. *Prostate,* 19**,** 91-8.

BOS, J. L., REHMANN, H. & WITTINGHOFER, A. 2007. GEFs and GAPs: Critical Elements in the Control of Small G Proteins. *Cell,* 129**,** 865-877.

BOSTWICK, D. G., PACELLI, A. & LOPEZ-BELTRAN, A. 1996. Molecular biology of prostatic intraepithelial neoplasia. *Prostate,* 29**,** 117-34.

BOUTROS, M., MIHALY, J., BOUWMEESTER, T. & MLODZIK, M. 2000. Signaling specificity by Frizzled receptors in Drosophila. *Science,* 288**,** 1825-1828.

BRAY, F., LORTET-TIEULENT, J., FERLAY, J., FORMAN, D. & AUVINEN, A. 2010. Prostate cancer incidence and mortality trends in 37 European countries: an overview. *Eur J Cancer,* 46**,** 3040-52.

BRUXVOORT, K. J., CHARBONNEAU, H. M., GIAMBERNARDI, T. A., GOOLSBY, J. C., QIAN, C. N., ZYLSTRA, C. R., ROBINSON, D. R., ROY-BURMAN, P., SHAW, A. K., BUCKNER-BERGHUIS, B. D., SIGLER, R. E., RESAU, J. H., SULLIVAN, R., BUSHMAN, W. & WILLIAMS, B. O. 2007. Inactivation of Apc in the mouse prostate causes prostate carcinoma. *Cancer Res,* 67**,** 2490-6.

BURGER, P. E., XIONG, X., COETZEE, S., SALM, S. N., MOSCATELLI, D., GOTO, K. & WILSON, E. L. 2005. Sca-1 expression identifies stem cells in the proximal region of prostatic ducts with high capacity to reconstitute prostatic tissue. *Proc Natl Acad Sci U S A,* 102**,** 7180-5.

BURMER, G. C., RABINOVITCH, P. S. & LOEB, L. A. 1991. Frequency and spectrum of c-Ki-ras mutations in human sporadic colon carcinoma, carcinomas arising in ulcerative colitis, and pancreatic adenocarcinoma. *Environ Health Perspect,* 93**,** 27-31.

BURRELL, R. A., MCGRANAHAN, N., BARTEK, J. & SWANTON, C. 2013. The causes and consequences of genetic heterogeneity in cancer evolution. *Nature,* 501**,** 338-45.

CADIGAN, K. M. & NUSSE, R. 1997. Wnt signaling: a common theme in animal development. *Genes Dev,* 11**,** 3286-305.

CAIRNS, P., OKAMI, K., HALACHMI, S., HALACHMI, N., ESTELLER, M., HERMAN, J. G., JEN, J., ISAACS, W. B., BOVA, G. S. & SIDRANSKY, D. 1997. Frequent inactivation of PTEN/MMAC1 in primary prostate cancer. *Cancer Res,* 57**,** 4997-5000.

CANALE, D., BARTELLONI, M., NEGRONI, A., MESCHINI, P., IZZO, P. L., BIANCHI, B. & MENCHINI-FABRIS, G. F. 1986. Zinc in human semen. *Int J Androl,* 9**,** 477-80.

CAPPELLO, A. R., GUIDO, C., SANTORO, A., SANTORO, M., CAPOBIANCO, L., MONTANARO, D., MADEO, M., ANDO, S., DOLCE, V. & AQUILA, S. 2012. The mitochondrial citrate carrier (CIC) is present and regulates insulin secretion by human male gamete. *Endocrinology,* 153**,** 1743-54.

CAREY, A. M., PRAMANIK, R., NICHOLSON, L. J., DEW, T. K., MARTIN, F. L., MUIR, G. H. & MORRIS, J. D. 2007. Ras-MEK-ERK signaling cascade regulates androgen receptor element-inducible gene transcription and DNA synthesis in prostate cancer cells. *Int J Cancer,* 121**,** 520-7.

CARTER, B. S., EPSTEIN, J. I. & ISAACS, W. B. 1990. ras gene mutations in human prostate cancer. *Cancer Res,* 50**,** 6830-2.

CARVER, B. S., CHAPINSKI, C., WONGVIPAT, J., HIERONYMUS, H., CHEN, Y., CHANDARLAPATY, S., ARORA, V. K., LE, C., KOUTCHER, J., SCHER, H., SCARDINO, P. T., ROSEN, N. & SAWYERS, C. L. 2011. Reciprocal feedback regulation of PI3K and androgen receptor signaling in PTEN-deficient prostate cancer. *Cancer Cell,* 19**,** 575-86.

CARVER, B. S., TRAN, J., GOPALAN, A., CHEN, Z., SHAIKH, S., CARRACEDO, A., ALIMONTI, A., NARDELLA, C., VARMEH, S., SCARDINO, P. T., CORDON-CARDO, C., GERALD, W. & PANDOLFI, P. P. 2009. Aberrant ERG expression cooperates with loss of PTEN to promote cancer progression in the prostate. *Nat Genet,* 41**,** 619-24.

CASTANO, J., RAURELL, I., PIEDRA, J. A., MIRAVET, S., DUNACH, M. & GARCIA DE HERREROS, A. 2002. B-catenin N- and C-terminal tails modulate the coordinated binding of adherens junction proteins to β-catenin. *J Biol Chem,* 277**,** 31541-31550.

CASTELLANO, E. & DOWNWARD, J. 2011. RAS Interaction with PI3K: More Than Just Another Effector Pathway. *Genes Cancer,* 2**,** 261-74.

CATALONA, W. J. 2012. Words of wisdom. Re: Radical prostatectomy versus observation for localized prostate cancer. *Eur Urol,* 62**,** 1195.

CAVALLO, R. A., COX, R. T., MOLINE, M. M., ROOSE, J., POLEVOY, G. A., CLEVERS, H., PEIFER, M. & BEJSOVEC, A. 1998. Drosophila Tcf and Groucho interact to repress Wingless signalling activity. *Nature Methods***,** 604-608.

CHALHOUB, N. & BAKER, S. J. 2009. PTEN and the PI3-kinase pathway in cancer. *Annu Rev Pathol,* 4**,** 127-50.

CHANG, W. Y. & PRINS, G. S. 1999. Estrogen receptor-beta: implications for the prostate gland. *Prostate,* 40**,** 115-24.

CHEN, C. D., WELSBIE, D. S., TRAN, C., BAEK, S. H., CHEN, R., VESSELLA, R., ROSENFELD, M. G. & SAWYERS, C. L. 2004a. Molecular determinants of resistance to antiandrogen therapy. *Nat Med,* 10**,** 33-9.

CHEN, G., FERNANDEZ, J., MISCHE, S. & COUREY, A. J. 1999. A functional interaction between the histone deacetylase Rpd3 and the co-repressor groucho in Drosophila development. *Genes Dev,* 13**,** 2218-2230.

CHEN, G., SHUKEIR, N., POTTI, A., SIRCAR, K., APRIKIAN, A., GOLTZMAN, D. & RABBANI, S. A. 2004b. Up-regulation of Wnt-1 and beta-catenin production in patients with advanced metastatic prostate carcinoma: potential pathogenetic and prognostic implications. *Cancer,* 101**,** 1345-56.

CHEN, M. S., WOODWARD, W. A., BEHBOD, F., PEDDIBHOTLA, S., ALFARO, M. P., BUCHHOLZ, T. A. & ROSEN, J. M. 2007. Wnt/beta-catenin mediates radiation resistance of Sca1+ progenitors in an immortalized mammary gland cell line. *J Cell Sci,* 120**,** 468-77.

CHEN, S. & PAUCHA, E. 1990. Identification of a region of simian virus 40 large T antigen required for cell transformation. *J Virol,* 64**,** 3350-7.

CHENG, J. Q., RUGGERI, B. & KLEIN, W. M. E. A. 1996. Amplification of AKT2 in human pancreatic cells and inhibition of AKT2 expression and tumorigenicity by antisense RNA. *Proc Natl Acad Sci USA,* 93**,** 3636-41.

CHESIRE, D. R., EWING, C. M., GAGE, W. R. & ISAACS, W. B. 2002. In vitro evidence for complex modes of nuclear beta-catenin signaling during prostate growth and tumorigenesis. *Oncogene,* 21**,** 2679-94.

CHESIRE, D. R., EWING, C. M., SAUVAGEOT, J., BOVA, G. S. & ISAACS, W. B. 2000. Detection and analysis of beta-catenin mutations in prostate cancer. *Prostate,* 45**,** 323-34.

CHIAVEROTTI, T., COUTO, S. S., DONJACOUR, A. A., MAO, J. H., NAGASE, H., CARDIFF, R. D., CUNHA, G. R. & BALMAIN, A. 2008. Dissociation of epithelial and neuroendocrine carcinoma lineages in the transgenic adenocarcinoma of mouse prostate model of prostate cancer. *Am J Pathol,* 172**,** 236-46.

CHIBA, S. 2006. Notch signaling in stem cell systems. *Stem Cells,* 24**,** 2437-47.

CHIN, L., TAM, A., POMERANTZ, J., WONG, M., HOLASH, J., BARDEESY, N. & SHEN, Q., ET AL. 1999. Essential role for oncogenic Ras in tumour maintenance. *Nature,* 400**,** 468-472.

CHOI, N., ZHANG, B., ZHANG, L., ITTMANN, M. & XIN, L. 2012. Adult murine prostate basal and luminal cells are self-sustained lineages that can both serve as targets for prostate cancer initiation. *Cancer Cell,* 21**,** 253-65.

CLARK, C. E., ET AL. 2007. Dynamics of the immune reaction to pancreatic cancer from inception to invasion. *Cancer Res,* 67**,** 9518-9527.

CLEVERS, H. 2006. Wnt/beta-catenin signaling in development and disease. *Cell,* 127**,** 469-80.

COLES-TAKABE, B. L., BRAIN, I., PURPURA, K. A., KARPOWICZ, P., ZANDSTRA, P. W., MORSHEAD, C. M. & VAN DER KOOY, D. 2008. Don't look: growing clonal versus nonclonal neural stem cell colonies. *Stem Cells,* 26**,** 2938-44.

COLLINS, A. T., BERRY, P. A., HYDE, C., STOWER, M. J. & MAITLAND, N. J. 2005. Prospective Identification of Tumorigenic Prostate Cancer Stem Cells. *Cancer Res,* 65 10946-10951.

COLLINS, A. T., HABIB, F. K., MAITLAND, N. J. & NEAL, D. E. 2001. Identification and isolation of human prostate epithelial stem cells based on alpha(2)beta(1)-integrin expression. *J Cell Sci,* 114**,** 3865-72.

CONDORELLI, R. A., LA VIGNERA, S., BELLANCA, S., VICARI, E. & CALOGERO, A. E. 2012. Myoinositol: does it improve sperm mitochondrial function and sperm motility? *Urology,* 79**,** 1290-5.

COUTO, S. S., CAO, M., DUARTE, P. C., BANACH-PETROSKY, W., WANG, S., ROMANIENKO, P., WU, H., CARDIFF, R. D., ABATE-SHEN, C. & CUNHA, G. R. 2009. Simultaneous haploinsufficiency of Pten and Trp53 tumor suppressor genes accelerates tumorigenesis in a mouse model of prostate cancer. *Differentiation,* 77**,** 103-11.

COX, A. D. & DER, C. J. 2003. The dark side of Ras: regulation of apoptosis. *Oncogene* 22**,** 8999-9006.

COX, R. T., PAI, L. M., KIRKPATRICK, C., STEIN, J. & PEIFER, M. 1999. Roles of the C terminus of armadillo in wingless signaling in Drosophila. *Genetics,* 153**,** 319-332.

CRAWFORD, H. C., FINGLETON, B. M., RUDOLPH-OWEN, L. A., GOSS, K. J., RUBINFELD, B., POLAKIS, P. & MATRISIAN, L. M. 1999. The metalloproteinase matrilysin is a target of beta-catenin transactivation in intestinal tumors. *Oncogene,* 18**,** 2883-91.

CRUK. 2012. *Prostate cancer - UK incidence statistics* [Online]. Available: http://info.cancerresearchuk.org/cancerstats/types/prostate [Accessed 01/06/12 2012].

CUNHA, G. R., COOKE, P. S. & KURITA, T. 2004. Role of stromal-epithelial interactions in hormonal responses. *Arch Histol Cytol,* 67**,** 417-34.

CUNHA, G. R., DONJACOUR, A. A., COOKE, P. S., MEE, S., BIGSBY, R. M., HIGGINS, S. J. & SUGIMURA, Y. 1987. The endocrinology and developmental biology of the prostate. *Endocr Rev,* 8**,** 338-62.

CUZICK, J., SWANSON, G. P., FISHER, G., BROTHMAN, A. R., BERNEY, D. M., REID, J. E., MESHER, D., SPEIGHTS, V. O., STANKIEWICZ, E., FOSTER, C. S., MOLLER, H., SCARDINO, P., WARREN, J. D., PARK, J., YOUNUS, A., FLAKE, D. D., 2ND, WAGNER, S., GUTIN, A., LANCHBURY, J. S., STONE, S. & TRANSATLANTIC PROSTATE, G. 2011. Prognostic value of an RNA expression signature derived from cell cycle proliferation genes in patients with prostate cancer: a retrospective study. *Lancet Oncol,* 12**,** 245-55.

D ' AMICO, A. V., CHEN, M. H., RENSHAW, A. A., LOFFREDO, M. & KANTOFF, P. W. 2008. Androgen suppression and radiation vs radiation alone for prostate cancer: a randomized trial. *JAMA,* 299**,** 289 - 95.

DAHIA, P. L. 2000. PTEN, a unique tumor suppressor gene. *Endocr Relat Cancer,* 7**,** 115-29.

DAVIES, E. L. & FULLER, M. T. 2008. Regulation of self-renewal and differentiation in adult stem cell lineages: lessons from the Drosophila male germ line. *Cold Spring Harb Symp Quant Biol,* 73**,** 137-45.

DE BONO, J. S., LOGOTHETIS, C. J., MOLINA, A., FIZAZI, K., NORTH, S., CHU, L., CHI, K. N., JONES, R. J., GOODMAN, O. B., JR., SAAD, F., STAFFURTH, J. N., MAINWARING, P., HARLAND, S., FLAIG, T. W., HUTSON, T. E., CHENG, T., PATTERSON, H., HAINSWORTH, J. D., RYAN, C. J., STERNBERG, C. N., ELLARD, S. L., FLECHON, A., SALEH, M., SCHOLZ, M., EFSTATHIOU, E., ZIVI, A., BIANCHINI, D., LORIOT, Y., CHIEFFO, N., KHEOH, T., HAQQ, C. M., SCHER, H. I. & INVESTIGATORS, C.-A.-. 2011. Abiraterone and increased survival in metastatic prostate cancer. *N Engl J Med,* 364**,** 1995-2005.

DE LA TAILLE, A., RUBIN, M. A., CHEN, M. W., VACHEROT, F., DE MEDINA, S. G., BURCHARDT, M., BUTTYAN, R. & CHOPIN, D. 2003. Beta-catenin-related anomalies in apoptosis-resistant and hormone-refractory prostate cancer cells. *Clin Cancer Res,* 9**,** 1801-7.

DE MARZO, A. M., NELSON, W. G., ISAACS, W. B. & EPSTEIN, J. I. 2003. Pathological and molecular aspects of prostate cancer. *Lancet Oncol,* 361**,** 955-64.

DE MARZO, A. M., NELSON, W. G., MEEKER, A. K. & COFFEY, D. S. 1998. Stem cell features of benign and malignant prostate epithelial cells. *J Urol,* 160**,** 2381-92.

DEPINHO, R. A. 2000. The age of cancer. *Nature,* 408**,** 248-54.

DERMER, G. B. 1978. Basal cell proliferation in benign prostatic hyperplasia. *Cancer,* 41**,** 1857-62.

DI CRISTOFANO, A., DE ACETIS, M., KOFF, A., CORDON-CARDO, C. & PANDOLFI, P. P. 2001. Pten and p27KIP1 cooperate in prostate cancer tumor suppression in the mouse. *Nat Genet,* 27**,** 222-4.

DIGIOVANNI, J., KIGUCHI, K., FRIJHOFF, A., WILKER, E., BOL, D. K., BELTRAN, L., MOATS, S., RAMIREZ, A., JORCANO, J. & CONTI, C. 2000. Deregulated expression of insulin-like growth factor 1 in prostate epithelium leads to neoplasia in transgenic mice. *Proc Natl Acad Sci U S A,* 97**,** 3455-60.

DING, Z., WU, C. J., CHU, G. C., XIAO, Y., HO, D., ZHANG, J., PERRY, S. R., LABROT, E. S., WU, X., LIS, R., HOSHIDA, Y., HILLER, D., HU, B., JIANG, S., ZHENG, H., STEGH, A. H., SCOTT, K. L., SIGNORETTI, S., BARDEESY, N., WANG, Y. A., HILL, D. E., GOLUB, T. R., STAMPFER, M. J., WONG, W. H., LODA, M., MUCCI, L., CHIN, L. & DEPINHO, R. A. 2011. SMAD4-dependent barrier constrains prostate cancer growth and metastatic progression. *Nature,* 470**,** 269-73.

DONG, J. T., LI, C. L., SIPE, T. W. & FRIERSON, H. F., JR. 2001. Mutations of PTEN/MMAC1 in primary prostate cancers from Chinese patients. *Clin Cancer Res,* 7**,** 304-8.

DONG, J. T., SIPE, T. W., HYYTINEN, E. R., LI, C. L., HEISE, C., MCCLINTOCK, D. E., GRANT, C. D., CHUNG, L. W. & FRIERSON, H. F., JR. 1998. PTEN/MMAC1 is infrequently mutated in pT2 and pT3 carcinomas of the prostate. *Oncogene,* 17**,** 1979-82.

DORFF, T. B., FLAIG, T. W., TANGEN, C. M., HUSSAIN, M. H., SWANSON, G. P., WOOD, D. P., JR., SAKR, W. A., DAWSON, N. A., HAAS, N. B., CRAWFORD, E. D., VOGELZANG, N. J., THOMPSON, I. M.

& GLODE, L. M. 2011. Adjuvant androgen deprivation for high-risk prostate cancer after radical prostatectomy: SWOG S9921 study. *J Clin Oncol,* 29**,** 2040-5.
DUBROVSKA, A., KIM, S., SALAMONE, R. J., WALKER, J. R., MAIRA, S. M., GARCIA-ECHEVERRIA, C., SCHULTZ, P. G. & REDDY, V. A. 2009. The role of PTEN/Akt/PI3K signaling in the maintenance and viability of prostate cancer stem-like cell populations. *Proc Natl Acad Sci U S A,* 106**,** 268-73.
ECKLE, V. S., BUCHMANN, A., BURSCH, W., SCHULTE-HERMANN, R. & SCHWARZ, M. 2004. Immunohistochemical detection of activated caspases in apoptotic hepatocytes in rat liver. *Toxicol Pathol,* 32**,** 9-15.
EL SEWEDY, T., FORNARO, M. & ALBERTI, S. 1998. Cloning of the murine TROP2 gene: Conservation of a PIP2-binding sequence in the cytoplasmic domain of TROP-2. *Int J Cancer,* 75**,** 324-330.
ELFIKY, A. A. & JIANG, Z. 2013. kyp. *Curr Cancer Drug Targets,* 13**,** 157-64.
ENGLISH, H. F., DRAGO, J. R. & SANTEN, R. J. 1985. Cellular response to androgen depletion and repletion in the rat ventral prostate: autoradiography and morphometric analysis. *Prostate,* 7**,** 41-51.
ENGLISH, H. F., SANTEN, R. J. & ISAACS, J. T. 1987. Response of glandular versus basal rat ventral prostatic epithelial cells to androgen withdrawal and replacement. *Prostate,* 11**,** 229-42.
EPSTEIN, J. I. 2010. An update of the Gleason grading system. *J Urol,* 183**,** 433-40.
EPSTEIN, J. I., ALLSBROOK JR, W. C., AMIN, M. B. & COMMITTEE, I. G. 2005. The 2005 International Society of Urologic Pathology (ISUP) Consensus Conference on Gleason grading of Prostatic Carcinoma. *Am J Surg Pathol,* 29**,** 1228-42.
EPSTEIN, J. I., PARTIN, A. W., SAUVAGEOT, J. & WALSH, P. C. 1996. Prediction of progression following radical prostatectomy. A multivariate analysis of 721 men with long-term follow-up. *Am J Surg Pathol,* 20**,** 286-92.
EVANS, G. S. & CHANDLER, J. A. 1987. Cell proliferation studies in the rat prostate: II. The effects of castration and androgen-induced regeneration upon basal and secretory cell proliferation. *Prostate,* 11**,** 339-51.
FAHMY, W. E. & BISSADA, N. K. 2003. Cryosurgery for prostate cancer. *Arch Androl,* 49**,** 397-407.
FAIR, W. R. & CORDONNIER, J. J. 1978. The pH of prostatic fluid: a reappraisal and therapeutic implications. *J Urol,* 120**,** 695-8.
FARNIE, G., CLARKE, R. B., SPENCE, K., PINNOCK, N., BRENNAN, K., ANDERSON, N. G. & BUNDRED, N. J. 2007. Novel cell culture technique for primary ductal carcinoma in situ: role of Notch and epidermal growth factor receptor signaling pathways. *J Natl Cancer Inst,* 99**,** 616-27.
FAUSTO, N. 2000. Liver regeneration. *J Hepatol,* 32**,** 19-31.
FEILOTTER, H. E., NAGAI, M. A., BOAG, A. H., ENG, C. & MULLIGAN, L. M. 1998. Analysis of PTEN and the 10q23 region in primary prostate carcinomas. *Oncogene,* 16**,** 1743-8.
FISHER, G. H., ET AL. 2001. Induction and apoptotic regression of lung adenocarcinomas by regulation of a K-Ras transgene in the presence and absence of tumor suppressor genes. *Genes Dev,* 15**,** 3249-3262.
FONG, D., ET AL. 2008. High expression of TROP2 correlates with poor prognosis in pancreatic cancer. *Br J Cancer,* 99**,** 1290-1295.
FORBES, S. A., BINDAL, N., BAMFORD, S., COLE, C., KOK, C. Y. & BEARE, D., ET AL. 2011. COSMIC: mining complete cancer genomes in the Catalogue of Somatic Mutations in Cancer. *Nucleic Acids Res,* 39**,** D945-50. URL: http://cancer.sanger.ac.uk/cancergenome/projects/cosmic/; accessed 26/09/13.
FORNARO, M., DELL'ARCIPRETE, R., STELLA, M., BUCCI, C., NUTINI, M., CAPRI, M. G. & ALBERTI, S. 1995. Cloning of the gene encoding Trop-2, a cell-surface glycoprotein expressed by human carcinomas. *Int J Cancer. 1995 Sep 4;():.* 62**,** 610-8.
FRANCIS, J. C., MCCARTHY, A., THOMSEN, M. K., ASHWORTH, A. & SWAIN, A. 2010. Brca2 and Trp53 deficiency cooperate in the progression of mouse prostate tumourigenesis. *PLoS Genet,* 6**,** e1000995.

FRANCIS, J. C., THOMSEN, M. K., TAKETO, M. M. & SWAIN, A. 2013. β-catenin is required for prostate development and cooperates with Pten loss to drive invasive carcinoma. *PLoS Genet,* 9**,** e1003180.

FRESNO VARA, J. A., CASADO, E., DE CASTRO, J., CEJAS, P., BELDA-INIESTA, C. & GONZÁLEZ-BARÓN, M. 2004. PI3K/Akt signalling pathway and cancer. *Cancer Treat Rev,* 30**,** 193-204.

GAO, A. C., LOU, W., DONG, J. T. & ISAACS, J. T. 1997. CD44 is a metastasis suppressor gene for prostatic cancer located on human chromosome 11p13. *Cancer Res,* 57**,** 846-9.

GAO, H., OUYANG, X., BANACH-PETROSKY, W. A., SHEN, M. M. & ABATE-SHEN, C. 2006. Emergence of androgen independence at early stages of prostate cancer progression in Nkx3.1; Pten mice. *Cancer Res,* 66**,** 7929-33.

GARABEDIAN, E. M., HUMPHREY, P. A. & GORDON, J. I. 1998. A transgenic mouse model of metastatic prostate cancer originating from neuroendocrine cells. *Proc Natl Acad Sci U S A,* 95**,** 15382-7.

GARBER, K. 2011. Beyond sequencing: new diagnostic tests turn to pathways. *J Natl Cancer Inst,* 103**,** 290-2.

GARRAWAY, I. P., SUN, W., TRAN, C. P., PERNER, S., ZHANG, B., GOLDSTEIN, A. S., HAHM, S. A., HAIDER, M., HEAD, C. S., REITER, R. E., RUBIN, M. A. & WITTE, O. N. 2010. Human prostate sphere-forming cells represent a subset of basal epithelial cells capable of glandular regeneration in vivo. *Prostate,* 70**,** 491-501.

GERSTEIN, A. V., ALMEIDA, T. A., ZHAO, G., CHESS, E., SHIH IE, M., BUHLER, K., PIENTA, K., RUBIN, M. A., VESSELLA, R. & PAPADOPOULOS, N. 2002. APC/CTNNB1 (beta-catenin) pathway alterations in human prostate cancers. *Genes Chromosomes Cancer,* 34**,** 9-16.

GHANI, K. R., GRIGOR, K., TULLOCH, D. N., BOLLINA, P. R. & MCNEILL, S. A. 2005. Trends in reporting Gleason score 1991 to 2001: changes in the pathologist's practice. *Eur Urol,* 47**,** 196-201.

GINESTIER, C., HUR, M. H., CHARAFE-JAUFFRET, E., MONVILLE, F., DUTCHER, J., BROWN, M., JACQUEMIER, J., VIENS, P., KLEER, C. G., LIU, S., SCHOTT, A., HAYES, D., BIRNBAUM, D., WICHA, M. S. & DONTU, G. 2007. ALDH1 is a marker of normal and malignant human mammary stem cells and a predictor of poor clinical outcome. *Cell Stem Cell,* 1**,** 555-67.

GINGRICH, J. R., BARRIOS, R. J., MORTON, R. A., BOYCE, B. F., DEMAYO, F. J., FINEGOLD, M. J., ANGELOPOULOU, R., ROSEN, J. M. & GREENBERG, N. M. 1996. Metastatic prostate cancer in a transgenic mouse. *Cancer Res,* 56**,** 4096-102.

GIOELI, D., KRAUS, S. & WEBER, M. J. 2008. Signal Transduction by the Ras–MAP Kinase Pathway in Prostate Cancer Progression. *In:* PESTELL, R. G., MILKEN, M., NEVALAINEN, M. T. & SPRINGERLINK (ONLINE SERVICE) (eds.) *Prostate Cancer Signaling Networks, Genetics, and New Treatment Strategies.* Totowa, NJ: Humana Press,.

GLEASON, D. F. & MELLINGER, G. T. 1974. Prediction of prognosis for prostatic adenocarcinoma by combined histological grading and clinical staging. *J Urol,* 111**,** 58-64.

GOLDIE, S. J., MULDER, K. W., TAN, D. W., LYONS, S. K., SIMS, A. H. & WATT, F. M. 2012. FRMD4A upregulation in human squamous cell carcinoma promotes tumor growth and metastasis and is associated with poor prognosis. *Cancer Res,* 72**,** 3424-36.

GOLDSTEIN, A. S., HUANG, J., GUO, C., GARRAWAY, I. P. & WITTE, O. N. 2010. Identification of a cell-of-origin for human prostate cancer. *Science,* 329**,** 568-71.

GOLDSTEIN, A. S., LAWSON, D. A., CHENG, D., SUN, W., GARRAWAY, I. P. & WITTE, O. N. 2008. Trop2 identifies a subpopulation of murine and human prostate basal cells with stem cell characteristics. *Proc Natl Acad Sci U S A,* 105**,** 20882-7.

GOUNARI, F., SIGNORETTI, S., BRONSON, R., KLEIN, L., SELLERS, W. R., KUM, J., SIERMANN, A., TAKETO, M. M., VON BOEHMER, H. & KHAZAIE, K. 2002. Stabilization of beta-catenin induces lesions reminiscent of prostatic intraepithelial neoplasia, but terminal squamous transdifferentiation of other secretory epithelia. *Oncogene,* 21**,** 4099-107.

GRASSO, C. S., WU, Y. M., ROBINSON, D. R., CAO, X., DHANASEKARAN, S. M., KHAN, A. P., QUIST, M. J., JING, X., LONIGRO, R. J., BRENNER, J. C., ASANGANI, I. A., ATEEQ, B., CHUN, S. Y.,

SIDDIQUI, J., SAM, L., ANSTETT, M., MEHRA, R., PRENSNER, J. R., PALANISAMY, N., RYSLIK, G. A., VANDIN, F., RAPHAEL, B. J., KUNJU, L. P., RHODES, D. R., PIENTA, K. J., CHINNAIYAN, A. M. & TOMLINS, S. A. 2012. The mutational landscape of lethal castration-resistant prostate cancer. *Nature,* 487**,** 239-43.

GREAVES, M. & MALEY, C. C. 2012. Clonal evolution in cancer. *Nature,* 481**,** 306-13.

GREEN, J. E., GREENBERG, N. M., ASHENDEL, C. L., BARRETT, J. C., BOONE, C., GETZENBERG, R. H., HENKIN, J., MATUSIK, R. J., JANUS, T. J. & SCHER, H. I. 1998. Workgroup 3: transgenic and reconstitution models of prostate cancer. *Prostate,* 36**,** 59-63.

GU, G., YUAN, J., WILLS, M. & KASPER, S. 2007. Prostate cancer cells with stem cell characteristics reconstitute the original human tumor in vivo. *Cancer Res,* 67**,** 4807-15.

GUERRA, C., MIJIMOLLE, N., DHAWAHIR, A., DUBUS, P., BARRADAS, M., SERRANO, M., CAMPUZANO, V. & BARBACID, M. 2003. Tumor induction by an endogenous K-ras oncogene is highly dependent on cellular context. *Cancer Cell,* 4**,** 111-20.

GUERTIN, D. A. & SABATINI, D. M. 2007. Defining the role of mTOR in cancer. *Cancer Cell,* 12**,** 9-22.

GUNIA, S., ALBRECHT, K., KOCH, S., HERRMANN, T., ECKE, T., LOY, V., LINKE, J., SIEGSMUND, M. & MAY, M. 2008. Ki67 staining index and neuroendocrine differentiation aggravate adverse prognostic parameters in prostate cancer and are characterized by negligible inter-observer variability. *World J Urol,* 26**,** 243-50.

GUO, C., LIU, H., ZHANG, B. H., CADANEANU, R. M., MAYLE, A. M. & GARRAWAY, I. P. 2012. Epcam, CD44, and CD49f distinguish sphere-forming human prostate basal cells from a subpopulation with predominant tubule initiation capability. *PLoS One,* 7**,** e34219.

HAGEN, T. & VIDAL-PUIG, A. 2002. Characterisation of the phosphorylation of beta-catenin at the GSK-3 priming site Ser45. *Biochem Biophys Res Commun,* 294**,** 324-8.

HALL, J. A., MAITLAND, N. J., STOWER, M. & LANG, S. H. 2002. Primary prostate stromal cells modulate the morphology and migration of primary prostate epithelial cells in type 1 collagen gels. *Cancer Res,* 62**,** 58-62.

HALL, J. C. & KILLIAN, G. J. 1987. Changes in rat sperm membrane glycosidase activities and carbohydrate and protein contents associated with epididymal transit. *Biol Reprod,* 36**,** 709-18.

HALVORSEN, O. J., HAUKAAS, S. A. & AKSLEN, L. A. 2003. Combined loss of PTEN and p27 expression is associated with tumor cell proliferation by Ki-67 and increased risk of recurrent disease in localized prostate cancer. *Clin Cancer Res,* 9**,** 1474-9.

HAN, K. R. & BELLDEGRUN, A. S. 2004. Third-generation cryosurgery for primary and recurrent prostate cancer. *BJU Int,* 93**,** 14-8.

HARADA, N., TAMAI, Y., ISHIKAWA, T., SAUER, B., TAKAKU, K., OSHIMA, M. & TAKETO, M. M. 1999. Intestinal polyposis in mice with a dominant stable mutation of the beta-catenin gene. *EMBO J,* 18**,** 5931-42.

HAYWARD, S. W. & CUNHA, G. R. 2000. The prostate: development and physiology. *Radiol Clin North Am,* 38**,** 1-14.

HE, T. C., SPARKS, A. B., RAGO, C., HERMEKING, H., ZAWEL, L., DA COSTA, L. T., MORIN, P. J., VOGELSTEIN, B. & KINZLER, K. W. 1998. Identification of c-MYC as a target of the APC pathway. *Science,* 281**,** 1509-12.

HEIDENREICH, A., BASTIAN, P., BELLMUNT, J., BOLLA, M., JONIAU, S., MASON, M., MATVEEV, V., MOTTET, N., VAN DER KWAST, T., WIEGEL, T. & ZATTONI, F. 2012. Guidelines on Prostate Cancer. European Association of Urology (EAU).

HENSLEY, P. J. & KYPRIANOU, N. 2012. Modeling prostate cancer in mice: limitations and opportunities. *J Androl,* 33**,** 133-44.

HISHA, H., TANAKA, T., KANNO, S., TOKUYAMA, Y., KOMAI, Y., OHE, S., YANAI, H., OMACHI, T. & UENO, H. 2013. Establishment of a novel lingual organoid culture system: generation of organoids having mature keratinized epithelium from adult epithelial stem cells. *Sci Rep,* 3**,** 3224.

HOCKENBERY, D. M., ZUTTER, M., HICKEY, W., NAHM, M. & KORSMEYER, S. J. 1991. BCL2 protein is topographically restricted in tissues characterized by apoptotic cell death. *PNAS,* 88**,** 6961-5.
HOROSZEWICZ, J. S., LEONG, S. S., CHU, T. M., WAJSMAN, Z. L., FRIEDMAN, M., PAPSIDERO, L., KIM, U., CHAI, L. S., KAKATI, S., ARYA, S. K. & SANDBERG, A. A. 1980. The LNCaP cell line--a new model for studies on human prostatic carcinoma. *Prog Clin Biol Res,* 37**,** 115-332.
HORVATH, L. G., HENSHALL, S. M., LEE, C. S., KENCH, J. G., GOLOVSKY, D., BRENNER, P. C., O'NEILL, G. F., KOONER, R., STRICKER, P. D., GRYGIEL, J. J. & SUTHERLAND, R. L. 2005. Lower levels of nuclear beta-catenin predict for a poorer prognosis in localized prostate cancer. *Int J Cancer,* 113**,** 415-22.
HOU, X., TAN, Y., LI, M., DEY, S. K. & DAS, S. K. 2004. Canonical Wnt signaling is critical to estrogen-mediated uterine growth. *Mol Endocrinol,* 18**,** 3035-49.
HU, H., XIA, S. H., LI, A. D., XU, X., CAI, Y., HAN, Y. L., WEI, F., CHEN, B. S., HUANG, X. P., HAN, Y. S., ZHANG, J. W., ZHANG, X., WU, M. & WANG, M. R. 2002. Elevated expression of p63 protein in human esophageal squamous cell carcinomas. *Int J Cancer,* 102**,** 580-3.
HUANG, H., ET AL. 2005. Aberrant expression of novel and previously described cell membrane markers in human breast cancer cell lines and tumors. *Clin Cancer Res,* 11**,** 4357-4364.
HUDSON, D. L., GUY, A. T., FRY, P., O'HARE, M. J., WATT, F. M. & MASTERS, J. R. 2001. Epithelial cell differentiation pathways in the human prostate: identification of intermediate phenotypes by keratin expression. *J Histochem Cytochem,* 49**,** 271-8.
HUGGINS, C. & HODGES, C. V. Feb 2002. Studies on prostatic cancer. I. The effect of castration, of estrogen and of androgen injection on serum phosphatase in metastatic carcinoma of the prostate. *J Urol,* 167**,** 948-951, discussion 952.
HUGGINS, C., STEVENS, R. E., JR & HODGES, C. V. 1941. Studies on prostate cancer. II. The effect of castration on advanced carcinoma of the prostate gland. *Arch Surg,* 43**,** 209-23.
HURT, E. M., KAWASAKI, B. T., KLARMANN, G. J., THOMAS, S. B. & FARRAR, W. L. 2008. CD44+ CD24(-) prostate cells are early cancer progenitor/stem cells that provide a model for patients with poor prognosis. *Br J Cancer,* 98**,** 756-65.
IKENOUCHI, J. & UMEDA, M. 2010. FRMD4A regulates epithelial polarity by connecting Arf6 activation with the PAR complex. *Proc Natl Acad Sci U S A,* 107**,** 748-53.
ISAACS, J. T. & COFFEY, D. S. 1989. Etiology and disease process of benign prostatic hyperplasia. *Prostate Suppl,* 2**,** 33-50.
ISAACS, J. T. & ISAACS, W. B. 2004. Androgen receptor outwits prostate cancer drugs. *Nat Med,* 10**,** 26-7.
ITTMANN, M., HUANG, J., RADAELLI, E., MARTIN, P., SIGNORETTI, S., SULLIVAN, R., SIMONS, B. W., WARD, J. M., ROBINSON, B. D., CHU, G. C., LODA, M., THOMAS, G., BOROWSKY, A. & CARDIFF, R. D. 2013. Animal Models of Human Prostate Cancer: The Consensus Report of the New York Meeting of the Mouse Models of Human Cancers Consortium Prostate Pathology Committee. *Cancer Res,* 73**,** 2718-2736.
IWAO, K., NAKAMORI, S., KAMEYAMA, M., IMAOKA, S., KINOSHITA, M., FUKUI, T., ISHIGURO, S., NAKAMURA, Y. & MIYOSHI, Y. 1998. Activation of the beta-catenin gene by interstitial deletions involving exon 3 in primary colorectal carcinomas without adenomatous polyposis coli mutations. *Cancer Res,* 58**,** 1021-1026.
IYIBOZKURT, A. C., BALCIK, P., BULGURCUOGLU, S., ARSLAN, B. K., ATTAR, R. & ATTAR, E. 2009. Effect of vascular endothelial growth factor on sperm motility and survival. *Reprod Biomed Online,* 19**,** 784-8.
JAGGUPILLI, A. & ELKORD, E. 2012. Significance of CD44 and CD24 as cancer stem cell markers: an enduring ambiguity. *Clin Dev Immunol,* 2012**,** 708036.
JANSSEN, K. P., ALBERICI, P., FSIHI, H., GASPAR, C., BREUKEL, C. & FRANKEN, P., ET AL. 2006. APC and oncogenic KRAS are synergistic in enhancing Wnt signaling in intestinal tumor formation and progression. *Gastroenterology,* 131**,** 1096-1109.

JENSEN, K. B. & WATT, F. M. 2006. Single-cell expression profiling of human epidermal stem and transit-amplifying cells: Lrig1 is a regulator of stem cell quiescence. *Proc Natl Acad Sci U S A,* 103**,** 11958-63.

JERONIMO, C., BASTIAN, P. J., BJARTELL, A., CARBONE, G. M., CATTO, J. W., CLARK, S. J., HENRIQUE, R., NELSON, W. G. & SHARIAT, S. F. 2011. Epigenetics in prostate cancer: biologic and clinical relevance. *Eur Urol,* 60**,** 753-66.

JESIK, C. J., HOLLAND, J. M. & LEE, C. 1982. An anatomic and histologic study of the rat prostate. *Prostate,* 3**,** 81-97.

JIA, S., LIU, Z. & ZHANG, S. E. A. 2008. Essential roles of PI(3)K-p110β in cell growth, metabolism and tumorigenesis. *Nature,* 454**,** 776-9.

JIAO, J., HINDOYAN, A., WANG, S., TRAN, L. M., GOLDSTEIN, A. S., LAWSON, D., CHEN, D., LI, Y., GUO, C., ZHANG, B., FAZLI, L., GLEAVE, M., WITTE, O. N., GARRAWAY, I. P. & WU, H. 2012. Identification of CD166 as a Surface Marker for Enriching Prostate Stem/Progenitor and Cancer Initiating Cells. *PLoS One,* 7**,** e42564.

JOHNSON, M. A., HERNANDEZ, I., WEI, Y. & GREENBERG, N. 2000. Isolation and characterization of mouse probasin: An androgen-regulated protein specifically expressed in the differentiated prostate. *Prostate,* 43**,** 255-62.

JONES, P. H., HARPER, S. & WATT, F. M. 1995. Stem cell patterning and fate in human epidermis. *Cell,* 60**,** 83-93.

JONES, R. G. & THOMPSON, C. B. 2009. Tumour suppressors and cell metabolism: a recipe for cancer growth. *Genes Dev,* 23**,** 537-548.

JORDAN, C. T., GUZMAN, M. L. & NOBLE, M. 2006. Cancer stem cells. *N Engl J Med,* 355**,** 1253-61.

KAIGHN, M. E., NARAYAN, K. S., OHNUKI, Y., LECHNER, J. F. & JONES, L. W. 1979. Establishment and characterization of a human prostatic carcinoma cell line (PC-3). *Invest Urol. 1979 Jul;17(1):16-23,* 17**,** 16-23.

KALLAKURY, B. V., SHEEHAN, C. E. & ROSS, J. S. 2001. Co-downregulation of cell adhesion proteins alpha- and beta-catenins, p120CTN, E-cadherin, and CD44 in prostatic adenocarcinomas. *Hum Pathol,* 32**,** 849-55.

KARANTANOS, T. & THOMPSON, T. C. 2013. GEMMs shine a light on resistance to androgen deprivation therapy for prostate cancer. *Cancer Cell,* 24**,** 11-3.

KARESKOSKI, M. & KATILA, T. 2008. Components of stallion seminal plasma and the effects of seminal plasma on sperm longevity. *Anim Reprod Sci,* 107**,** 249-56.

KASPER, S. 2005. Survey of genetically engineered mouse models for prostate cancer: analyzing the molecular basis of prostate cancer development, progression, and metastasis. *J Cell Biochem,* 94**,** 279-97.

KASPER, S. & MATUSIK, R. J. 2000. Rat probasin: structure and function of an outlier lipocalin. *Biochim Biophys Acta,* 1482**,** 249-58.

KASPER, S., SHEPPARD, P. C., YAN, Y., PETTIGREW, N., BOROWSKY, A. D., PRINS, G. S., DODD, J. G., DUCKWORTH, M. L. & MATUSIK, R. J. 1998. Development, progression, and androgen-dependence of prostate tumors in probasin-large T antigen transgenic mice: a model for prostate cancer. *Lab Invest,* 78**,** 1-15.

KELAVKAR, U. P., PARWANI, A. V., SHAPPELL, S. B. & MARTIN, W. D. 2006. Conditional expression of human 15-lipoxygenase-1 in mouse prostate induces prostatic intraepithelial neoplasia: the FLiMP mouse model. *Neoplasia,* 8**,** 510-22.

KEOHAVONG, P., DEMICHELE, M. A., MELACRINOS, A. C., LANDRENEAU, R. J., WEYANT, R. J. & SIEGFRIED, J. M. 1996. Detection of K-ras mutations in lung carcinomas: relationship to prognosis. *Clin Cancer Res,* 2**,** 411-418.

KHOR, L. Y., BAE, K., PAULUS, R., AL-SALEEM, T., HAMMOND, M. E., GRIGNON, D. J., CHE, M., VENKATESAN, V., BYHARDT, R. W., ROTMAN, M., HANKS, G. E., SANDLER, H. M. & POLLACK, A. 2009. MDM2 and Ki-67 predict for distant metastasis and mortality in men treated with

radiotherapy and androgen deprivation for prostate cancer: RTOG 92-02. *J Clin Oncol,* 27**,** 3177-84.
KIM, M. J., CARDIFF, R. D., DESAI, N., BANACH-PETROSKY, W. A., PARSONS, R., SHEN, M. M. & ABATE-SHEN, C. 2002. Cooperativity of Nkx3.1 and Pten loss of function in a mouse model of prostate carcinogenesis. *Proc Natl Acad Sci U S A,* 99**,** 2884-9.
KINBARA, H., CUNHA, G. R., BOUTIN, E., HAYASHI, N. & KAWAMURA, J. 1996. Evidence of stem cells in the adult prostatic epithelium based upon responsiveness to mesenchymal inductors. *Prostate,* 29**,** 107-16.
KING, J. C., XU, J., WONGVIPAT, J., HIERONYMUS, H., CARVER, B. S., LEUNG, D. H., TAYLOR, B. S., SANDER, C., CARDIFF, R. D., COUTO, S. S., GERALD, W. L. & SAWYERS, C. L. 2009. Cooperativity of TMPRSS2-ERG with PI3-kinase pathway activation in prostate oncogenesis. *Nat Genet,* 41**,** 524-6.
KISHIDA, M., KOYAMA, S., KISHIDA, S., MATSUBARA, K., NAKASHIMA, S., HIGANO, K., TAKADA, R., TAKADA, S. & KIKUCHI, A. 1999. Axin prevents Wnt-3a-induced accumulation of beta-catenin. *Oncogene* 18**,** 979-985.
KLOTZ, L. H., GOLDENBERG, S. L., JEWETT, M. A., FRADET, Y., NAM, R., BARKIN, J., CHIN, J., CHATTERJEE, S. & CANADIAN URO-ONCOLOGY, G. 2003. Long-term followup of a randomized trial of 0 versus 3 months of neoadjuvant androgen ablation before radical prostatectomy. *J Urol,* 170**,** 791-4.
KOLLIGS, F. T., BOMMER, G. & GOKE, B. 2002. Wnt/beta-catenin/tcf signaling: a critical pathway in gastrointestinal tumorigenesis. *Digestion,* 66**,** 131-44.
KOMIYA, Y. & HABAS, R. 2008. Wnt signal transduction pathways. *Organogenesis,* 4**,** 68-75.
KOMPIER, L. C., LURKIN, I., VAN DER AA, M. N., VAN RHIJN, B. W., VAN DER KWAST, T. H. & ZWARTHOFF, E. C. 2010. FGFR3, HRAS, KRAS, NRAS and PIK3CA mutations in bladder cancer and their potential as biomarkers for surveillance and therapy. *PLoS One,* 5**,** e13821.
KORSTEN, H., ZIEL-VAN DER MADE, A., MA, X., VAN DER KWAST, T. & TRAPMAN, J. 2009. Accumulating progenitor cells in the luminal epithelial cell layer are candidate tumor initiating cells in a Pten knockout mouse prostate cancer model. *PLoS One,* 4**,** e5662.
KOZMA, S. C. & THOMAS, G. 2002. Regulation of cell size in growth, development and human disease: PI3K, PKB and S6K. *Bioessays,* 24**,** 65-71.
KRISTIANSEN, G. 2012. Diagnostic and prognostic molecular biomarkers for prostate cancer. *Histopathology,* 60**,** 125-41.
KURITA, T., MEDINA, R. T., MILLS, A. A. & CUNHA, G. R. 2004. Role of p63 and basal cells in the prostate. *Development,* 131**,** 4955-64.
KURODA, T., LEE, M. M., HAQQ, C. M., POWELL, D. M., MANGANARO, T. F. & DONAHOE, P. K. 1990. Mullerian inhibiting substance ontogeny and its modulation by follicle-stimulating hormone in the rat testes. *Endocrinology,* 127**,** 1825-32.
KYPTA, R. M. & WAXMAN, J. 2012. Wnt/beta-catenin signalling in prostate cancer. *Nat Rev Urol*.
LAITINEN, S., MARTIKAINEN, P. M., TOLONEN, T., ISOLA, J., TAMMELA, T. L. & VISAKORPI, T. 2008. EZH2, Ki-67 and MCM7 are prognostic markers in prostatectomy treated patients. *Int J Cancer,* 122**,** 595-602.
LANE, J. A., HAMDY, F. C., MARTIN, R. M., TURNER, E. L., NEAL, D. E. & DONOVAN, J. L. 2010. Latest results from the UK trials evaluating prostate cancer screening and treatment: the CAP and ProtecT studies. *Eur J Cancer,* 46**,** 3095-101.
LANG, S. H., ANDERSON, E., FORDHAM, R. & COLLINS, A. T. 2010. Modeling the prostate stem cell niche: an evaluation of stem cell survival and expansion in vitro. *Stem Cells Dev,* 19**,** 537-46.
LASNITZKI, I., TAKEDA, H. & MIZUNO, T. 1989. Autoradiographic studies of androgen-binding sites in human benign prostatic hyperplasia in vitro. *J Endocrinol,* 120**,** 167-70.
LAWRENCE, M. G., TAYLOR, R. A., TOIVANEN, R., PEDERSEN, J., NORDEN, S., POOK, D. W., FRYDENBERG, M., AUSTRALIAN PROSTATE CANCER BIORESOURCE, PAPARGIRIS, M. M., NIRANJAN, B., RICHARDS, M. G., WANG, H., COLLINS, A. T., MAITLAND, N. J. & RISBRIDGER,

G. P. 2013. A preclinical xenograft model of prostate cancer using human tumors. *Nat Protoc,* 8**,** 836-48.
LAWSON, D. A., XIN, L., LUKACS, R. U., CHENG, D. & WITTE, O. N. 2007. Isolation and functional characterization of murine prostate stem cells. *Proc Natl Acad Sci U S A,* 104**,** 181-6.
LE CALVE, M., SEGALEN, J., QUERNEE, D., LAVAULT, M. T. & LESCOAT, D. 1995. Diamine oxidase activity and biochemical markers in human seminal plasma. *Hum Reprod,* 10**,** 1141-4.
LEE, C., SENSIBAR, J. A., DUDEK, S. M., HIIPAKKA, R. A. & LIAO, S. T. 1990. Prostatic ductal system in rats: regional variation in morphological and functional activities. *Biol Reprod,* 43**,** 1079-86.
LEE, E., MADAR, A., DAVID, G., GARABEDIAN, M. J., DASGUPTA, R. & LOGAN, S. K. 2013. Inhibition of androgen receptor and beta-catenin activity in prostate cancer. *Proc Natl Acad Sci U S A,* 110**,** 15710-5.
LEE, E., YIM, S., LEE, S. K. & PARK, H. 2002. Two transactivation domains of hypoxia-inducible factor 1α regulated by the MEK 1/p42/p44 MAPK pathway. *Mod Cells,* 14**,** 9-15.
LEE, J. O., YANG, H., GEORGESCU, M. M., DI CRISTOFANO, A., MAEHAMA, T., SHI, Y., DIXON, J. E., PANDOLFI, P. & PAVLETICH, N. P. 1999a. Crystal structure of the PTEN tumor suppressor: implications for its phosphoinositide phosphatase activity and membrane association. *Cell,* 99**,** 323-334.
LEE, J. S., ISHIMOTO, A. & YANAGAWA, S. 1999b. Characterization of mouse dishevelled (Dvl) proteins in Wnt/Wingless signaling pathway. *J Biol Chem,* 274**,** 21464-1470.
LEFEVRE, P. L., PALIN, M. F. & MURPHY, B. D. 2011. Polyamines on the reproductive landscape. *Endocr Rev,* 32**,** 694-712.
LEONG, K. G. & GAO, W. Q. 2008. The Notch pathway in prostate development and cancer. *Differentiation,* 76**,** 699-716.
LEONG, K. G., WANG, B. E., JOHNSON, L. & GAO, W. Q. 2008. Generation of a prostate from a single adult stem cell. *Nature,* 456**,** 804-8.
LEUNG, E. L., FISCUS, R. R., TUNG, J. W., TIN, V. P., CHENG, L. C., SIHOE, A. D., FINK, L. M., MA, Y. & WONG, M. P. 2010. Non-small cell lung cancer cells expressing CD44 are enriched for stem cell-like properties. *PLoS One,* 5**,** e14062.
LI, L. & CLEVERS, H. 2010. Coexistence of quiescent and active adult stem cells in mammals. *Science,* 327**,** 542-5.
LI, Z. G., YANG, J., VAZQUEZ, E. S., ROSE, D., VAKAR-LOPEZ, F., MATHEW, P., LOPEZ, A., LOGOTHETIS, C. J., LIN, S. H. & NAVONE, N. M. 2008. Low-density lipoprotein receptor-related protein 5 (LRP5) mediates the prostate cancer-induced formation of new bone. *Oncogene,* 27**,** 596-603.
LIAO, C. P., ADISETIYO, H., LIANG, M. & ROY-BURMAN, P. 2010. Cancer-associated fibroblasts enhance the gland-forming capability of prostate cancer stem cells. *Cancer Res,* 70**,** 7294-303.
LIAW, D., MARSH, D. J., LI, J., DAHIA, P. L., WANG, S. I., ZHENG, Z., BOSE, S., CALL, K. M., TSOU, H. C. & PEACOCKE, M. 1997. Germline mutations of the PTEN gene in Cowden disease, an inherited breast and thyroid cancer syndrome. *Nat Genet,* 16**,** 64-67.
LIU, A. Y., TRUE, L. D., LATRAY, L., NELSON, P. S., ELLIS, W. J., VESSELLA, R. L., LANGE, P. H., HOOD, L. & VAN DEN ENGH, G. 1997. Cell-cell interaction in prostate gene regulation and cytodifferentiation. *Proc Natl Acad Sci U S A,* 94**,** 10705-10.
LIU, C., LI, Z., BI, L., LI, K., ZHOU, B., XU, C., HUANG, J. & XU, K. 2014. NOTCH1 signaling promotes chemoresistance via regulating ABCC1 expression in prostate cancer stem cells. *Mol Cell Biochem,* 393**,** 265-70.
LIU, J. L., SHENG, X., HORTOBAGYI, Z. K., MAO, Z., GALLICK, G. E. & YUNG, W. K. 2005. Nuclear PTEN-mediated growth suppression is independent of Akt down-regulation. *Mol Cell Biol,* 25**,** 6211-24.
LIU, L., ZHU, S., GONG, Z. & LOW, B. C. 2008. K-ras/PI3K-Akt signaling is essential for zebrafish hematopoiesis and angiogenesis. *PLoS One,* 3**,** e2850.

LIU, R., WANG, X., CHEN, G. Y., DALERBA, P., GURNEY, A., HOEY, T., SHERLOCK, G., LEWICKI, J., SHEDDEN, K. & CLARKE, M. F. 2007 The prognostic role of a gene signature from tumorigenic breast-cancer cells. *N Engl J Med,* 356**,** 217-26.

LOHMANN, S., WOLLSCHEID, U., HUBER, C. & SELIGER, B. 1996. Multiple levels of MHC class I down-regulation by ras oncogenes. *Scand J Immunol,* 43**,** 537-544.

LOPEZ, J. I., CAMENISCH, T. D., STEVENS, M. V., SANDS, B. J., MCDONALD, J. & SCHROEDER, J. A. 2005. CD44 attenuates metastatic invasion during breast cancer progression. *Cancer Res,* 65**,** 6755-63.

LOWRANCE, W. T., ELKIN, E. B., YEE, D. S., FEIFER, A., EHDAIE, B., JACKS, L. M., ATORIA, C. L., ZELEFSKY, M. J., SCHER, H. I., SCARDINO, P. T. & EASTHAM, J. A. 2012. Locally advanced prostate cancer: a population-based study of treatment patterns. *BJU Int,* 109**,** 1309-14.

LUKACS, R. U., GOLDSTEIN, A. S., LAWSON, D. A., CHENG, D. & WITTE, O. N. 2010. Isolation, cultivation and characterization of adult murine prostate stem cells. *Nat Protoc,* 5**,** 702-13.

LUKACS, R. U., LAWSON, D. A., XIN, L., ZONG, Y., GARRAWAY, I., GOLDSTEIN, A. S., MEMARZADEH, S. & WITTE, O. N. 2008. Epithelial stem cells of the prostate and their role in cancer progression. *Cold Spring Harb Symp Quant Biol,* 73**,** 491-502.

MA, X., ZIEL-VAN DER MADE, A. C., AUTAR, B., VAN DER KORPUT, H. A., VERMEIJ, M., VAN DUIJN, P., CLEUTJENS, K. B., DE KRIJGER, R., KRIMPENFORT, P., BERNS, A., VAN DER KWAST, T. H. & TRAPMAN, J. 2005. Targeted biallelic inactivation of Pten in the mouse prostate leads to prostate cancer accompanied by increased epithelial cell proliferation but not by reduced apoptosis. *Cancer Res,* 65**,** 5730-9.

MA, X. M. & BLENIS, J. 2009. Molecular mechanisms of mTOR-mediated translational control. *Nature Rev Mol Cell Biol,* 10**,** 307-318.

MA, Y. Y., WEI, S. J. & LIN, Y. C. E. A. 2000. PIK3CA as an oncogene in cervical cancer. *Oncogene,* 19**,** 2739-44.

MACDONALD, B. T., TAMAI, K. & HE, X. 2009. Wnt/beta-catenin signaling: components, mechanisms, and diseases. *Dev Cell,* 17**,** 9-26.

MADDISON, K. & CLARKE, A. R. 2005. New approaches for modelling cancer mechanisms in the mouse. *J Pathol,* 205**,** 181-93.

MADDISON, L. A., NAHM, H., DEMAYO, F. & GREENBERG, N. M. 2000. Prostate specific expression of Cre recombinase in transgenic mice. *Genesis,* 26**,** 154-6.

MADDISON, L. A., SUTHERLAND, B. W., BARRIOS, R. J. & GREENBERG, N. M. 2004. Conditional deletion of Rb causes early stage prostate cancer. *Cancer Res,* 64**,** 6018-25.

MAEHAMA, T. & DIXON, J. E. 1998. The tumor suppressor, PTEN/MMAC1, dephosphorylates the lipid second messenger, phosphatidylinositol 3,4,5-trisphosphate. *J Biol Chem,* 273**,** 13375-78.

MAIER, U., KIRCHHEIMER, J. C., HIENERT, G., CHRIST, G. & BINDER, B. R. 1991. Fibrinolytic parameters in spermatozoas and seminal plasma. *J Urol,* 146**,** 906-8.

MAITLAND, N. J., FRAME, F. M., POLSON, E. S., LEWIS, J. L. & COLLINS, A. T. 2011. Prostate cancer stem cells: do they have a basal or luminal phenotype? *Horm Cancer,* 2**,** 47-61.

MALANCHI, I., PEINADO, H., KASSEN, D., HUSSENET, T., METZGER, D., CHAMBON, P., HUBER, M., HOHL, D., CANO, A., BIRCHMEIER, W. & HUELSKEN, J. 2008. Cutaneous cancer stem cell maintenance is dependent on beta-catenin signalling. *Nature,* 452**,** 650-3.

MANIATIS, T. 1999. A ubiquitin ligase complex essential for the NF-kappaB, Wnt/Wingless, and Hedgehog signaling pathways. *Genes Dev,* 13**,** 505-510.

MANNING, B. D. & CANTLEY, L. C. 2007. AKT/PKB signaling: navigating downstream. *Cell,* 129**,** 1261-1274.

MAROTTA, L. L. & POLYAK, K. 2009. Cancer stem cells: a model in the making. *Curr Opin Genet Dev,* 19**,** 44-50.

MARSH, D. J., KUM, J. B., LUNETTA, K. L., BENNETT, M. J., GORLIN, R. J., AHMED, S. F., BODURTHA, J., CROWE, C., CURTIS, M. A. & DASOUKI, M. 1999. PTEN mutation spectrum and genotype-

phenotype correlations in Bannayan- Riley-Ruvalcaba syndrome suggest a single entity with Cowden syndrome. *Hum Mol Genet,* 8.

MASER, R. S., CHOUDHURY, B., CAMPBELL, P. J., FENG, B., WONG, K. K., PROTOPOPOV, A., O'NEIL, J., GUTIERREZ, A., IVANOVA, E., PERNA, I., LIN, E., MANI, V., JIANG, S., MCNAMARA, K., ZAGHLUL, S., EDKINS, S., STEVENS, C., BRENNAN, C., MARTIN, E. S., WIEDEMEYER, R., KABBARAH, O., NOGUEIRA, C., HISTEN, G., ASTER, J., MANSOUR, M., DUKE, V., FORONI, L., FIELDING, A. K., GOLDSTONE, A. H., ROWE, J. M., WANG, Y. A., LOOK, A. T., STRATTON, M. R., CHIN, L., FUTREAL, P. A. & DEPINHO, R. A. 2007. Chromosomally unstable mouse tumours have genomic alterations similar to diverse human cancers. *Nature,* 447**,** 966-71.

MATSUI, M., FOWLER, J. H. & WALLING, L. L. 2006. Leucine aminopeptidases: diversity in structure and function. *Biol Chem,* 387**,** 1535-44.

MAUDSLEY, D. J., BATEMAN, W. J. & MORRIS, A. G. 1991. Reduced stimulation of helper T cells by K-ras transformed cells. *Immunology,* 72**,** 277-281.

MCMANUS, E. J., SAKAMOTO, K., ARMIT, L. J., RONALDSON, L., SHPIRO, N., MARQUEZ, R. & ALESSI, D. R. 2005. Role that phosphorylation of GSK3 plays in insulin and Wnt signalling defined by knockin analysis. *EMBO J,* 24**,** 1571-83.

MCMENAMIN, M. E., SOUNG, P., PERERA, S., KAPLAN, I., LODA, M. & SELLERS, W. R. 1999. Loss of PTEN expression in paraffin-embedded primary prostate cancer correlates with high Gleason score and advanced stage. *Cancer Res,* 59**,** 4291-6.

MCNEAL, J. E. 1969. Origin and development of carcinoma in the prostate. *Cancer,* 23**,** 24-34.

MCNEAL, J. E. 1981a. Normal and pathologic anatomy of prostate. *Urology,* 17**,** 11-6.

MCNEAL, J. E. 1981b. The zonal anatomy of the prostate. *Prostate,* 2**,** 35-49.

MCNEAL, J. E. 1992. Cancer volume and site of origin of adenocarcinoma in the prostate: relationship to local and distant spread. *Hum Pathol,* 23**,** 258-66.

MCNEAL, J. E., REDWINE, E. A., FREIHA, F. S. & STAMEY, T. A. 1988. Zonal distribution of prostatic adenocarcinoma. Correlation with histologic pattern and direction of spread. *Am J Surg Pathol,* 12**,** 897-906.

MELLINGER, G. T., GLEASON, D. F. & BAILAR III, J. 1967. The histology and prognosis of prostatic cancer. *J Urol,* 97**,** 331-7.

MESSING, E. M., MANOLA, J., YAO, J., KIERNAN, M., CRAWFORD, D., WILDING, G., DI'SANTAGNESE, P. A., TRUMP, D. & EASTERN COOPERATIVE ONCOLOGY GROUP STUDY, E. S. T. 2006. Immediate versus deferred androgen deprivation treatment in patients with node-positive prostate cancer after radical prostatectomy and pelvic lymphadenectomy. *Lancet Oncol,* 7**,** 472-9.

MIKI, J., FURUSATO, B., LI, H., GU, Y., TAKAHASHI, H., EGAWA, S., SESTERHENN, I. A., MCLEOD, D. G., SRIVASTAVA, S. & RHIM, J. S. 2007. Identification of putative stem cell markers, CD133 and CXCR4, in hTERT-immortalized primary nonmalignant and malignant tumor-derived human prostate epithelial cell lines and in prostate cancer specimens. *Cancer Res,* 67**,** 3153-61.

MISSOL-KOLKA, E., KARBANOVÁ, J., JANICH, P., HAASE, M., FARGEAS, C. A., HUTTNER, W. B. & CORBEIL, D. 2011. Prominin-1 (CD133) is not restricted to stem cells located in the basal compartment of murine and human prostate. *Prostate Cancer Prostatic Dis,* 71**,** 254-67.

MIYAKE, H., MURAMAKI, M., KURAHASHI, T., TAKENAKA, A. & FUJISAWA, M. 2010. Expression of potential molecular markers in prostate cancer: correlation with clinicopathological outcomes in patients undergoing radical prostatectomy. *Urol Oncol,* 28**,** 145-51.

MIYOSHI, Y., IWAO, K., NAGASAWA, Y., AIHARA, T., SASAKI, Y., IMAOKA, S., MURATA, M., SHIMANO, T. & NAKAMURA, Y. 1998. Activation of the beta-catenin gene in primary hepatocellular carcinomas by somatic alterations involving exon3. *Cancer Res,* 58**,** 2524–2527.

MOLENAAR, M., VAN DE WETERING, M., OOSTERWEGEL, M., PETERSON-MADURO, J., GODSAVE, S., KORINEK, V., ROOSE, J., DESTREE, O. & CLEVERS, H. 1996. Tcf-3 transcription factor mediates beta-catenin-induced axis formation in Xenopus embryos. *Cell,* 86.

MONTIRONI, R., MAZZUCCHELI, R., SCARPELLI, M., LOPEZ-BELTRAN, A., FELLEGARA, G. & ALGABA, F. 2005. Gleason grading of prostate cancer in needle biopsies or radical prostatectomy specimens: contemporary approach, current clinical significance and sources of pathology discrepancies. *BJU Int,* 95**,** 1146-52.

MONTPETIT, M., ABRAHAMS, P., CLARK, A. F. & TENNISWOOD, M. 1988. Androgen-independent epithelial cells of the rat ventral prostate. *Prostate,* 12**,** 13-28.

MORI, H., NINOMIYA, K., KINO-OKA, M., SHOFUDA, T., ISLAM, M. O., YAMASAKI, M., OKANO, H., TAYA, M. & KANEMURA, Y. 2006. Effect of neurosphere size on the growth rate of human neural stem/progenitor cells. *J Neurosci Res,* 84**,** 1682-91.

MULHOLLAND, D. J., DEDHAR, S., WU, H. & NELSON, C. C. 2006. PTEN and GSK3beta: key regulators of progression to androgen-independent prostate cancer. *Oncogene,* 25**,** 329-37.

MULHOLLAND, D. J., KOBAYASHI, N., RUSCETTI, M., ZHI, A., TRAN, L. M., HUANG, J., GLEAVE, M. & WU, H. 2012. Pten loss and RAS/MAPK activation cooperate to promote EMT and metastasis initiated from prostate cancer stem/progenitor cells. *Cancer Res,* 72**,** 1878-89.

MULHOLLAND, D. J., XIN, L., MORIM, A., LAWSON, D., WITTE, O. & WU, H. 2009. Lin-Sca-1+CD49fhigh stem/progenitors are tumor-initiating cells in the Pten-null prostate cancer model. *Cancer Res,* 69**,** 8555-62.

MUNDY, G. R. 2002. Metastasis to bone: causes, consequences and therapeutic opportunities. *Nat Rev Cancer,* 2**,** 584-93.

MUNSTERBERG, A. & LOVELL-BADGE, R. 1991. Expression of the mouse anti-mullerian hormone gene suggests a role in both male and female sexual differentiation. *Development,* 113**,** 613-24.

NAOR, D., NEDVETZKI, S., GOLAN, I., MELNIK, L. & FAITELSON, Y. 2002. CD44 in cancer. *Crit Rev Clin Lab Sci,* 39**,** 527-79.

NG, S. S., MAHMOUDI, T., DANENBERG, E., BEJAOUI, I., DE LAU, W., KORSWAGEN, H. C., SCHUTTE, M. & CLEVERS, H. 2009. Phosphatidylinositol 3-kinase signaling does not activate the wnt cascade. *J Biol Chem,* 284**,** 35308-13.

NICE, N. I. F. H. A. C. E. 2014. Prostate cancer: diagnosis and treatment. Velindre NHS Trust, Cardiff, Wales: National Collaborating Centre for Cancer.

NIESSEN, C. M. 2007. Tight junctions/adherens junctions: basic structure and function. *J Invest Dermatol,* 127**,** 2525-32.

NOLLET, F., BERX, G., MOLEMANS, F. & VAN ROY, F. 1996. Genomic organization of the human beta-catenin gene (CTNNB1). *Genomics,* 32**,** 413-24.

NUSSE, R. & VARMUS, H. E. 1992. Wnt genes. *Cell,* 69**,** 1073-87.

OHMACHI, T., ET AL. 2006. Clinical significance of TROP2 expression in colorectal cancer. *Clin Cancer Res,* 12**,** 3057-3063.

OLDRIDGE, E. E., PELLACANI, D., COLLINS, A. T. & MAITLAND, N. J. 2012. Prostate cancer stem cells: are they androgen-responsive? *Mol Cell Endocrinol,* 360**,** 14-24.

OSHEROFF, J. E., VISCONTI, P. E., VALENZUELA, J. P., TRAVIS, A. J., ALVAREZ, J. & KOPF, G. S. 1999. Regulation of human sperm capacitation by a cholesterol efflux-stimulated signal transduction pathway leading to protein kinase A-mediated up-regulation of protein tyrosine phosphorylation. *Mol Hum Reprod,* 5**,** 1017-26.

OSHIMA, H., ROCHAT, A., KEDZIA, C., KOBAYASHI, K. & BARRANDON, Y. 2001. Morphogenesis and renewal of hair follicles from adult multipotent stem cells. *Cell,* 104**,** 233-45.

PALAPATTU, G. S., WU, C., SILVERS, C. R., MARTIN, H. B., WILLIAMS, K., SALAMONE, L., BUSHNELL, T., HUANG, L. S., YANG, Q. & HUANG, J. 2009. Selective expression of CD44, a putative prostate cancer stem cell marker, in neuroendocrine tumor cells of human prostate cancer. *Prostate,* 69**,** 787-98.

PANNUTI, A., FOREMAN, K., RIZZO, P., OSIPO, C., GOLDE, T., OSBORNE, B. & MIELE, L. 2010. Targeting Notch to target cancer stem cells. *Clin Cancer Res,* 16**,** 3141-52.

PARADIS, V., DARGERE, D., LAURENDEAU, I., BENOIT, G., VIDAUD, M., JARDIN, A. & BEDOSSA, P. 1999. Expression of the RNA component of human telomerase (hTR) in prostate cancer, prostatic intraepithelial neoplasia, and normal prostate tissue. *J Pathol,* 189**,** 213-8.

PARK, K. S., JEON, S. H., KIM, S. E., BAHK, Y. Y., HOLMEN, S. L., WILLIAMS, B. O., CHUNG, K. C., SURH, Y. J. & CHOI, K. Y. 2006. APC inhibits ERK pathway activation and cellular proliferation induced by RAS. *J Cell Sci,* 119**,** 819-27.

PARKER, C., SYDES, M. R., CATTON, C., KYNASTON, H., LOGUE, J., MURPHY, C., MORGAN, R. C., MELLON, K., MORASH, C., PARULEKAR, W., PARMAR, M. K., PAYNE, H., SAVAGE, C., STANSFELD, J. & CLARKE, N. W. 2007. Radiotherapy and androgen deprivation in combination after local surgery (RADICALS): a new Medical Research Council/National Cancer Institute of Canada phase III trial of adjuvant treatment after radical prostatectomy. *BJU Int,* 99**,** 1376-9.

PASTRANA, E., SILVA-VARGAS, V. & DOETSCH, F. 2011. Eyes wide open: a critical review of sphere-formation as an assay for stem cells. *Cell Stem Cell,* 8**,** 486-98.

PEARSON, H. B., PHESSE, T. J. & CLARKE, A. R. 2009. K-ras and Wnt signaling synergize to accelerate prostate tumorigenesis in the mouse. *Cancer Res,* 69**,** 94-101.

PEEHL, D. M. 2005. Primary cell cultures as models of prostate cancer development. *Endocr Relat Cancer,* 12**,** 19-47.

PERENTESIS, J. P., BHATIA, S., BOYLE, E., SHAO, Y., SHU, X. O., STEINBUCH, M., SATHER, H. N., GAYNON, P., KIFFMEYER, W., ENVALL-FOX, J. & ROBISON, L. L. 2004. RAS oncogene mutations and outcome of therapy for childhood acute lymphoblastic leukemia. *Leukemia,* 18**,** 685-692.

PERSAD, S., TROUSSARD, A. A., MCPHEE, T. R., MULHOLLAND, D. J. & DEDHAR, S. 2001. Tumor suppressor PTEN inhibits nuclear accumulation of beta-catenin and T cell/lymphoid enhancer factor 1-mediated transcriptional activation. *J Cell Biol,* 153**,** 1161-74.

PFEIFFER, M. J. & SCHALKEN, J. A. 2010. Stem cell characteristics in prostate cancer cell lines. *Eur Urol,* 57**,** 246-254.

PIEDRA, J., MARTINEZ, D., CASTANO, J., MIRAVET, S., DUNACH, M. & DE HERREROS, A. G. 2001. Regulation of beta-catenin structure and activity by tyrosine phosphorylation. *J Biol Chem,* 276**,** 20436-20443.

PIGNON, J. C., GRISANZIO, C., GENG, Y., SONG, J., SHIVDASANI, R. A. & SIGNORETTI, S. 2013. p63-expressing cells are the stem cells of developing prostate, bladder, and colorectal epithelia. *Proc Natl Acad Sci U S A,* 110**,** 8105-10.

PILEPICH, M. V., WINTER, K., LAWTON, C. A., KRISCH, R. E., WOLKOV, H. B., MOVSAS, B., HUG, E. B., ASBELL, S. O. & GRIGNON, D. 2005. Androgen suppression adjuvant to definitive radiotherapy in prostate carcinoma - long-term results of phase III RTOG 85-31. *Int J Radiat Oncol Biol Phys,* 61**,** 1285-90.

PODSYPANINA, K., ELLENSON, L. H., NEMES, A., GU, J., TAMURA, M., YAMADA, K. M., CORDON-CARDO, C., CATORETTI, G., FISHER, P. E. & PARSONS, R. 1999. Mutation of Pten/Mmac1 in mice causes neoplasia in multiple organ systems. *Proc Natl Acad Sci U S A,* 96**,** 1563-8.

POINTIS, G., LATREILLE, M. T. & CEDARD, L. 1980. Gonado-pituitary relationships in the fetal mouse at various times during sexual differentiation. *J Endocrinol,* 86**,** 483-8.

PONTIER, S. M. & MULLER, W. J. 2009. Integrins in mammary-stem-cell biology and breast-cancer progression--a role in cancer stem cells? *J Cell Sci,* 122**,** 207-14.

POTOSKY, A. L., MILLER, B. A., ALBERTSEN, P. C. & KRAMER, B. S. 1995. The role of increasing detection in the rising incidence of prostate cancer. *JAMA,* 273**,** 548-52.

POWELL, A. E., WANG, Y., LI, Y., POULIN, E. J., MEANS, A. L., WASHINGTON, M. K., HIGGINBOTHAM, J. N., JUCHHEIM, A., PRASAD, N., LEVY, S. E., GUO, Y., SHYR, Y., ARONOW, B. J., HAIGIS, K. M., FRANKLIN, J. L. & COFFEY, R. J. 2012. The pan-ErbB negative regulator Lrig1 is an intestinal stem cell marker that functions as a tumor suppressor. *Cell,* 149**,** 146-58.

PRICE, D. 1963. Comparative Aspects of Development and Structure in the Prostate. *Natl Cancer Inst Monogr,* 12**,** 1-27. In SHARMA, P. & SCHREIBER-AGUS, N. 1999. Mouse models of prostate cancer. Oncogene, 18, 5349-55.

PRIOR, I. A., LEWIS, P. D. & MATTOS, C. 2012. A Comprehensive Survey of Ras Mutations in Cancer. *Cancer Res,* 72**,** 2457-2467.

PRIULLA, M., CALASTRETTI, A., BRUNO, P., AZZARITI, A., PARADISO, A., CANTI, G. & NICOLIN, A. 2007. Preferential chemosensitization of PTEN-mutated prostate cells by silencing the Akt kinase. *Prostate,* 67**,** 782-9.

PROTECT ISRCTN20141297. Prostate Testing for Cancer and Treatment (ProtecT). NIHR Health Technology Assessment programme.

PULLEN, N., DENNIS, P. B., ANDJELKOVIC, M., DUFNER, A., KOZMA, S. C., HEMMINGS, B. A. & THOMAS, G. 1998. Phosphorylation and activation of p70s6k by PDK1. *Science,* 279**,** 707-10.

PYLAYEVA-GUPTA, Y., GRABOCKA, E. & BAR-SAGI, D. 2011. RAS oncogenes: weaving a tumorigenic web. *Nat Rev Cancer,* 11**,** 761-774.

QUINTANA, E., SHACKLETON, M., SABEL, M. S., FULLEN, D. R., JOHNSON, T. M. & MORRISON, S. J. 2008. Efficient tumour formation by single human melanoma cells. *Nature,* 456**,** 593-598.

REES, J., PATEL, B., MACDONAGH, R. & PERSAD, R. 2004. Cryosurgery for prostate cancer. *BJU Int,* 93**,** 710-4.

REYA, T., MORRISON, S. J., CLARKE, M. F. & WEISSMAN, I. L. 2001. Stem cells, cancer, and cancer stem cells. *Nature,* 414**,** 105-11.

RICHARDSON, G. D., ROBSON, C. N., LANG, S. H., NEAL, D. E., MAITLAND, N. J. & COLLINS, A. T. 2004. CD133, a novel marker for human prostatic epithelial stem cells. *J Cell Sci,* 117**,** 3539-45.

RICHTER, R., BISTRIAN, R., ESCHER, S., FORSSMANN, W. G., VAKILI, J., HENSCHLER, R., SPODSBERG, N., FRIMPONG-BOATENG, A. & FORSSMANN, U. 2005. Quantum proteolytic activation of chemokine CCL15 by neutrophil granulocytes modulates mononuclear cell adhesiveness. *J Immunol,* 175**,** 1599-608.

RIMM, D. L., CACA, K., HU, G., HARRISON, F. B. & FEARON, E. R. 1999. Frequent nuclear/cytoplasmic localization of beta-catenin without exon 3 mutations in malignant melanoma. *Am J Pathol,* 154**,** 325-329.

RISBRIDGER, G. P., ELLEM, S. J. & MCPHERSON, S. J. 2007. Estrogen action on the prostate gland: a critical mix of endocrine and paracrine signaling. *J Mol Endocrinol,* 39**,** 183-8.

RISBRIDGER, G. P., WANG, H., FRYDENBERG, M. & CUNHA, G. 2001. The metaplastic effects of estrogen on mouse prostate epithelium: proliferation of cells with basal cell phenotype. *Endocrinology,* 142**,** 2443-50.

RIZZO, S., ATTARD, G. & HUDSON, D. L. 2005. Prostate epithelial stem cells. *Cell Prolif. 2005 Dec;38(6):363-74.,* 38**,** 363-74.

ROACH, M., III, BAE, K., SPEIGHT, J., WOLKOV, H. B., RUBIN, P., LEE, R. J., LAWTON, C., VALICENTI, R., GRIGNON, D. & PILEPICH, M. V. 2008. Short-term neoadjuvant androgen deprivation therapy and external-beam radiotherapy for locally advanced prostate cancer: long-term results of RTOG 8610. *J Clin Oncol,* 26**,** 585-91.

ROBINSON, E. J., NEAL, D. E. & COLLINS, A. T. 1998. Basal cells are progenitors of luminal cells in primary cultures of differentiating human prostatic epithelium. *Prostate,* 37**,** 149-60.

ROCA, H., VARSOS, Z. & PIENTA, K. J. 2008. CCL2 protects prostate cancer PC3 cells from autophagic death via phosphatidylinositol 3-kinase/AKT-dependent survivin up-regulation. *J Biol Chem,* 283**,** 25057-73.

ROMANO, R. A., ORTT, K., BIRKAYA, B., SMALLEY, K. & SINHA, S. 2009. An active role of the DeltaN isoform of p63 in regulating basal keratin genes K5 and K14 and directing epidermal cell fate. *PLoS One,* 4**,** e5623.

ROOSE, J., MOLENAAR, M., PETERSON, J., HURENKAMP, J., BRANTJES, H., MOERER, P., VAN DE WETERING, M., DESTREE, O. & CLEVERS, H. 1998. The Xenopus Wnt effector XTcf-3 interacts with Groucho-related transcriptional repressors. *Nature,* 395.

ROSEN, J. M. & JORDAN, C. T. 2009. The increasing complexity of the cancer stem cell paradigm. *Science* 324**,** 1670-1673.
ROY-BURMAN, P., WU, H., POWELL, W. C., HAGENKORD, J. & COHEN, M. B. 2004. Genetically defined mouse models that mimic natural aspects of human prostate cancer development. *Endocr Relat Cancer,* 11**,** 225-54.
RUBINFELD, B., ALBERT, I., PORFIRI, E., FIOL, C., MUNEMITSU, S. & POLAKIS, P. 1996. Binding of GSK3beta to the APC-beta-catenin complex and regulation of complex assembly. *Science,* 272**,** 1023-1026.
RUBINSTEIN, S. & BREITBART, H. 1990 Transport and localization of spermine in Ram spermatozoa. *Bio Reprod,* 42**,** Suppl 1, Abstr 139.
RUPTIER, C., DE GASPERIS, A., ANSIEAU, S., GRANJON, A., TANIERE, P., LAFOSSE, I., SHI, H., PETITJEAN, A., TARANCHON-CLERMONT, E., TRIBOLLET, V., VOELTZEL, T., SCOAZEC, J. Y., MAGUER-SATTA, V., PUISIEUX, A., HAINAUT, P., CAVARD, C. & CARON DE FROMENTEL, C. 2011. TP63 P2 promoter functional analysis identifies beta-catenin as a key regulator of DeltaNp63 expression. *Oncogene,* 30**,** 4656-65.
SARKER, D., REID, A. H., YAP, T. A. & DE BONO, J. S. 2009. Targeting the PI3K/AKT pathway for the treatment of prostate cancer. *Clin Cancer Res,* 15**,** 4799-805.
SATO, T., VAN ES, J. H., SNIPPERT, H. J., STANGE, D. E., VRIES, R. G., VAN DEN BORN, M., BARKER, N., SHROYER, N. F., VAN DE WETERING, M. & CLEVERS, H. 2011. Paneth cells constitute the niche for Lgr5 stem cells in intestinal crypts. *Nature,* 469**,** 415-8.
SAUER, B. & HENDERSON, N. 1989. Cre-stimulated recombination at loxP-containing DNA sequences placed into the mammalian genome. *Nucleic Acids Res,* 17**,** 147-61.
SAWICKI, J. A. & ROTHMAN, C. J. 2002. Evidence for stem cells in cultures of mouse prostate epithelial cells. *Prostate,* 50**,** 46-53.
SCHALKEN, J. A. & VAN LEENDERS, G. 2003. Cellular and molecular biology of the prostate: stem cell biology. *Urology,* 62**,** 11-20.
SCHERL, A., LI, J. F., CARDIFF, R. D. & SCHREIBER-AGUS, N. 2004. Prostatic intraepithelial neoplasia and intestinal metaplasia in prostates of probasin-RAS transgenic mice. *Prostate,* 59**,** 448-59.
SCHMELZ, M., MOLL, R., HESSE, U., PRASAD, A. R., GANDOLFI, J. A., HASAN, S. R., BARTHOLDI, M. & CRESS, A. E. 2005. Identification of a stem cell candidate in the normal human prostate gland. *Eur J Cell Biol,* 84**,** 341-54.
SCHMIDT, E. K., FICHELSON, S. & FELLER, S. M. 2004. PI3 kinase is important for Ras, MEK and Erk activation of Epo-stimulated human erythroid progenitors. *BMC Biol,* 2**,** 7.
SCHNEIDER, C. A., RASBAND, W. S. & ELICEIRI, K. W. 2012. NIH Image to ImageJ: 25 years of image analysis. *Nature Methods,* 9**,** 671-675.
SCHUBBERT, S., SHANNON, K. & BOLLAG, G. 2007. Hyperactive Ras in developmental disorders and cancer. *Nat Rev Cancer,* 7**,** 295-308.
SCHULMAN, C. C., DEBRUYNE, F. M., FORSTER, G., SELVAGGI, F. P., ZLOTTA, A. R. & WITJES, W. P. 2000. 4-Year follow-up results of a European prospective randomized study on neoadjuvant hormonal therapy prior to radical prostatectomy in T2-3N0M0 prostate cancer. European Study Group on Neoadjuvant Treatment of Prostate Cancer. *Eur Urol,* 38**,** 706-13.
SELIGER, B., ET AL. 1996. Suppression of MHC class I antigens in oncogenic transformants: association with decreased recognition by cytotoxic T lymphocytes. *Exp Hematol,* 24**,** 1275-1279.
SELVARAJ, N., BUDKA, J. A., FERRIS, M. W., JERDE, T. J. & HOLLENHORST, P. C. 2014. Prostate cancer ETS rearrangements switch a cell migration gene expression program from RAS/ERK to PI3K/AKT regulation. *Mol Cancer,* 13**,** 61.
SETH, A. & WATSON, D. K. 2005. ETS transcription factors and their emerging roles in human cancer. *Eur J Cancer,* 41**,** 2462-78.
SHACKLETON, M., QUINTANA, E., FEARON, E. R. & MORRISON, S. J. 2009. Heterogeneity in cancer: cancer stem cells versus clonal evolution. *Cell,* 138**,** 822-829.

SHAH, A., SWAIN, W. A., RICHARDSON, D., EDWARDS, J., STEWART, D. J., RICHARDSON, C. M., SWINSON, D. E., PATEL, D., JONES, J. L. & O'BYRNE, K. J. 2005. Phospho-akt expression is associated with a favorable outcome in non-small cell lung cancer. *Clin Cancer Res,* 11**,** 2930-6.

SHANNON, J. M. & CUNHA, G. R. 1983. Autoradiographic localization of androgen binding in the developing mouse prostate. *Prostate,* 4**,** 367-73.

SHAPPELL, S. B., THOMAS, G. V., ROBERTS, R. L., HERBERT, R., ITTMANN, M. M., RUBIN, M. A., HUMPHREY, P. A., SUNDBERG, J. P., ROZENGURT, N., BARRIOS, R., WARD, J. M. & CARDIFF, R. D. 2004. Prostate pathology of genetically engineered mice: definitions and classification. The consensus report from the Bar Harbor meeting of the Mouse Models of Human Cancer Consortium Prostate Pathology Committee. *Cancer Res,* 64**,** 2270-305.

SHARMA, M., CHUANG, W. W. & SUN, Z. 2002. Phosphatidylinositol 3-kinase/Akt stimulates androgen pathway through GSK3beta inhibition and nuclear beta-catenin accumulation. *J Biol Chem,* 277**,** 30935-41.

SHAYESTEH, L., LU, Y. & KUO, W. L. E. A. 1999. PIK3CA is implicated as an oncogene in ovarian cancer. *Nat Genet,* 21**,** 99-102.

SHELLEY, M. D., KUMAR, S., COLES, B., WILT, T., STAFFURTH, J. & MASON, M. D. 2009a. Adjuvant hormone therapy for localised and locally advanced prostate carcinoma: a systematic review and meta-analysis of randomised trials. *Cancer Treat Rev,* 35**,** 540-6.

SHELLEY, M. D., KUMAR, S., WILT, T., STAFFURTH, J., COLES, B. & MASON, M. D. 2009b. A systematic review and meta-analysis of randomised trials of neo-adjuvant hormone therapy for localised and locally advanced prostate carcinoma. *Cancer Treat Rev,* 35**,** 9-17.

SHEN, M. M. & ABATE-SHEN, C. 2007. Pten inactivation and the emergence of androgen-independent prostate cancer. *Cancer Res,* 67**,** 6535-8.

SHMELKOV, S. V., BUTLER, J. M., HOOPER, A. T., HORMIGO, A., KUSHNER, J. & MILDE, T. E. A. 2008. CD133 expression is not restricted to stem cells, and both CD133+ and CD133- metastatic colon cancer cells initiate tumors. *J Clin Invest,* 118**,** 2111-2120.

SHOU, J., ROSS, S., KOEPPEN, H., DE SAUVAGE, F. J. & GAO, W. Q. 2001. Dynamics of notch expression during murine prostate development and tumorigenesis. *Cancer Res,* 61**,** 7281-7.

SHTUTMAN, M., ZHURINSKY, J., SIMCHA, I., ALBANESE, C., D'AMICO, M., PESTELL, R. & BEN-ZE'EV, A. 1999. The cyclin D1 gene is a target of the beta-catenin/LEF-1 pathway. *Proc Natl Acad Sci U S A,* 96**,** 5522-7.

SIGNORETTI, S., WALTREGNY, D., DILKS, J., ISAAC, B., LIN, D., GARRAWAY, L., YANG, A., MONTIRONI, R., MCKEON, F. & LODA, M. 2000. p63 is a prostate basal cell marker and is required for prostate development. *Am J Pathol,* 157**,** 1769-75.

SINGEC, I., KNOTH, R., MEYER, R. P., MACIACZYK, J., VOLK, B., NIKKHAH, G., FROTSCHER, M. & SNYDER, E. Y. 2006. Defining the actual sensitivity and specificity of the neurosphere assay in stem cell biology. *Nat Methods,* 3**,** 801-6.

SINGH, A. S. & FIGG, W. D. 2005. In vivo models of prostate cancer metastasis to bone. *J Urol,* 174**,** 820-6.

SINGH, S. K., HAWKINS, C., CLARKE, I. D., SQUIRE, J. A., BAYANI, J. & HIDE, T., ET AL. 2004. Identification of human brain tumour initiating cells. *Nature,* 432**,** 396-401.

SIROVICH, B. E., SCHWARTZ, L. M. & WOLOSHIN, S. 2003. Screening men for prostate and colorectal cancer in the United States: does practice reflect the evidence? *JAMA,* 289**,** 1414-20.

SLOMIANY, M. G., DAI, L., TOLLIVER, L. B., GRASS, G. D., ZENG, Y. & TOOLE, B. P. 2009. Inhibition of Functional Hyaluronan-CD44 Interactions in CD133-positive Primary Human Ovarian Carcinoma Cells by Small Hyaluronan Oligosaccharides. *Clin Cancer Res,* 15**,** 7593-7601.

SMALLEY, M. J., SARA, E., PATERSON, H., NAYLOR, S., COOK, D., JAYATILAKE, H., FRYER, M. G., HUTCHINSON, L., FRY, M. J. & DALE, T. C. 1999. Interaction of axin and Dvl-2 proteins regulates Dvl-2-stimulated TCF- dependent transcription. *EMBO J,* 18**,** 2823-2835.

SNIPPERT, H. J. & CLEVERS, H. 2011. Tracking adult stem cells. *EMBO Rep,* 12**,** 113-122.

SOLANAS, G., MIRAVET, S., CASAGOLDA, D., CASTANO, J., RAURELL, I., CORRIONERO, A., DE HERREROS, A. G. & DUNACH, M. 2004. Beta-catenin and plakoglobin N- and C-tails determine ligand specificity. *J Biol Chem,* 279**,** 49849-49856.

SONG, L. N. & GELMANN, E. P. 2005. Interaction of beta-catenin and TIF2/GRIP1 in transcriptional activation by the androgen receptor. *J Biol Chem,* 280**,** 37853-67.

SONG, M. S., SALMENA, L. & PANDOLFI, P. P. 2012. The functions and regulation of the PTEN tumour suppressor. *Nat Rev Mol Cell Biol,* 13**,** 283-96.

SONTAG, E., FEDOROV, S., KAMIBAYASHI, C., ROBBINS, D., COBB, M. & MUMBY, M. 1993. The interaction of SV40 small tumor antigen with protein phosphatase 2A stimulates the map kinase pathway and induces cell proliferation. *Cell,* 75**,** 887-97.

SORIANO, P. 1999. Generalized lacZ expression with the ROSA26 Cre reporter strain. *Nat Genet,* 21**,** 70-1.

STAACK, A., DONJACOUR, A. A., BRODY, J., CUNHA, G. R. & CARROLL, P. 2003. Mouse urogenital development: a practical approach. *Differentiation,* 71**,** 402-13.

STAMBOLIC, V., TSAO, M. S., MACPHERSON, D., SUZUKI, A., CHAPMAN, W. B. & MAK, T. W. 2000. High incidence of breast and endometrial neoplasia resembling human Cowden syndrome in pten+/- mice. *Cancer Res,* 60**,** 3605-11.

STASIAK, P. C., PURKIS, P. E., LEIGH, I. M. & LANE, E. B. 1989. Keratin 19: predicted amino acid sequence and broad tissue distribution suggest it evolved from keratinocyte keratins. *J Invest Dermatol,* 92**,** 707-16.

STERNBERG, N. & HAMILTON, D. 1981. Bacteriophage P1 site-specific recombination. I. Recombination between loxP sites. *J Mol Biol,* 150**,** 467-86.

STERNBERG, N., HAMILTON, D. & HOESS, R. 1981. Bacteriophage P1 site-specific recombination. II. Recombination between loxP and the bacterial chromosome. *J Mol Biol,* 150**,** 487-507.

STONE, K. R., MICKEY, D. D., WUNDERLI, H., MICKEY, G. H. & PAULSON, D. F. 1978. Isolation of a human prostate carcinoma cell line (DU 145). *Int J Cancer,* 21**,** 274-81.

STOYANOVA, T., GOLDSTEIN, A. S., CAI, H., DRAKE, J. M., HUANG, J. & WITTE, O. N. 2012. Regulated proteolysis of Trop2 drives epithelial hyperplasia and stem cell self-renewal via beta-catenin signaling. *Genes Dev,* 26**,** 2271-85.

STRAIN, A. J. & CROSBY, H. A. 2000. Hepatic stem cells. *Gut,* 46**,** 743-5.

SUGIMURA, Y., CUNHA, G. R. & DONJACOUR, A. A. 1986a. Morphogenesis of ductal networks in the mouse prostate. *Biol Reprod,* 34**,** 961-71.

SUGIMURA, Y., CUNHA, G. R., DONJACOUR, A. A., BIGSBY, R. M. & BRODY, J. R. 1986b. Whole-mount autoradiography study of DNA synthetic activity during postnatal development and androgen-induced regeneration in the mouse prostate. *Biol Reprod,* 34**,** 985-95.

SUN, Y., CAMPISI, J., HIGANO, C., BEER, T. M., PORTER, P., COLEMAN, I., TRUE, L. & NELSON, P. S. 2012. Treatment-induced damage to the tumor microenvironment promotes prostate cancer therapy resistance through WNT16B. *Nat Med,* 18**,** 1359-68.

SUNAYAMA, J., MATSUDA, K., SATO, A., TACHIBANA, K., SUZUKI, K., NARITA, Y., SHIBUI, S., SAKURADA, K., KAYAMA, T., TOMIYAMA, A. & KITANAKA, C. 2010. Crosstalk between the PI3K/mTOR and MEK/ERK pathways involved in the maintenance of self-renewal and tumorigenicity of glioblastoma stem-like cells. *Stem Cells,* 28**,** 1930-9.

SUTHERLAND, B. W., KNOBLAUGH, S. E., KAPLAN-LEFKO, P. J., WANG, F., HOLZENBERGER, M. & GREENBERG, N. M. 2008. Conditional deletion of insulin-like growth factor-I receptor in prostate epithelium. *Cancer Res,* 68**,** 3495-504.

SUZUKI, A., YAMAGUCHI, M. T., OHTEKI, T., SASAKI, T., KAISHO, T., KIMURA, Y., YOSHIDA, R., WAKEHAM, A., HIGUCHI, T., FUKUMOTO, M., TSUBATA, T., OHASHI, P. S., KOYASU, S., PENNINGER, J. M., NAKANO, T. & MAK, T. W. 2001. T cell-specific loss of Pten leads to defects in central and peripheral tolerance. *Immunity,* 14**,** 523-34.

SUZUKI, H., FREIJE, D., NUSSKERN, D. R., OKAMI, K., CAIRNS, P., SIDRANSKY, D., ISAACS, W. B. & BOVA, G. S. 1998. Interfocal heterogeneity of PTEN/MMAC1 gene alterations in multiple metastatic prostate cancer tissues. *Cancer Res,* 58**,** 204-209.

TAKEDA, H. & CHANG, C. 1991. Immunohistochemical and in-situ hybridization analysis of androgen receptor expression during the development of the mouse prostate gland. *J Endocrinol,* 129**,** 83-9.

TAKEDA, H., MIZUNO, T. & LASNITZKI, I. 1985. Autoradiographic studies of androgen-binding sites in the rat urogenital sinus and postnatal prostate. *J Endocrinol,* 104**,** 87-92.

TAYLOR, B. S., SCHULTZ, N., HIERONYMUS, H., GOPALAN, A., XIAO, Y., CARVER, B. S., ARORA, V. K., KAUSHIK, P., CERAMI, E., REVA, B., ANTIPIN, Y., MITSIADES, N., LANDERS, T., DOLGALEV, I., MAJOR, J. E., WILSON, M., SOCCI, N. D., LASH, A. E., HEGUY, A., EASTHAM, J. A., SCHER, H. I., REUTER, V. E., SCARDINO, P. T., SANDER, C., SAWYERS, C. L. & GERALD, W. L. 2010. Integrative genomic profiling of human prostate cancer. *Cancer Cell,* 18**,** 11-22.

TAYLOR, G., LEHRER, M. S., JENSEN, P. J., SUN, T. T. & LAVKER, R. M. 2000. Involvement of follicular stem cells in forming not only the follicle but also the epidermis. *Cell,* 102**,** 451-61.

TESTA, J. R. & BELLACOSA, A. 2001. AKT plays a central role in tumorigenesis. *Proc Natl Acad Sci USA,* 98**,** 10983-5.

THOMPSON, I. M., TANGEN, C. M., PARADELO, J., LUCIA, M. S., MILLER, G., TROYER, D., MESSING, E., FORMAN, J., CHIN, J., SWANSON, G., CANBY-HAGINO, E. & CRAWFORD, E. D. 2009. Adjuvant radiotherapy for pathological T3N0M0 prostate cancer significantly reduces risk of metastases and improves survival: long-term followup of a randomized clinical trial. *J Urol,* 181**,** 956-62.

TIMMS, B. G. 2008. Prostate development: a historical perspective. *Differentiation,* 76**,** 565-77.

TIMMS, B. G., MOHS, T. J. & DIDIO, L. J. 1994. Ductal budding and branching patterns in the developing prostate. *J Urol,* 151**,** 1427-32.

TOMLINS, S. A., RHODES, D. R., PERNER, S., DHANASEKARAN, S. M., MEHRA, R., SUN, X. W., VARAMBALLY, S., CAO, X., TCHINDA, J., KUEFER, R., LEE, C., MONTIE, J. E., SHAH, R. B., PIENTA, K. J., RUBIN, M. A. & CHINNAIYAN, A. M. 2005. Recurrent fusion of TMPRSS2 and ETS transcription factor genes in prostate cancer. *Science,* 310**,** 644-8.

TRAN THANG, N. N., ET AL. 2010. Immune infiltration of spontaneous mouse astrocytomas is dominated by immunosuppressive cells from early stages of tumor development. *Cancer Res,* 70**,** 4829-4839.

TREROTOLA, M., LI, J., ALBERTI, S. & LANGUINO, L. R. 2012. Trop-2 inhibits prostate cancer cell adhesion to fibronectin through the beta1 integrin-RACK1 axis. *J Cell Physiol,* 227**,** 3670-7.

TRIMBOLI, A. J., CANTEMIR-STONE, C. Z., LI, F., WALLACE, J. A., MERCHANT, A. & CREASAP, N. E. A. 2009. Pten in stromal fibroblasts suppresses mammary epithelial tumours. *Nature,* 461**,** 1084-1091.

TROTMAN, L. C., NIKI, M., DOTAN, Z. A., KOUTCHER, J. A., DI CRISTOFANO, A., XIAO, A., KHOO, A. S., ROY-BURMAN, P., GREENBERG, N. M., VAN DYKE, T., CORDON-CARDO, C. & PANDOLFI, P. P. 2003. Pten dose dictates cancer progression in the prostate. *PLoS Biol,* 1**,** E59.

TRUICA, C. I., BYERS, S. & GELMANN, E. P. 2000. Beta-catenin affects androgen receptor transcriptional activity and ligand specificity. *Cancer Res,* 60**,** 4709-13.

TSUJII, M. E. A. 1998. Cyclooxygenase regulates angiogenesis induced by colon cancer cells. *Cell,* 93**,** 705-716.

TSUJIKAWA, M., ET AL. 1999. Identification of the gene responsible for gelatinous drop-like corneal dystrophy. *Nat Genet,* 21**,** 420-423.

TSUJIMURA, A., FUJITA, K., KOMORI, K., TAKAO, T., MIYAGAWA, Y., TAKADA, S., MATSUMIYA, K., NONOMUR, N. & OKUYAMA, A. 2007. Prostatic stem cell marker identified by cDNA microarray in mouse. *J Urol,* 178**,** 686-91.

TSUJIMURA, A., KOIKAWA, Y., SALM, S., TAKAO, T., COETZEE, S., MOSCATELLI, D., SHAPIRO, E., LEPOR, H., SUN, T. T. & WILSON, E. L. 2002. Proximal location of mouse prostate epithelial stem cells: a model of prostatic homeostasis. *J Cell Biol,* 157**,** 1257-65.

UCHIDA, N., BUCK, D. W., HE, D., REITSMA, M. J., MASEK, M. & PHAN, T. V., ET AL. 2000. Direct isolation of human central nervous system stem cells. *PNAS USA,* 97**,** 14720-14725.

UICC, U. F. I. C. C. 2009. TNM Classification of Malignant Tumours 7th Edition. *Prostate Cancer.* UICC.

VADLAKONDA, L., PASUPULETI, M. & PALLU, R. 2013. Role of PI3K-AKT-mTOR and Wnt Signaling Pathways in Transition of G1-S Phase of Cell Cycle in Cancer Cells. *Front Oncol,* 3**,** 85.

VALKENBURG, K. C. & WILLIAMS, B. O. 2011. Mouse models of prostate cancer. *Prostate Cancer,* 2011**,** 895238.

VAN DE SANDE, T., ROSKAMS, T., LERUT, E., JONIAU, S., VAN POPPEL, H., VERHOEVEN, G. & SWINNEN, J. V. 2005. High-level expression of fatty acid synthase in human prostate cancer tissues is linked to activation and nuclear localization of Akt/PKB. *J Pathol,* 206**,** 214-9.

VAN DER KWAST, T. H., TETU, B., SUBURU, E. R., GOMEZ, J., LEMAY, M. & LABRIE, F. 1998. Cycling activity of benign prostatic epithelial cells during long-term androgen blockade: evidence for self-renewal of luminal cells. *J Pathol,* 186**,** 406-9.

VAN LEENDERS, G., DIJKMAN, H., HULSBERGEN-VAN DE KAA, C., RUITER, D. & SCHALKEN, J. 2000. Demonstration of intermediate cells during human prostate epithelial differentiation in situ and in vitro using triple-staining confocal scanning microscopy. *Lab Invest,* 80**,** 1251-8.

VANDER HAAR, E., LEE, S. I., BANDHAKAVI, S., GRIFFIN, T. J. & KIM, D. H. 2007. Insulin signalling to mTOR mediated by the Akt/PKB substrate PRAS40. *Nature Cell Biol,* 9**,** 316-323.

VASKO, V., SAJI, M., HARDY, E., KRUHLAK, M., LARIN, A., SAVCHENKO, V., MIYAKAWA, M., ISOZAKI, O., MURAKAMI, H., TSUSHIMA, T., BURMAN, K. D., DE MICCO, C. & RINGEL, M. D. 2004. Akt activation and localisation correlate with tumour invasion and oncogene expression in thyroid cancer. *J Med Genet,* 41**,** 161-70.

VERHAGEN, A. P., RAMAEKERS, F. C., AALDERS, T. W., SCHAAFSMA, H. E., DEBRUYNE, F. M. & SCHALKEN, J. A. 1992. Colocalization of basal and luminal cell-type cytokeratins in human prostate cancer. *Cancer Res,* 52**,** 6182-7.

VERHAGEN, P. C., VAN DUIJN, P. W., HERMANS, K. G., LOOIJENGA, L. H., VAN GURP, R. J., STOOP, H., VAN DER KWAST, T. H. & TRAPMAN, J. 2006. The PTEN gene in locally progressive prostate cancer is preferentially inactivated by bi-allelic gene deletion. *J Pathol,* 208**,** 699-707.

VERHEYEN, E. M. & GOTTARDI, C. J. 2010. Regulation of Wnt/beta-catenin signaling by protein kinases. *Dev Dyn,* 239**,** 34-44.

VERMEULEN, L., DE SOUSA, E. M. F., VAN DER HEIJDEN, M., CAMERON, K., DE JONG, J. H., BOROVSKI, T., TUYNMAN, J. B., TODARO, M., MERZ, C., RODERMOND, H., SPRICK, M. R., KEMPER, K., RICHEL, D. J., STASSI, G. & MEDEMA, J. P. 2010. Wnt activity defines colon cancer stem cells and is regulated by the microenvironment. *Nat Cell Biol,* 12**,** 468-76.

VISVADER, J. E. & LINDEMAN, G. J. 2008. Cancer stem cells in solid tumours: accumulating evidence and unresolved questions. *Nat Rev Cancer,* 8**,** 755-68.

VIVANCO, I. E. A. 2007. Identification of the JNK signaling pathway as a functional target of the tumor suppressor PTEN. *Cancer Cell,* 11**,** 555-569.

VOELLER, H. J., TRUICA, C. I. & GELMANN, E. P. 1998. Beta-catenin mutations in human prostate cancer. *Cancer Res,* 58**,** 2520-3.

WALZ, J., BURNETT, A. L., COSTELLO, A. J., EASTHAM, J. A., GRAEFEN, M., GUILLONNEAU, B., MENON, M., MONTORSI, F., MYERS, R. P., ROCCO, B. & VILLERS, A. 2009. A Critical Analysis of the Current Knowledge of Surgical Anatomy Related to Optimization of Cancer Control and Preservation of Continence and Erection in Candidates for Radical Prostatectomy. *European Urology,* 57**,** 179-192.

WANDZIOCH, E., EDLING, C. E., PALMER, R. H., CARLSSON, L. & HALLBERG, B. 2004. Activation of the MAP kinase pathway by c-Kit is PI-3 kinase dependent in hematopoietic progenitor/stem cell lines. *Blood,* 104**,** 51-7.

WANG, G., WANG, J. & SADAR, M. D. 2008. Crosstalk between the androgen receptor and beta-catenin in castrate-resistant prostate cancer. *Cancer Res,* 68**,** 9918-27.
WANG, S., GAO, J., LEI, Q., ROZENGURT, N., PRITCHARD, C., JIAO, J., THOMAS, G. V., LI, G., ROY-BURMAN, P., NELSON, P. S., LIU, X. & WU, H. 2003. Prostate-specific deletion of the murine Pten tumor suppressor gene leads to metastatic prostate cancer. *Cancer Cell,* 4**,** 209-21.
WANG, S., GARCIA, A. J., WU, M., LAWSON, D. A., WITTE, O. N. & WU, H. 2006. Pten deletion leads to the expansion of a prostatic stem/progenitor cell subpopulation and tumor initiation. *Proc Natl Acad Sci U S A,* 103**,** 1480-5.
WANG, X., KRUITHOF-DE JULIO, M., ECONOMIDES, K. D., WALKER, D., YU, H., HALILI, M. V., HU, Y. P., PRICE, S. M., ABATE-SHEN, C. & SHEN, M. M. 2009. A luminal epithelial stem cell that is a cell of origin for prostate cancer. *Nature,* 461**,** 495-500.
WANG, X. D., ET AL. 2007. Expression profiling of the mouse prostate after castration and hormone replacement: Implication of H-cadherin in prostate tumorigenesis. *Differentiation,* 75**,** 219-234.
WANG, X. D., SHOU, J., WONG, P., FRENCH, D. M. & GAO, W. Q. 2004. Notch1-expressing cells are indispensable for prostatic branching morphogenesis during development and re-growth following castration and androgen replacement. *J Biol Chem,* 279**,** 24733-44.
WANG, Y., KRIVTSOV, A. V., SINHA, A. U., NORTH, T. E., GOESSLING, W., FENG, Z., ZON, L. I. & ARMSTRONG, S. A. 2010. The Wnt/beta-catenin pathway is required for the development of leukemia stem cells in AML. *Science,* 327**,** 1650-3.
WANG, Z. A., MITROFANOVA, A., BERGREN, S. K., ABATE-SHEN, C., CARDIFF, R. D., CALIFANO, A. & SHEN, M. M. 2013. Lineage analysis of basal epithelial cells reveals their unexpected plasticity and supports a cell-of-origin model for prostate cancer heterogeneity. *Nat Cell Biol,* 15**,** 274-83.
WANG, Z. A. & SHEN, M. M. 2011. Revisiting the concept of cancer stem cells in prostate cancer. *Oncogene,* 30**,** 1261-71.
WARDE, P., MASON, M., DING, K., KIRKBRIDE, P., BRUNDAGE, M., COWAN, R., GOSPODAROWICZ, M., SANDERS, K., KOSTASHUK, E., SWANSON, G., BARBER, J., HILTZ, A., PARMAR, M. K., SATHYA, J., ANDERSON, J., HAYTER, C., HETHERINGTON, J., SYDES, M. R., PARULEKAR, W. & INVESTIGATORS, N. C. P. M. U. P. 2011. Combined androgen deprivation therapy and radiation therapy for locally advanced prostate cancer: a randomised, phase 3 trial. *Lancet,* 378**,** 2104-11.
WATT, F. M. & DRISKELL, R. R. 2010. The therapeutic potential of stem cells. *Philos Trans R Soc Lond B Biol Sci,* 365**,** 155-63.
WCISU 2009. Urological Cancers; Cancers in Wales, 1995-2009. 1=13.
WEBER, M. J. & GIOELI, D. 2004. Ras signaling in prostate cancer progression. *J Cell Biochem,* 91**,** 13-25.
WEI, C., GUOMIN, W., YUJUN, L. & RUIZHE, Q. 2007. Cancer stem-like cells in human prostate carcinoma cells DU145: the seeds of the cell line? *Cancer Biol Ther,* 6**,** 763-768.
WELSH CANCER INTELLIGENCE AND SURVEILLANCE UNIT, W. C. I. S. U. 2009. Urological Cancers; Cancers in Wales, 1995-2009.
WHITAKER, H. C., GIRLING, J., WARREN, A. Y., LEUNG, H., MILLS, I. G. & NEAL, D. E. 2008. Alterations in beta-catenin expression and localization in prostate cancer. *Prostate,* 68**,** 1196-205.
WIDMARK, A., KLEPP, O., SOLBERG, A., DAMBER, J. E., ANGELSEN, A., FRANSSON, P., LUND, J. A., TASDEMIR, I., HOYER, M., WIKLUND, F., FOSSÅ, S. D., STUDY, S. P. C. G. & ONCOLOGY, S. A. F. U. 2009. Endocrine treatment, with or without radiotherapy, in locally advanced prostate cancer (SPCG-7/SFUO-3): an open randomised phase III trial. *Lancet,* 373**,** 301-8.
WIEGEL, T., BARTKOWIAK, D., BOTTKE, D., BRONNER, C., STEINER, U., SIEGMANN, A., GOLZ, R., STORKEL, S., WILLICH, N., SEMJONOW, A., STOCKLE, M., RUBE, C., REBMANN, U., KALBLE, T., FELDMANN, H. J., WIRTH, M., HOFMANN, R., ENGENHART-CABILLIC, R., HINKE, A.,

HINKELBEIN, W. & MILLER, K. 2014. Adjuvant Radiotherapy Versus Wait-and-See After Radical Prostatectomy: 10-year Follow-up of the ARO 96-02/AUO AP 09/95 Trial. *Eur Urol*.

WIELENGA, V. J., SMITS, R., KORINEK, V., SMIT, L., KIELMAN, M., FODDE, R., CLEVERS, H. & PALS, S. T. 1999. Expression of CD44 in Apc and Tcf mutant mice implies regulation by the WNT pathway. *Am J Pathol,* 154**,** 515-23.

WILLIAMS, D. A. 1993. Ex vivo expansion of hematopoietic stem and progenitor cells--robbing Peter to pay Paul? *Blood,* 81**,** 3169-72.

WILT, T. J., BRAWER, M. K., JONES, K. M., BARRY, M. J., ARONSON, W. J., FOX, S., GINGRICH, J. R., WEI, J. T., GILHOOLY, P., GROB, B. M., NSOULI, I., IYER, P., CARTAGENA, R., SNIDER, G., ROEHRBORN, C., SHARIFI, R., BLANK, W., PANDYA, P., ANDRIOLE, G. L., CULKIN, D., WHEELER, T. & PROSTATE CANCER INTERVENTION VERSUS OBSERVATION TRIAL STUDY, G. 2012. Radical prostatectomy versus observation for localized prostate cancer. *N Engl J Med,* 367**,** 203-13.

WOODWARD, W. A., CHEN, M. S., BEHBOD, F., ALFARO, M. P., BUCHHOLZ, T. A. & ROSEN, J. M. 2007. WNT/beta-catenin mediates radiation resistance of mouse mammary progenitor cells. *Proc Natl Acad Sci U S A,* 104**,** 618-23.

WRIGHT, K., WILSON, P., MORLAND, S., CAMPBELL, I., WALSH, M., HURST, T., WARD, B., CUMMINGS, M. & CHENEVIX-TRENCH, G. 1999. Beta-catenin mutation and expression analysis in ovarian cancer: Exon 3 mutations and nuclear translocation in 16% of endometrioid tumours. *Int J Cancer,* 82**,** 625-629.

WU, X., WU, J., HUANG, J., POWELL, W. C., ZHANG, J., MATUSIK, R. J., SANGIORGI, F. O., MAXSON, R. E., SUCOV, H. M. & ROY-BURMAN, P. 2001. Generation of a prostate epithelial cell-specific Cre transgenic mouse model for tissue-specific gene ablation. *Mech Dev,* 101**,** 61-9.

XIN, L., LAWSON, D. A. & WITTE, O. N. 2005. The Sca-1 cell surface marker enriches for a prostate-regenerating cell subpopulation that can initiate prostate tumorigenesis. *Proc Natl Acad Sci U S A,* 102**,** 6942-7.

XIN, L., LUKACS, R. U., LAWSON, D. A., CHENG, D. & WITTE, O. N. 2007. Self-renewal and multilineage differentiation in vitro from murine prostate stem cells. *Stem Cells,* 25**,** 2760-9.

XING, Y., K., T., LIU, J., BERNDT, J. D., ZHENG, J. J., MOON, R. T. & XU, W. 2008. Crystal structure of a full-length beta-catenin. *Structure* 16**,** 478-87.

XUE, Y., SMEDTS, F., DEBRUYNE, F. M., DE LA ROSETTE, J. J. & SCHALKEN, J. A. 1998. Identification of intermediate cell types by keratin expression in the developing human prostate. *Prostate,* 34**,** 292-301.

YAMAMOTO, H., KISHIDA, S., KISHIDA, M., IKEDA, S., TAKADA, S. & KIKUCHI, A. 1999. Phosphorylation of axin, a Wnt signal negative regulator, by glycogen synthase kinase-3beta regulates its stability. *J Biol Chem,* 274**,** 10681-10684.

YAN, Y., SHEPPARD, P. C., KASPER, S., LIN, L., HOARE, S., KAPOOR, A., DODD, J. G., DUCKWORTH, M. L. & MATUSIK, R. J. 1997. Large fragment of the probasin promoter targets high levels of transgene expression to the prostate of transgenic mice. *Prostate,* 32**,** 129-39.

YANAGISAWA, N., MIKAMI, T., SAEGUSA, M. & OKAYASU, I. 2001. More frequent beta-catenin exon 3 mutations in gallbladder adenomas than in carcinomas indicate different lineages. *Cancer Res,* 61**,** 19-22.

YANG, X., CHEN, M. W., TERRY, S., VACHEROT, F., BEMIS, D. L., CAPODICE, J., KITAJEWSKI, J., DE LA TAILLE, A., BENSON, M. C., GUO, Y. & BUTTYAN, R. 2006. Complex regulation of human androgen receptor expression by Wnt signaling in prostate cancer cells. *Oncogene,* 25**,** 3436-44.

YARDY, G. W., BICKNELL, D. C., WILDING, J. L., BARTLETT, S., LIU, Y., WINNEY, B., TURNER, G. D., BREWSTER, S. F. & BODMER, W. F. 2009. Mutations in the AXIN1 gene in advanced prostate cancer. *Eur Urol,* 56**,** 486-94.

YARDY, G. W. & BREWSTER, S. F. 2005. Wnt signalling and prostate cancer. *Prostate Cancer Prostatic Dis,* 8**,** 119-26.

YOSHIMOTO, M., CUNHA, I. W., COUDRY, R. A., FONSECA, F. P., TORRES, C. H., SOARES, F. A. & SQUIRE, J. A. 2007. FISH analysis of 107 prostate cancers shows that PTEN genomic deletion is associated with poor clinical outcome. *Br J Cancer,* 97**,** 678-85.

YOSHIMOTO, M., CUTZ, J. C., NUIN, P. A., JOSHUA, A. M., BAYANI, J., EVANS, A. J., ZIELENSKA, M. & SQUIRE, J. A. 2006. Interphase FISH analysis of PTEN in histologic sections shows genomic deletions in 68% of primary prostate cancer and 23% of high-grade prostatic intra-epithelial neoplasias. *Cancer Genet Cytogenet,* 169**,** 128-37.

YU, X., WANG, Y., DEGRAFF, D. J., WILLS, M. L. & MATUSIK, R. J. 2011. Wnt/beta-catenin activation promotes prostate tumor progression in a mouse model. *Oncogene,* 30**,** 1868-79.

YU, X., WANG, Y., JIANG, M., BIERIE, B., ROY-BURMAN, P., SHEN, M. M., TAKETO, M. M., WILLS, M. & MATUSIK, R. J. 2009. Activation of beta-Catenin in mouse prostate causes HGPIN and continuous prostate growth after castration. *Prostate,* 69**,** 249-62.

YUN, M. S., KIM, S. E., JEON, S. H., LEE, J. S. & CHOI, K. Y. 2005. Both ERK and Wnt/beta-catenin pathways are involved in Wnt3a-induced proliferation. *J Cell Sci,* 118**,** 313-22.

ZAHEER, A., CHO, S. Y. & POMPER, M. G. 2009. New agents and techniques for imaging prostate cancer. *J Nucl Med,* 50**,** 1387-90.

ZHANG, S. E. A. 2011. Combating trastuzumab resistance by targeting SRC, a common node downstream of multiple resistance pathways. *Nature Med,* 17**,** 461-469.

ZHOU, Z., FLESKEN-NIKITIN, A., CORNEY, D. C., WANG, W., GOODRICH, D. W., ROY-BURMAN, P. & NIKITIN, A. Y. 2006. Synergy of p53 and Rb deficiency in a conditional mouse model for metastatic prostate cancer. *Cancer Res,* 66**,** 7889-98.

ZHU, J. Y., ABATE, M., RICE, P. W. & COLE, C. N. 1991. The ability of simian virus 40 large T antigen to immortalize primary mouse embryo fibroblasts cosegregates with its ability to bind to p53. *J Virol,* 65**,** 6872-80.

ZHU, Q., YOUN, H. & TANG, J. E. A. 2008. Phosphoinositide3-OH kinase p85α and p110β are essential for androgen receptor transactivation and tumor progression in prostate cancers. *Oncogene,* 27**,** 4569-79.

ZOLLER, M. 2011. CD44: can a cancer-initiating cell profit from an abundantly expressed molecule? *Nat Rev Cancer,* 11**,** 254-67.

ZONCU, R., EFEYAN, A. & SABATINI, D. M. 2011. mTOR: from growth signal integration to cancer, diabetes and ageing. *Nature Rev Mol Cell Biol,* 12**,** 21-35.